

EFFECTS OF ENERGY DEPENDENCE IN THE ELECTRONIC DENSITY OF
STATES ON SOME NORMAL STATE AND SUPERCONDUCTING PROPERTIES

By



BOŽIDAR MITROVIĆ, B.SC., M.SC.

A Thesis

Submitted to the School of Graduate Studies

in Partial Fulfilment of the Requirements

for the Degree

Doctor of Philosophy

McMaster University

July 1981

NONCONSTANT ELECTRONIC DENSITY OF STATES
IN SUPERCONDUCTORS

DOCTOR OF PHILOSOPHY (1981)
(Physics)

McMASTER UNIVERSITY
Hamilton, Ontario.

TITLE: Effects of Energy Dependence in the
Electronic Density of States on Some Normal
State and Superconducting Properties.

AUTHOR: Božidar Mirtrović, B.Sc (Belgrade University)
M.Sc (McMaster University)

SUPERVISOR: Professor J.P. Carbotte

NUMBER OF PAGES: xi, 210

ABSTRACT

We study the effects of energy dependence in the electronic density of states (EDOS) on the electron quasiparticle properties in the normal state, the single particle tunneling characteristics into superconductors and the superconducting thermodynamic properties. The Migdal-Eliashberg equations generalized to include nonconstant EDOS are derived in detail in the isotropic approximation. By numerical solution of the electron self-energy equations in the normal state we assess the effect of the interplay of the energy dependence in EDOS, the electron-phonon interaction and/or elastic impurity scattering on the electron quasiparticle properties. The frequency dependence of the inverse lifetime due to the electron-phonon interaction is significantly affected by energy dependence in EDOS on the scale of several Debye energies around the Fermi level E_F . The analysis of single-particle tunneling density of states into superconductor with nonconstant EDOS via solution of the three generalized Eliashberg equations and inversion of the calculated tunneling conductances shows that the effects of the peaks in EDOS, on a scale of several Debye energies, are important and cannot necessarily be reproduced within the usual Eliashberg theory, by working with some effective values of $\alpha^2 F$ and/or μ^* without introducing unphysical features of these parameters. We

derive the expression for the free energy difference between the normal state and superconducting state for a symmetric Lorentzian model of EDOS starting from Eliashberg's expression for the grand thermodynamic potential of an interacting electron-phonon system. From the solution of the generalized Eliashberg equations on the imaginary frequency axis we calculate the superconducting critical field deviation function $D(t)$. Also, by analytical continuation of the imaginary axis solutions via N-point Padé approximants we calculate the corresponding ratios $(2\Delta_0)/(k_B T_C)$. We show that for a peak in EDOS near E_F with a half-width less than the Debye energy one can describe the effect of this peak on the above mentioned thermodynamic quantities only within the full Eliashberg theory modified to include the energy dependence in EDOS. However for a peak half-width greater than the Debye energy, the influence of the structure in EDOS on $D(t)$, T_C and $(2\Delta_0)/(k_B T_C)$ is small.

ACKNOWLEDGMENTS

I would like to thank my supervisor, Professor J.P. Carbotte for his guidance and encouragement in the course of this project.

I owe many thanks to Dr. J.M. Daams for proofreading the major part of this thesis. Her computer programs made possible the numerical calculation of the thermodynamic properties.

I have benefited from discussions with Dr. W.B. Cowan, Dr. C.R. Leavens, Dr. S.G. Lie, Dr. F.W. Kus and Dr. P. Ummat.

Mrs. Helen Kennelly, who typed this difficult manuscript, deserves my sincere gratitude.

I would like to thank Mrs. Dorothy Matthews for making the typing corrections.

Finally, I gratefully acknowledge the financial support of McMaster University in the form of a Graduate Assistantship, the Dawes Memorial Bursary and the Dalley Fellowship, and of the National Science and Engineering Research Council of Canada in the form of Research grants to Dr. Carbotte.

TABLE OF CONTENTS

	<u>Page</u>
CHAPTER I INTRODUCTION	1
I.1 Introduction to the Subject of of the Thesis	1
I.2 Scope of the Thesis	7
CHAPTER II ELECTRON SELF-ENERGIES IN THE NORMAL STATE DUE TO THE ELECTRON-PHONON INTERACTION AND TO ORDINARY IMPURITY SCATTERING FOR THE CASE OF A NON- CONSTANT ELECTRONIC DENSITY OF STATES	10
II.1 Theoretical Background	10
II.2 Effects of the Interplay between a Sharp Structure in the Elec- tronic Density of States near the Fermi Level, the Electron-Phonon Interaction and Ordinary Impurity Scattering, on the Electron Quasi- particle Properties in the Normal State at $T=0$	31
III.3 Effects of the Interplay between a Sharp Peak in the Electronic Density of States and Electron- Phonon Interaction at Finite T	77
CHAPTER III THE EFFECTS OF A SHARP STRUCTURE IN THE ELECTRONIC DENSITY OF STATES ON THE SINGLE PARTICLE TUNNELING CHARAC- TERISTICS AND THERMODYNAMIC PROPERTIES OF SUPERCONDUCTORS.	90
III.1 The Eliashberg Equations for Strong Coupling Superconductors Generalized to Include the Energy Dependent Electronic Density of States	90
III.2 Tunneling in a Superconductor with an Energy Dependent Elec- tronic Density of States	104

	<u>Page</u>
III.3 Thermodynamic Properties of a Superconductor with a Symmetric Lorentzian Electronic Density of States	126
CHAPTER IV SUMMARY AND CONCLUSIONS	144
APPENDIX 1 SOME PROPERTIES OF THE GREEN'S FUNCTIONS	148
APPENDIX 2 EVALUATION OF SOME INTEGRALS WHICH APPEAR IN THE SELF-ENERGY	152
APPENDIX 3 THE GRAND THERMODYNAMIC POTENTIAL FOR THE INTERACTING ELECTRON-PHONON SYSTEM IN THE NORMAL AND SUPERCONDUCTING STATE. THE FREE ENERGY DIFFERENCE BETWEEN THE SUPERCONDUCTING AND NORMAL STATE	166
APPENDIX 4 DERIVATION OF THE FORMULA FOR THE FREE ENERGY DIFFERENCE BETWEEN THE SUPERCONDUCTING AND NORMAL STATE FOR THE SYMMETRIC LORENTZIAN MODEL FOR $N(\epsilon)$	184
REFERENCES	202

LIST OF FIGURES

<u>Figure No.</u>		<u>Page</u>
II.1	Feynman diagram for the self-energy part	11
II.2	Feynman diagrams for several impurity scattering processes	15
II.3	The Feynman diagram for the polarization part	16
II.4	Contours for the integration	21
II.5	Some processes contributing to the excitation energy	33
II.6	The real part of the electron-phonon self-energy	40
II.7	The imaginary part of the electron-phonon self-energy	41
II.8	The real part of the normal state renormalization function	44
II.9	The imaginary part of the normal state renormalization function	45
II.10	Real and imaginary parts of the self-energy component which describes the shift of the chemical potential	46
II.11	The quasiparticle density of states	47
II.12	The frequency dependence of λ at $T=0$	52
II.13	The frequency derivative of $1/(2\tau)$ at $T=0$	54
II.14	A multiphonon process	55
II.15	Schematic illustration of the basic process contributing to the damping rate	56
II.16	The symmetrized frequency derivative of $1/(2\tau)$	58
II.17	Feynman diagrams which are summed to produce the impurity contribution to the self-energy part	61

<u>Figure No.</u>		<u>Page</u>
II.18	Quasiparticle density of states for the elastic impurity scattering	65
II.19	The dependence of imaginary part of the impurity self-energy on the impurity concentration	67
II.20	The real part of the electron self-energy due to the elastic impurity scattering	68
II.21	The dependence of the impurity renormalization parameter on the impurity concentration	69
II.22	The real part of the electron self-energy	71
II.23	The imaginary part of the electron self-energy	72
II.24	The quasiparticle density of states normalized to $N(0)$.	73
II.25	The real part of the electron self-energy at four different temperatures	80
II.26	The imaginary part of the electron self-energy at four different temperatures	81
II.27	The quasiparticle density of states at four different temperatures	82
II.28	Temperature dependence of the quasiparticle density of states at the chemical potential	84
II.29	Temperature dependence of the electron-phonon mass renormalization parameter	85
II.30	Temperature dependence of $\lambda(T)/\lambda(0)$	86
III.1	Solutions of Eliashberg equations	108
III.2	Normalized tunneling conductances	112
III.3	Normalized tunneling conductances obtained with Lorentzian models for $N(\epsilon)$	113
III.4	Effective electron-phonon spectra	118
III.5	Comparison of tunneling conductances	119

<u>Figure</u>		<u>Page</u>
III.6	Comparison of tunneling conductances	121
III.7	The effective electron-phonon spectrum	122
III.8	$D(t)$ for several Lorentzian half-widths	135
III.9	$D(t)$ for several values of $S/(\pi a)$	137
III.10	$D(t)$ for two values of $S/(\pi a)$	139
III.11	$D(t)$ for a narrow Lorentzian peak in $N(\epsilon)$	142
A3.1	Feynman diagram for calculating Ω	170
A3.2	Feynman diagram which gives small contribution to Ω	170
A3.3	Feynman diagrams for calculating Ω in the superconducting state	174
A3.4	Feynman diagram for impurity contribution to Ω	176
A3.5	Two Feynman diagrams which are taken to be equal when calculating Ω	181

LIST OF TABLES

	<u>Page</u>
III.1 The T_C and the corresponding ratio of the gap edge to the T_C for several Lorentzian half-widths	134
III.2 The T_C and the corresponding ratio of the gap edge to the T_C for several $S(\pi a)$ -values and fixed $a = 1.5 \omega_{\max}$	136
III.3 The T_C and the corresponding ratio of the gap edge to the T_C for two values of $S/(\pi a)$ and fixed $a = 0.25 \omega_{\max}$	138
A.1 Several values of Z_s , Z_n and Z_{ns}	200

CHAPTER I

INTRODUCTION

I.1 INTRODUCTION TO THE SUBJECT OF THE THESIS

In recent years there has been a considerable number of attempts (Refs. 1-8) to incorporate the effects of a rapidly varying electronic density of states (EDOS) near the Fermi level E_F into the so-called strong coupling (or Eliashberg) theory of superconductivity, which takes into account the details of the basic interactions in superconductors. The motivation for these attempts is that some A-15 superconducting materials with the formula A_3B ($A = V, Nb, \dots$, $B = Si, Ge, Al, Ga, Sn$), which possess the highest superconducting critical temperatures ($\sim 20^\circ K$), have long been suspected of having unusually sharp peaks in EDOS near E_F (for review see Refs. 9, 10, 11), with structure on the scale of Debye energy ω_D ($\hbar = 1$), which is of the order of several tens of meV. Originally, in the early sixties, peaks in EDOS were invoked¹²⁾ to explain the anomalous temperature dependence of the magnetic susceptibility and Knight shift of several vanadium based A-15 materials. Subsequently Weger¹³⁾ suggested that the concept of sharp peaks in EDOS $N(E)$ is consistent with the presence of A-atom linear chains in A-15 A_3B structure. The rapid variation in $N(E)$ near E_F was also used to

explain unusual elastic properties of these materials, including the structural transformation from the cubic to the tetragonal phase, which occurs in some of the A-15 compounds^{9,10,11}.

Indeed, several recent band structure calculations⁽¹⁴⁻¹⁸⁾ have confirmed the possibility of sharp peaks in EDOS for materials with A-15 crystal structure. Unfortunately, at present there is not enough agreement between various band structure calculations on the scale of ω_D to make their results completely convincing (see for example Ref. 19). Therefore, model EDOS are still being used to fit various properties of these materials^{20,21}). Nevertheless, a quite general argument has been given by Ho et al.¹⁵⁾ which explains why one can expect sharp peaks in EDOS of A-15 compounds and another class of materials, the Chevrel-phase compounds, having a relatively large number of transition element atoms per unit cell. In the A-15 materials there are six transition metal atoms per unit cell and therefore $6 \times 5 = 30$ d bands within the energy interval ~ 10 eV. Ho et al. state that the strong interaction between the bands and the requirement of no band crossing off symmetry planes results in sharp peaks in $N(E)$ from each band. Since the peak width in Nb is less than 1 eV, they estimate that the peak widths in A-15 materials should be less than 150 meV. It should be noted that according to more recent band structure calculations¹⁴⁻¹⁸⁾ peaks in the EDOS have nothing to do with the singular nature of one-dimensional band-structure²²⁾.

The influence of the above described feature of EDOS of A-15 materials on their superconducting properties was first treated by Labé et al.²³⁾. First of all, sharp peaks in EDOS should imply large values of $N(E_F)$. This large degeneracy around the Fermi level is favourable for superconductivity since there are then a large number of electrons to participate in the pairing correlations. Normally, the finite width of the phonon spectrum limits the attractive range of the electron-phonon interaction which brings about superconductivity. Labé et al.²³⁾ conclude that in A-15 compounds, however, the narrowness of the peak in $N(\epsilon)$ (they used the Labé-Fredel model $N(E) = N(0) (E+E_m)^{-1/2}$ with $E_m = 1.8$ meV) limits the attractive range of interaction.

Since all of the A-15 materials with high superconducting critical temperature T_c , except V_3Si , are expected to be strong coupling superconductors, i.e. ones where retardation and damping effects play a significant role, it is of interest to analyze the effects of rapid variation in $N(E)$ in the context of strong coupling theory of superconductivity. The general formalism which takes into account all the complexities of the band structure has been developed by Garland²⁴⁾. A limiting case of Garland's formalism, which ignores all anisotropy effects and possible energy dependence of the electron-phonon coupling, but retains the energy dependence of $N(E)$, has been applied in the analysis of T_c in some A-15

materials by Horsch and Rietschel¹⁾ and independently by Nettel and Thomas²⁾. Both groups have neglected the damping effects in their analysis. Nettel and Thomas²⁾ reach a conclusion which is analogous to that of Labé et.al.²³⁾, while Horsch and Rietschel¹⁾ claimed that a particular placement of the Fermi level within the peak may lead to enhancement of T_c due to the suppression of the repulsive part of the electron-phonon interaction. Lie and Carbotte³⁾ calculated the functional derivative $\delta T_c / \delta N(E)$ by using the complete Eliashberg theory^{24,25)} in its imaginary axis formulation; thus damping effects were included in their analysis. Lie and Carbotte found from their calculated $\delta T_c / \delta N(E)$ that the values of $N(E)$ only within 5 to 10 T_c 's around the chemical potential have appreciable effect on T_c ($\delta T_c / \delta N(\epsilon)$ is approximately of Lorentzian form centred at the chemical potential $\epsilon = 0$ and becomes negative only at larger energies $\epsilon > 50 T_c$). Ho et al. were first to point out that the effective smearing of the normal state EDOS at T_c due to the damping effects at finite T may be a limiting mechanism for achieving still higher superconducting critical temperatures in A-15 compounds¹⁵⁾. In their semiquantitative analysis based on the results of the band structure calculations, experimental resistivity data and uncertainty principle,

$$\Delta \epsilon \tau \sim 1 ;$$

according to which for given life-time τ any fine structure in

$N(\epsilon)$ on the scale $\Delta\epsilon$ is smeared out, they conclude that the measured T_c of Nb_3Ge is several degrees lower than what would follow from $T = 0$ band-structure properties. By rewriting the strong coupling Eliashberg equations at T_c on the real frequency axis with certain approximations Pickett⁴⁾ has shown explicitly how the damping effects influence $N(\epsilon)$ and thereby the critical temperature.

In recent years a new experimental method has been employed in studying the superconducting properties of A-15 compounds, (see Ref. 26 and references therein). By changing the intrinsic properties of A-15 materials through radiation damage and then measuring the resulting changes in the physical properties one expects to gain more understanding of the essential microscopic features of these difficult materials. Since the fluence of the radiation can be controlled, one can study the dependence of various physical properties on the amount of alteration of the original structure. Analogous methods are the changing of the composition or alloying. In most cases the superconducting critical temperature of A-15 compounds decreases with increasing fluence. Various explanations of this behaviour have been given^{19,26,27)}, the most prominent being the smearing of the peak in EDOS. The point is that other explanations of the reduction in T_c , such as the washing out of gap anisotropy²⁷⁾, cannot account for the increase in the superconducting critical temperature of

Mo_3Ge ²⁸⁾ with increasing fluence. Most likely²⁶⁾ the Fermi level of Mo_3Ge is located in a valley in the electronic density of states, between the bonding and antibonding peak, and the smearing of the structure in EDOS results in an effective increase of $N(E_F)$, which implies an increase in T_c .

From radiation damage experiments it is possible to obtain a rough estimate of the energy scale on which $N(E)$ varies²⁶⁾. From these experiments it has been deduced²⁶⁾ that for V_3Si structure on the scale of 100°K is possible. However, since in these analyses of radiation damage experiments oversimplified formulae of at best limited accuracy are used for T_c it is of interest to study the effects of smearing in EDOS within the context of rigorous Eliashberg theory modified to include energy dependence in $N(E)$. This study has been carried out by Lie and Carbotte⁵⁾ and by Müller et al.⁷⁾ who treated the broadening of EDOS due to static disorder in a phenomenological way. More recently Schachinger et al.²⁹⁾ treated a similar problem, including the scattering of ordinary or paramagnetic impurities in a more exact way.

Since the superconducting critical temperature is a fairly complicated functional of the basic microscopic parameters it is of interest to study the influence of energy dependence in EDOS on other superconducting properties. One expects that the study of single particle tunneling experiments^{30, 31)}, which are known to provide the most detailed in-

formation about basic microscopic interactions in superconductors, may give more direct information about EDOS than the other superconducting properties. The preliminary results of such a study were published by Lie et al.⁶⁾ and the more detailed analysis was done by Mitrović and Carbotte⁸⁾.

Obviously the study of superconducting properties in the presence of sharp peaks in EDOS should be paralleled by an analogous investigation of the normal state properties, in particular the effects of the electron-phonon interaction in the normal state. A nonselfconsistent quantitative analysis of the effects of the interplay between the electron-phonon interaction and energy dependence in $N(E)$ was given by Fradín³²⁾, while a selfconsistent, but formal, treatment of the same problem was given by Pickett⁴⁾.

I.2 SCOPE OF THE THESIS

In this thesis we investigate the effects of sharp structure in EDOS near the Fermi level on some superconducting and normal state properties. In Chapter II we study the effects of the interplay between energy dependence in $N(E)$, electron-phonon interaction, and/or elastic impurity scattering on the electron quasiparticle properties in the normal state. In Section II.1 we present a fairly detailed derivation of the self-energy equations relevant to the problem under consideration. In Sec. II.2, the electron self-energy equation

is solved for the electron-phonon problem and/or impurity problem at $T=0$. The resulting quantities determine the electron quasiparticle properties in the normal state. In Sec. II.3 we analyze the problem of the electron phonon interaction in the normal state for finite temperature in the presence of sharp peaks in $N(E)$. The temperature dependence of the electron-phonon mass enhancement parameter $\lambda(T)$ is calculated for two model electronic densities of states.

In Chapter III we consider tunneling into superconductor with nonconstant $N(E)$ and calculate some thermodynamic properties. In Section III.1 of this chapter we give the derivation of the Eliashberg equations for the superconducting state generalized to include variation in EDOS on the scale of a few Debye energies around E_F . Section III.2 contains an analysis of the single-particle tunneling experiments at $T=0$ for the case of nonconstant $N(E)$. In Sec. III.3 we present numerical results for the superconducting critical field deviation function and the corresponding ratios $(2\Delta_0)/(k_B T_c)$ obtained with several Lorentzian models for $N(E)$.

Chapter IV contains summary and conclusions.

In Appendix 1 we summarize, for convenience, some Green's function properties and many-body perturbation theory diagrammatic rules. Appendix 2 contains the derivation of several integrals appearing in the self-energy equations. Appendix 3 contains an analysis of Eliashberg's expression

for the grand thermodynamic potential of an interacting electron-phonon system in both the normal and superconducting state. We show how this expression is to be generalized to include short-range Coulomb repulsion in the superconducting state and scattering by ordinary (or paramagnetic) impurities. In Appendix 4 we present a detailed derivation of the expression for the free energy difference between superconducting and normal state for a symmetric Lorentzian model of $N(\epsilon)$.

CHAPTER II

ELECTRON SELF-ENERGIES IN THE NORMAL STATE DUE TO THE ELECTRON-PHONON INTERACTION AND TO ORDINARY IMPURITY SCATTERING FOR THE CASE OF A NONCONSTANT ELECTRONIC DENSITY OF STATES

II.1 THEORETICAL BACKGROUND

The problem of the electron-phonon interaction and ordinary impurity scattering in metals is well known and has been formulated and reviewed in several books, formal articles and review articles (see in particular refs. (33) - (61)). Here we will briefly present those aspects of the problem which are of interest in this thesis, namely the energy dependence in the electronic density of states (EDOS) and the effects of the interplay between the electron-phonon interaction (or ordinary impurity scattering) and energy dependence in the EDOS.

The normal state electronic self-energy part due to the electron-phonon interaction and to scattering by ordinary (non-magnetic) impurities is given by (see Fig. II.1)

$$\Sigma(k; i\omega_n) = \Sigma_{ep}(k, i\omega_n) + \Sigma_{iN}(k, i\omega_n) \quad (II.1)$$

where (we take the volume of the system $V = 1$)

$$\Sigma_{ep}(k, i\omega_n) = -T \sum_{k'} \sum_{m=-\infty}^{+\infty} \sum_{\lambda} |g_{kk', \lambda}|^2 D_{\lambda}(k-k', i\omega_n - i\omega_m) G(k', i\omega_m) \quad (II.2)$$

is the self-energy part coming from the electron-phonon interac-

tion and

$$\Sigma_{iN}(k, i\omega_n) = n_N \sum_{k'} | \langle k | V_N | k' \rangle |^2 G(k', i\omega_n) \quad (\text{II.3})$$

is the contribution due to ordinary impurity scattering.

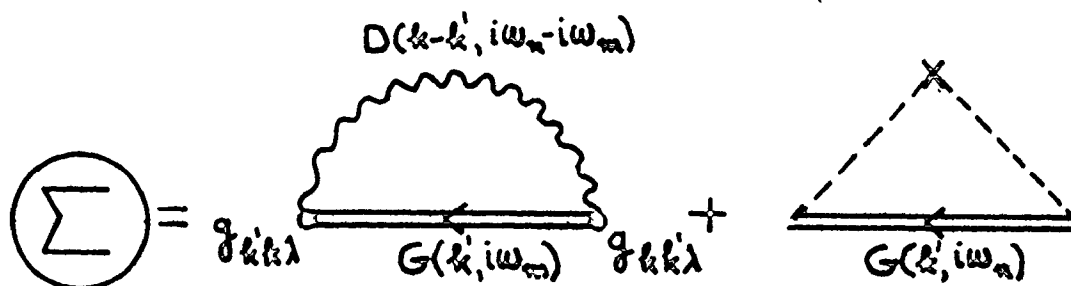


Fig. II.1

Here $k = (\vec{k}, n)$, where \vec{k} is the wave-vector in the first Brillouin zone, n is the band index and $i\omega_n$ are the Fermion thermal or Matsubara frequencies

$$\omega_n = \pi T(2n-1) \quad , \quad n = 0, \pm 1, \pm 2, \dots \quad (\text{II.4})$$

where T is the absolute temperature (we use the system of units in which Boltzmann's constant $k_B = 1$ and $\hbar = 1$).

$G(k, i\omega_n)$ is the electron thermodynamic Green's function (see Appendix I), which is related to the noninteracting electron thermodynamic Green's function

$$G_0(k, i\omega_n) = \frac{1}{i\omega_n - \epsilon_k} \quad (\text{II.5})$$

and to the self-energy part $\Sigma(k, i\omega_n)$ by the Dyson equation

$$G^{-1}(k, i\omega_n) = G_0^{-1}(k, i\omega_n) - \Sigma(k, i\omega_n) . \quad (\text{II.6})$$

Here ϵ_k are the Bloch energies measured with respect to the true interacting chemical potential μ , which is determined by the equation

$$\begin{aligned} \bar{N} &= \text{tr} \{ \exp[-\frac{1}{T} (\hat{H} - \mu \hat{N})] \hat{N} \} / \text{tr} \{ \exp[-\frac{1}{T} (\hat{H} - \mu \hat{N})] \} \\ &= 2T \sum_k \sum_{n=-\infty}^{+\infty} G(k, i\omega_n) e^{i\omega_n 0^+} \end{aligned} \quad (\text{II.7})$$

where \bar{N} is the average number of electrons in the system, \hat{H} is the Hamiltonian of the system, \hat{N} - particle number operator and 0^+ is a positive infinitesimal.

In equation (II.2) $D_\lambda(\vec{q}, i\nu_n)$ is the phonon thermodynamic Green's function defined by

$$D_\lambda(\vec{q}, i\nu_n) = \int_0^{+\infty} d\Omega B_\lambda(\vec{q}, \Omega) \left[\frac{1}{i\nu_n - \Omega} - \frac{1}{i\nu_n + \Omega} \right] , \quad (\text{II.8})$$

where

$$i\nu_n = i\pi T 2n \quad (n = 0, \pm 1, \pm 2, \dots) \quad (\text{II.9})$$

and $B_\lambda(\vec{q}, \Omega)$ is the phonon spectral weight function for the wave-vector \vec{q} and polarization λ (\vec{q} is restricted to the first Brill-

lounin zone). $D_\lambda(\vec{q}, i\nu_n)$ is related to its noninteracting counterpart

$$D_{\lambda 0}(\vec{q}, i\nu_n) = \frac{2\Omega_{\vec{q}\lambda}^0}{(i\nu_n)^2 - (\Omega_{\vec{q}\lambda}^0)^2} \quad (II.10)$$

(where $\Omega_{\vec{q}\lambda}^0$ is the unrenormalized (or bare) phonon frequency for the wave-vector \vec{q} and polarization λ) and to the polarization part $\Pi_\lambda(\vec{q}, i\nu_n)$ through the Dyson equation

$$D_\lambda^{-1}(\vec{q}, i\nu_n) = D_{\lambda 0}^{-1}(\vec{q}, i\nu_n) - \Pi_\lambda(\vec{q}, i\nu_n) \quad (II.11)$$

In the quasiparticle approximation for phonons (i.e. for long lived phonons)

$$B_\lambda(\vec{q}, \Omega) = \delta(\Omega - \Omega_{\vec{q}\lambda}) \quad (II.12)$$

where $\Omega_{\vec{q}\lambda}$ is the renormalized phonon frequency for wave-vector \vec{q} and polarization λ which is the physical phonon frequency measured in experiments. We note that

$$F(\Omega) = \sum_{\vec{q}, \lambda} B_\lambda(\vec{q}, \Omega) \quad (II.13)$$

is the phonon density of states at frequency Ω .

$g_{kk', \lambda}$ is the electron-phonon coupling function defined by

$$g_{kk', \lambda} = - \left(\frac{\hbar N_c}{2\Omega_{\vec{k}-\vec{k}', \lambda}} \right)^{1/2} \sum_{\alpha} \langle \vec{k}' | \nabla_i U_{i\alpha} | \vec{k} \rangle \cdot \vec{\epsilon}_{\vec{k}-\vec{k}', \lambda}(\alpha) e^{i(\vec{k}-\vec{k}') \cdot \vec{\rho}_{\alpha}^0} \quad (II.14)$$

where N_c is the number of unit cells per unit volume, M_c is the net mass of the ions within a unit cell. $|k\rangle$ and $|k'\rangle$ are Bloch states and $U_{i\alpha}$ is the screened and Coulomb vertex corrected one-body potential on the i -th electron due to the α -th ion in the unit cell located at its equilibrium position \vec{p}_α^0 with respect to the origin. The $\vec{\epsilon}_{k-k',\lambda}$'s are phonon polarization vectors.

We assume that the effects of the Coulomb interaction between the electrons are included in calculating the electronic band-structure as well as screening and Coulomb vertex corrections for the electron-phonon coupling function. We also assume that the static screening approximation is applicable. How good this approximation is for transition metals and their compounds, where one can expect a sharp structure in the electronic density of states, remains an open question^{19,62}.

The impurity contribution $\Sigma_{iN}(k, i\omega_n)$ given by the Eq. (II.3) is obtained in the standard way^{40,61} by diagrammatic expansion, ensemble averaging over impurity configurations, whereby it is assumed that the impurity concentration n_{iN} is small, and assuming that the Born approximation is applicable so that diagrams given in Figs. II.2 b,c (and higher order ones) give small contribution compared to the second diagram in Fig. II.1

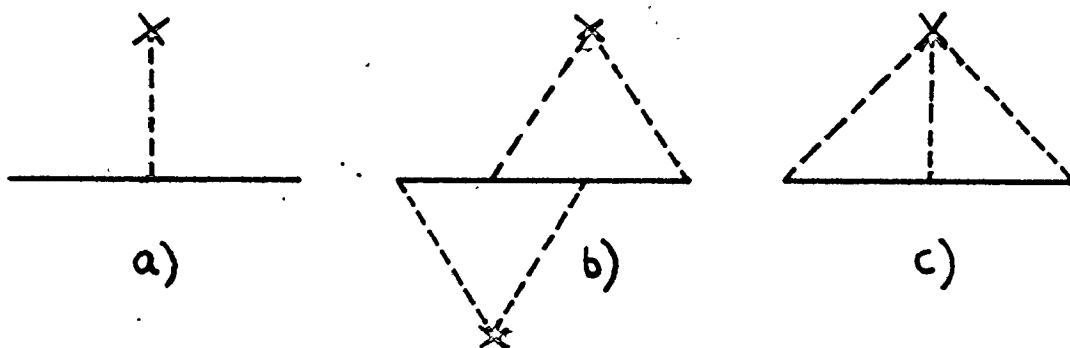


Fig. II.2

It should be noted that the diagram in Fig. II.2a) which corresponds to the single scattering by one impurity gives a constant term upon ensemble averaging, if the Bloch states are approximated by plane-waves and leads to a constant shift of the chemical potential. In the case of Bloch states this graph leads to a non-rigid shift of the bands and can be handled implicitly by taking for the unperturbed states $|k\rangle$ the eigenstates of the redefined average crystal potential⁵⁹⁾.

Before we proceed to isolate the effects of the energy dependence in the electronic density of states in Eqs. (II.2) and (II.3) we complete the solution of the electron-phonon problem by giving the expression for the polarization part $\Pi(\vec{q}, i\nu_n)$ (see Fig. II.3)

$$\Pi(\vec{q}, i\nu_n) = 2T \sum_{\vec{k}} \sum_{m=-\infty}^{+\infty} |g_{\vec{k}, \vec{k}+\vec{q}, \lambda}|^2 G(\vec{k}+\vec{q}, i\nu_n + i\omega_m) G(\vec{k}, i\omega_m) \quad (\text{II.15})$$

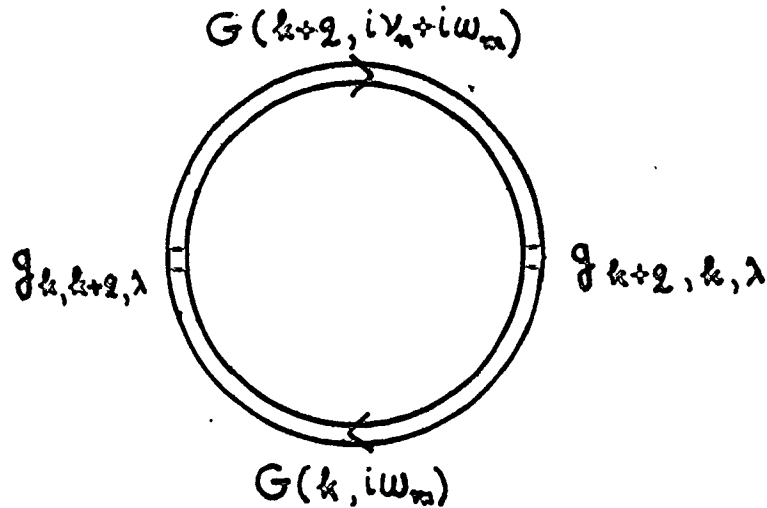


Fig. II.3

Equations (II.2) and (II.14) are essentially Migdal's equations ³³⁾ for the electron-phonon problem in the normal state. It should be noted that Migdal's equations have limited validity ³⁸⁾. They break down for $q \rightarrow 0$ optical phonons whose phase velocity is greater than the Fermi velocity and one has to include higher order vertex corrections to the simple electron-phonon vertex $g_{\vec{k}\vec{k}+\vec{q}, \lambda}$. However, we shall ignore this difficulty. This may not be completely justified for A-15 compounds where it has been suggested ⁶³⁾ that coupling to the optical modes plays an important role.

In order to isolate effects of the energy dependence of $N(\epsilon)$ in Eqs. (1) and (2) it is convenient ⁴⁾ to define for any quantity $Q(k)$

$$Q(\epsilon) = [\sum_k Q(k) \delta(\epsilon - \epsilon_k)] / N(\epsilon) \quad (\text{II.16})$$

where $N(\epsilon)$ is the single spin band-structure electronic density of states per unit volume at energy ϵ measured with respect to the true chemical potential; then Eqs. (II.2) and (II.8) give

$$\begin{aligned} \Sigma_{ep}(\epsilon, i\omega_n) &= \frac{1}{N(\epsilon)} \sum_k \Sigma_{ep}(k, i\omega_n) \delta(\epsilon - \epsilon_k) = \\ &= T \sum_{m=-\infty}^{+\infty} \int_0^{+\infty} d\Omega \frac{2\Omega}{(\omega_n - \omega_m)^2 + \Omega^2} \sum_k \sum_{k'} \sum_{\lambda} |g_{kk', \lambda}|^2 B_{\lambda}(k - k', \Omega) \times \\ &\quad \times \frac{\delta(\epsilon - \epsilon_k)}{N(\epsilon)} \int_{-\infty}^{+\infty} d\epsilon' \delta(\epsilon' - \epsilon_{k'}) G(k', i\omega_m) \\ &= T \sum_{m=-\infty}^{+\infty} \int_0^{+\infty} d\Omega \frac{2\Omega}{(\omega_n - \omega_m)^2 + \Omega^2} \int_{-\infty}^{+\infty} d\epsilon' \frac{1}{N(\epsilon)} \sum_k \delta(\epsilon - \epsilon_k) \sum_{k'} \sum_{\lambda} |g_{kk', \lambda}|^2 \times \\ &\quad \times B_{\lambda}(k - k', \Omega) G(k', i\omega_m) \delta(\epsilon' - \epsilon_{k'}) . \end{aligned}$$

We will assume that the equality

$$\frac{1}{N(\epsilon)} \sum_k Q_1(k) Q_2(k) \delta(\epsilon - \epsilon_k) = Q_1(\epsilon) Q_2(\epsilon) \quad (\text{II.17})$$

is valid which amounts to ignoring all anisotropy effects. Then

We can write

$$\begin{aligned}
 \sum_{k'} \sum_{\lambda} |g_{kk'\lambda}|^2 B_{\lambda}(k-k', \Omega) G(k', i\omega_m) \delta(\epsilon' - \epsilon_{k'}) &= \\
 &= \frac{1}{N(\epsilon')} \sum_{k''} G(k'', i\omega_m) \delta(\epsilon' - \epsilon_{k''}) \sum_{k'} \sum_{\lambda} |g_{kk'\lambda}|^2 B_{\lambda}(k-k', \Omega) \delta(\epsilon' - \epsilon_{k'}) \\
 &= G(\epsilon', i\omega_m) \sum_{k'} \sum_{\lambda} |g_{kk'\lambda}|^2 B_{\lambda}(k-k', \Omega) \delta(\epsilon' - \epsilon_{k'})
 \end{aligned}$$

and

$$\begin{aligned}
 \Sigma_{ep}(\epsilon, i\omega_n) &= T \sum_{m=-\infty}^{+\infty} \int_{-\infty}^{+\infty} d\epsilon' \frac{N(\epsilon')}{N(0)} G(\epsilon', i\omega_m) \int_0^{+\infty} d\Omega \alpha^2 F(\Omega; \epsilon, \epsilon') \times \\
 &\times \frac{2\Omega}{(\omega_n - \omega_m)^2 + \Omega^2} \quad (II.18)
 \end{aligned}$$

where

$$\begin{aligned}
 \alpha^2 F(\Omega; \epsilon, \epsilon') &\equiv N(0) \sum_k \sum_{k'} \sum_{\lambda} |g_{kk'\lambda}|^2 B_{\lambda}(k-k', \Omega) \times \\
 &\times \delta(\epsilon - \epsilon_k) \delta(\epsilon' - \epsilon_{k'}) / N(\epsilon) N(\epsilon') \quad (II.19)
 \end{aligned}$$

The same type of algebra leads to

$$\Sigma_{iN}(\epsilon, i\omega_n) = \int_{-\infty}^{+\infty} d\epsilon' \frac{N(\epsilon')}{N(0)} \frac{1}{2\pi\tau_{iN}(\epsilon, \epsilon')} G(\epsilon', i\omega_n) \quad (II.20)$$

where

$$\frac{1}{2\tau_{iN}(\epsilon, \epsilon')} = n_{iN} \pi N(0) \sum_k \sum_{k'} |\langle k' | V_N | k \rangle|^2 \delta(\epsilon - \epsilon_k) \delta(\epsilon - \epsilon_{k'}) / N(\epsilon) N(\epsilon') \quad (II.21)$$

and V_N is the change in the crystal potential due to ordinary (normal) impurities.

For calculating the equilibrium thermodynamic properties of the interacting electron-phonon system in the normal state (which may contain small amounts of ordinary impurities) in principle one needs only the thermodynamic Green's functions $G(k, i\omega_n)$, $D_\lambda(\vec{q}, i\nu_n)$ and the corresponding self-energy parts $\Sigma(k, i\omega_n)$, $\Pi_\lambda(\vec{q}, i\nu_n)$. However, in order to calculate other properties of this system such as, for example, the electron quasiparticle properties, one needs the retarded electron Green's function $G_R(k, Z)$ and the corresponding self-energy part $\Sigma_R(k, z)$ for the real values of the complex argument Z (see Appendix 1). It can be shown that for the real values of ω

$$G_R(k, \omega) = G(k, \omega + i\delta) \quad , \quad (\text{II.22a})$$

$$\Sigma_R(k, \omega) = \Sigma(k, \omega + i\delta) \quad , \quad (\text{II.22b})$$

where δ is a positive infinitesimal and $\Sigma(k, \omega + i\delta)$ should be a bounded function of ω .

When performing an analytic continuation it is worth noting that for $\omega_n > 0$ ($\omega_n < 0$) $G(\epsilon, i\omega_n)$ is equal to $G_R(\epsilon, i\omega_n)$ ($G_A(\epsilon, i\omega_n)$ -advanced Green's function) which is analytic and nonvanishing in the upper half (lower half) complex plane. Therefore (II.18) can be rewritten in the form

$$\begin{aligned}
\Sigma_{ep}(\epsilon, i\omega_n) = & -T \int_{-\infty}^{+\infty} d\epsilon' \frac{N(\epsilon')}{N(0)} \int_0^{\infty} d\Omega \alpha^2 F(\Omega; \epsilon, \epsilon') \times \\
& \times \left\{ \sum_{m=1}^{\infty} G_R(\epsilon, i\omega_m) \left[\frac{1}{i\omega_n - i\omega_m - \Omega} - \frac{1}{i\omega_n - i\omega_m + \Omega} \right] + \right. \\
& \left. + \sum_{m=0}^{\infty} G_A(\epsilon, i\omega_{-m}) \left[\frac{1}{i\omega_n - i\omega_{-m} - \Omega} - \frac{1}{i\omega_n - i\omega_{-m} + \Omega} \right] \right\}. \quad (II.23)
\end{aligned}$$

It is convenient to use identities ($\beta \equiv 1/T$)

$$\sum_{n=1}^{\infty} F_1(i\omega_n) = \pm \frac{1}{2\pi iT} \oint_{C_1} dz \frac{F_1(z)}{e^{\mp\beta z} + 1} \quad (II.24a)$$

$$\sum_{n=0}^{\infty} F_2(i\omega_{-n}) = \mp \frac{1}{2\pi iT} \oint_{C_2} dz \frac{F_2(z)}{e^{\mp\beta z} + 1} \quad (II.24b)$$

where F_1 (F_2) is analytic and nonvanishing in the neighbourhood of the positive (negative) imaginary axis and contours C_1 and C_2 are shown in Fig. II.4a. For a given $\omega_n > 0$ and any Ω from the open interval $]0, +\infty[$ the function

$$G_R(\epsilon, Z) = \frac{1}{i\omega_n - Z + \Omega}$$

is nonvanishing in the upper-half complex Z -plane and has a simple pole at $Z = i\omega_n + \Omega$ which is off the positive imaginary axis, while

$$G_A(\epsilon, Z) = \frac{1}{i\omega_n - Z + \Omega}$$

is nonvanishing and analytic in the lower-half complex plane.

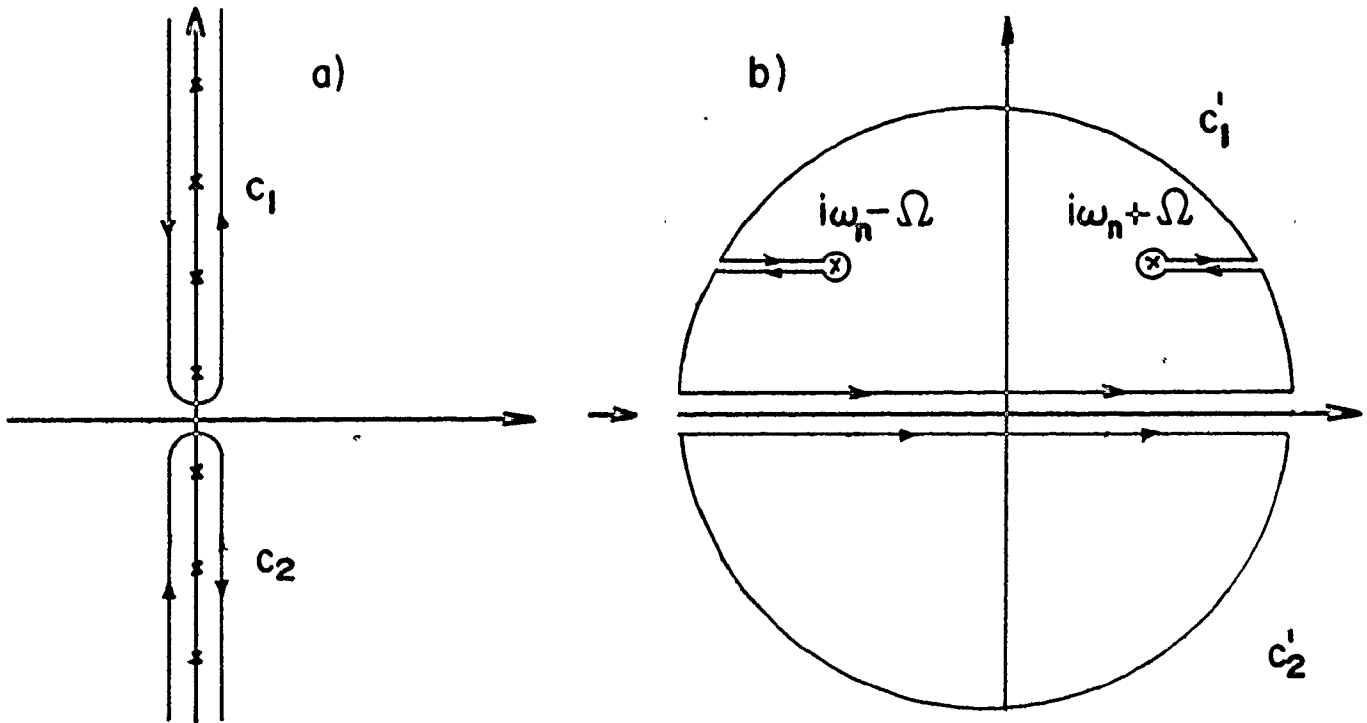


Fig. II-4

Then for a given $\omega_n > 0$ and $\Omega > 0$ contours C_1 and C_2 in Fig. II.4a can be deformed into C_1' and C_2' of Fig. II.4b, respectively. Since $G_R(\epsilon, Z) = O(1/Z)$ and $G_A(\epsilon, Z) = O(1/Z)$ for $|Z| \rightarrow \infty$ the contributions from the large semi-circles vanish and one has

$$\sum_{m=1}^{\infty} G_R(\varepsilon, i\omega_m) \frac{1}{i\omega_n - i\omega_m + \bar{\Omega}} = \pm \frac{1}{2\pi i T} \int_{-\infty}^{+\infty} d\omega' G_R(\varepsilon, \omega') \frac{1}{i\omega_n - \omega' + \bar{\Omega}} \times$$

$$\times \frac{1}{e^{\bar{\beta}\omega'} + 1} - 2\pi i \left(\pm \frac{1}{2\pi i T} \right) G_R(\varepsilon, i\omega_n + \bar{\Omega}) \frac{1}{-e^{(\bar{\beta}) + \bar{\Omega}} + 1} (-1) \quad (\text{II.25a})$$

and

$$\sum_{m=0}^{\infty} G_A(\varepsilon, i\omega_{-m}) \frac{1}{i\omega_n - i\omega_{-m} + \bar{\Omega}} = \mp \frac{1}{2\pi i T} \int_{-\infty}^{+\infty} d\omega' G_A(\varepsilon, \omega') \frac{1}{i\omega_n - \omega' + \bar{\Omega}} \times$$

$$\times \frac{1}{e^{\bar{\beta}\omega'} + 1} \quad (\text{II.25b})$$

Putting (II.25a) and (II.25b) back into (II.23) we obtain

$$\Sigma_{ep}(\varepsilon, i\omega_n) = - \frac{1}{2\pi i} \int_{-\infty}^{+\infty} d\varepsilon' \frac{N(\varepsilon')}{N(0)} \int_0^{+\infty} d\Omega \alpha^2 F(\Omega; \varepsilon, \varepsilon') \times$$

$$\times \left\{ \int_{-\infty}^{+\infty} d\omega' [G_R(\varepsilon', \omega') - G_A(\varepsilon', \omega')] \left[\frac{1}{i\omega_n - \omega' - \Omega} \frac{1}{e^{-\beta\omega'} + 1} + \right. \right.$$

$$\left. + \frac{1}{i\omega_n - \omega' + \Omega} \frac{1}{e^{\beta\omega'} + 1} \right] - 2\pi i \frac{G_R(\varepsilon, i\omega_n - \Omega) + G_R(\varepsilon, i\omega_n + \Omega)}{e^{\beta\Omega} - 1} \right\}.$$

Since

$$G_R(\varepsilon, \omega) - G_A(\varepsilon, \omega) = 2i \text{Im} G_R(\varepsilon, \omega) = 2i \text{Im} G(\varepsilon, \omega + i\delta)$$

(see Appendix 1), we have

$$\begin{aligned}
\Sigma_{ep}(\epsilon, i\omega_n) &= \int_{-\infty}^{+\infty} d\omega' \int_{-\infty}^{+\infty} d\epsilon' \frac{N(\epsilon')}{N(0)} \left\{ -\frac{1}{\pi} \text{Im}G(\epsilon', \omega' + i\delta) \right\} \times \\
&\times \int_0^{+\infty} d\Omega \alpha^2 F(\Omega; \epsilon, \epsilon') \left[\frac{1}{i\omega_n - \omega' - \Omega} \frac{1}{e^{-\beta\omega'} + 1} + \frac{1}{i\omega_n - \omega' + \Omega} \frac{1}{e^{\beta\omega'} + 1} \right] + \\
&+ \int_{-\infty}^{+\infty} d\epsilon' \frac{N(\epsilon')}{N(0)} \int_0^{+\infty} d\Omega \frac{\alpha^2 F(\Omega; \epsilon, \epsilon')}{e^{\beta\Omega} - 1} [G_R(\epsilon', i\omega_n - \Omega) + G_R(\epsilon', i\omega_n + \Omega)] .
\end{aligned}
\tag{II.26}$$

Now, setting $i\omega_n \rightarrow \omega + i\eta$, where η is a positive infinitesimal we finally obtain

$$\begin{aligned}
\Sigma_{ep}(\epsilon, \omega + i\eta) &= \int_{-\infty}^{+\infty} d\omega' \int_{-\infty}^{+\infty} d\epsilon' \frac{N(\epsilon')}{N(0)} \left\{ -\frac{1}{\pi} \text{Im}G(\epsilon', \omega' + i\delta) \right\} \times \\
&\times \int_0^{+\infty} d\Omega \alpha^2 F(\Omega; \epsilon, \epsilon') \left[\frac{1}{\omega - \omega' - \Omega + i\eta} \frac{1}{e^{-\beta\omega'} + 1} + \frac{1}{\omega - \omega' + \Omega + i\eta} \frac{1}{e^{\beta\omega'} + 1} \right] + \\
&+ \int_{-\infty}^{+\infty} d\epsilon' \frac{N(\epsilon')}{N(0)} \int_0^{+\infty} d\Omega \frac{\alpha^2 F(\Omega; \epsilon, \epsilon')}{e^{\beta\Omega} - 1} [G(\epsilon', \omega - \Omega + i\eta) + G(\epsilon', \omega + \Omega + i\eta)] .
\end{aligned}
\tag{II.27}$$

It is trivial to analytically continue the impurity contribution, Eq. (II.20):

$$\Sigma_{iN}(\epsilon, \omega + i\eta) = \int_{-\infty}^{+\infty} d\epsilon' \frac{N(\epsilon')}{N(0)} \frac{1}{2\pi\tau_{iN}(\epsilon, \epsilon')} G(\epsilon', \omega + i\eta) . \tag{II.28}$$

We now have the major approximation in this thesis by assuming that $\alpha^2 F(\Omega; \epsilon, \epsilon')$ does not depend on ϵ, ϵ' on the scale of

several times the Debye energy ω_D around the Fermi level, or better that the $\varepsilon, \varepsilon'$ -dependence of $\alpha^2 F(\Omega; \varepsilon, \varepsilon')$ is much weaker than the ε' dependence of $N(\varepsilon')$ for $\varepsilon, \varepsilon'$ in the indicated energy range. The point is that one is interested in the values of $\Sigma_{ep}(\varepsilon, i\omega_n)$ or $\Sigma_{ep}(\varepsilon, \omega + i\eta)$ for $\varepsilon, |\omega_n|, |\omega|$ in the range of a few times ω_D around the Fermi level. Since the phonon frequencies Ω fall in the range from zero to $\sim \omega_D$ the factor $\int_0^{+\infty} d\Omega \alpha^2 F(\Omega; \varepsilon, \varepsilon') \frac{2\Omega}{(\omega_n - \omega_m)^2 + \Omega^2}$ in (II.18) is a rapidly decreasing function of ω_m for $|\omega_m| > \text{a few times } \omega_D$ with $|\omega_n|$ in the interval from zero to several times ω_D . Therefore the major contribution to the \hat{m} -sum in (II.18) comes from the values of $|\omega_m|$ in the interval from zero to a few times ω_D . On the other hand, since $G(\varepsilon', i\omega_m) = [i\omega_m - \varepsilon' - \Sigma(\varepsilon', i\omega_m)]^{-1}$, the main contribution to the ε' -integration will come from the values of ε' in the same energy interval. This is the reason why one considers the variation in $N(\varepsilon)$ and $\alpha^2 F(\Omega; \varepsilon, \varepsilon')$ for $\varepsilon, \varepsilon'$ in the indicated energy range.

The approximation

$$\alpha^2 F(\Omega; \varepsilon, \varepsilon') = \alpha^2 F(\Omega; 0, 0) \equiv \alpha^2(\Omega) F(\Omega) \quad (\text{II.29})$$

simplifies the treatment considerably since the self-energy $\Sigma_{ep}(\varepsilon, i\omega_n)$ (or $\Sigma_{ep}(\varepsilon, \omega + i\eta)$) now depends only on frequency as can be seen from Eq. (II.18) (or (II.27)). We emphasize that such an approximation is an ad hoc assumption and a full microscopic justification, presumably on the basis of a detailed cal-

culation of the electron-phonon coupling function in a material where $N(\epsilon)$ varies rapidly near the Fermi level, is required. It should be noted that Horsch and Rietschel¹⁾, who together with Nettel and Thomas²⁾ were the first to explicitly analyze the effect of sharp structure in EDOS near the Fermi level on the superconducting critical temperature T_c , in the context of the strong-coupling theory, state that for the case of the interchain scattering model for the electron-phonon interaction in the A-15 compounds calculations show that such an approximation is justified (see also Ref. 64). Here we restrict ourselves to the case where only the energy dependence in $N(\epsilon)$ is retained. Before the complete solution to the problem of electron-phonon coupling in A-15 materials can be given, it seems appropriate to first catalogue the effects of ϵ -dependence in $N(\epsilon)$, (ϵ, ϵ') -dependence in $\alpha^2 F(\Omega; \epsilon, \epsilon')$ and anisotropy effects one at a time. This work is concerned only with the effects of rapid variation in the electronic density of states.

Assuming that (II.29) is valid Eq. (II.27) reduces to

$$\begin{aligned}
 \Sigma_{ep}(\omega + i\eta) = & \int_{-\infty}^{+\infty} d\omega' \int_{-\infty}^{+\infty} d\epsilon' \frac{N(\epsilon')}{N(0)} \left\{ -\frac{1}{\pi} \text{Im } G(\epsilon', \omega' + i\delta) \right\} \times \\
 & \times \int_0^{+\infty} d\Omega \alpha^2(\Omega) F(\Omega) \left[\frac{1}{\omega - \omega' - \Omega + i\eta} \frac{1}{e^{-\beta\omega'} + 1} + \frac{1}{\omega - \omega' + \Omega + i\eta} \frac{1}{e^{\beta\omega'} + 1} \right] + \\
 & + \int_0^{+\infty} d\Omega \frac{\alpha^2(\Omega) F(\Omega)}{e^{\beta\Omega} - 1} \int_{-\infty}^{+\infty} d\epsilon' \frac{N(\epsilon')}{N(0)} [G(\epsilon', \omega - \Omega + i\eta) + G(\epsilon', \omega + \Omega + i\eta)]
 \end{aligned}
 \tag{II.30}$$

Ordinarily it is assumed that $N(\varepsilon)$ can be taken constant in the range of several times ω_D around the Fermi level and then, since only this range contributes to the ε' -integral as discussed previously

$$\begin{aligned} \int_{-\infty}^{+\infty} d\varepsilon' \frac{N(0)}{N(0)} \left\{ -\frac{1}{\pi} \operatorname{Im} G(\varepsilon', \omega + i\delta) \right\} &= \\ &= -\frac{1}{\pi} \int_{-\infty}^{+\infty} d\varepsilon' \frac{\operatorname{Im} \Sigma(\omega + i\delta) - \delta}{[\varepsilon' - (\omega - \operatorname{Re} \Sigma(\omega + i\delta))]^2 + [\operatorname{Im} \Sigma(\omega + i\delta) - \delta]^2} = 1 \quad (\text{II.31}) \end{aligned}$$

where we have used the fact that the self-energy has a negative imaginary part in the upper-half complex plane (see Appendix 1). Also

$$\int_{-\infty}^{+\infty} d\varepsilon' \frac{N(0)}{N(0)} G(\varepsilon', \omega' + \Omega + i\delta) = -i\pi. \quad (\text{II.32})$$

Note that the results (II.31) and (II.32) do not depend on what is used for Σ in G as long as the imaginary part of Σ has the right sign, and the simplest choice is to use instead of G the noninteracting Green's function $G_0(\varepsilon, \omega + i\delta) = 1/(\omega + i\delta - \varepsilon)$. This conclusion is based on: 1) Σ does not depend on momentum (or, equivalently, ε) and 2) the electronic density of states $N(\varepsilon)$ can be assumed to be constant. As soon as one of these two conditions is not valid Eq. (II.27) or Eq. (II.30) has to be solved self-consistently for Σ .

It should be stressed that the quantity

$$\begin{aligned}
N(0)\tilde{N}(\omega') &\stackrel{\text{d}}{=} \int_{-\infty}^{+\infty} d\varepsilon' N(\varepsilon') \left\{ -\frac{1}{\pi} \text{Im} G(\varepsilon', \omega' + i\delta) \right\} = \\
&= \int \frac{d^3\vec{k}}{(2\pi)^3} A(\vec{k}, \omega') , \tag{II.33}
\end{aligned}$$

where $A(\vec{k}, \omega')$ is the electron spectral function (see Appendix I), gives the quasiparticle density of states. Strictly speaking this term is somewhat artificial since it is well known³⁸⁾ that the concept of the quasiparticle loses its meaning, in the case of a strong electron-phonon interaction even at $T=0$, for excitation energies of the order of typical phonon-frequencies (provided one defines the quasiparticle as an excitation whose level width is much smaller than the energy of the excitation). The term is reminiscent of the case when G in Eq.

(II.33) can be replaced by the noninteracting Green's function $G_0(\varepsilon', \omega' + i\delta) = [\omega' + i\delta - \varepsilon']^{-1}$ (or equivalently $A_0(\vec{k}, \omega') = \delta(\varepsilon_{\vec{k}} - \omega')$) since then Eq. (II.33) gives

$$N(0)\tilde{N}(\omega') = N(\omega') . \tag{II.34}$$

However, such an interpretation of $N(0)\tilde{N}(\omega')$ is never necessary for calculating various properties of the interacting electron-phonon system. At the same time this quantity embodies in a precise way the qualitative ideas about smearing, or better-depletion, of the peak in the electronic density of states due to the electron-phonon interaction at $T > 0$ (or due to the impurity scattering), which were mentioned in Ch. 1 and were based on the uncertainty principle. To see this, let us assume that the

EDOS has the form of a Lorentzian superimposed on the constant background at least for the values of $|\epsilon|$ which are within several times ω_D around the Fermi level $\epsilon = 0$

$$N(\epsilon) = N_b \left(1 + \frac{s}{\pi} \frac{a}{a^2 + \epsilon^2} \right) . \quad (\text{II.35})$$

As discussed before, the quantity $N(0)\tilde{N}(\omega)$ defined by Eq. (II.33) appears in the self-energy equation (II.30) and in the context of that equation the main contribution to the integral over ϵ' in Eq. (II.33) is coming from the interval of several Debye energies around $\epsilon = 0$. Therefore it is legitimate to assume that $N(\epsilon)$ is given by (II.35) for all values of ϵ , since it simplifies the evaluation of the integral. With this choice for $N(\epsilon)$ we have (see Appendix II)

$$N(0)\tilde{N}(\omega) = N_b \left[1 + \frac{s}{\pi} \frac{a + |\text{Im}\Sigma(\omega + i\delta)|}{(\omega - \text{Re}\Sigma(\omega + i\delta))^2 + (a + |\text{Im}\Sigma(\omega + i\delta)|)^2} \right] \quad (\text{II.36})$$

which has the form of a broadened EDOS given by Eq. (II.35).

At finite $T > 0$ $\text{Im}\Sigma(\omega + i\delta)$ is finite everywhere and the function $N(0)\tilde{N}(\omega)$ has a lower maximum than the original electronic density of states. This is the precise statement of the qualitative idea relating to smearing of the peak in EDOS. Another important point is that what appears in 'Lorentzian form', Eq. (II.36), is the renormalized energy $\omega - \text{Re}\Sigma(\omega + i\delta)$, instead of just the energy ω . In Sec. II.2 the results of numerical calculations will be presented and the effect of this renormalization will be

clarified. From Eq. (II.36) it is evident that for $\alpha \lesssim \omega_D$ and $s/(\pi a)$ of the order of 1 it is important to solve Eq. (II.30) self-consistently.

The completely self-consistent solution of the electron-phonon problem should include the subsystem of phonons as well (see Eqs. (II.15) and (II.11)). It was pointed out by Knapp et al.⁶⁵⁾ that the sharp structure in the d-band density of states near the Fermi level causes a strong temperature dependence of the bare phonon frequencies renormalization which results in phonon softening as the temperature is decreased. However such a completely self-consistent solution of the self-energy equations is an extremely difficult problem and the shortcut solution would be to use at each temperature phonon frequencies, that is $\alpha^2(\Omega)F(\Omega)$, determined from experiments at that temperature and solve self-consistently only the electron self-energy equation, Eq. (II.30). We will restrict ourselves to the low temperature regime, that is we will consider the temperatures which are at most 30% of ω_D and assume that in this temperature range $\alpha^2(\Omega)F(\Omega)$ can be taken as temperature independent. Schweiss et al.⁶⁶⁾ have performed inelastic neutron scattering experiments on several A-15 compounds and Chevrel phase materials. They have measured a generalized phonon density of states $G(\Omega)$, a quantity closely related to ordinary phonon density of states $F(\Omega)$, and found, for high T_c materials, a considerable shift in weight under $G(\Omega)$ towards the lower

frequencies upon cooling from room temperature to the liquid helium temperature. Since in our calculations the temperature will not exceed 80°K it is hoped, upon comparing the amount of softening in V_3Si between 297°K and 77°K and in Nb_3Sn between 297°K and 5.6°K (see Ref. 66), that our approximation of a temperature independent $\alpha^2(\Omega)F(\Omega)$ is not a bad one.

We will conclude this section by simplifying the impurity contribution to the electron-self energy, Eq. (II.28). We consider elastic impurity scattering and will assume that $1/\tau_{iN}(\epsilon, \epsilon')$ defined by Eq. (II.21) can be set equal to a constant $1/\tau_{iN}$, thus assuming that the potential V_N is short ranged. Eq. (II.28) then reads

$$\Sigma_{iN}(\epsilon, \omega + i\eta) = \frac{1}{2\pi\tau_{iN}} \int_{-\infty}^{+\infty} d\epsilon' \frac{N(\epsilon')}{N(0)} G(\epsilon', \omega + i\eta) . \quad (II.37)$$

Equation (II.37), or the one which is obtained when the electron phonon contribution and the impurity contribution are summed to give the total electron self-energy, has to be solved self-consistently. We note that our treatment of impurity scattering is quite similar to the one of Williamson et al.⁶⁷⁾ (see also Ref. 68).

II.2 EFFECTS OF THE INTERPLAY BETWEEN A SHARP STRUCTURE IN THE ELECTRONIC DENSITY OF STATES NEAR THE FERMİ LEVEL, THE ELECTRON-PHONON INTERACTION AND ORDINARY IMPURITY SCATTERING, ON THE ELECTRON QUASIPARTICLE PROPERTIES IN THE NORMAL STATE AT $T = 0$

In this section we will present numerical solutions of the self-energy equations (II.30), (II.37) and (II.1) for several model electronic densities of states (EDOS). In this way we will illustrate the possible effects of the interplay between sharp peaks in the EDOS, the electron-phonon interaction and/or ordinary impurity scattering.

At zero temperature Eq. (II.30) reduces to

$$\begin{aligned} \Sigma_{ep}(\omega+i\eta) = & \int_{-\infty}^{+\infty} d\omega' \int_{-\infty}^{+\infty} d\varepsilon' \frac{N(\varepsilon')}{N(0)} \left\{ -\frac{1}{\pi} \text{Im}G(\varepsilon', \omega'+i\delta) \right\} \times \\ & \times \int_0^{+\infty} d\Omega \alpha^2(\Omega) F(\Omega) \left[\frac{1}{\omega-\omega'-\Omega+i\eta} \theta(\omega') + \frac{1}{\omega-\omega'+\Omega+i\eta} \theta(-\omega') \right] \quad (\text{II.38}) \end{aligned}$$

In the constant density of states approximation Eq. (II.38) takes the form (see Eq. II.31)

$$\Sigma_{ep}(\omega+i\eta) = \int_{-\infty}^{+\infty} d\omega' \int_0^{+\infty} d\Omega \alpha^2(\Omega) F(\Omega) \left[\frac{1}{\omega-\omega'-\Omega+i\eta} \theta(\omega') + \frac{1}{\omega-\omega'+\Omega+i\eta} \theta(-\omega') \right]$$

or

$$\Sigma_{ep}(\omega+i\eta) = \int_0^{+\infty} d\omega' \int_0^{+\infty} d\Omega \alpha^2(\Omega) F(\Omega) \left[\frac{1}{\omega-\omega'-\Omega+i\eta} + \frac{1}{\omega+\omega'+\Omega+i\eta} \right] \quad (\text{II.39})$$

from which it can be easily seen that $\text{Re } \Sigma_{ep}(\omega+i\eta)$ is an odd

function of ω , while $\text{Im } \Sigma_{ep}(\omega+i\eta)$ is an even function. The quantity $\text{Re } \Sigma_{ep}(0+i\eta)$ gives the shift of the chemical potential due to the electron-phonon interaction^{38,69}). Thus in the constant EDOS approximation (and assuming that the self-energy is not momentum dependent) $\text{Re } \Sigma_{ep}(0+i\eta) = 0$, i.e. the electron-phonon interaction does not shift the chemical potential (to an accuracy of $(m/M)^{1/2}$, where m is the electron mass and M is the ion mass). This can be easily understood on the basis of usual second order perturbation theory arguments for the calculation of the energy shift due to the electron phonon interaction⁴³. This argument will also help to understand that, in the case when the electronic density of states $N(E)$ does not possess particle-hole symmetry around the band structure chemical potential at $E=0$ (i.e. when $N(E) \neq N(-E)$ close to $E=0$ on the scale of several Debye energies), one can expect a shift of the chemical potential due to the electron-phonon interaction. There are two effects contributing to the energy of the interacting electron-phonon system at $T=0$ when an extra particle is added to the system in momentum state \vec{p} , with $|\vec{p}| > p_F$ (p_F is the Fermi momentum). First, the added particle can virtually emit a phonon of energy $\Omega_{\vec{p}-\vec{p}',\lambda}$, go over to the state \vec{p}' , with $|\vec{p}'| > p_F$ (due to the Pauli principle) and then reabsorb this phonon returning to the original state \vec{p} (see Fig. II.5a). The contribution ΔE_1 of this type of process to the energy of the system will, among other things

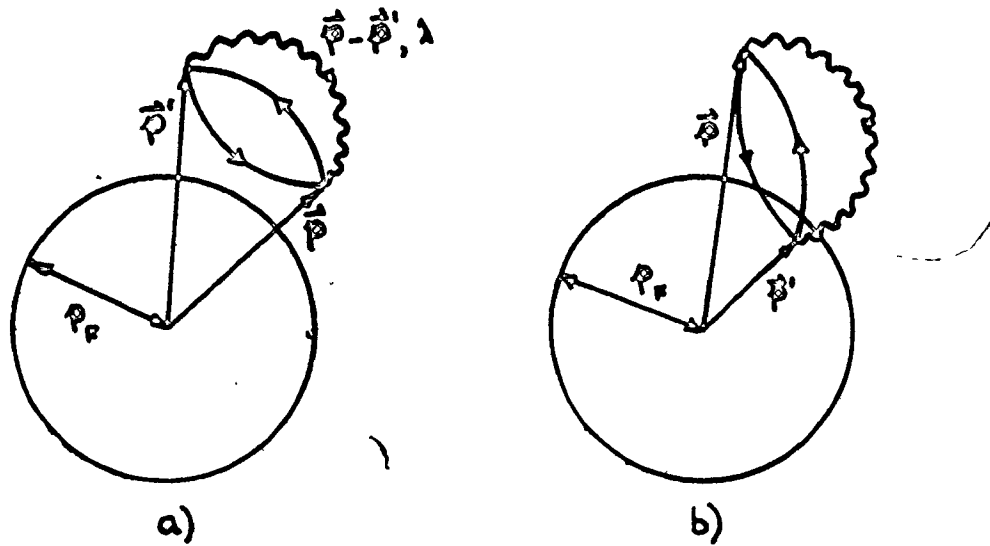


Fig. II.5

depend on the density of intermediate states \vec{p}' , $|\vec{p}'| > p_F$, available to the added electron at \vec{p} . Furthermore, in the absence of the added electron, there are virtual fluctuations of the system due to the electron-phonon interaction contributing to the ground state energy, in which an electron in the state \vec{p}' within the Fermi sea, $|\vec{p}'| < p_F$, virtually emits a phonon of energy $\Omega_{\vec{p}-\vec{p}', \lambda}$ (or equivalently absorbs a phonon $\Omega_{\vec{p}', -\vec{p}, \lambda}$) going over to the intermediate state \vec{p} , with $|\vec{p}| > p_F$ (due to the Pauli principle) and then returns to the original state by reabsorbing this phonon. Now, when the particle is added to the system in the momentum state \vec{p} with $|\vec{p}| > p_F$, these fluctuations of the system in which particles in momentum states \vec{p}' with $|\vec{p}'| < p_F$ go over to the state \vec{p} and then return back

to the original state by virtually emitting and reabsorbing a phonon, are blocked by the Pauli principle and the corresponding contribution ΔE_2 to the ground state energy has to be subtracted. For the given state \vec{p} , $|\vec{p}| > p_F$, the later contribution will depend on the density of states \vec{p}' with $|\vec{p}'| < p_F$. Now letting $|\vec{p}| \rightarrow p_F$, in order to find the shift of the chemical potential due to the electron phonon interaction, we see that if the electronic density of states is constant or symmetric around $E=0$ we can expect a zero shift of the chemical potential, while if $N(E)$ is not symmetric around $E=0$ there will be a finite shift of the chemical potential, since ΔE_1 and ΔE_2 do not cancel each other.

Moreover, if the electronic density of states is not symmetric around $E=0$ on the scale of a few Debye energies there is no reason to expect that $\text{Im } \Sigma_{ep}(\omega+i\eta)$ will be an even function of ω or that $\text{Re } \Sigma_{ep}(\omega+i\eta)$ will be an odd function of ω , as in the case of a constant electronic density of states.

We have solved Eq. (II.38) by taking the following form of the band electronic density of states

$$N(E) = \begin{cases} B, & \text{for } E \leq E_1 = -100 \text{ meV} \\ B + \frac{P-B}{E_2-E_1} (E-E_1), & \text{for } E_1 < E \leq E_2 = -10 \text{ meV} \\ B + \frac{B-P}{E_3-E_2} (E-E_2), & \text{for } E_2 < E \leq E_3 = 25 \text{ meV} \\ B, & \text{for } E > E_3 \end{cases} \quad (\text{II.40})$$

with $B/N(E=0) = 0.44$ and $P/N(E=0) = 1.22$ which has the form of a triangle superimposed on a constant background of height B . It should be noted that the 'bare' band structure chemical potential ($T=0^\circ\text{K}$) is located at $E=0$. This choice of $N(E)$ was made to reduce the numerical work when solving Eq. (II.38) and to approximate the detailed band structure EDOS for Nb_3Sn as calculated by Klein et al. 14) (see also Ref. 7, where the effects of lifetime broadening due to static disorder have been approximately taken into account for the band EDOS of Ref. 14). The electronic band density of states appears in Eq. (II.38) in the form $N(\epsilon')$ where ϵ' is measured with respect to the true interacting chemical potential. The two energies are related by

$$E(\epsilon') = \epsilon' + \text{Re } \Sigma_{\text{ep}}(0 + i\eta) \quad (\text{II.41})$$

or equivalently

$$N(\epsilon') = \begin{cases} B, & \text{for } \epsilon' \leq \epsilon_1 \equiv E_1 - \text{Re } \Sigma_{ep}(0+i\eta) \\ B + \frac{P-B}{\epsilon_2 - \epsilon_1} (\epsilon' - \epsilon_1) & \text{for } \epsilon_1 < \epsilon' \leq \epsilon_2 \equiv E_2 - \text{Re } \Sigma_{ep}(0+i\eta) \\ B + \frac{B-P}{\epsilon_3 - \epsilon_1} (\epsilon' - \epsilon_3) & \text{for } \epsilon_2 < \epsilon' \leq \epsilon_3 \equiv E_3 - \text{Re } \Sigma_{ep}(0+i\eta) \\ B, & \text{for } \epsilon' > \epsilon_3 \end{cases} \quad (\text{II.42})$$

At every stage of iteration of Eq. (II.38) the band density of states $N(\epsilon')$ was redefined according to Eq. (II.42) on the basis of $\text{Re } \Sigma_{ep}(0+i\eta)$ obtained as a result of the previous iteration. The iterations were started with the noninteracting guess $\Sigma(\omega+i\eta) = 0$. Instead of redefining $N(\epsilon')$ at every stage of iteration, the equivalent procedure would be to subtract from the solution $\text{Re } \Sigma(\omega+i\eta)$ the number $\text{Re } \Sigma(0+i\eta)$, as is evident from the structure of Eq. (II.33). However, since the number of frequencies ω at which $\Sigma(\omega+i\eta)$ was calculated was much larger (typically 1081 nonuniformly spaced frequencies) than the number of intervals at which $N(E)$ varies linearly (only 4 for $N(E)$ given by Eq. (II.39)) the first procedure was more economical from the computational point of view. The integral over ϵ' can be carried out analytically for any piecewise linear function and we give the results of such an integration for EDOS given by Eq. (II.42) in Appendix II. It should be noted that since at $T=0$ the imaginary part of the electron-phonon self-energy vanishes at $\omega=0$ (position of the interacting chemical potential) we have, with an arbitrary $N(\epsilon)$

$$\begin{aligned}
N(0)\tilde{N}(0) &= -\frac{1}{\pi} \operatorname{Im} \int_{-\infty}^{+\infty} d\varepsilon N(\varepsilon) \frac{1}{-\varepsilon - \operatorname{Re} \Sigma(0+i\delta) + i\delta} = \\
&= N(\varepsilon = -\operatorname{Re} \Sigma(0+i\delta))
\end{aligned} \tag{II.43}$$

which is exactly the value of the band structure electronic density of states at the band structure chemical potential $E=0$ (see Eq. (II.41)). Thus, at $T=0^\circ\text{K}$ the value of the electronic density of states is 'pinned' to the chemical potential (at $T=0$ and very close to $\omega=0$ one can talk about quasiparticles even in the case of a strong electron-phonon interaction).

As the input $\alpha^2(\Omega)F(\Omega)$ -spectrum we have taken Shen's result for Nb_3Sn obtained from the tunneling experiments⁹¹⁾ with

$$\lambda \equiv 2 \int_0^{+\infty} d\Omega \alpha^2(\Omega) F(\Omega) / \Omega = 1.7 \tag{II.44}$$

and a maximum phonon frequency $\omega_{\max} = 28.9 \text{ meV}$ ($\hbar = 1$). The $\Sigma_{\text{ep}}(\omega+i\eta)$ solution of Eq. (II.38) was obtained in the interval $|\omega| \leq \omega_c = 150 \text{ meV}$. The ω' integration in (II.38) was carried from $-\infty$ to $+\infty$ by assuming that

$$\tilde{N}(\omega') = -\frac{1}{\pi} \operatorname{Im} \int_{-\infty}^{+\infty} d\varepsilon (N(\varepsilon)/N(0)) G(\varepsilon, \omega' + i\eta)$$

is constant for $|\omega'| > \omega_c$. Connected to this latter point we note that if one wants to solve Eq. (II.38) with the actual band structure calculation result for $N(E)$, like the one in Ref. (14), it is useful to assume that $N(-E) = N(E) = \text{const.}$ for $|E| > \omega_c$ in order to be able to carry the integration over ω' in Eq. (II.38) from $-\infty$ to $+\infty$. This is essential in order not to underestimate the renormalization effects by cutting off the ω' -integration in Eq. (II.38) at $\pm \omega_c^{47}$. For $|\omega| \leq \omega_c$ where ω_c is of the order of $5 \omega_{\text{max}}$ to $10 \omega_{\text{max}}$, Eq. (II.38) can be rewritten as (assuming $\tilde{N}(\omega') = \tilde{N}(\omega_c)$ for $|\omega'| > \omega_c$)

$$\begin{aligned} \Sigma_{\text{ep}}(\omega+i\eta) = & \int_{-\omega_c}^{+\omega_c} d\omega' \tilde{N}(\omega') \int_0^{\omega_{\text{max}}} d\Omega \alpha^2(\Omega) F(\Omega) \times \\ & \times \left[\frac{1}{\omega - \omega' - \Omega + i\eta} \theta(\omega') + \frac{1}{\omega - \omega' + \Omega + i\eta} \theta(-\omega') \right] + \\ & + \tilde{N}(\omega_c) \int_{\omega_c}^{+\infty} d\omega' \left\{ \left[P \int_0^{\omega_{\text{max}}} d\Omega \alpha^2(\Omega) F(\Omega) \frac{1}{\Omega + \omega' + \omega} - \right. \right. \\ & - P \int_0^{\omega_{\text{max}}} d\Omega \alpha^2(\Omega) F(\Omega) P \frac{1}{\Omega + (\omega' - \omega)} \left. \right] - i\pi [\alpha^2 F(-(\omega' - \omega)) + \\ & + \alpha^2 F(-(\omega' + \omega))] \} . \end{aligned}$$

Since $\alpha^2(\Omega)F(\Omega)$ is zero outside the interval $[0, \omega_{\text{max}}]$ one has $\alpha^2 F(-(\omega' - \omega)) = \alpha^2 F(-(\omega' + \omega)) = 0$ for $\omega' > \omega_c > |\omega|$, so that the second term in the above formula can be written in the form

$$\tilde{N}(\omega_c) \int_0^{\omega_{\max}} d\Omega \alpha^2(\Omega) F(\Omega) \ln \frac{\Omega + \omega_c - \omega}{\Omega + \omega_c + \omega}.$$

In Fig. (II.6) we present the real part of the solution of Eq. (II.38) (solid line) for the electronic density of states $N(E)$ given by Eq. (II.40). For comparison we present in the same figure the corresponding solution for the case of a constant electronic density of states equal to the value of $N(E)$ given by Eq. (II.40) at $E=0$. We will refer to these two cases as Case 1) and Case 2), respectively. In both of these cases the same $\alpha^2(\Omega)F(\Omega)$ spectrum was used. From Fig. (II.6) it can be seen that $\text{Re } \Sigma_{\text{ep}}(\omega+i\eta)$ in Case 1) is not an anti-symmetric function of ω . This is a consequence of the asymmetry of the band EDOS given by Eq. (II.40). As was anticipated in the previous qualitative description of the processes contributing to the excitation energy of the interacting electron-phonon system, this asymmetry of the band EDOS results in the finite shift of the chemical potential. For the model EDOS $N(E)$, Eq. (II.40), this shift is $\text{Re } \Sigma_{\text{ep}}(0+i\eta) = 6.43$ meV which is about 20% of ω_{\max} .

In Fig. (II.7) we plot the $-\text{Im } \Sigma_{\text{ep}}(\omega+i\eta)$ for Case 1) (solid line) and Case 2) (dotted line). Again $\text{Im } \Sigma_{\text{ep}}(\omega+i\eta)$ in the case of a nonconstant electronic density of states, is not an even function of ω , thus reflecting the asymmetry of the underlying band EDOS. It is worthwhile to define, in particular for the treatment of the superconducting state, the

Fig.II.6

The real part of the electron-phonon self-energy.

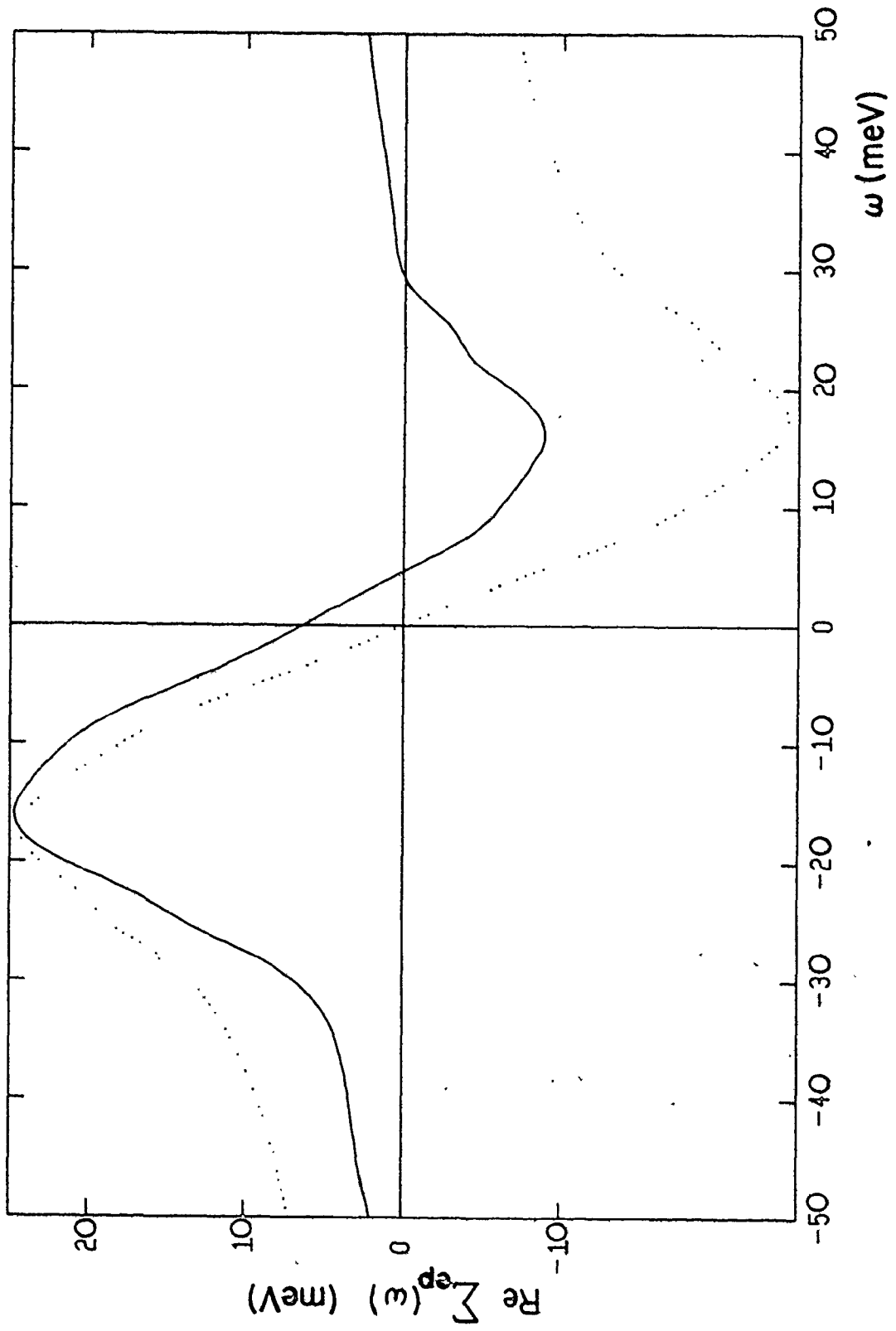
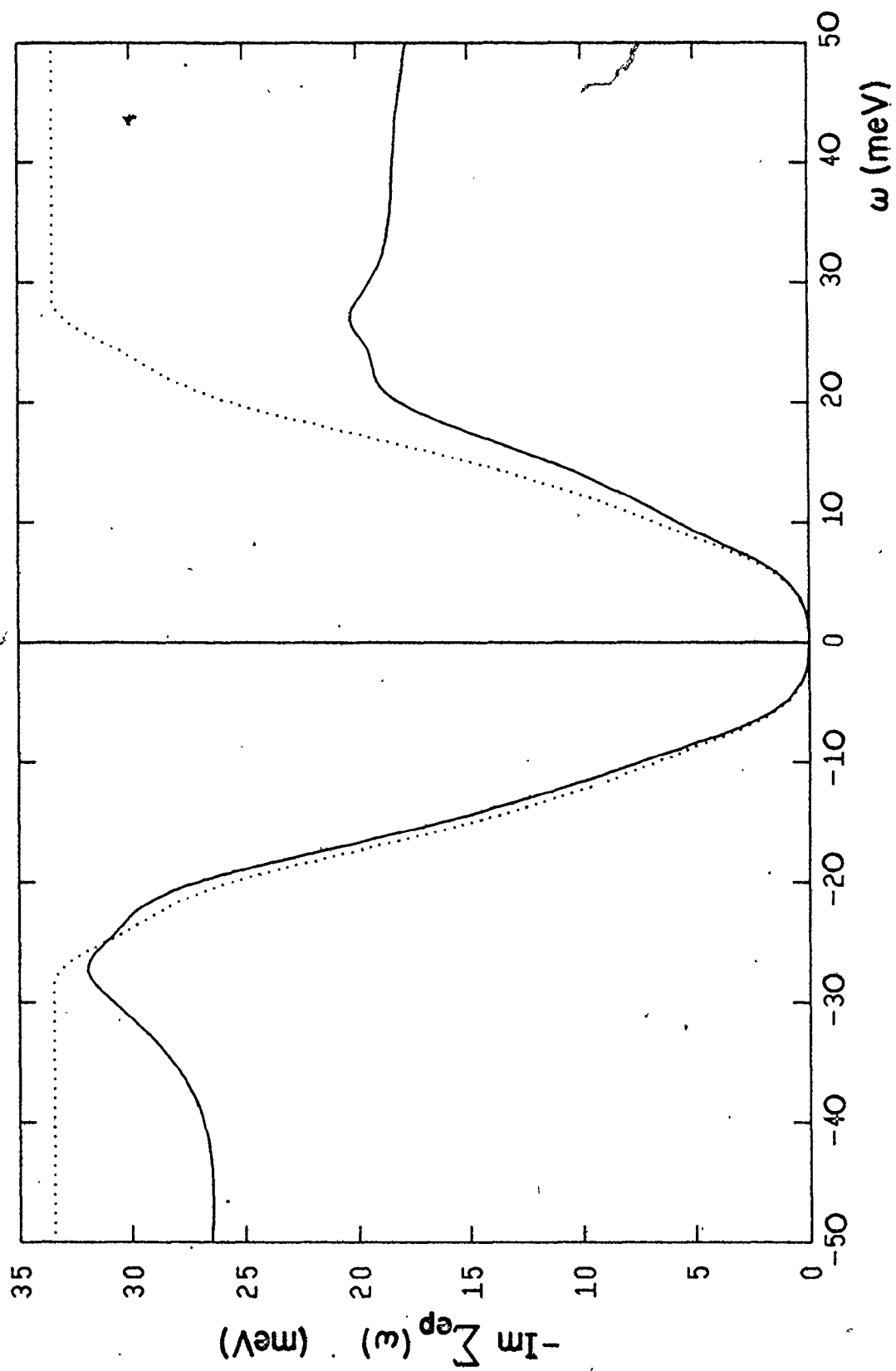


Fig.II.7

The imaginary part of the electron-phonon self-energy.



even and odd part of $\Sigma(i\omega_n)$ in Matsubara frequencies $i\omega_n$ (see Sec. II.1) by

$$\chi(i\omega_n) \equiv \frac{1}{2}[\Sigma(i\omega_n) + \Sigma(-i\omega_n)] \quad (\text{II.45a})$$

$$i\omega_n(1-Z(i\omega_n)) \equiv \frac{1}{2}[\Sigma(i\omega_n) - \Sigma(-i\omega_n)] \quad (\text{II.45b})$$

In order to find the analytic continuation $\chi(\omega+i\eta)$, where η is positive infinitesimal by letting $i\omega_n \rightarrow \omega+i\eta$ in the upper half complex plane, it should be remembered that

$$\Sigma(i\omega_n) = \Sigma_R(i\omega_n) \quad , \quad \omega_n > 0 \quad (\text{II.46a})$$

$$\Sigma(i\omega_n) = \Sigma_A(i\omega_n) \quad , \quad \omega_n < 0 \quad (\text{II.46b})$$

with $\Sigma_R(i\omega_n)$ and $\Sigma_A(i\omega_n)$ analytic in the upper and lower half complex plane respectively (see Appendix I). Thus

$$\chi(\omega+i\eta) = \frac{1}{2}[\Sigma_R(\omega+i\eta) + \Sigma_A(-\omega-i\eta)] \quad (\text{II.47a})$$

$$\omega(1-Z(\omega+i\eta)) = \frac{1}{2}[\Sigma_R(\omega+i\eta) - \Sigma_A(-\omega-i\eta)] \quad , \quad (\text{II.47b})$$

or after using the relation (see Appendix I)

$$\Sigma_A(\omega-i\eta) = \Sigma_R^*(\omega+i\eta) \quad , \quad (\text{II.48})$$

$$\chi(\omega+i\eta) = \frac{1}{2} [\Sigma(\omega+i\eta) + \Sigma^*(-\omega+i\eta)] \quad (\text{II.49a})$$

$$\omega(1-Z(\omega+i\eta)) = \frac{1}{2} [\Sigma(\omega+i\eta) - \Sigma^*(-\omega+i\eta)] \quad . \quad (\text{II.49b})$$

The function $Z(\omega+i\eta)$ is known as the renormalization function. In Figs. (II.8) and (II.9) we present the real and imaginary part of Z , respectively, for Case 1 (solid lines) and Case 2) (dotted lines). The reduction in the renormalization, i.e. in $\text{Re } Z$, for the case of the peak in the EDOS is the obvious consequence of the overall reduction in weight under $N(E)$ given by (Eq. II.40) in the interval of several ω_{max} around $E = 0$, as compared to the constant EDOS equal to $N(E = 0)$. The imaginary part of Z , Fig. (II.9) contains more information about the local variation in ω of the symmetrized EDOS, or more precisely $\frac{1}{2}(\tilde{N}(\omega') + \tilde{N}(-\omega'))$, which will be discussed in more detail below. In Fig. II.10 we give the real (solid line) and the imaginary part (dotted line) of χ calculated for the peaked EDOS (χ vanishes for the case of a constant electronic density of states as is obvious from the definition, Eq. (II.45a)).

In Fig. II.11 we plot the quasiparticle density of states $N(0)\tilde{N}(\omega) = - (1/\pi) \text{Im} \int_{-\infty}^{+\infty} d\varepsilon N(\varepsilon) G(\varepsilon, \omega+i\delta)$ divided by the value of the band structure EDOS at the band structure chemical potential, $N(E=0)$ (solid line) and the band EDOS $N(\omega)$ normalized to $N(E=0)$ (dotted line). The position of the true interacting chemical potential is at $\omega = 0$ and the circle denotes the position of the bare band chemical potential at $T = 0$. We note that several iterations of Eq. (II.38) are required before the condition (II.43) was satisfied to suffi-

Fig.II.8

The real part of the normal state renormalization function.

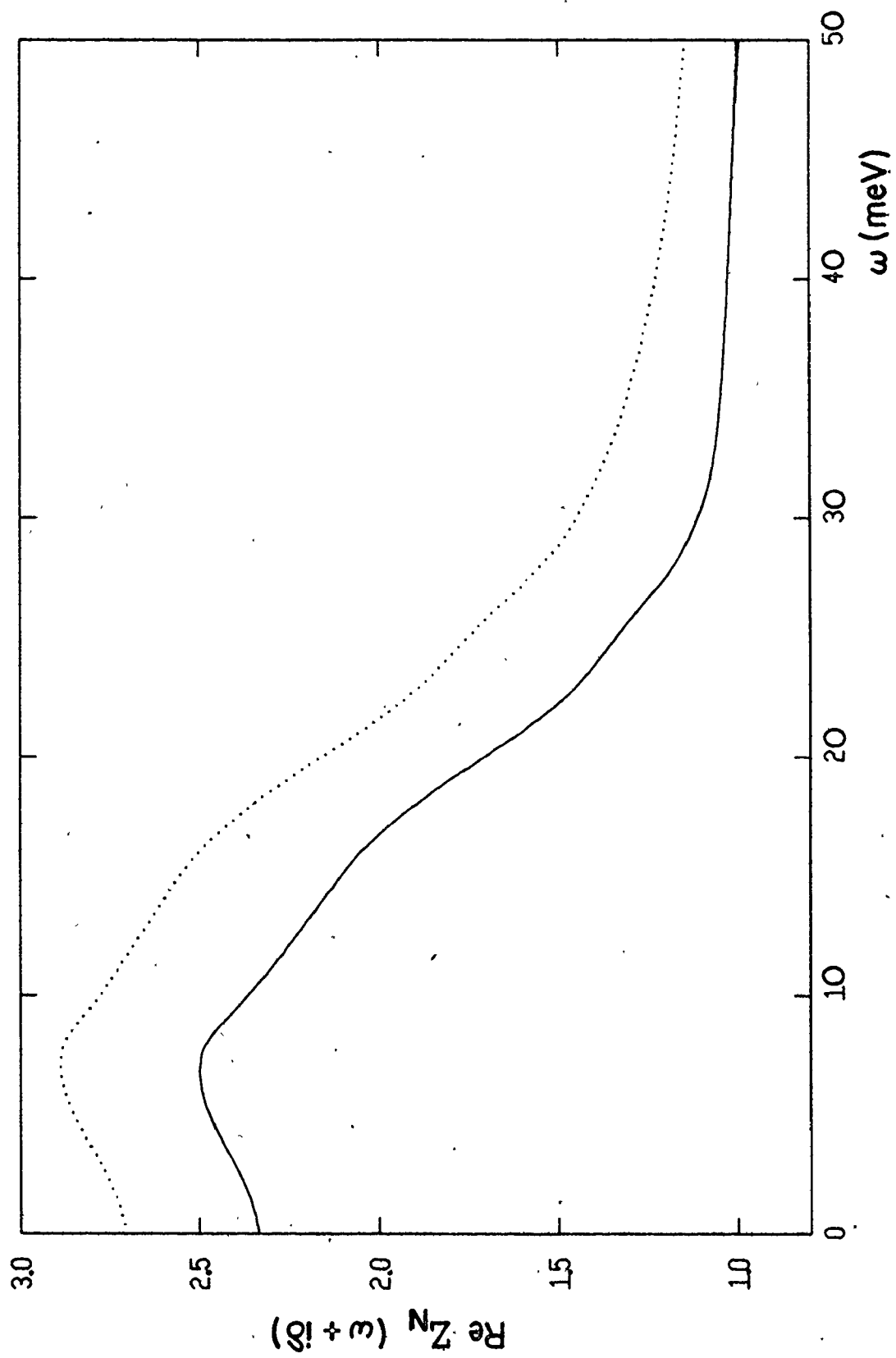


Fig.II.9

Imaginary part of the normal state renormalization function.

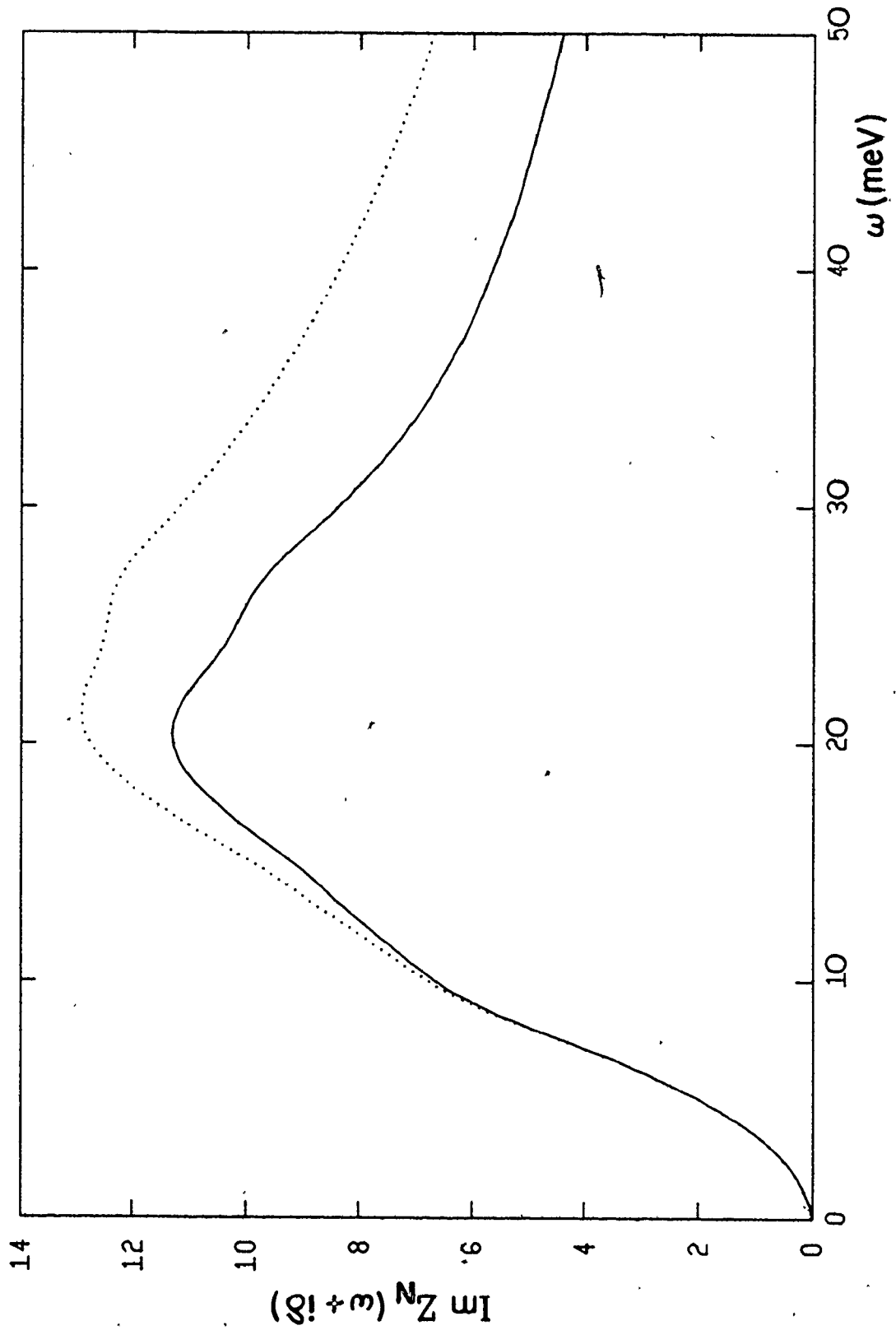


Fig.II.10

Real and imaginary parts of the self-energy component which describes the shift of the chemical potential.

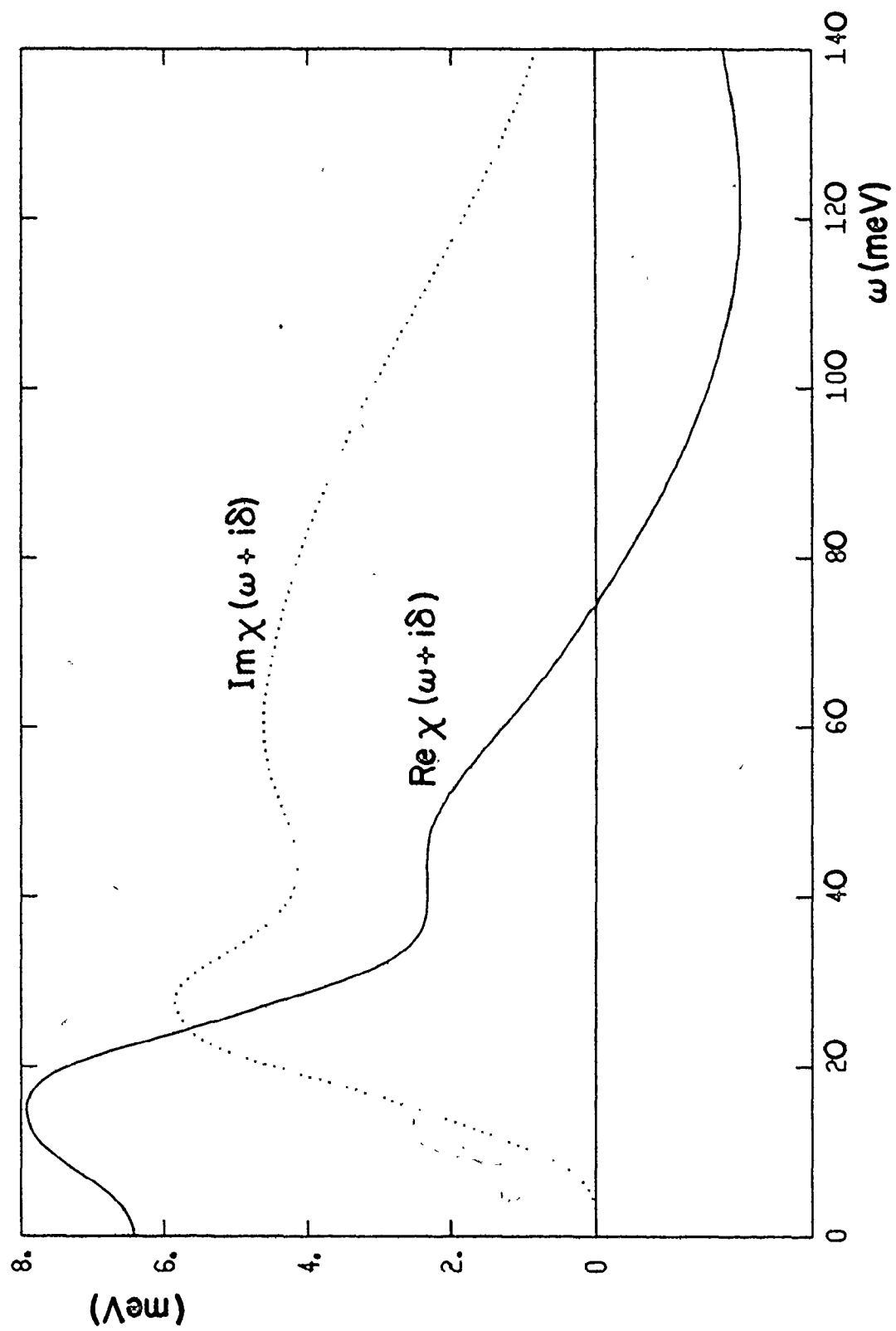
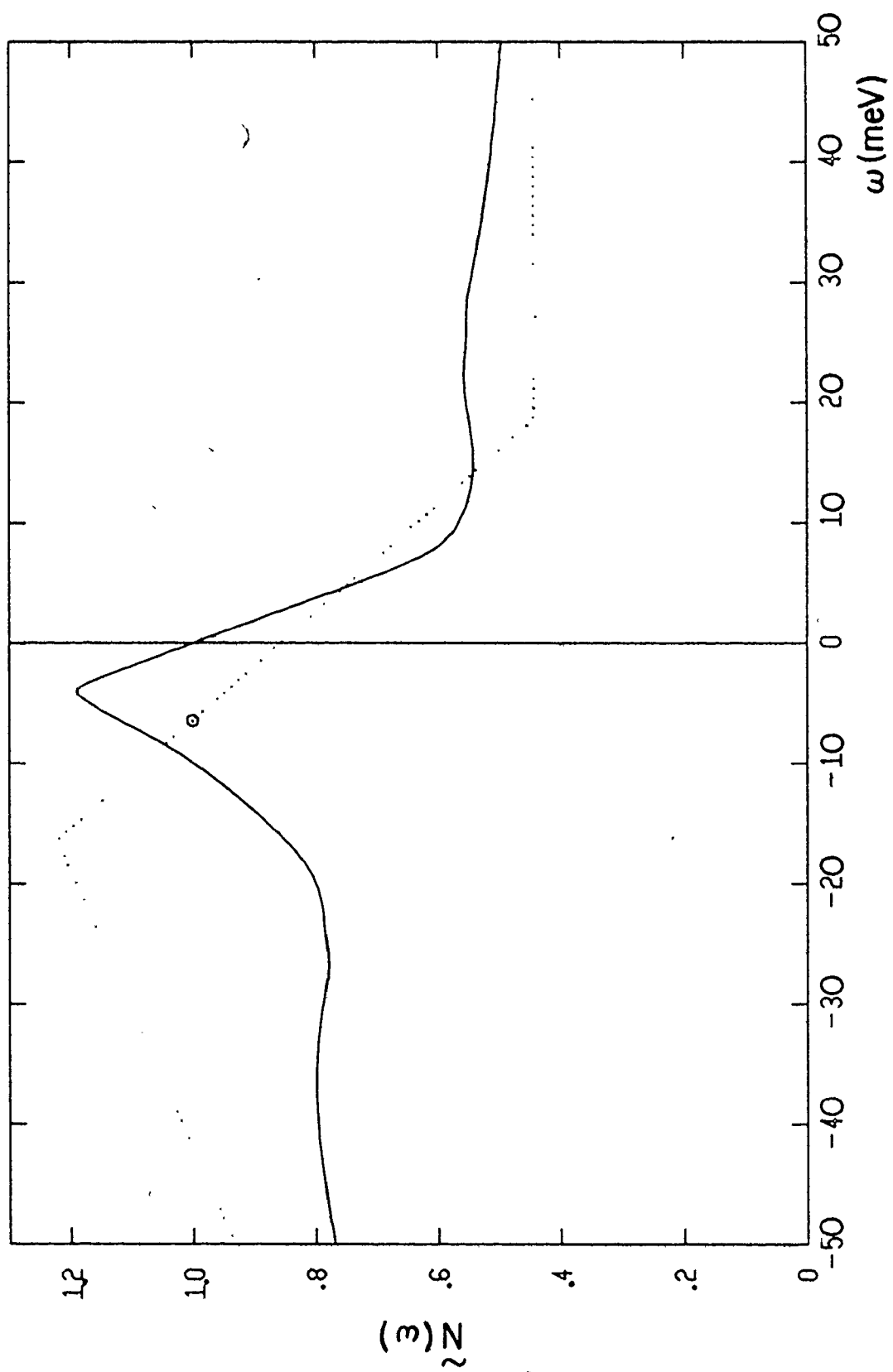


Fig.II.11

The quasiparticle density of states normalized to $N(0)$ (—) and the band electronic density of states normalized to $N(0)$ (.....).



cient numerical accuracy. (It took 16 iterations of Eq. (II.38) to converge the solution $\Sigma(\omega+i\delta)$ at each of 1081 frequencies between -150 meV and +150 meV to the 12 decimal places on the McMaster's CDC Cyber 170 machine.)

The effective narrowing of the peak in the quasiparticle density of states as compared to the bare band EDOS results from the energy renormalization due to the electron-phonon interaction. To see this we consider the energy range $\omega \ll \omega_D$ at $T=0^\circ\text{K}$ where the imaginary part of the self-energy is very small. Then

$$\begin{aligned}
 N(0)\tilde{N}(\omega) &= -\frac{1}{\pi} \text{Im} \int_{-\infty}^{+\infty} d\epsilon N(\epsilon) G(\epsilon, \omega+i\delta) = \\
 &= \int_{-\infty}^{+\infty} d\epsilon N(\epsilon) \frac{1}{\pi} \frac{|\text{Im}\Sigma(\omega+i\delta)|}{[\epsilon - (\omega - \text{Re}\Sigma(\omega+i\delta))]^2 + |\text{Im}\Sigma(\omega+i\delta)|^2} \\
 &\approx N(\epsilon = (\omega - \text{Re}\Sigma(\omega+i\delta))) = N(\epsilon = (\omega \text{Re}Z_n(\omega+i\delta) - \text{Re}\chi(\omega+i\delta))) \\
 &= N(E = \omega \text{Re}Z_n(\omega+i\delta)) \\
 &= N(E = \omega(1+\lambda_{\text{eff}})) \tag{II.50}
 \end{aligned}$$

where λ_{eff} is defined by

$$\lambda_{\text{eff}} \equiv Z_N(0+i\delta) - 1 \tag{II.51}$$

(to be distinguished in the case of a nonconstant EDOS from the 'spectral' λ defined by Eq. (II.44) Thus the value of the quasiparticle density of states at the energy $\omega (\ll \omega_D)$

with respect to the true interacting chemical potential is the same as the value of the bare band EDOS at the energy $E = \omega(1+\lambda_{\text{eff}})$ with respect to the band chemical potential. If the band EDOS varies linearly near $E = 0$, $N(E) = aE+b$ (as in the case of our choice, Eq. (II.40)) then the quasiparticle density of states varies as $N(0)\tilde{N}(\omega) = a(1+\lambda_{\text{eff}})\omega+b$ near $\omega = 0$, that is, the effective slope $a_{\text{eff}} = a(1+\lambda_{\text{eff}})$ is increased by a factor $(1+\lambda_{\text{eff}})$. For λ_{eff} in the range from 1 to 2 this gives a factor of 2 to 3. If the electronic density of states was assumed to be a constant in the range from $-\omega_D$ to $+\omega_D$ this effect would go away and one would obtain the well known result⁵³⁾ that the electron-phonon interaction does not affect the quasiparticle density of states in the normal state.

It should be noted that the above described narrowing of the quasiparticle density of states due to the electron-phonon interaction is one of the reasons for solving Eq. (II.30) self-consistently, since the amount of narrowing depends on $\text{Re } \Sigma(\omega+i\delta)$, which is in turn determined by $\tilde{N}(\omega')$. Upon examination, the slope of the normalized quasiparticle density of states $\tilde{N}(\omega)$, given by the solid line in Fig. II.11, around $\omega = 0$ we find $(d\tilde{N}(\omega)/d\omega)_{\omega=0} = -0.0519 \text{ meV}^{-1}$ which is to be compared $((dN(E)/dE)_{E=0}/N(0)) \times Z(0+i\delta) = -0.77 \text{ meV}^{-1} \times 2.33435 = -0.0519 \text{ meV}^{-1}$ thus confirming our previous analysis. The reduction in the effective renormalization parameter $\lambda_{\text{eff}} = 1.33435$ (see Eq. (II.51)) compared to the spectral $\lambda = 1.7$ (see Eq. (II.44)) is 21.5%.

By using a contour integration analogous to the one in Sec. II.1 it can be shown (see also ref. 70) that the equation for the chemical potential μ in terms of the average number of particles (per unit volume, since in this work we set $V=1$), Eq. (II.7), can be written in the form

$$\begin{aligned} N &= 2 \int_{-\infty}^{+\infty} d\omega \frac{1}{e^{\beta\omega} + 1} \left\{ -\frac{1}{\pi} \operatorname{Im} \int_{-\infty}^{+\infty} d\varepsilon N(\varepsilon) G(\varepsilon, \omega + i\delta) \right\} \\ &= 2 \int_{-\infty}^{+\infty} d\omega \frac{1}{e^{\beta\omega} + 1} N(0) \tilde{N}(\omega) \end{aligned} \quad (\text{II.52})$$

where

$$N(\varepsilon) = \begin{cases} 0, & \text{for } \varepsilon \leq -\mu \\ \neq 0, & \text{for } \varepsilon > -\mu \end{cases} \quad (\text{II.53})$$

is the band single spin EDOS measured with respect to the true interaction chemical potential. This equation (II.52), replaces the commonly used equation

$$N = 2 \int_{-\infty}^{+\infty} d\varepsilon \frac{1}{e^{\beta\varepsilon} + 1} N(\varepsilon) \quad (\text{II.54})$$

which is appropriate only in the absence of interactions (other than those explicitly included in calculating the band structure). Hence, the above described sharpening of the structure in $N(0)\tilde{N}(\omega)$ as compared to $N(\omega)$ in the range from $\sim -\omega_D$ to $\sim +\omega_D$ (due to the electron-phonon interaction which, as it will be seen below, persists even at finite T) may be related to the fact that the models for the bare band EDOS used to fit

the (anomalous) temperature dependence of the various normal state properties of A-15 materials are often pathologically sharp (see Ch. I).

In Fig. (II.12) we present the frequency dependent re-normalization parameter

$$\lambda(\omega, T=0) \equiv - \frac{\partial}{\partial \omega} \text{Re } \Sigma_{\text{ep}}(\omega, T=0) \quad (\text{II.55})$$

obtained by numerical differentiation, for the case of a non-constant EDOS given by Eq. (II.40).

In Fig. (II.13) we give the corresponding derivative of the $|\text{Im } \Sigma_{\text{ep}}(\omega, T=0)| \equiv \Gamma(\omega, T=0)$. The quantity $\Gamma(\omega, T)$ is equal to $1/(2\tau(\omega, T))$ where $\tau(\omega, T)$ is the (unrenormalized) lifetime of the 'quasiparticle'. In the constant EDOS approximation and at $T=0$, Eq. (II.39), one has

$$\Gamma(\omega, T=0) = \pi \int_0^{|\omega|} d\omega' d^2 F(|\omega| - \omega') = \pi \int_0^{|\omega|} d\omega' \alpha^2 F(\omega') \quad (\text{II.56})$$

and thus

$$\frac{\partial \Gamma(\omega, T=0)}{\partial \omega} = \pi \alpha^2 F(|\omega|) \text{sgn} \omega . \quad (\text{II.57})$$

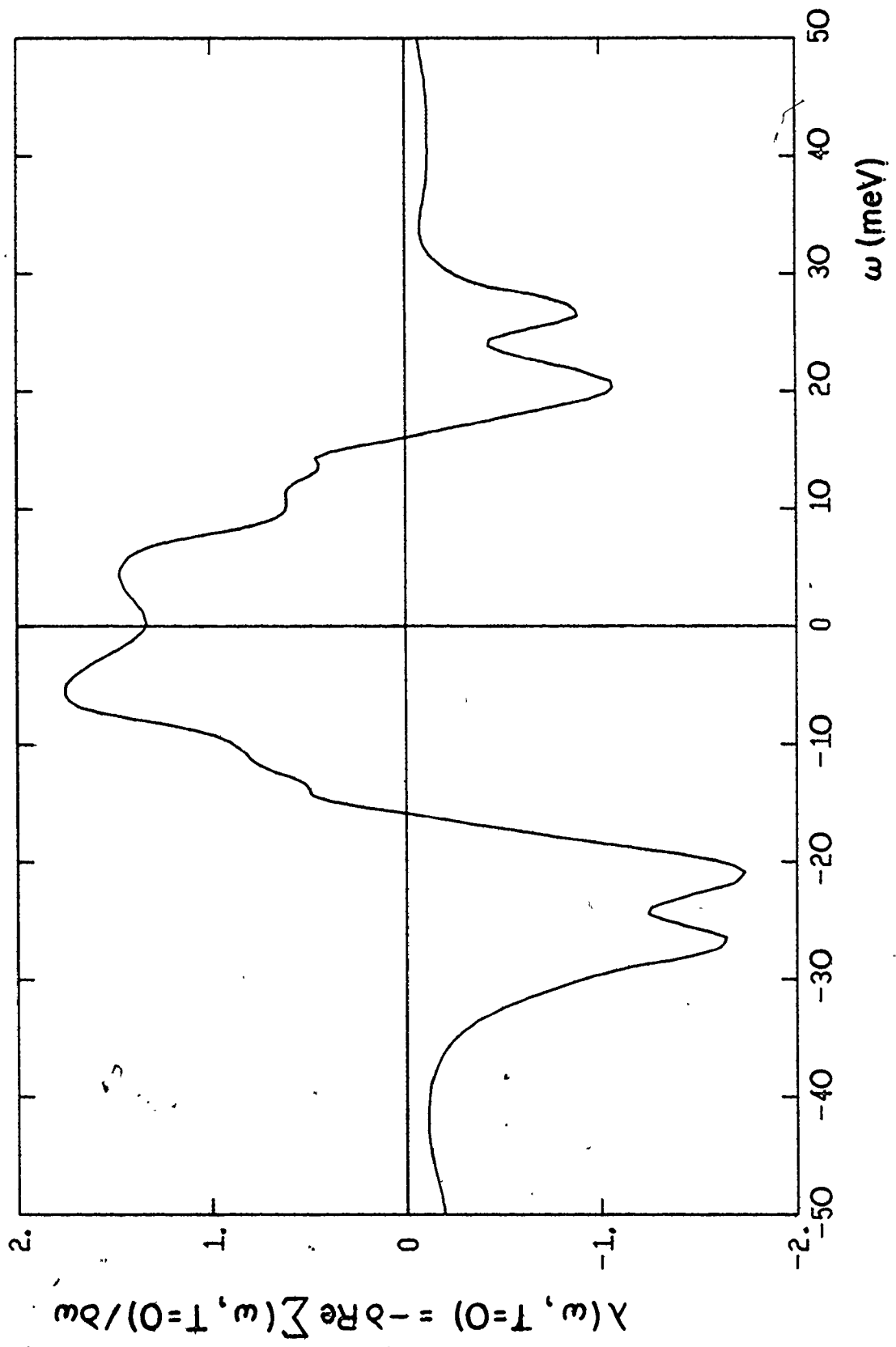
In the case of a nonconstant EDOS and at $T=0$ Eq. (II.38) gives

$$\Gamma(\omega, T) = \pi \int_0^{|\omega|} d\omega' [\theta(\omega) \tilde{N}(\omega') + \theta(-\omega) \tilde{N}(-\omega')] \alpha^2 F(|\omega| - \omega') \quad (\text{II.58})$$

Upon differentiating this expression with respect to ω and using

Fig.II.12

The frequency dependence of electron-phonon renormalization parameter at $T=0$.



the trivial identity

$$\frac{\partial}{\partial \omega} \alpha^2 F(|\omega| - \omega') = -\text{sgn}(\omega) \frac{\partial}{\partial \omega'} \alpha^2 F(|\omega| - \omega')$$

(where we have assumed that $\alpha^2 F(\Omega)$ is differentiable) as well as

$$\begin{aligned} \alpha^2 F(0) &= 0, \\ \tilde{N}(0) &= 1, \end{aligned}$$

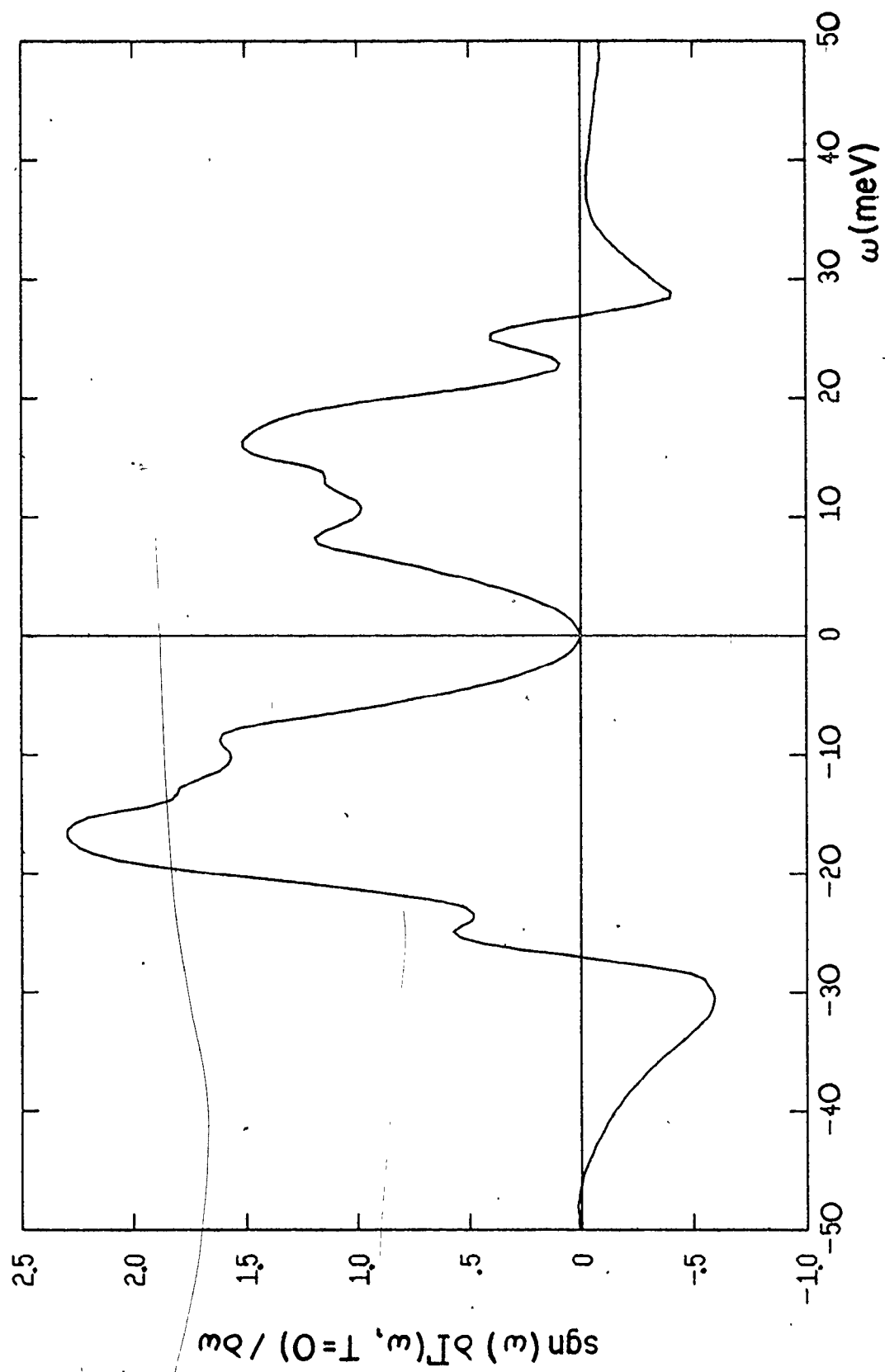
we obtain

$$\frac{\partial \Gamma(\omega, T=0)}{\partial \omega} = \pi \text{sgn}(\omega) [\alpha^2 F(|\omega|) + \int_0^{|\omega|} d\omega' \alpha^2 F(|\omega| - \omega') \frac{\partial \tilde{N}(\text{sgn}(\omega) \omega')}{\partial \omega'}] \quad (\text{II.59})$$

In the case of a constant EDOS this reduces to Eq. (II.57). In Fig. (II.13) we have plotted $\text{sgn}(\omega) \partial \Gamma(\omega, T=0) / \partial \omega$ for the EDOS given by Eq. (II.40). This derivative was calculated numerically by differentiating $\text{Im } \Sigma_{\text{ep}}(\omega + i\delta)$. The negative tails result from the drop in $|\text{Im } \Sigma_{\text{ep}}(\omega + i\delta)|$ for $|\omega| \gtrsim \omega_{\text{max}}$, as can be seen from Fig. (II.7), which is directly related to the fact (see Eq. (II.58)) that $\tilde{N}(\omega)$ drops as one moves away from the origin because of the particular form of the underlying band EDOS. Here we have a qualitative difference between the constant EDOS case and the one where the EDOS is sharply peaked in the range from $\sim -\omega_D$ to $\sim \omega_D$ around the Fermi level. In the constant EDOS approximation one has

Fig.II.13

The frequency derivative of the inverse life-time due to the electron-phonon interaction at $T=0$.



$$\Gamma(\omega, T=0) = \pi A, \quad \omega \geq \omega_{\max} \quad (\text{II.60})$$

where

$$A = \int_0^{\omega_{\max}} d\Omega \alpha^2(\Omega) F(\Omega) \quad (\text{II.61})$$

is the area under the electron-phonon spectral function. The reasons that at $T=0$ the damping rate Γ above the (upper) threshold ω_{\max} for the phonon emission is constant are:

- 1) The multiphonon processes, like the one in Fig. II.14 do not contribute to the damping rate due to the assumption that $N(\epsilon) = N(0)$ for $-\infty < \epsilon < +\infty$ ³⁸⁾.
- 2) If the 'quasiparticle' is added to the system at the energy $\omega > \omega_{\max}$ it has at its disposal all the phonons to emit and the density of final states is constant no matter what the initial energy $\omega > \omega_{\max}$. Here, we talk about single phonon emission processes and the damping rates

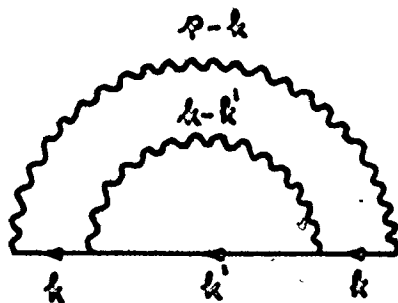


Fig. II.14

due to each of these individual processes have to be added to produce the total damping rate.

Leaving for the moment point 1) we see that in the case of a peaked EDOS an analysis similar to the one given in 2) leads us to the conclusion that the damping rate is not necessarily constant. This is illustrated schematically in Fig. II.15 where we have assumed an Einstein model for

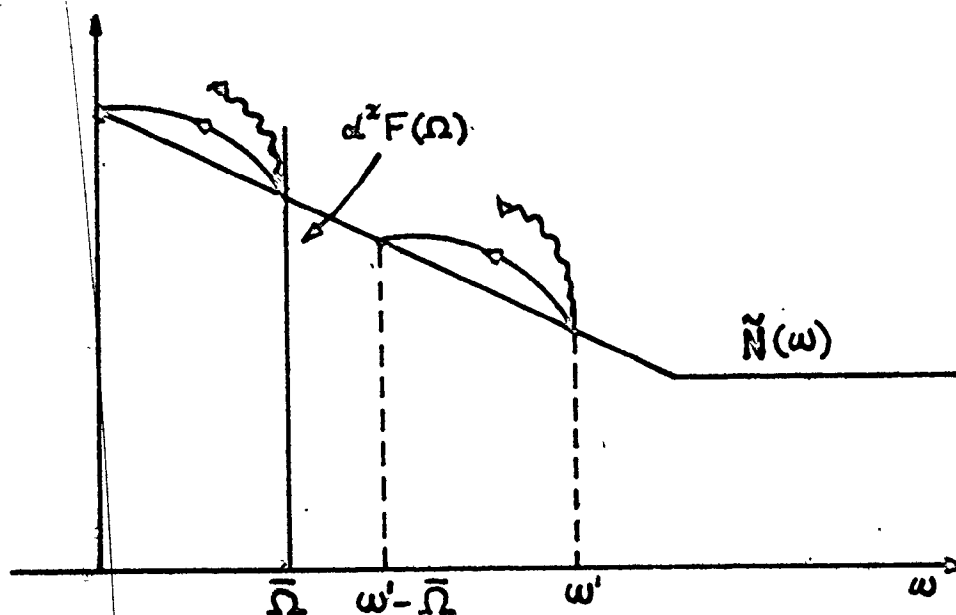


Fig. II.15

$\alpha^2(\Omega)F(\Omega) = A\delta(\Omega - \bar{\Omega})$. With this model for $\alpha^2(\Omega)F(\Omega)$ Eq. (II.58) gives

$$\Gamma(\omega, T=0) = \pi A N(\omega - \bar{\Omega}) \quad , \quad \text{for } \omega > \bar{\Omega} \quad (\text{II.62})$$

in accord with the above more or less intuitive argument. This is precisely what is happening in our full treatment with the EDOS given by Eq. (II.40).

In Fig. II.16 we plot $\frac{1}{2\pi} (\partial\Gamma(\omega, T=0)/\partial\omega + \partial\Gamma(-\omega, T=0)/\partial\omega)$ for our triangular model of $N(E)$ (solid line) and the corresponding quantity for the case of the flat EDOS ($\tilde{N}(\omega) = 1$) - dotted line - which is just the input electron-phonon spectral density $\alpha^2(\Omega)F(\Omega)$ (see Eq. (II.57)). This function is equal to

$$\frac{1}{2\pi} \frac{d}{d\omega} [\omega \text{Im} Z_N(\omega + i\delta)] = \frac{d}{d\omega} \int_0^\omega d\omega' \alpha^2 F(\omega - \omega') \frac{1}{2} [\tilde{N}(\omega') + \tilde{N}(-\omega')] , \quad (II.63)$$

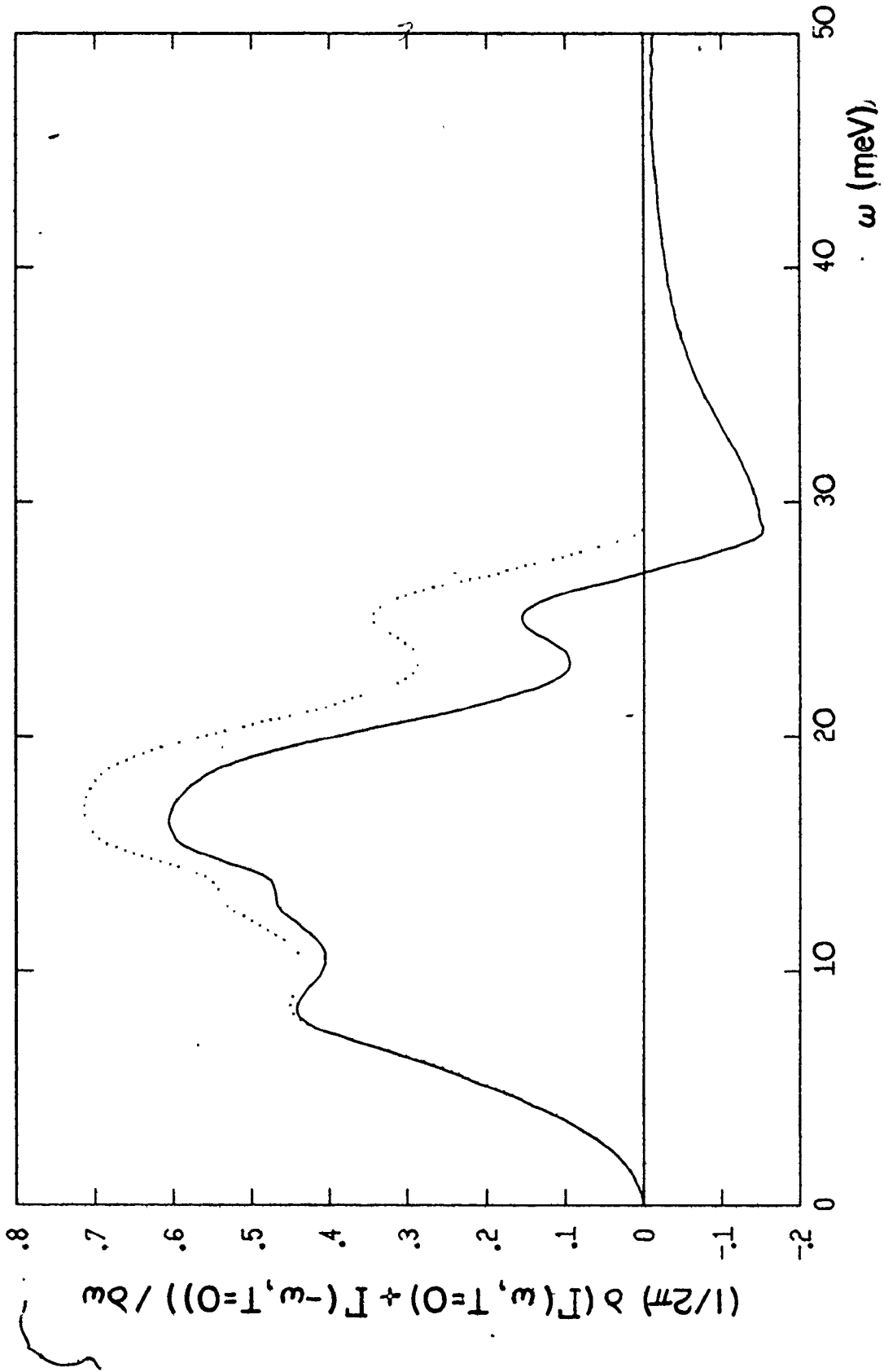
$\omega > 0$.

Thus, $\text{Im} Z_N(\omega + i\delta)$ contains the information about the local variation in $\frac{1}{2} [\tilde{N}(\omega') + \tilde{N}(-\omega')]$. The fact that at low frequencies the solid curve in Fig. II.16 agrees with the input $\alpha^2(\Omega)F(\Omega)$ spectrum is the consequence of $\tilde{N}(\omega')$ being a linear function in ω' , for small values of $|\omega'|$ so that in this range $\frac{1}{2} \tilde{N}(\omega') + \tilde{N}(-\omega') = \tilde{N}(0) = 1$.

It is evident that in some cases the effects of a nonconstant EDOS cannot be simulated within the usual theory of the electron-phonon interaction in the normal state by working with some effective electron-phonon spectrum $\alpha^2 F_{\text{eff}}$ provided one requires that this spectrum possess the usual properties, for instance that it is non-negative. Similar effects will persist in the superconducting state, as will be

Fig.II.16

(——) The function which in the constant electronic density of states case is equal to the input electron-phonon spectral density (.....).



seen in Sec. III.1, where we solve the Eliashberg equations generalized to include an energy dependent EDOS and analyze the tunneling characteristics into a superconductor.

We have mentioned that in the constant EDOS approximation the multiphonon processes, like the one in Fig. II.14, do not contribute to the self-energy part $\Sigma_{ep}(\omega+i\delta)$, although they are implicitly included in the treatment of the electron-phonon problem outlined in Sec. II.1 (see the first diagram in Fig. II.1 where the electron line is the full line). This fact was pointed out by Engelsberg and Schrieffer³⁸⁾ in their treatment of the electron-phonon problem in the Einstein model for the lattice. The reason for this is³⁸⁾ that, for instance, the contribution of the diagram in Fig. (II.14) contains the factor

$$\int_{-\infty}^{+\infty} d\varepsilon_k N(\varepsilon_k) \frac{1}{(\omega - \varepsilon_k + i\delta \operatorname{sgn} \varepsilon_k)^2} \quad (\text{II.64})$$

which gives zero if one assumes

$$N(\varepsilon_k) = N(0) \quad , \quad -\infty < \varepsilon_k < +\infty . \quad (\text{II.65})$$

However if the EDOS is not assumed to satisfy the condition (II.65) the multiphonon processes will contribute to Σ_{ep} and our self-consistent treatment of the electron-phonon interaction in the normal state with nonconstant $N(E)$ includes these processes.

The contribution to the total self-energy part due to the elastic impurity scattering, (Eq. (II.37)), gives

$$\text{Re}\Sigma_{iN}(\omega+i\delta) = \text{Re} \frac{1}{2\pi\tau_{iN}} \int_{-\infty}^{+\infty} d\epsilon' \frac{N(\epsilon')}{N(0)} G(\epsilon', \omega+\delta) \quad (\text{II.66a})$$

$$\text{Im}\Sigma_{iN}(\omega+i\delta) = - \frac{1}{2\tau_{iN}} \tilde{N}(\omega) . \quad (\text{II.66b})$$

In the constant density of states approximation the real part of this self-energy vanishes and the imaginary part reduces to the familiar result $-i/(2\tau_{iN})$. Note that if the full Green's function G in the expression (II.37) was replaced by a noninteracting (retarded) Green's function $G_0(\epsilon, \omega) = 1/(\omega - \epsilon_k + i\delta)$ Eqs. (II.66a) and (II.66) would give

$$\text{Re}\Sigma_{iN}(\omega-i\delta) = \frac{1}{2\pi\tau_{iN}} \frac{1}{N(0)} P \int_{-\infty}^{+\infty} d\epsilon \frac{N(\epsilon)}{\omega - \epsilon} \quad (\text{II.67a})$$

$$\text{Im}\Sigma_{iN}(\omega+i\delta) = - \frac{1}{2\tau_{iN}} N(\omega) \quad (\text{II.67b})$$

which are just the 'textbook'⁶¹⁾ results obtained in second order perturbation theory. The scattering rate given by Eq. (II.67b) is proportional to the EDOS to which the particle can be elastically scattered, while the corresponding formula (II.66b) contains the quasiparticle density of states. The difference between Eqs. (II.66a)-(II.66b) on the one hand and Eqs. (II.67a)-(II.67b) on the other is that in the latter case

we have summed all the diagrams for G given in Fig. II.17a, while

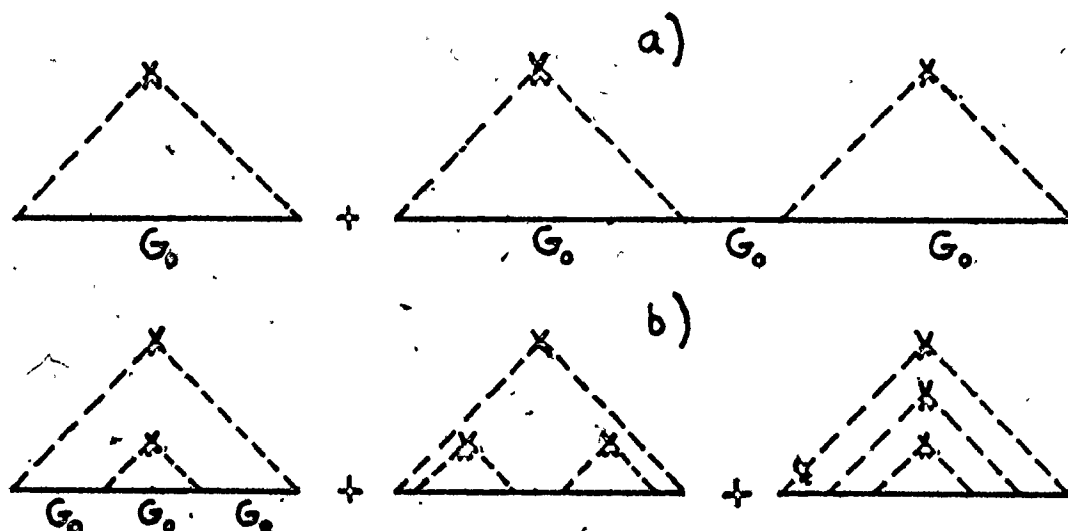


Fig. II.17

in the former case we have included besides the diagrams in Fig. II.17a all the nested diagrams in Fig. II.17b. If the EDOS was assumed to be constant, all the nested diagrams would give a zero contribution in analogy with the electron-phonon interaction and the two treatments would be identical.

Since the impurity contribution $\Sigma_{iN}(\omega)$ has a finite imaginary part for all ω , we cannot, as in the case of electron-phonon interaction at $T=0$, locate the position of the chemical potential by the frequency at which $\text{Im}\Sigma_{iN}(\omega)$ vanishes ⁷¹⁾. Instead, one has to solve Eq. (II.52) which is the equation for the interacting chemical potential in terms of the average number of particles. We will restrict ourselves to the case when the EDOS has the form of a Lorentzian

superimposed on a constant background and which is symmetric around the band chemical potential,

$$N(E) = N_b \left(1 + \frac{s}{\pi} \frac{a}{a^2 + E^2} \right), \quad -\mu_0 \leq E < +\infty. \quad (\text{II.68})$$

and we will assume $\mu_0 \gg a, s$. Thus, we will ignore any shift of the chemical potential and will instead focus on the exact form of the smearing in the quasiparticle density of states due to the impurity scattering. More specifically, in several recent attempts^[7,72] to account for lifetime effects on the band density of states, a phenomenological approach has been taken in which the lifetime broadening of the energy levels is described by

$$\langle N(E) \rangle = \int dE' N(E') S(E, E', E_b) \quad (\text{II.69})$$

where $S(E, E', E_b)$ is some broadening function, usually taken to be a Lorentzian

$$S(E, E', E_b) \propto \frac{E_b}{E_b^2 + (E - E')^2} \quad (\text{II.70})$$

or a derivative of the Fermi function

$$S(E, E', E_b) \propto \frac{\partial}{\partial E'} \left[\frac{1}{e^{(E' - E)/E_b} + 1} \right] \quad (\text{II.71})$$

The input consisted of $N(E)$, $v(E)$ etc. obtained from band

structure calculations and several average quantities were calculated on the basis of an averaging procedure, similar to the one given by Eq. (II.69). The number of states was preserved and the chemical potential was changed accordingly.

Instead, we will choose the Lorentzian model previously described which simplifies the treatment considerably from the computational point of view, but we will treat life-time effects exactly. It should be noted that, recently, this Lorentzian model has been successfully used in fitting the temperature dependence of several normal state properties for the series of A-15 $(V_{1-x}Cr_x)_3Si$ alloys^{20,21}). With this model for EDOS Eqs. (II.66a) and (II.66b) give (see Appendix II)

$$\text{Re}\Sigma_{iN}(\omega+i\delta) = \frac{1}{2\pi\tau_{iN}} \frac{Nb}{N(0)} S \frac{\omega - \text{Re}\Sigma(\omega+i\delta)}{(a + |\text{Im}\Sigma(\omega+i\delta)|)^2 + (\omega - \text{Re}\Sigma(\omega+i\delta))^2} \quad (\text{II.72a})$$

$$\text{Im}\Sigma_{iN}(\omega+i\delta) = - \frac{1}{2\tau_{iN}} \tilde{N}(\omega) \quad (\text{II.72b})$$

with (see Eq. (II.36))

$$N(0)\tilde{N}(\omega) = N_b \left[1 + \frac{S}{\pi} \frac{a + |\text{Im}\Sigma(\omega+i\delta)|}{(a + |\text{Im}\Sigma(\omega+i\delta)|)^2 + (\omega - \text{Re}\Sigma(\omega+i\delta))^2} \right] \quad (\text{II.72c})$$

We have solved Eqs. (II.72a)-(II.72c), assuming that only impurity scattering is present, i.e. $\Sigma(\omega+i\delta) = \Sigma_{iN}(\omega+i\delta)$ with $a \approx 9.6$ meV, $S = \pi a$ for two different values of the parameter $1/2\tau = 1$ meV and 10 meV. The choice of these Lorentzian para-

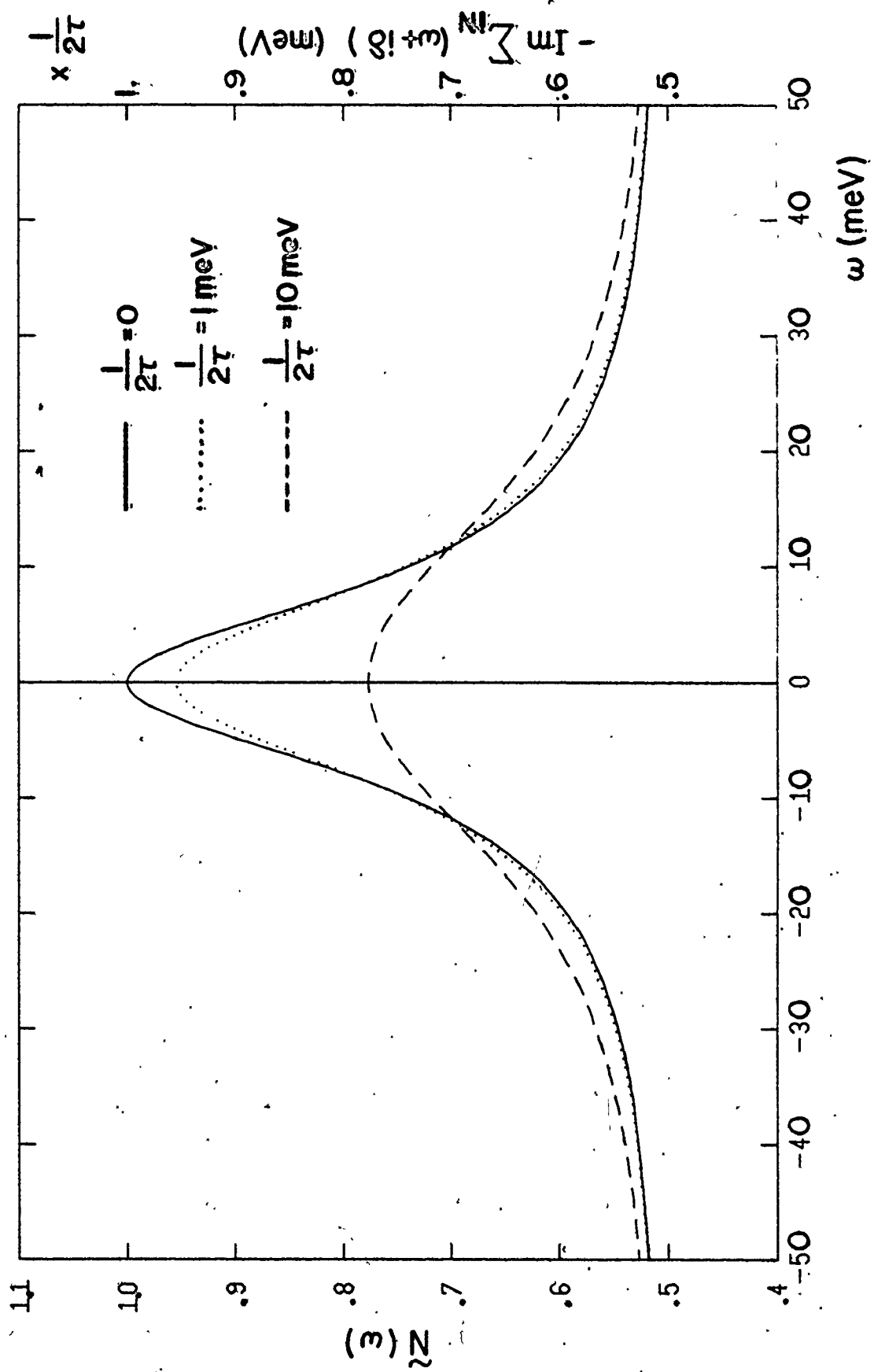
meters was made to simulate the size of the peak in the EDOS for Nb_3Ge which was obtained from self-consistent pseudopotential band-structure calculations¹⁶⁾, with the Fermi level situated at the center of the peak¹⁵⁾. Also, the half-widths of the model Lorentzian peaks used in Ref. 20 are comparable to our choice.

In Fig. II.18 we plot the band EDOS normalized to $N(0)$ (solid line), $\tilde{N}(\omega)$ for $1/(2\tau_{iN}) = 1$ meV (dotted line) and for $1/(2\tau_{iN}) = 10$ meV (dashed line). These quantities, upon multiplying by the corresponding $1/2\tau_{iN}$, also give the decay rates (Eq. (II.66b)). Note that if the impurity problem was treated by the second order nonselfconsistent perturbation theory, Eqs. (II.67a)-(II.67b), the decay rates would be given by multiplying the solid line in Fig. II.18 with the corresponding $1/(2\tau_{iN})$. Thus, in the full self-consistent treatment the scattering by the impurities is, in a sense, self-limiting due to the smearing of the quasiparticle density of states. The increase in the value of the parameter $1/(2\tau_{iN})$ from 1 meV to 10 meV should be interpreted as an increase in impurity concentration of a factor of 10 (see Eqs. (II.20) and (II.21)). In the constant EDOS case or in a nonselfconsistent treatment of the impurity scattering, Eqs. (II.67a)-(II.67b), this would correspond to an increase in the scattering rate at the Fermi surface of a factor of 10 while it is only 8 in the full self-consistent calculation. In other words, the impurity scat-



Fig.II.18

Quasiparticle densities of states for the elastic impurity scattering.

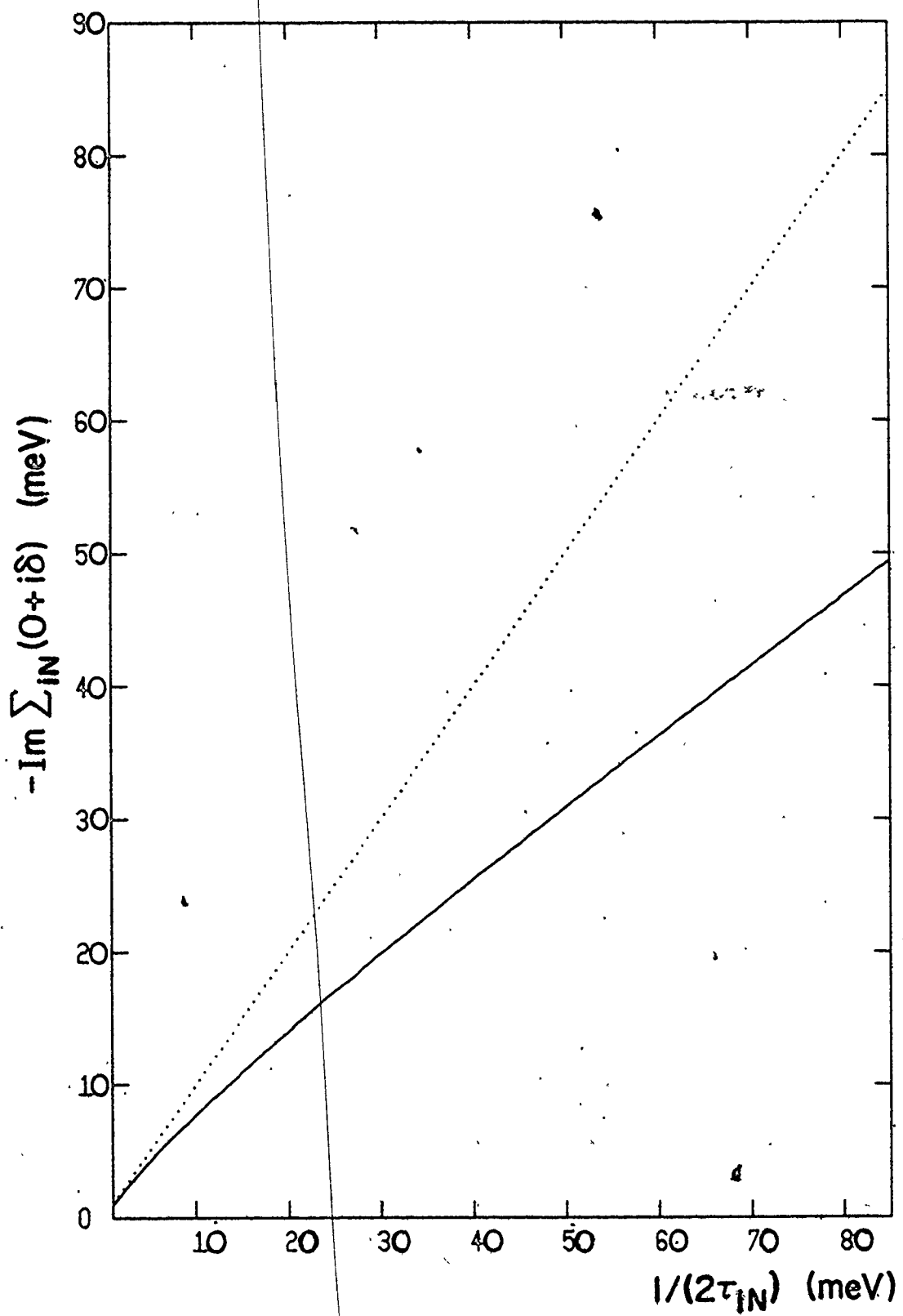


tering rate is not necessarily linear in concentration when the EDOS cannot be assumed to be constant. In Fig. II.19 we plot the scattering rate at the Fermi surface (solid line) vs. $1/(2\tau_N)$, the latter parameter being linearly proportional to the concentration, for the Lorentzian model of the EDOS. (It should be noted that, strictly speaking, our treatment of the elastic impurity scattering problem is valid only in the limit of small impurity concentration, as explained in Sec. II.1.) Once the peak has been largely smeared out, i.e. for $1/(2\tau_{iN}) > 60$ meV the linear dependence is again approximately recovered with the slope ~ 0.5 (dotted line is the simple linear dependence with the slope 1).

In Fig. II.20 we plot the real part of $\Sigma_{iN}(\omega+i\delta)$ for $1/(2\tau_{iN}) = 1$ meV (dotted line) and for $1/(2\tau_{iN}) = 10$ meV. Thus, elastic impurity scattering contributes to the renormalization, i.e. $\lambda_{imp} = -[\partial \text{Re}\Sigma_{iN}(\omega+i\delta)/\partial \omega]_{\omega=0} \neq 0$, once the EDOS cannot be assumed to be constant. This is also true in the case of a nonselfconsistent second order perturbation theory treatment, Eqs. (II.67a)-(II.67b), with the renormalization parameter being linearly proportional to the concentration (or $1/(2\tau_{iN})$). However in the full self-consistent treatment this ceases to be the case due to the smearing of the peak as is evident from Fig. II.21, where we plot $-\lambda_{imp}$ vs. $1/(2\tau_{iN})$. The shape of this curve can be understood qualitatively if after differentiating Eq. (II.72a) at $\omega = 0$ we ignore λ_{imp} compared to 1 and

Fig.II.19

Imaginary part of the self-energy due to elastic impurity scattering as a function of the parameter which is proportional to the impurity concentration.






Fig.II.20

The real part of the electron self-energy due to the elastic impurity scattering.

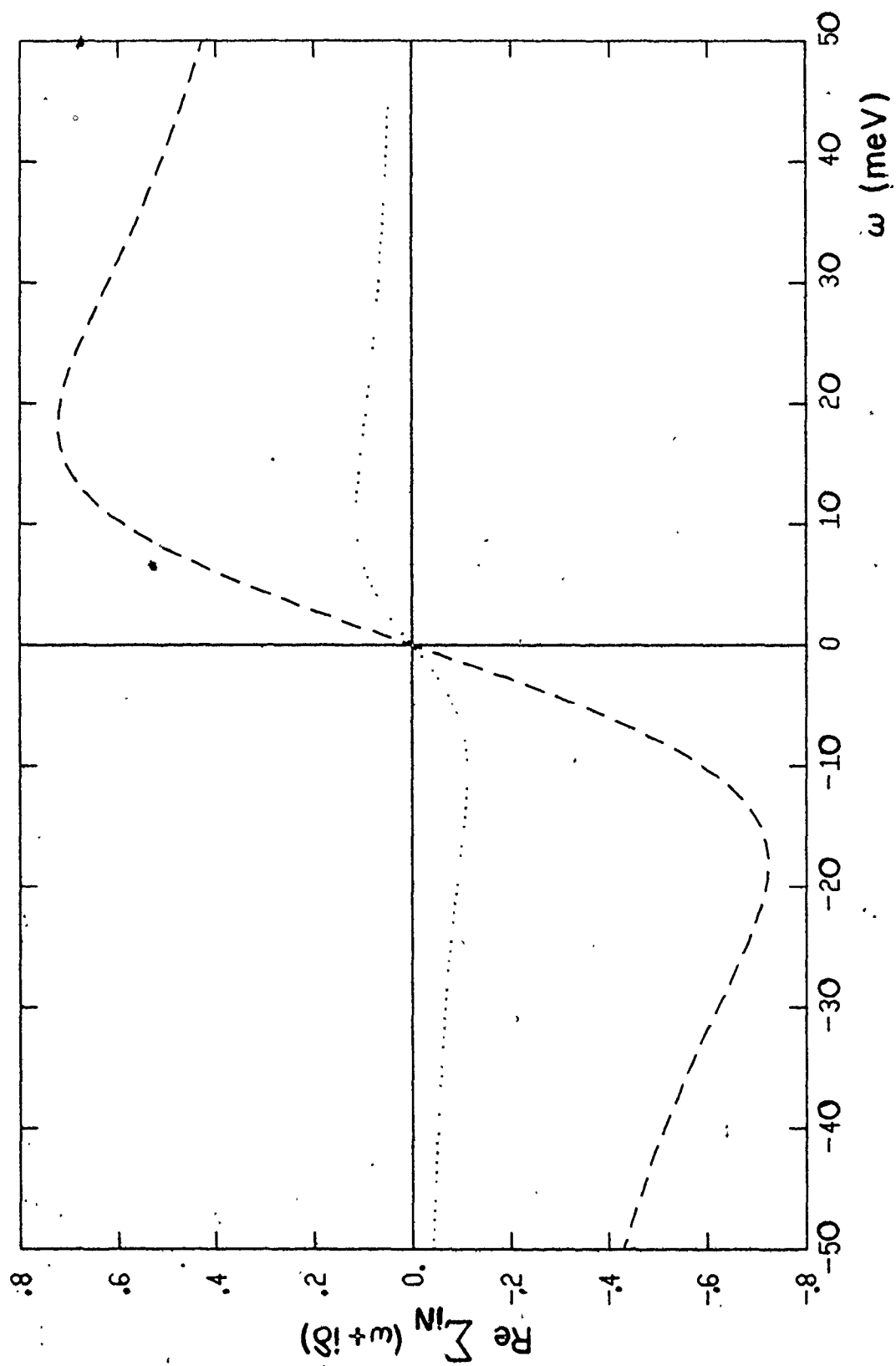
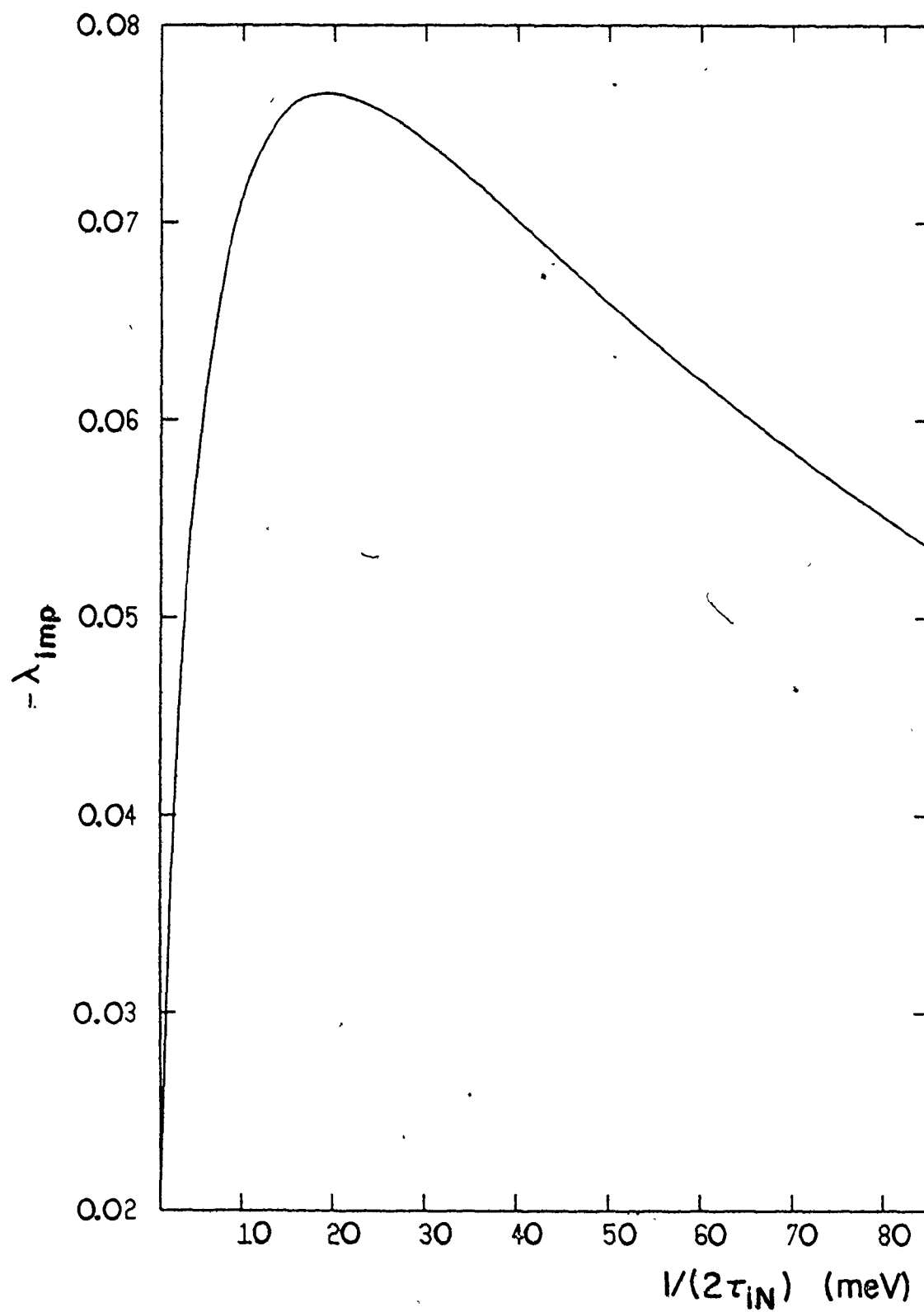


Fig.II.21

Renormalization parameter due to Elastic impurity scattering as a function of the quantity which is linear in the impurity concentration.



replace $-\text{Im}\Sigma_{iN}(0+i\delta)$ with $1/(2\tau_{iN})$. The result is

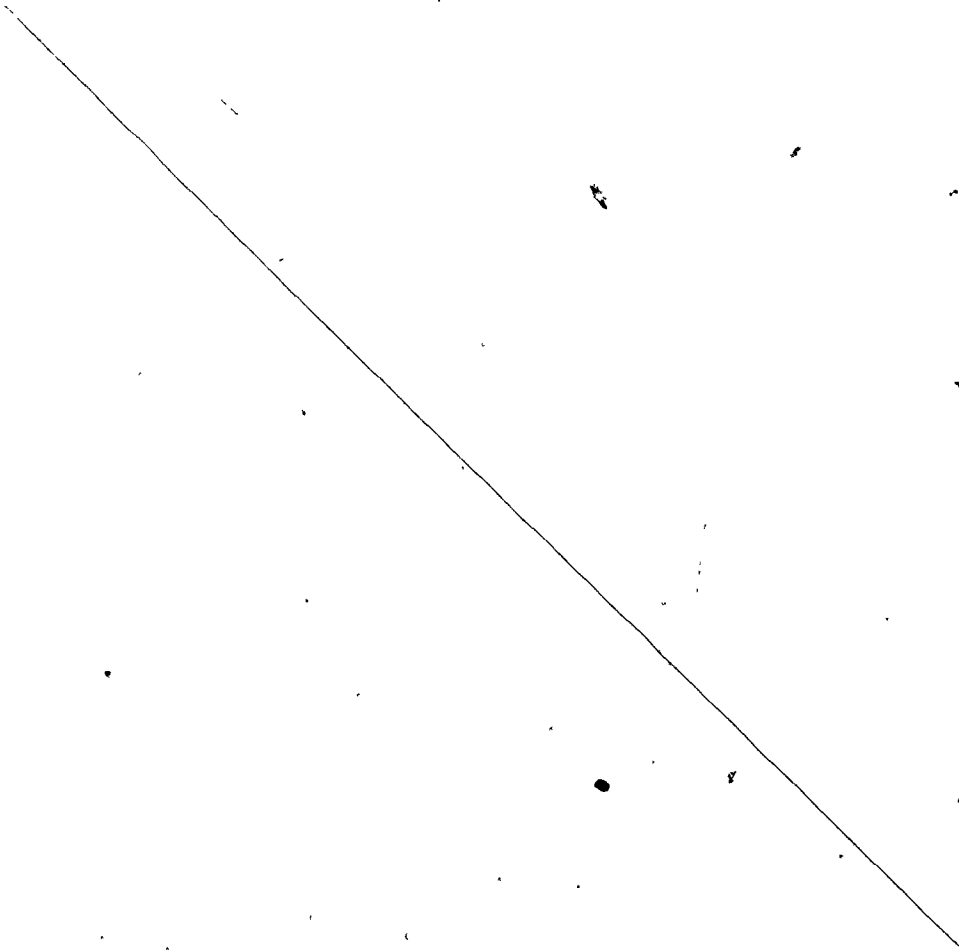
$$-\lambda_{\text{imp}} \propto \frac{(1/2\tau_{iN})}{(a+1/2\tau_{iN})^2}$$

This formula would predict the maximum at $1/(2\tau_{iN}) = a$, while in fact the maximum is near $1/(2\tau_{iN}) = 2a$. The reason for this is that $-\text{Im}\Sigma_{iN}(0+i\delta)$ is of order of magnitude $1/2\tau_{iN}$ and it would be more appropriate to take $-\text{Im}\Sigma_{iN}(0+i\delta) = C(1/(2\tau_{iN}))(1/(2\tau_{iN}))$ with $C(1/(2\tau_{iN}))$ between 1 and 0.5 with our model for EDOS (see Fig. II.19).

We have also solved the complete self-energy equation at $T=0$ when both the electron-phonon interaction and elastic impurity scattering are present, for the same Lorentzian model. The input electron-phonon spectrum was the one for Nb_3Sn and we have chosen $1/(2\tau_{iN}) = 10$ meV. In Fig. II.22 we plot the real part of the total self-energy when only the electron-phonon interaction is present (solid line), when the impurity contribution is also present (dotted line) and when the real part of the impurity self-energy is ignored (dashed line). Note that all three curves are odd in ω due to assumed symmetry of EDOS with respect to the chemical potential. In Fig. II.23 we plot $-\text{Im}\Sigma(\omega+i\delta)$ for these three cases and in Fig. II.24 we plot the EDOS normalized to $N(0)$ (solid line): $\tilde{N}(\omega)$ when only the electron phonon interaction is present (dotted line), $\tilde{N}(\omega)$ when the elastic impurity scattering is also included (dashed line) and $\tilde{N}(\omega)$ when the real part of the im-

Fig.II.22

The real part of the electron self-energy.

A single, straight diagonal line is drawn across the lower half of the page, starting from the left margin and extending towards the right margin. The line is slightly curved and has a few small dark spots or artifacts along its length.

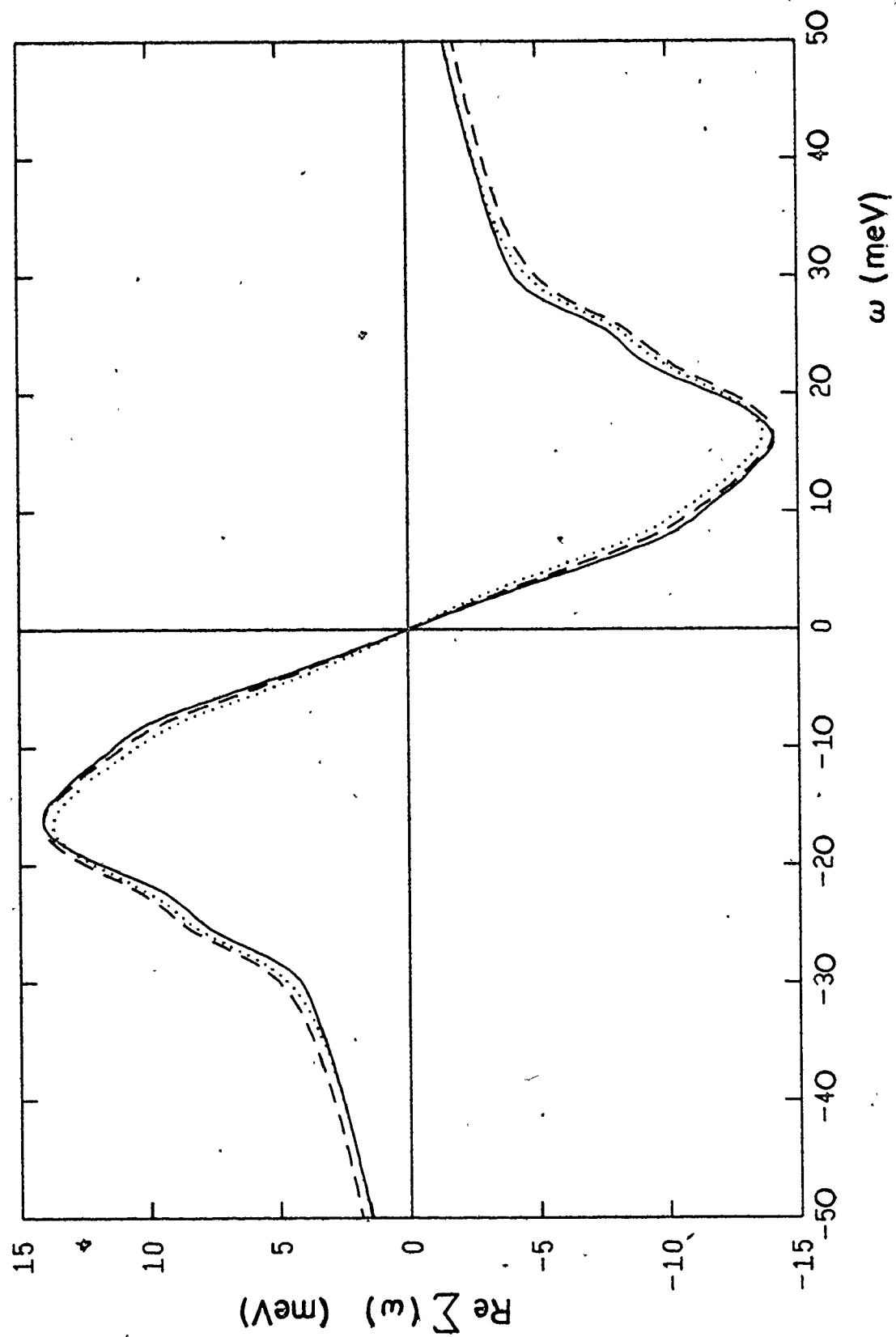


Fig.II.23

The imaginary part of the electron self-energy.

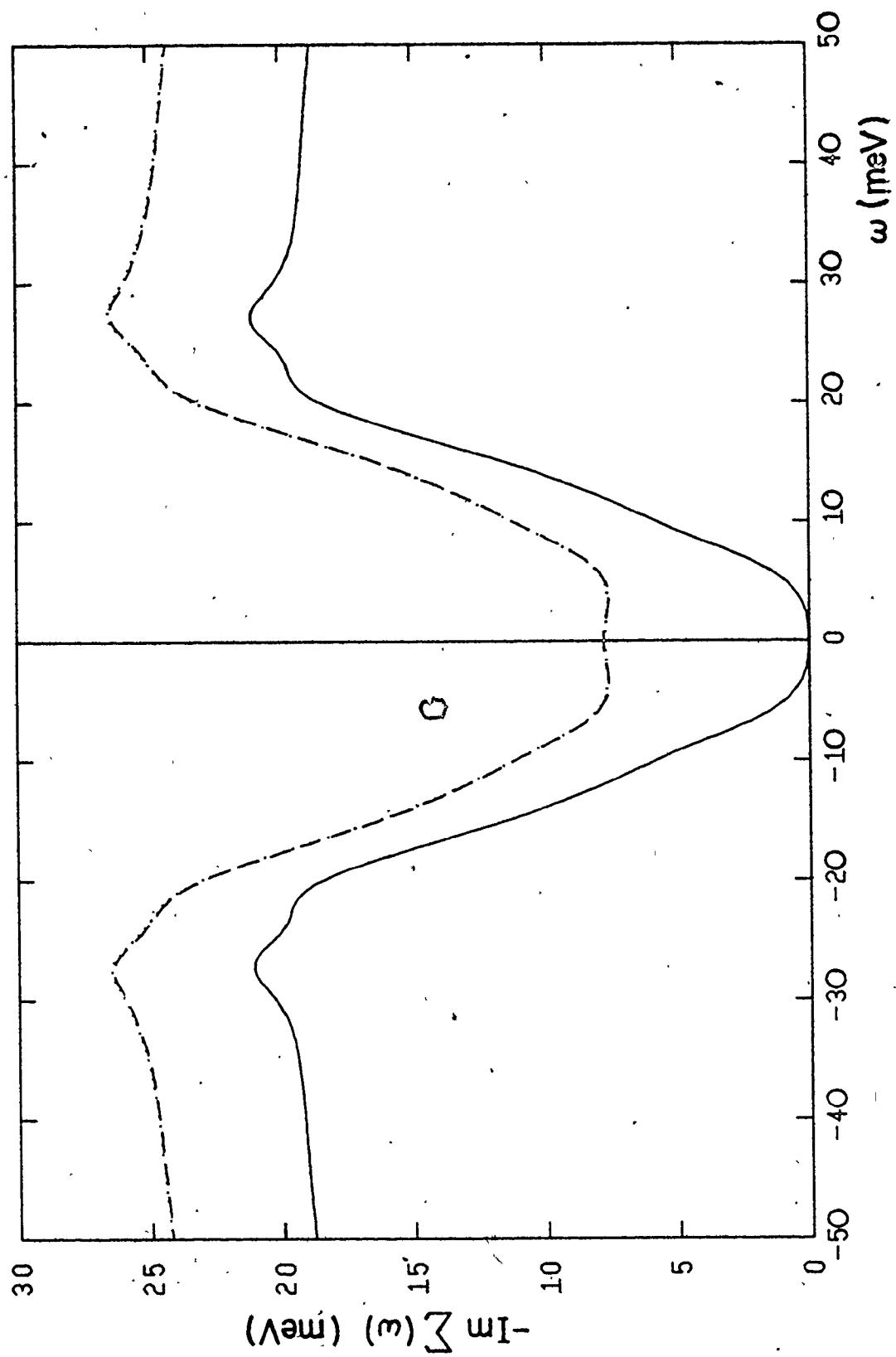
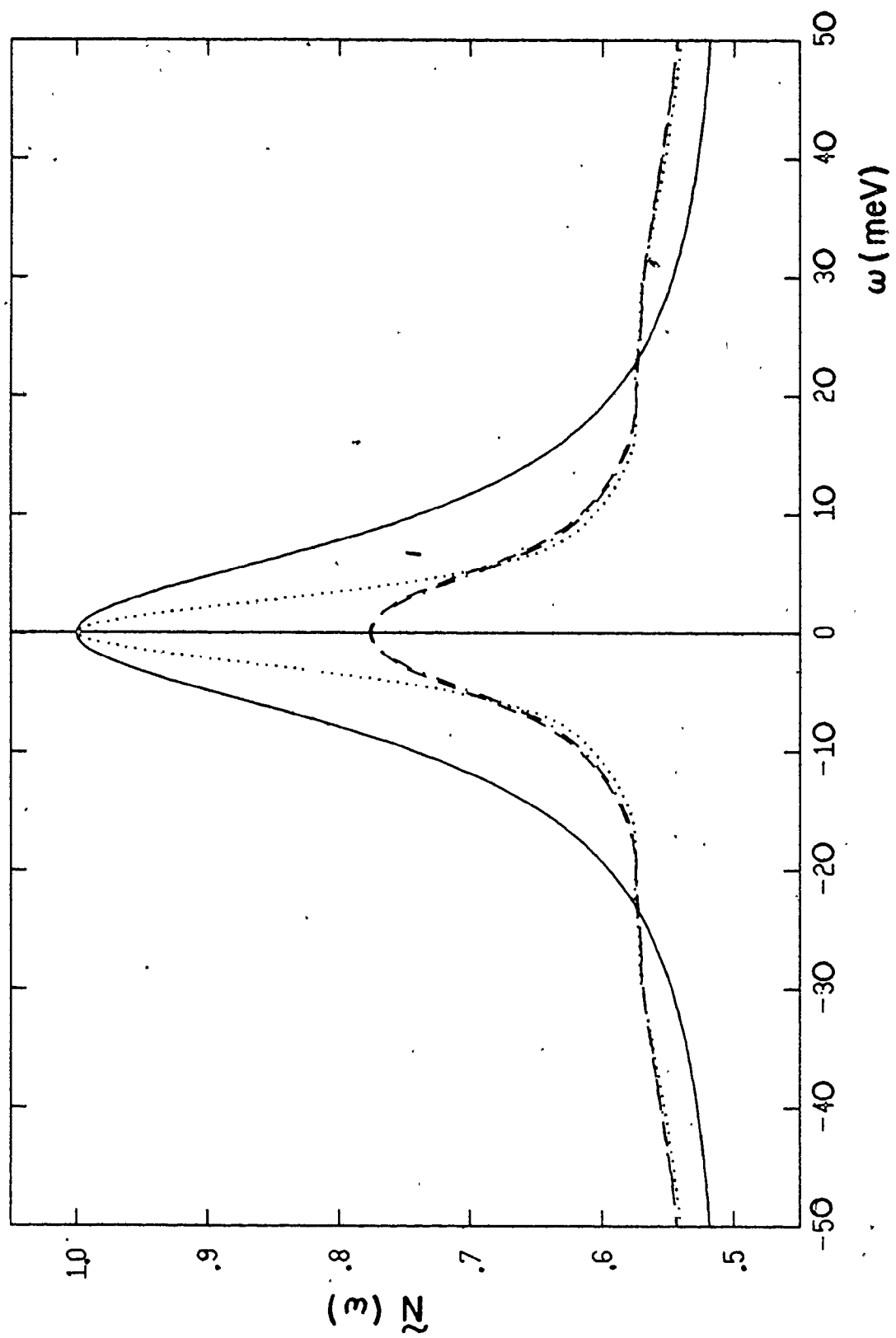


Fig.II.24

The quasiparticle density of states normalized to $N(0)$.



impurity self-energy is ignored (dash-dot). The reason that we consider the case when the real part of the impurity self-energy is ignored is that in the recent treatment of the same problem by Pickett⁴⁾ the real part of the impurity self-energy does not appear due to the mathematical approximations which went into his analysis.

Here again we have considerable 'sharpening' of the structure in the quasiparticle density of states as compared to the bare band EDOS due to renormalization by the strong electron-phonon interaction. Of course, the peak is heavily depleted by the impurity scattering but is at the same time narrowed compared to the case when the electron-phonon interaction is 'switched-off' (see the dashed curve in Fig. II.18).

The value of the effective renormalization parameter $\lambda_{\text{eff}} = -[\partial \text{Re}\Sigma(\omega+i\delta)/\partial\omega]_{\omega=0}$ in the case when only the electron-phonon interaction is present is $\lambda_{\text{eff}}(\text{ep}) = 1.1577$. The same quantity for the case when elastic impurity scattering is also included has the value $\lambda_{\text{eff}}(\text{ep+imp}) = 0.9532$, or if the real part of the impurity self-energy is left out from the considerations $\lambda'_{\text{eff}}(\text{ep+imp}) = 1.0829$. The difference $\lambda_{\text{eff}}(\text{ep}) - \lambda'_{\text{eff}}(\text{ep+imp}) = 0.0748$ is coming from the depletion of the peak in the quasiparticle density of states close to $\omega = 0$, due to the impurity scattering. This depletion is about the same, whether one includes or not the real part of the impurity self-energy as can be seen from Fig. II.24. Therefore, most of the difference between $\lambda_{\text{eff}}(\text{ep})$ and $\lambda_{\text{eff}}(\text{ep+imp})$, $\lambda_{\text{eff}}(\text{ep}) -$

$\lambda_{\text{eff}}(\text{ep+imp}) = 0.2045$ is coming from the impurity renormalization parameter, $\lambda_{\text{imp}} = -[\partial \text{Re}\Sigma_{iN}(\omega+i\delta)/\partial\omega]_{\omega=0}$ which is negative for our model of EDOS. It is interesting to ask why the value of $|\lambda_{\text{imp}}| \approx \lambda'_{\text{eff}}(\text{ep+imp}) - \lambda_{\text{eff}}(\text{ep+imp}) = 0.1297$ is almost twice the value $|\lambda_{\text{imp}}| = 0.0714$ when only impurity scattering is present with the same $1/(2\tau_{iN}) = 10$ meV. The reason for this is that the effective narrowing of the peak in the quasiparticle density of states due to the electron-phonon interaction as compared to the corresponding case (the same $1/(2\tau_{iN})$) when there is only elastic impurity scattering, increases the value of the impurity renormalization parameter (for the given model of EDOS). To see this it is best to consider the result for $\text{Re}\Sigma_{iN}(\omega+i\delta)$ which is obtained in nonselfconsistent second order perturbation theory

$$\text{Re}\Sigma_{iN}(\omega+i\delta) = \frac{1}{2\pi\tau} \frac{1}{N(0)} P \int_{-\infty}^{+\infty} d\varepsilon \frac{N(\varepsilon)}{\omega - \varepsilon} = \frac{1}{2\pi\tau_{iN}} \frac{N_b}{N(0)} S \frac{\omega}{a^2 + \omega^2}$$

which after differentiation gives

$$\begin{aligned} \lambda_{\text{imp}} &= -[\partial \text{Re}\Sigma_{iN}(\omega+i\delta)/\partial\omega]_{\omega=0} = - \frac{1}{2\tau_{iN}} \frac{N_b}{N(0)} \frac{S}{\pi a} \frac{1}{a} = \\ &= - \frac{1}{2\tau_{iN}} \frac{N_b}{(1 + \frac{S}{\pi a})} \frac{S}{\pi a} \frac{1}{a} . \end{aligned}$$

For a given peak height over the background, i.e. for a given $S/(a\pi)$ and N_b , and for a given $1/(2\tau_{iN})$ $|\lambda_{\text{imp}}| \propto \frac{1}{a}$. Since at

$T = 0$ the electron-phonon interaction does not give any damping at $\omega = 0$ the heights of the two curves, the dashed one in Fig. II.18 and the dashed one in Fig. II.24, are almost the same (since the parameter $1/(2\tau_{iN})$ has one and the same value) while the effective half-width of the latter is about one half of the former. Thus the value of the λ_{imp} when the electron-phonon interaction is present is about twice the value when this interaction is switched off.

The natural question is, to what extent are the conclusions of our analysis dependent on the particular model for EDOS, i.e. the symmetric Lorentzian model? We believe that the details will depend on the details of the particular band structure EDOS. The common effect which will always be present is the smearing of the structure in the EDOS due to lifetime effects and the sharpening of the possible structure close to $\omega = 0$ due to electron-phonon renormalization effects. The last effect has been overlooked, although it is implicitly present, in several recent works concerned with similar topics¹⁻⁴). To see how the details of the EDOS come in, suppose that in our analysis of the impurity problem we would start with the model of a displaced Lorentzian, for example the solid curve in Fig. II.18 displaced by some amount to the left. By adding impurities to the system this curve would be smeared so that the corresponding quasiparticle densities of states would

be given by the displaced dotted and dashed curves in Fig.

II.18. Obviously, depending on the original displacement, the smearing may result in a decrease or increase in the value of the quasiparticle density of states at the chemical potential, compared to its value when there are no impurities present. This can, for example, lead to a decrease or increase in the decay rate at the chemical potential over which one would obtain from Eqs. (II.67a)-(II.67b), etc. However if the position of the Fermi level is only slightly displaced from the center of the Lorentzian our conclusions should remain more or less unchanged.

II.3 EFFECTS OF THE INTERPLAY BETWEEN A SHARP PEAK IN THE ELECTRONIC DENSITY OF STATES AND ELECTRON-PHONON INTERACTION AT FINITE T

We conclude this chapter by presenting the solutions of Eq. (II.30) at finite temperature, for two models of the electronic density of states (EDOS). At $T > 0$ the average number of phonons with frequency Ω becomes non-vanishing and is given by $N(\Omega) = 1/(e^{\beta\Omega} - 1)$, $\beta = 1/T$ ($\hbar = 1$, Boltzmann's constant $k_B = 1$). As a consequence there is a finite damping at all ω , i.e. the imaginary part of the $\Sigma_{ep}(\omega + i\delta)$ becomes nonvanishing for all ω . If the EDOS cannot be assumed to be constant in the range of several Debye energies around the Fermi level it is necessary to locate the position of the true interacting chemical potential by solving Eq. (II.52), as we have explained in Sec. II.2 in

connection with the problem of elastic impurity scattering. To simplify the numerical calculations we will assume, as was the case with the impurity problem, that the EDOS is symmetric around the 'bare' band chemical potential. More specifically, we will work with the symmetric Lorentzian model (see Sec. II.2, Eq. (II.68)) previously described and with the symmetric triangular model

$$N(E) = \begin{cases} 0 & , E \leq -\mu_0 \\ B & , -\mu_0 < E \leq -E_W \\ B + \frac{P-B}{E_W} (E+E_W) & , -E_W < E \leq 0 \\ B + \frac{B-P}{E_W} (E-E_W) & , 0 < E \leq E_W \\ B & , E > E_W \end{cases} \quad (\text{II.73})$$

By assuming $\mu_0 \gg E_W$, we can neglect any shift in the chemical potential. Thus we are primarily interested in the effects of the decrease in the EDOS as one moves away from $E = 0$.

The problem of the electron-phonon interaction at finite temperature in the presence of sharp structure in the EDOS near the Fermi level was treated by Fradin³²⁾ and Pickett⁴⁾. Fradin's analysis is within the framework of nonselfconsistent second order perturbation theory for the electron-phonon interaction. Pickett's approach is similar to ours, i.e. it is self-consistent, but we do not perform (unnecessary) mathema-

tical approximations which are present in his analysis.

In Fig. II.25 we give the real part of $\Sigma_{ep}(\omega+i\delta, T)$ with the Lorentzian model for the EDOS ($a = 9.6$ meV, $S/(\pi a) = 1$) at four temperatures: $T = 0^\circ$ (solid line), $T = 10^\circ\text{K}$ (dotted line), $T = 20^\circ\text{K}$ (dashed line) and at $T = 80^\circ\text{K}$ (dash-dot). Incidentally, the superconducting critical temperature for this EDOS and input α^2F spectrum described in Sec. II.2, is $T_c = 15^\circ\text{K}$ (with $\mu^*(\omega_c) = 0.1747$ and $\omega_c = 240$ meV). The corresponding imaginary parts are given in Fig. II.26. In Fig. II.27 we plot the bare band EDOS (—) and quasiparticle densities of states at $T = 0^\circ\text{K}$ (.....), $T = 10^\circ\text{K}$ (----), $T = 20^\circ\text{K}$ (-.-.-) and $T = 80^\circ\text{K}$ (-.-.-.-), all curves being normalized to $N(E=0)$.

It can be seen that the effective narrowing in the quasiparticle density of states due to renormalization by the electron-phonon interaction, persist at finite T . At the same time, however, there is a progressive depletion and relative broadening with increasing temperature, caused by the increase in damping. The change of the normalized quasiparticle density of states, $\tilde{N}(\omega, T)$, at $\omega = 0$ with temperature is illustrated by the solid line in Fig. II.28. This effect, i.e. the temperature smearing of the peak in the electronic density of states, was first pointed out by Ho et al.¹⁵⁾ on the basis of uncertainty principle arguments. By using the results of their self-consistent pseudopotential band-structure calculations for



Fig.II.25

The real part of the electron self-energy at four different temperatures.

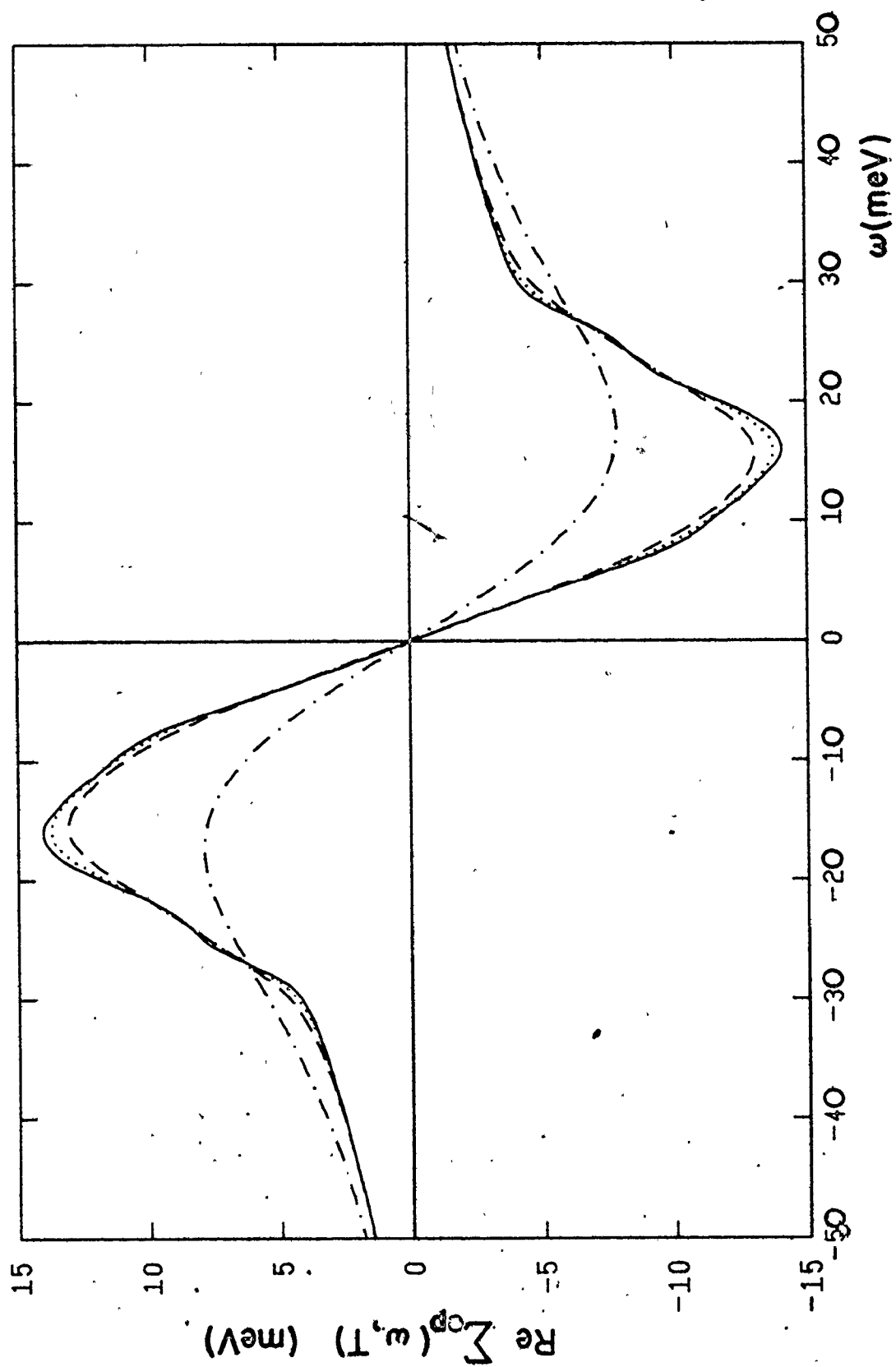


Fig.II.26

The imaginary part of the electron self-energy at four different temperatures.



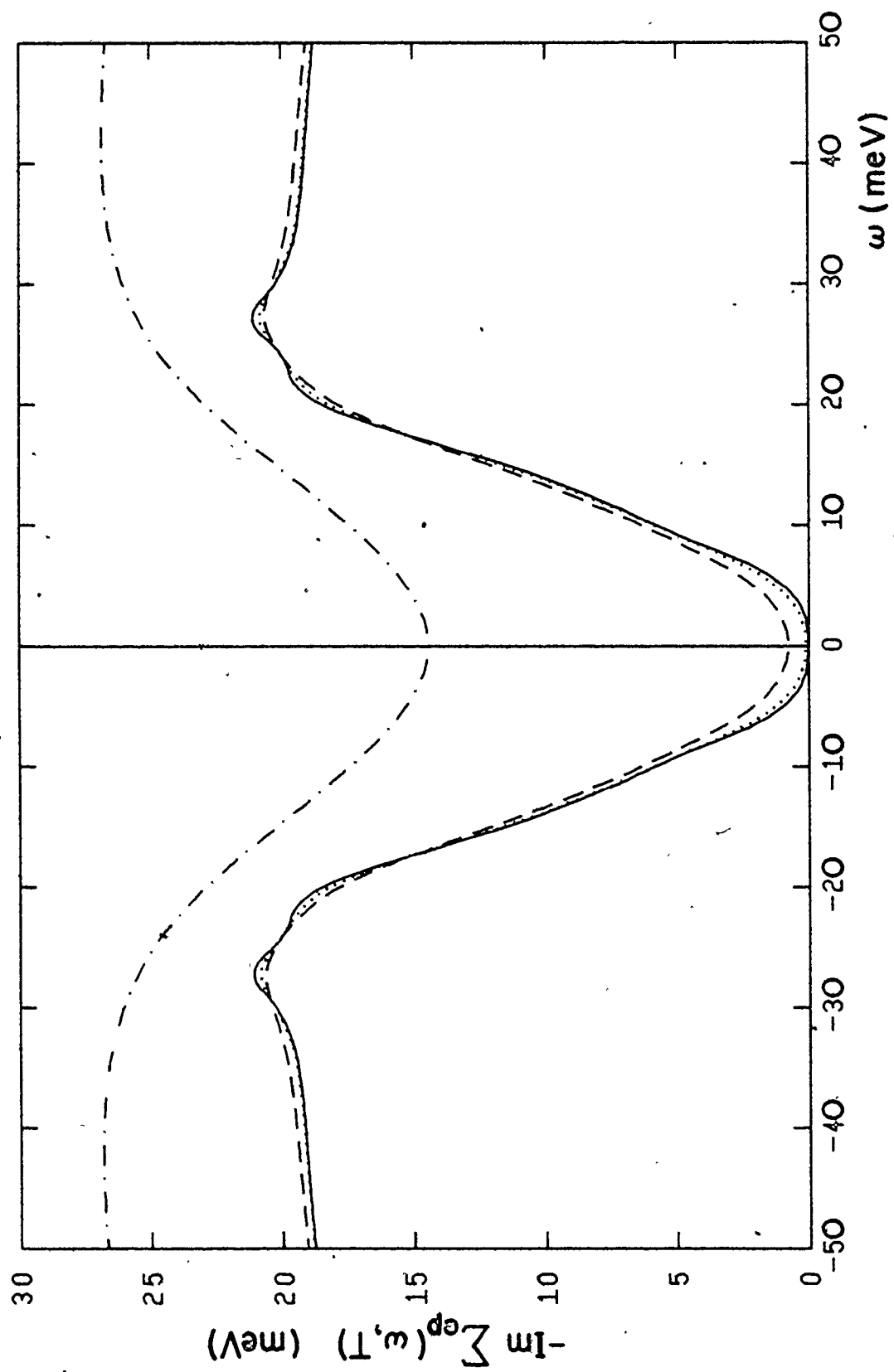


Fig.II.27

The quasiparticle density of states at four different temperatures.

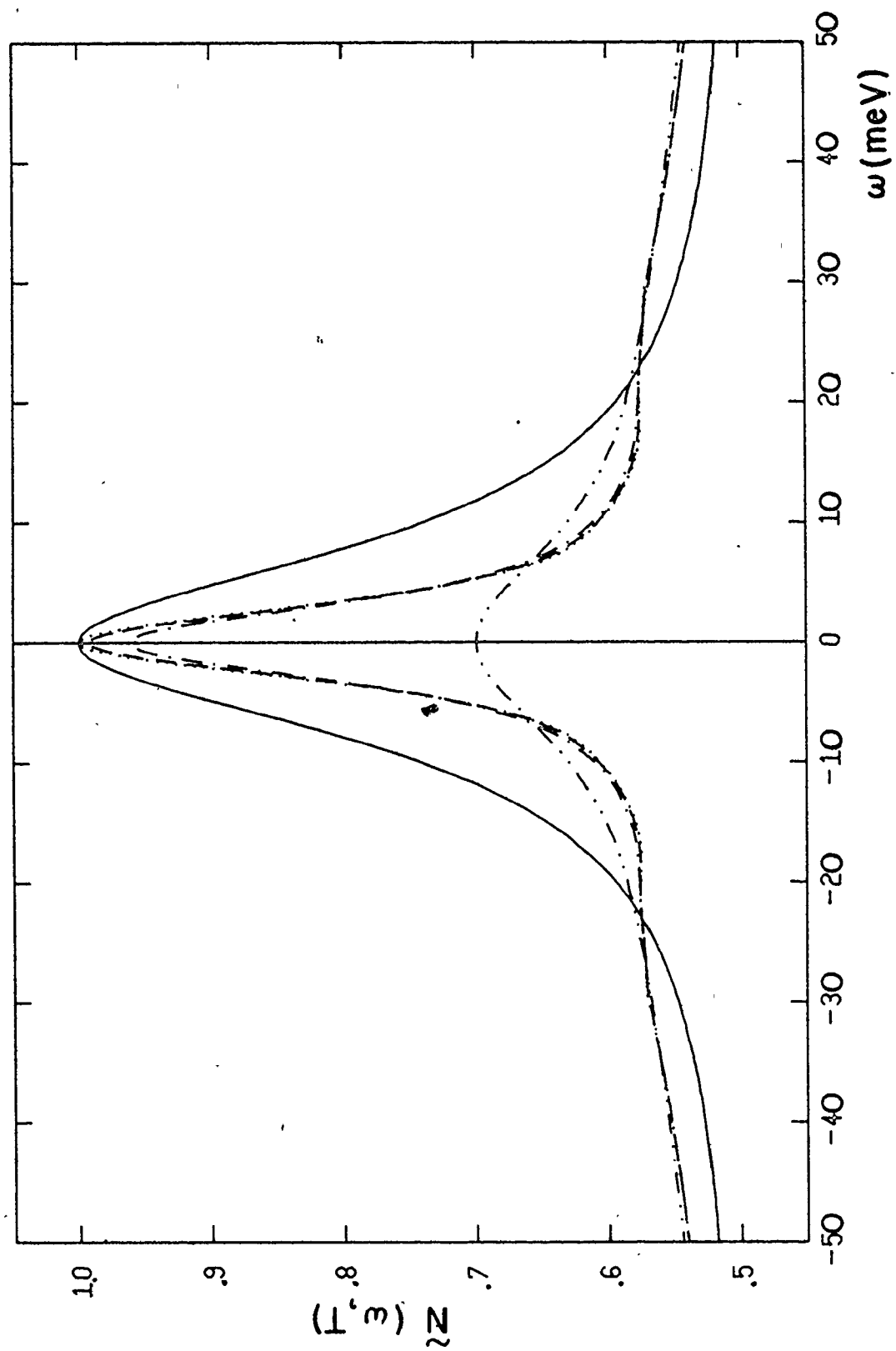
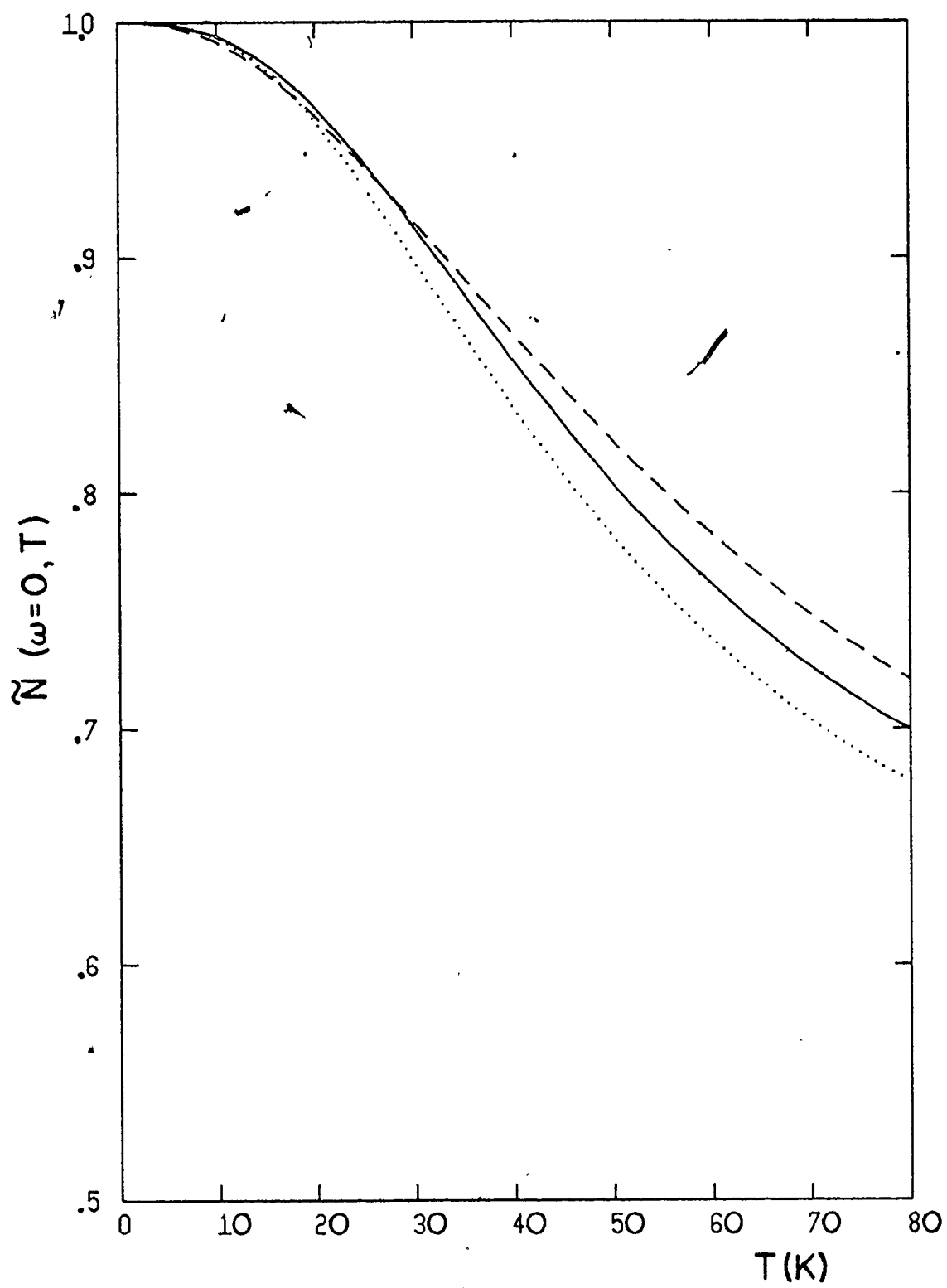


Fig.II.28

Temperature Dependence of the quasiparticle density of states at the chemical potential.



Nb_3Ge and Nb_3Al ¹⁶⁾ and experimental data on resistivity they have estimated that the peaks in EDOS for these two materials (with the size of the peak for Nb_3Ge similar to our choice) are virtually destroyed at $T = 80^\circ\text{K}$ and $T = 75^\circ\text{K}$, respectively, assuming the value of the electron-phonon mass enhancement parameter $\lambda = 1.7$. However, it is strictly speaking the quasiparticle density of states $N(0)\tilde{N}(\omega')$, defined by Eq. (II.33), that contains the information about the band structure EDOS and incorporates the lifetime effects. Our accurate numerical calculation, with the similar input parameters shows that their conclusion is more or less correct.

We have also calculated the temperature dependence of the electron mass enhancement parameter

$$\lambda(T) = -(\partial \text{Re}\Sigma_{\text{ep}}(\omega, T)/\partial \omega)_{\omega=0} \quad (\text{II.74})$$

which can normally be measured in cyclotron resonance experiments (for review see Ref. 58). We have calculated the temperature dependence of $\lambda(T)$ in the following four cases:

- 1) with the Lorentzian model ($a = 9.6 \text{ meV}$, $S/(\pi a) = 1$) for EDOS within the full self-consistent theory as described by Eq. (II.38) (solid lines in Figs. (II.29) and (II.30));
- 2) with the same Lorentzian model but taking the non self-consistent approach of Fradin which amounts to using the non-interacting Green's function in place of the full Green's

Fig.II.29

Temperature dependence of the electron-phonon mass renormalization parameter.

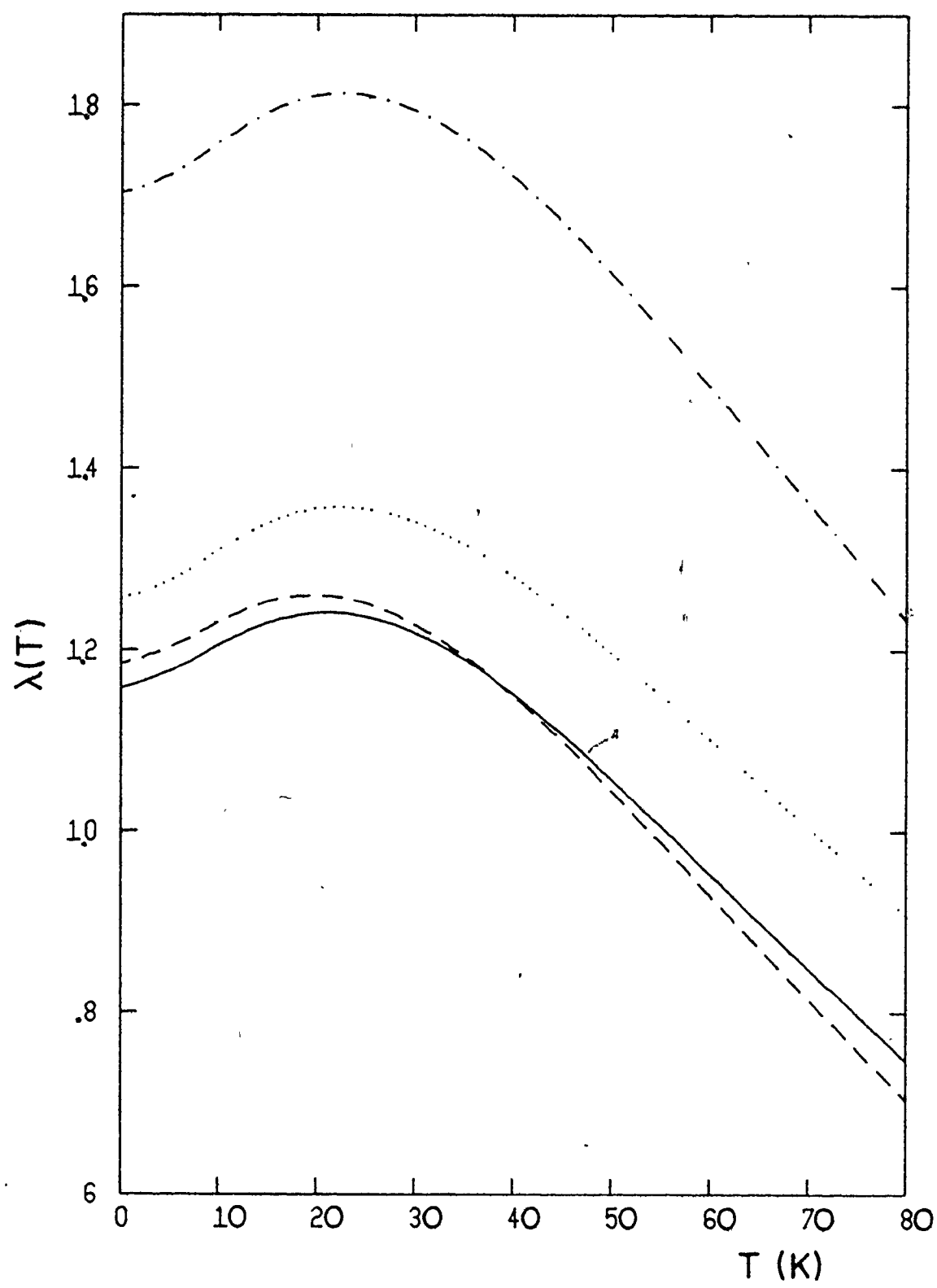
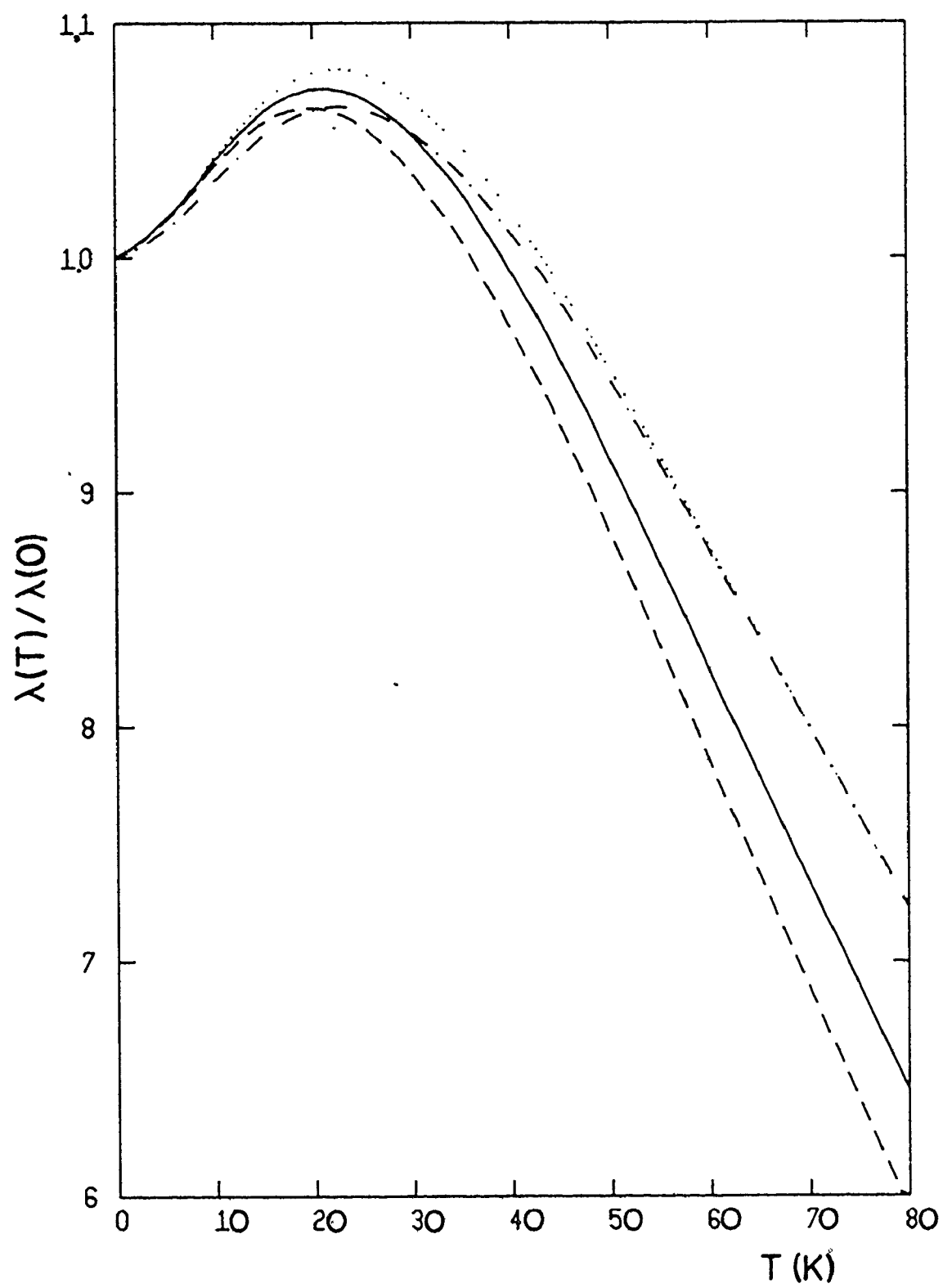


Fig.II.30

Temperature dependence of the electron-phonon mass renormalization parameter normalized to the value at $T=0$.



function in Eq. (II.30) (dotted lines in Figs. (II.29) and (II.30)). 3) By using the symmetric triangular model, Eq. (II.73), with $P-B = B$, and $E = 28.9$ meV so that it has approximately the same size as the above Lorentzian model (dashed lines). 4) Assuming a flat EDOS (dash-dot lines). In all four cases the input $\alpha^2 F$ -spectrum was the same, i.e. the one obtained by Shen from tunneling experiments on Nb_3Sn .

By comparing the solid and the dotted lines in Figs. (II.29) and (II.30) we see that the non self-consistent treatment overestimates the value of $\lambda(T)$ at all temperatures. At low T ($\lesssim 10^\circ K$) this overestimate is mainly coming from the lack of narrowing due to the renormalization of the quasi-particle density of states in the non self-consistent treatment. At temperatures $T \gtrsim 10^\circ K$ the effect of smearing $N(0)\tilde{N}(\omega)$ starts to play an important role.

In the case of a flat EDOS the quantity $\lambda(T)/\lambda(0)$ does not depend on the scale of the particular $\alpha^2(\Omega)F(\Omega)$ but on its shape as can be easily seen from Eq. (II.30) (see also ref. 73). Here however, the differences are coming from the fact that the EDOS is energy dependent in the range of several Debye energies around the Fermi level.

We point out that the above values of $\lambda(T)$ were calculated by numerical differentiation of the $\text{Re}\Sigma_{ep}(\omega, T)$ at $\omega = 0$, since in the case of energy dependent EDOS the thermal phonon term in Eq. (II.30) starts contributing to the renormalization

in analogy with the case of elastic impurity scattering. This prohibits the derivation of a simple formula for $\lambda(T)$, analogous to the Grimvall's expression⁷³⁾ in the case of a flat EDOS, which would be valid at all T . Even if one neglects the contribution of thermal phonons (i.e. the one coming from the last term in Eq. (II.30)) to $\lambda(T)$, the resulting expression

$$\lambda(T) = \int_0^{+\infty} d\omega \tilde{N}(\omega) \int_0^{+\infty} d\Omega \alpha^2(\Omega) F(\Omega) \left[\frac{f(-\omega)}{(\Omega+\omega)^2} + \frac{f(\omega)}{(\Omega-\omega)^2} \right] \quad (\text{II.75})$$

where we have assumed that $\tilde{N}(\omega)$ is even in ω , is of little use since the quantity $\tilde{N}(\omega)$ is unknown, unless one solves the complete problem. The formula analogous to (Eq. II.75) has been derived by Pickett⁴⁾.

The dashed curve in Fig. II.28 gives the temperature dependence of the normalized quasiparticle density of states at the chemical potential for the triangular model of EDOS. The dotted curve describes the same quantity for the Lorentzian model which is obtained after just one iteration. By comparing the solid and the dotted curve in Fig. II. 29 it is seen that, as in the case of impurity scattering, the temperature smearing of $\tilde{N}(\omega)$ caused by the electron-phonon interaction is to some extent self-limiting.

At present there is very little experimental information about the effects of the electron-phonon interaction in the normal state of the A-15 compounds with high superconducting

critical temperature, where one expects sharp peaks in EDOS. One of the main reasons for this is that the high upper critical fields in these materials require large magnetic fields (up to 400 kOe) to quench the superconducting state. Only very recently have the de Haas-van Alphen measurements been performed on Nb_3Sn and V_3Si in order to study the band structure in these materials near E_F ⁷⁴⁾.

In general, the single particle tunneling experiments into superconductors can provide the most detailed information about the electron-phonon interaction. In the following chapter we will analyse effects of sharp structure in EDOS on these experiments.

CHAPTER III

THE EFFECTS OF SHARP STRUCTURE IN THE ELECTRONIC DENSITY OF STATES ON THE SINGLE PARTICLE TUNNELING CHARACTERISTICS AND THERMODYNAMIC PROPERTIES OF SUPERCONDUCTORS.

III.1 THE ELIASHBERG EQUATIONS FOR STRONG COUPLING SUPERCONDUCTORS GENERALIZED TO INCLUDE THE ENERGY DEPENDENT ELECTRONIC DENSITY OF STATES

The problem of generalizing Eliashberg's theory for strong coupling superconductors to include all the complexities of the underlying band structure was first treated by Garland²⁴⁾. Only very recently, several more specific studies¹⁻⁴⁾ analyzed the effects of sharp structure in the electronic density of states (EDOS) on the superconducting critical temperature within the framework of Garland's formalism. Here we will give a brief outline of the Eliashberg equations generalized to include the effects of energy dependent EDOS, following the review article of P.B. Allen⁶⁰⁾ (see also ²⁴⁾).

In order to describe the pairing correlations in the superconducting state it is traditional to use Nambu's two-component formalism⁷⁵⁾. Within this formalism one can still apply the Feynman-Dyson many-body diagrammatic technique, with only a slight modification of the rules appropriate for the normal state (see Appendix 1). The two central objects of the

theory are the 2×2 matrix electron thermodynamic Green's function $\hat{G}(k, i\omega_n)$ and the corresponding self-energy part $\hat{\Sigma}(k, i\omega_n)$ which are related by the Dyson equation

$$\hat{G}^{-1}(k, i\omega_n) = \hat{G}_0^{-1}(k, i\omega_n) - \hat{\Sigma}(k, i\omega_n) . \quad (\text{III.1})$$

Here, $\hat{G}_0(k, i\omega_n)$ is the noninteracting electron thermodynamic Green's function

$$\hat{G}_0(k, i\omega_n) = \begin{pmatrix} 1/(i\omega_n - \epsilon_k) & 0 \\ 0 & -1/(i\omega_n + \epsilon_k) \end{pmatrix} . \quad (\text{III.2})$$

The meaning of other symbols is the same as in Sec. II.1.

In close analogy with the normal state, the electron-phonon contribution to $\hat{\Sigma}(k, i\omega_n)$ is given by (see Sec. II.1, Eq. (II.2))

$$\hat{\Sigma}_{\text{ep}}(k, i\omega_n) = -T \sum_{k'} \sum_{m=-\infty}^{+\infty} \sum_{\lambda} |g_{kk', \lambda}|^2 D_{\lambda}(k-k', i\omega_n - i\omega_m) \hat{\tau}_3 \hat{G}(k, i\omega_m) \hat{\tau}_3 \quad (\text{III.3})$$

where

$$\hat{\tau}_3 = \begin{pmatrix} 1 & 0 \\ 0 & -1 \end{pmatrix} \quad (\text{III.4})$$

and the other symbols have meanings analogous to those in the normal state (Sec. II.1). Eq. (III.3) is essentially Eliashberg's generalization of Migdal's equation (II.2) to the superconducting state³⁴⁻³⁵).

In the normal state the effect of the Coulomb interactions were included in the band-structure energies, screening and Coulomb vertex corrections of the electron-phonon coupling function. To include the effects of short-range screened Coulomb repulsion between the electrons on the pairing correlations it is necessary to add onto $\hat{\Sigma}_{ep}(k, i\omega_n)$ ⁶⁰⁾

$$\hat{\Sigma}_C(k) = -T \sum_{k'} \sum_{m=-\infty}^{+\infty} |V_{SC}(k-k')|^2 \hat{\tau}_3 \{ \hat{G}(k', i\omega_m) - \hat{G}_n(k', i\omega_m) \} \hat{\tau}_3 \quad (\text{III.5})$$

where $V_{SC}(k-k')$ is the screened Coulomb matrix element, which is assumed to depend only on the momentum transfer. Also, the static screening approximation is assumed. \hat{G}_n is the normal state limit of \hat{G} and is subtracted from it in order not to double count the effects of the Coulomb interaction, which have already been included in calculating the band structure energies. Since the off-diagonal part of \hat{G} , \hat{G}^{od} , corresponds to the pairing correlations ⁷⁵⁾, it is legitimate to approximate $\hat{G} - \hat{G}_n$, within the context of Eq. (III.5) for the Coulomb self-energy, with \hat{G}^{od}

$$\hat{G} - \hat{G}_n = \hat{G}^{od} \quad (\text{III.6})$$

This approximation is justified by the scales of characteristic energies ⁵⁷⁾ for the Coulomb interaction (1 eV per atom), electron-phonon interaction (10^{-4} eV per atom) and superconducting pairing correlations (10^{-7} eV per atom). Thus we take

$$\hat{\Sigma}_c(k) = -T \sum_k \sum_{m=-\infty}^{+\infty} |V_{sc}(k-k')|^2 \hat{\tau}_3 \hat{G}^{od}(k', i\omega_m) \hat{\tau}_3 \quad (\text{III.7})$$

as the Coulomb contribution to the total self-energy part in the superconducting state,

$$\hat{\Sigma}(k, i\omega_n) = \hat{\Sigma}_{ep}(k, i\omega_n) + \hat{\Sigma}_c(k, i\omega_n) \quad (\text{III.8})$$

After some algebra, identical to that which leads to Eq. (II.18), we obtain

$$\hat{\Sigma}_{ep}(i\omega_n) = T \sum_{m=-\infty}^{+\infty} \lambda(n-m) \int_{-\infty}^{+\infty} d\varepsilon \frac{N(\varepsilon)}{N(0)} \hat{\tau}_3 \hat{G}(\varepsilon, i\omega_m) \hat{\tau}_3 \quad (\text{III.9})$$

with

$$\lambda(n-m) = \int_0^{+\infty} d\Omega \alpha^2(\Omega) F(\Omega) \frac{2\Omega}{\Omega^2 + (\omega_n - \omega_m)^2} \quad (\text{III.10})$$

Here, we have made use of the approximation that the $\alpha^2 F(\Omega; \varepsilon, \varepsilon')$ defined by Eq. (II.19) does not depend on $\varepsilon, \varepsilon'$ in the range of several Debye energies around the chemical potential, as discussed in Sec. II.1.

An analogous treatment of the Coulomb contribution, Eq. (III.7), gives

$$\hat{\Sigma}_c(\varepsilon) = -T \sum_{m=-\infty}^{+\infty} \int_{-\infty}^{+\infty} d\varepsilon' N(\varepsilon') V_{sc}(\varepsilon, \varepsilon') \hat{\tau}_3 \hat{G}^{od}(\varepsilon', i\omega_m) \hat{\tau}_3 \quad (\text{III.11})$$

where

$$V_{sc}(\epsilon, \epsilon') = \left[\sum_{k, k'} |V_{sc}(k-k')|^2 \delta(\epsilon - \epsilon_k) \delta(\epsilon - \epsilon_{k'}) \right] / (N(\epsilon) N(\epsilon')) \quad (III.12)$$

For computation purposes it is convenient to exploit the above mentioned relation between the characteristic energy scales of the basic interactions and rewrite Eq. (III.11) in a form which involves only the sum over the excitation energies within a range about one order of magnitude larger than the maximum phonon frequency $\omega_{\max} (\approx \omega_D)$. For $|\omega_m| > \omega_c$, with $\omega_c \sim 10 \omega_{\max}$

$$\hat{G}^{od}_{(\epsilon', i\omega_m)} \approx \frac{\hat{\Sigma}_c(\epsilon')}{(i\omega_m)^2 - \epsilon'^2} \quad (III.13)$$

and since

$$\hat{\tau}_3 \hat{G} \hat{\tau}_3 = \hat{\tau}_3 (\hat{G}^d + \hat{G}^{od}) \hat{\tau}_3 = \hat{G}^d - \hat{G}^{od} \quad (III.14)$$

Eq. (II.11) can be written as

$$\begin{aligned} & \int_{-\infty}^{+\infty} d\epsilon' \{ \delta(\epsilon - \epsilon') + T \sum_{|\omega_m| > \omega_c} N(\epsilon') \frac{V_{sc}(\epsilon, \epsilon')}{\omega_m^2 + \epsilon'^2} \} \hat{\Sigma}_c(\epsilon') = \\ & = - T \sum_{|\omega_m| < \omega_c} \int_{-\infty}^{+\infty} d\epsilon' N(\epsilon') V_{sc}(\epsilon, \epsilon') \hat{\tau}_3 \hat{G}^{od}_{(\epsilon', i\omega_m)} \hat{\tau}_3 \quad (III.15) \end{aligned}$$

The left-hand side of the above equation has the structure

$$\int_{-\infty}^{+\infty} d\epsilon' M(\epsilon, \epsilon') \hat{\Sigma}_c(\epsilon') \quad (III.16)$$

with

$$M(\varepsilon, \varepsilon') = \delta(\varepsilon - \varepsilon') + TN(\varepsilon') V_{SC}(\varepsilon, \varepsilon') \sum_{|\omega_m| > \omega_c} \frac{1}{\omega_m^2 + \varepsilon'^2} \quad (\text{III.17})$$

Since the second term in the kernel $M(\varepsilon, \varepsilon')$ is positive, the linear integral operator $\int_{-\infty}^{+\infty} d\varepsilon' M(\varepsilon, \varepsilon')$ cannot map a nonzero function into zero, i.e. it is nonsingular. Therefore, it can be inverted. By applying the inverse, $\int_{-\infty}^{+\infty} d\varepsilon' M'(\varepsilon, \varepsilon')$, of the above operator to both sides of Eq. (III.15) we obtain

$$\hat{\Sigma}_C(\varepsilon) = -T \sum_{m=-\infty}^{+\infty} \theta(\omega_c - |\omega_m|) \int_{-\infty}^{+\infty} d\varepsilon' \frac{N(\varepsilon')}{N(0)} U(\varepsilon, \varepsilon') \hat{\tau}_3 \hat{G}^{od}(\varepsilon', i\omega_m) \hat{\tau}_3 \quad (\text{III.18})$$

where

$$U(\varepsilon, \varepsilon') = N(0) \int_{-\infty}^{+\infty} d\varepsilon'' M'(\varepsilon, \varepsilon'') V_{SC}(\varepsilon'', \varepsilon') \quad (\text{III.19})$$

is the so-called Coulomb pseudopotential. An integral equation for $U(\varepsilon, \varepsilon')$ can be obtained by applying the operator $\int_{-\infty}^{+\infty} d\varepsilon M(\varepsilon_1, \varepsilon)$ on both sides of Eq. (III.19). The result is (see Eq. (III.17))

$$\begin{aligned} U(\varepsilon_1, \varepsilon') + T \int_{-\infty}^{+\infty} d\varepsilon \frac{N(\varepsilon)}{N(0)} N(0) V_{SC}(\varepsilon_1, \varepsilon) U(\varepsilon, \varepsilon') \sum_{|\omega_m| > \omega_c} \frac{1}{\omega_m^2 + \varepsilon^2} \\ = N(0) V_{SC}(\varepsilon_1, \varepsilon') \end{aligned} \quad (\text{II.20})$$

We are interested in $\hat{\Sigma}_C(\epsilon)$ for ϵ in the vicinity of $\epsilon=0$. Since the factor $\hat{\tau}_3 \hat{G}^{od} \hat{\tau}_3$ in Eq. (III.18) drops off very rapidly for $\epsilon > \omega_C$ (see below) and since, as can be seen from Eq. (III.20), $U(0, \epsilon')$ varies slowly for $|\epsilon'| < \omega_C$ (the scale of variation in $U(0, \epsilon')$ with ϵ' is the same as for $V(0, \epsilon')$, of the order of Fermi energy) $U(\epsilon, \epsilon')$ in Eq. (III.18) will be evaluated at $\epsilon = \epsilon' = 0$. Calling

$$\mu^*(\omega_C) = U(0, 0) \quad (III.21)$$

our final result for the Coulomb contribution to the total self-energy part is

$$\hat{\Sigma}_C = -T \sum_{m=-\infty}^{+\infty} \mu^*(\omega_C) \theta(\omega_C - |\omega_m|) \int_{-\infty}^{+\infty} d\epsilon' \frac{N(\epsilon')}{N(0)} \hat{\tau}_3 \hat{G}^{od}(\epsilon', i\omega_m) \hat{\tau}_3. \quad (III.22)$$

It is convenient to decompose $\hat{\Sigma}(i\omega_n)$ into the various (linearly independent) matrix components. Since Pauli matrices together with the unit 2×2 matrix

$$\hat{\tau}_1 = \begin{pmatrix} 0 & 1 \\ 1 & 0 \end{pmatrix}, \quad \hat{\tau}_2 = \begin{pmatrix} 0 & -i \\ i & 0 \end{pmatrix}, \quad \hat{\tau}_3 = \begin{pmatrix} 1 & 0 \\ 0 & -1 \end{pmatrix}, \quad \hat{\tau}_0 = \begin{pmatrix} 1 & 0 \\ 0 & 1 \end{pmatrix},$$

form a basis in the four-dimensional complex vector space of 2×2 matrices it is possible to write

$$\hat{\Sigma}(i\omega_n) = i\omega_n (1 - Z(i\omega_n)) \hat{\tau}_0 + \phi(i\omega_n) \hat{\tau}_1 + \bar{\phi}(i\omega_n) \hat{\tau}_2 + \chi(i\omega_n) \hat{\tau}_3. \quad (III.24)$$

Also, from (III.1) and (III.2)

$$\hat{G}(\varepsilon, i\omega_n) = [i\omega_n Z(i\omega_n) \hat{\tau}_0 + (\varepsilon_k + \chi(i\omega_n)) \hat{\tau}_3 + \phi(i\omega_n) \hat{\tau}_1 + \bar{\phi}(i\omega_n) \hat{\tau}_2] / \det G^{-1}(\varepsilon, i\omega_n) \quad (\text{III.25})$$

$$\det(\hat{G}^{-1}) = (i\omega_n Z(i\omega_n))^2 - (\varepsilon + \chi(i\omega_n))^2 - \phi^2(i\omega_n) - \bar{\phi}^2(i\omega_n). \quad (\text{III.26})$$

By substituting (III.24), (III.25) and (III.26) into (III.8), with $\hat{\Sigma}_{ep}$ and $\hat{\Sigma}_c$ given by (III.10) and (III.22) respectively, and by equating coefficients of the various Pauli matrices, the following equations can be obtained:

$$i\omega_n Z(i\omega_n) = i\omega_n + \pi T \sum_{m=-\infty}^{+\infty} \lambda(n-m) \left[\frac{1}{\pi} \int_{-\infty}^{+\infty} d\varepsilon \frac{N(\varepsilon)}{N(0)} \frac{i\omega_m Z(i\omega_m)}{(-\det G^{-1}(\varepsilon, i\omega_m))} \right] \quad (\text{III.27a})$$

$$\chi(i\omega_n) = -\pi T \sum_{m=-\infty}^{+\infty} \lambda(n-m) \left[\frac{1}{\pi} \int_{-\infty}^{+\infty} d\varepsilon \frac{N(\varepsilon)}{N(0)} \frac{\varepsilon + \chi}{(-\det G^{-1}(\varepsilon, i\omega_m))} \right] \quad (\text{III.27b})$$

$$\phi(i\omega_n) = \pi T \sum_{m=-\infty}^{+\infty} [\lambda(n-m) - \mu^*(\omega_c) \theta(\omega_c - |\omega_m|)] \left[\frac{1}{\pi} \int_{-\infty}^{+\infty} d\varepsilon \frac{N(\varepsilon)}{N(0)} \frac{\phi(i\omega_m)}{(-\det G^{-1}(\varepsilon, i\omega_m))} \right] \quad (\text{III.27c})$$

and an equation for $\bar{\phi}(i\omega_n)$ which has the form identical to the Eq. (III.27). At the superconducting critical temperature T_c the pairing self-energies ϕ , $\bar{\phi}$ become small and the ϕ^2 , $\bar{\phi}^2$ appearing in $\det G^{-1}(\varepsilon, i\omega_n)$ can be set equal to zero. Thus at T_c Eqs. (III.27a) and (III.27b) decouple from Eq. (III.27c) and the corresponding equation for $\bar{\phi}$. Also, equations for ϕ and $\bar{\phi}$ become linear homogeneous equations independent of each other.

For $T \geq T_c$ the quantities $Z(i\omega_n)$ and $\chi(i\omega_n)$ are the ones defined by Eqs. (II.45a) and (II.45b) and therefore they are even functions of $i\omega_n$. Assuming that there is no spin dependent interaction one can show ⁶⁰⁾ that $G_{11}(k, i\omega_n) = -G_{22}(-k, -i\omega_n)$. Therefore $\phi^2(i\omega_n) + \bar{\phi}^2(i\omega_n)$ must be an even function of $i\omega_n$. Since at T_c ϕ and $\bar{\phi}$ are not coupled, each one of them must be an even function of $i\omega_n$.

For calculating the equilibrium properties the $\hat{\tau}_2$ -component of $\hat{\Sigma}$ can be transformed away by choosing the phases of single-particle states $|k\rangle$, used to define creation ($C_{k\sigma}^\dagger$) and destruction ($C_{k\sigma}$) operators, in the appropriate way (see Ref. 75, Eq. (2.20)). Therefore, one has only to solve Eqs. (III.27a)-(III.27c) plus the equation for the chemical potential in terms of the average number of particles \bar{N}

$$\bar{N} = 2T \sum_k \sum_{m=-\infty}^{+\infty} \hat{G}_{11}(k, i\omega_n) e^{i\omega_n O^+} \quad (\text{III.28})$$

where \hat{G}_{11} is (1,1)-component of the matrix \hat{G} . Eq. (III.28) is completely analogous to Eq. (II.7), appropriate to the normal state.

In Sec. (III.3) we shall study the thermodynamic properties of a strong coupling superconductor taking a symmetric Lorentzian model for EDOS. For that purpose it is sufficient to consider only the imaginary axis form of the Eliashberg equations (III.27a)-(III.27c). On the other hand, to

study, for example, the single particle tunneling experiments (Sec. III.2) one needs the retarded 2×2 matrix thermodynamic Green's function and the corresponding self-energy part for the real values of their frequency arguments, i.e. $\hat{G}(\epsilon, \omega + i\delta)$, $\hat{\Sigma}(\omega + i\delta)$. There are two alternatives for obtaining $\hat{G}(\epsilon, \omega + i\delta)$ and $\hat{\Sigma}(\omega + i\delta)$. The first one is to set up and solve the Eliashberg equations on the real frequency axis; the second is to find some numerical procedure for analytic continuation of the imaginary frequency axis solution. Serene and Vidberg⁷⁶⁾ have found a method for an analytic continuation by means of N-point Padé approximants. The method of Serene and Vidberg works well⁷⁶⁾ at low temperatures when the spacing between successive Matsubara⁽²⁾ frequencies is small. However, even then the method does not give analytically continued functions which are exactly the same as the corresponding solutions of the Eliashberg equations on the real frequency axis. This is, presumably, due to the intrinsic limitations of the N-point Padé approximant method⁷⁶⁾. We have used this method to calculate the normalized tunneling conductance $\sigma(\omega)$ from the imaginary frequency axis solutions of the Eliashberg equations generalized to include the rapidly varying EDOS⁶⁾. Although certain trends were observable, we did not know to what extent the modifications in calculated $\sigma(\omega)$, compared to its form when the EDOS is assumed to be flat, resulted just from the intrinsic limitations of the method, especially in the

range $\omega \gtrsim \omega_{\max}$ where it is expected⁷⁶⁾ that the method starts to fail and where the modifications turned out to be large. For this reason we have decided to formulate and solve the modified Eliashberg equations on the real frequency axis. It turned out that the method of N-point Padé approximants was describing correctly the trends in the changes of $\sigma(\omega)$ due to peaks in EDOS throughout the whole frequency range considered (from $\omega = \Delta_0$ up to $\omega = 1.5 \omega_{\max} + \Delta_0$), but the details were somewhat different from the real axis solutions.

To obtain the analytic continuation of Eqs. (III.3) and (III.5) to the real frequency axis it is necessary to repeat step by step the procedure given in Sec. (II.1). The result is

$$\begin{aligned} \hat{\Sigma}_{\text{ep}}(\omega+i\eta) = & \int_{-\infty}^{+\infty} d\omega' \left\{ -\frac{1}{\pi} \operatorname{Im} \int_{-\infty}^{+\infty} d\varepsilon \frac{N(\varepsilon)}{N(0)} \hat{\tau}_3 \hat{G}(\varepsilon, \omega' + i\delta) \hat{\tau}_3 \right\} \times \\ & \times \int_0^{+\infty} d\Omega \alpha^2(\Omega) F(\Omega) \left\{ \frac{1}{\omega - \omega' - \Omega + i\eta} \frac{1}{e^{\beta\omega'} + 1} + \frac{1}{\omega - \omega' + \Omega + i\eta} \frac{1}{e^{\beta\omega'} + 1} \right\} + \\ & + \int_0^{+\infty} d\Omega \frac{\alpha^2(\Omega) F(\Omega)}{e^{\beta\Omega} - 1} \int_{-\infty}^{+\infty} d\varepsilon \frac{N(\varepsilon)}{N(0)} [\hat{\tau}_3 \hat{G}(\varepsilon, \omega - \Omega + i\eta) \hat{\tau}_3 + \hat{\tau}_3 \hat{G}(\varepsilon, \omega + \Omega + i\eta) \hat{\tau}_3] \end{aligned} \quad (\text{III.29})$$

and

$$\begin{aligned} \hat{\Sigma}_{\text{c}}(\varepsilon) = & \int_{-\infty}^{+\infty} d\omega \left\{ -\frac{1}{\pi} \operatorname{Im} \int_{-\infty}^{+\infty} d\varepsilon' N(\varepsilon') V_{\text{sc}}(\varepsilon, \varepsilon') \hat{\tau}_3 \hat{G}^{\text{od}}(\varepsilon', \omega + i\delta) \hat{\tau}_3 \right\} \times \\ & \times \frac{1}{2} \tanh\left(\frac{\beta\omega}{2}\right) \end{aligned} \quad (\text{III.30})$$

where η and δ are positive infinitesimals.

From Eqs. (II.49a) and (II.49b) it follows that in the normal state

$$\chi(-\omega+i\eta) = \chi^*(\omega+i\eta) \quad , \quad Z(-\omega+i\eta) = Z^*(\omega+i\eta) \quad (\text{II.31a,b,})$$

These relations should hold in the superconducting state as well.

Therefore (see Eq. (III.26)) $\phi^2(\omega+i\eta)$ must have a property

analogous to (III.31a,b), which implies $\phi(-\omega+i\delta) = \pm\phi^*(\omega+i\delta)$.

From the spectral representation for, say, \hat{G}_{12}^{77} and the fact that $\phi(i\omega_n)$ is an even function of $i\omega_n$ it follows that

$$\phi(-\omega+i\delta) = \phi^*(\omega+i\delta) \quad . \quad (\text{II.31c})$$

By using (III.31a,b,c) one finds

$$\text{Im}[\hat{\tau}_3 \hat{G}^{\text{od}}(\epsilon', -\omega' + i\delta) \hat{\tau}_3] = -\text{Im}[\hat{\tau}_3 \hat{G}^{\text{od}}(\epsilon', \omega' + i\delta) \hat{\tau}_3] \quad .$$

Also the $\hat{\tau}_0$ -component of $\text{Im} \hat{\tau}_3 \hat{G}^{\text{d}}(\epsilon', \omega + i\delta) \hat{\tau}_3$ does not change sign when $\omega \rightarrow -\omega$, while its $\hat{\tau}_3$ component does change sign under such a transformation. Knowing this we can transform Eq. (II.29) into

$$\begin{aligned} \hat{\Sigma}_{\text{ep}}^{\text{d}}(\omega+i\eta) = & \hat{\tau}_0 \int_0^{+\infty} d\omega' \tilde{N}_Z(\omega' + i\delta) [f(-\omega') K_-(\omega, \omega') + f(\omega') K_-(\omega, -\omega')] + \\ & + \hat{\tau}_3 \int_0^{+\infty} d\omega' \tilde{N}_X(\omega' + i\delta) [f(-\omega') K_+(\omega, \omega') - f(\omega') K_+(\omega, -\omega')] \\ & + \int_0^{+\infty} d\Omega \frac{\alpha^2(\Omega) F(\Omega)}{e^{\beta\Omega} - 1} \int_{-\infty}^{+\infty} d\epsilon \frac{N(\epsilon)}{N(0)} [\hat{\tau}_3 \hat{G}^{\text{d}}(\epsilon, \omega - \Omega + i\delta) \hat{\tau}_3 + \hat{\tau}_3 \hat{G}^{\text{d}}(\epsilon, \omega + \Omega + i\delta) \hat{\tau}_3] \end{aligned} \quad (\text{III.32})$$

$$\begin{aligned}
\hat{\Sigma}_{ep}^{od}(\omega+i\eta) = & \int_0^{+\infty} d\omega' \tilde{N}_{\Delta}(\omega'+i\delta) [f(-\omega')K_+(\omega, \omega') - f(\omega')K_+(\omega, -\omega')] \hat{\tau}_1 + \\
& + \int_0^{+\infty} d\Omega \frac{\alpha^2(\Omega)F(\Omega)}{e^{\beta\Omega}-1} \int_{-\infty}^{+\infty} d\varepsilon \frac{N(\varepsilon)}{N(0)} [\hat{\tau}_3 \hat{G}^{od}(\varepsilon, \omega-\Omega+i\eta) \hat{\tau}_3 + \\
& + \hat{\tau}_3 \hat{G}^{od}(\varepsilon, \omega+\Omega+i\eta) \hat{\tau}_3] .
\end{aligned} \tag{III.33}$$

Here

$$\tilde{N}_Z(\omega+i\delta) = -\frac{1}{\pi} \text{Im} \int_{-\infty}^{+\infty} d\varepsilon \frac{N(\varepsilon)}{N(0)} \frac{\omega Z(\omega+i\delta)}{D(\varepsilon, \omega+i\delta)} \tag{III.34a}$$

$$\tilde{N}_\chi(\omega+i\delta) = \frac{1}{\pi} \text{Im} \int_{-\infty}^{+\infty} d\varepsilon \frac{N(\varepsilon)}{N(0)} \frac{\varepsilon + \chi(\omega+i\delta)}{D(\varepsilon, \omega+i\delta)} \tag{III.34b}$$

$$\tilde{N}_{\Delta}(\omega+i\delta) = -\frac{1}{\pi} \text{Im} \int_{-\infty}^{+\infty} d\varepsilon \frac{N(\varepsilon)}{N(0)} \frac{\phi(\omega+i\delta)}{D(\varepsilon, \omega+i\delta)} \tag{III.34c}$$

with

$$D(\varepsilon, \omega+i\delta) = \omega^2 Z^2(\omega+i\delta) - \phi^2(\omega+i\delta) - (\varepsilon + \chi(\omega+i\delta))^2 . \tag{III.34d}$$

Also

$$K_{\pm}(\omega, \omega') = \int_0^{+\infty} d\Omega \alpha^2(\Omega) F(\Omega) \left[\left(\frac{1}{\omega' + \omega + \Omega - i\eta} \right)^* \pm \left(\frac{1}{\omega' - \omega + \Omega - i\eta} \right) \right] \tag{III.35}$$

Since the function under the ω' -integral in (III.30) is even in ω' , the Coulomb contribution can be written in the form

$$\hat{\Sigma}_C = -\hat{\tau}_1 \int_0^{+\infty} d\omega' \tilde{N}_\Delta(\omega' + i\delta) \tanh\left(\frac{\beta\omega'}{2}\right) \mu^*(\omega_C) \theta(\omega_C - \omega') \quad (\text{III.36})$$

where the Coulomb pseudopotential $(\omega_C, \mu^*(\omega_C))$ has been introduced in a way analogous to our previous treatment of the imaginary frequency equations.

In the following section we will solve these generalized Eliashberg equations on the real frequency axis at $T=0$ to study the zero temperature single particle tunneling experiments in a superconductor with rapidly varying EDOS near the Fermi level.

III.2 TUNNELING IN A SUPERCONDUCTOR WITH AN ENERGY DEPENDENT ELECTRONIC DENSITY OF STATES

In this section we solve generalized Eliashberg equations on the real frequency axis at $T = 0$ for the model electronic density of states (EDOS), Eq. (II.40), which approximates the result of the band structure calculations¹⁴⁾ for Nb_3Sn . We also study the effects of a rapidly varying EDOS on single particle tunneling experiments. These experiments can provide the most detailed information about the electron-phonon interaction, i.e. $\alpha^2(\Omega)F(\Omega)$, in superconducting materials via inversion of Eliashberg equations³⁰⁾. It is precisely within the context of these experiments in numerous polyvalent simple metals and their alloys³¹⁾ that the accuracy of the usual Eliashberg theory, which assumes a constant EDOS, was confirmed to within a few percent (see Ref. 30, Sec. VI.C). However, such experiments on transition metals and their compounds have been difficult to perform and interpret⁷⁸⁻⁸³⁾. The main reason for this difficulty is that with these materials it is very difficult to produce good quality tunneling barriers by the usual thermal oxidation method⁷⁸⁾. Experimental results suggest^{78,80)} that when the tunneling barrier is thermally grown, a thin layer of normal material having a much smaller critical temperature T_c may form between the superconductor and insulating tunneling barrier. Thus in the tunneling experiment one is sampling

not the bulk properties of the superconductor which is being studied but rather the properties of superconductor-normal layer proximity sandwich. Only very recently a quantitative analysis of such an experimental situation has been proposed⁸⁴⁾ and performed on several transition metals⁸⁵⁻⁸⁷⁾, their alloys⁸⁵⁾ and compounds such as A-15 compounds⁸⁷⁻⁹⁰⁾. In this procedure⁸⁶⁾, the normal layer is characterized by two parameters which are then self-consistently determined by the inversion program modified to include the presence of the proximity sandwich, along with the bulk values of $\alpha^2(\Omega)F(\Omega)$ and $\mu^*(\omega_c)$.

However, it is not always clear whether a normal layer is formed⁸⁶⁻⁸⁹⁾ particularly for some A-15 materials where the tunneling junctions were fabricated by first depositing a thin layer of Si on the superconducting film before exposure to the atmosphere⁸⁹⁾. There, the attitude is taken that if the usual McMillan-Rowell inversion procedure³⁰⁾ gives anomalous values for α^2F and μ^* (too small values of $\lambda = 2 \int_0^\infty d\Omega \alpha^2(\Omega)F(\Omega)/\Omega$ and negative values of μ^*) the existence of a proximity sandwich is assumed and the experimental results are inverted by taking into account the proximity effect⁸⁴⁾. It should be noted that in the case of Nb an alternative explanation of the anomalous results of the tunneling experiments has been given⁹⁰⁾; transparency of the tunneling barrier was assumed and the experimental results were inverted by taking into account this transparency, with as much success as in the case

of proximity sandwich model.

Here we will illustrate the possible effects of a sharp structure in EDOS on the $T=0$ single particle tunneling experiments assuming an ideal tunneling experiment in which none of the above difficulties with the tunneling barrier is present.

At $T=0$ the Eliashberg equations generalized to include EDOS are (see Sec. III.1)

$$\Delta(\omega+i\eta)Z(\omega+i\eta) = \int_0^{+\infty} d\omega' \tilde{N}_\Delta(\omega'+i\delta) [K_+(\omega, \omega') - \mu^*(\omega_c) \theta(\omega_c - \omega')] \quad (\text{III.37a})$$

$$\omega(1-Z(\omega+i\eta)) = \int_0^{+\infty} d\omega' \tilde{N}_Z(\omega'+i\delta) K_-(\omega, \omega') \quad (\text{III.37b})$$

$$\chi(\omega+i\eta) = \int_0^{+\infty} d\omega' \tilde{N}_\chi(\omega'+i\delta) K_+(\omega, \omega') , \quad (\text{III.37c})$$

where

$$\Delta^*(\omega+i\delta) \equiv \phi(\omega+i\delta)/Z(\omega+i\delta) \quad (\text{III.37d})$$

is the so-called gap-function. We have solved these equations for EDOS $N(E)$ given by Eq. (II.40). For the input $\alpha^2(\Omega)F(\Omega)$ -spectrum we have taken Shen's result for Nb_3Sn ($\lambda = 1.7$) and $\mu^*(\omega_c) = 0.18$ with $\omega_c = 180 \text{ meV}^{91}$.

Note that, as in the normal state, EDOS appearing in

Eqs. (III-37a)-(III.37c) via \tilde{N}_Δ , \tilde{N}_Z and \tilde{N}_χ (see their definition in Sec. III.1) is $N(\epsilon)$, where ϵ is measured with respect to the true interacting chemical potential. The relationship between the band-structure energies E , measured with respect to the bare band chemical potential, and ϵ is

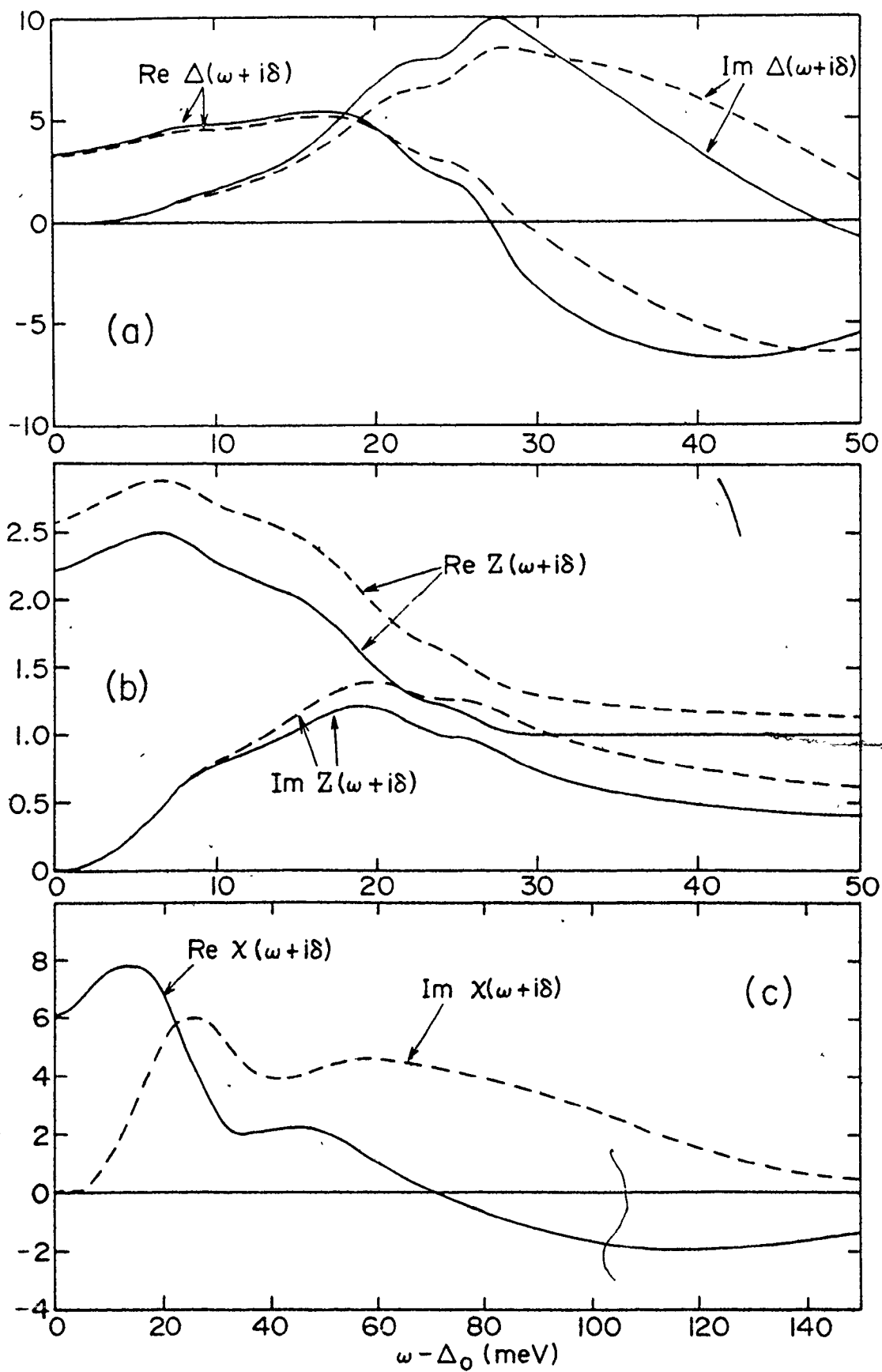
$$E(\epsilon) = \epsilon + \text{Re}\chi(0+i\delta) . \quad (\text{III.38})$$

As in the normal state calculations which were described in Sec. II.2, $N(\epsilon)$ was redefined at each stage of iteration according to Eq. (III.38). The quantities \tilde{N}_Δ , \tilde{N}_Z and \tilde{N}_χ were calculated analytically for the given $N(\tilde{E})$ (see Appendix II).

In Figs. (III.1a)-(III.1c) we present solutions of Eqs. (III.37a)-(III.37c) (solid lines) together with corresponding solutions when the electronic density of states is taken to be constant and equal to $N(E=0)$ (dashed lines). Note the strong resemblance to the corresponding results of the normal state calculations (Figs. (II.8), (II.9) and (II.11)), as one would expect for the diagonal part of the superconducting self-energy. However, since quite different numerical routines were followed in the superconducting and normal state calculations, with the algorithm for the superconducting state being more complicated and tedious than in the case of the usual Eliashberg equations, we find such resemblance very reassuring.

Fig.III.1

Solutions of Eliashberg equations. Dashed lines in (a) and (c) correspond to the case of constant electronic density of states equal to $N(0)$.



Upon careful examination of the expressions for \tilde{N}_Δ and \tilde{N}_Z for the triangular model of EDOS one can argue that the first two equations for Δ and Z , Eqs. (III.37a)-(III.37b), are largely independent of Eq. (III.37c) for χ . More precisely, one can argue that χ can be set equal to zero when solving Eqs. (III.37a) and (III.37b) for Δ and Z . (This is equivalent to stating that χ vanishes.) We have verified this argument explicitly for our model of EDOS, Eq. (II.40), by numerical solution of Eqs. (III.37a) and (III.37b) where χ was set equal to zero as an external constraint.

The main effect of energy dependence in $N(E)$ is that the quasiparticle density of states

$$N(0)(\tilde{N}_Z(\omega+i\eta) - \tilde{N}_\chi(\omega+i\eta)) = -\frac{1}{\pi} \operatorname{Im} \int_{-\infty}^{+\infty} d\varepsilon N(\varepsilon) G_{11}(\varepsilon, \omega+i\eta) \quad (\text{III.39})$$

and the analogous quantity in the gap equation, $N(0)\tilde{N}_\Delta$, are modulated by the underlying band-structure EDOS. Close to the gap edge $\Delta_0 = \operatorname{Re}\Delta(\omega=\Delta_0)$ these quantities are dominated by the superconducting square-root singularity while for $\omega \gtrsim \omega_{\max}$ ($\approx \omega_D$) the quasiparticle density of states is mainly determined by $N(\varepsilon)$. The actual analytic expressions for \tilde{N}_Δ , \tilde{N}_Z and \tilde{N}_χ with the triangular model for $N(E)$, Eq. (II.40), are long and uninteresting (see Appendix II). For the symmetric Lorentzian model $N(\varepsilon) = N_b(1 + (s/\pi)a/(a^2 + \varepsilon^2))$ the quasiparticle density of states is

$$\begin{aligned}
N(0)\tilde{N}_Z(\omega+i\delta) = & \operatorname{Re}[\omega/(\omega^2-\Delta^2(\omega))^{1/2}] \{ [N_b [1 + \frac{s}{\pi} \operatorname{Re} \frac{a+iZ(\omega)(\omega^2-\Delta^2(\omega))^{1/2}}{a^2+Z^2(\omega)(\omega^2-\Delta^2(\omega))}] - \\
& - N_b \frac{s}{\pi} \operatorname{Im}[\omega/(\omega^2-\Delta^2(\omega))^{1/2}] \operatorname{Im} \frac{a+iZ(\omega)(\omega^2-\Delta^2(\omega))^{1/2}}{a^2+Z^2(\omega)(\omega^2-\Delta^2(\omega))}] \} \quad (\text{III.40})
\end{aligned}$$

We note that the root $(\omega^2-\Delta^2(\omega))^{1/2}$ is chosen in such a way that $Z(\omega)(\omega^2-\Delta^2(\omega))^{1/2}$ has a positive imaginary part. Although the above expression is less transparent than the corresponding formula for the quasiparticle density of states in the normal state, Eq. (II.36), it can be seen that the renormalization due to the electron-phonon interaction acts in the similar way as in the normal state, i.e. the energies become renormalized $(\omega \rightarrow \omega Z(\omega))$.

In order to calculate the normalized tunneling conductance³⁰⁾ $\sigma(\omega) \equiv (dI/dV)_S / (dI/dV)_N$ we have assumed that the tunneling matrix element is given by the WKB result⁹²⁾, which is the standard assumption⁵¹⁾. This result gives for the tunneling matrix element an expression which is inversely proportional to the electronic density of states perpendicular to the barrier and one recovers the usual strong-coupling expression for $\sigma(\omega)$

$$\sigma(\omega) = \operatorname{Re} \left[\frac{\omega}{(\omega^2-\Delta^2(\omega))^{1/2}} \right] \quad (\text{III.41})$$

Note, however, that $N(0)\sigma(\omega)$ is not equal to the quasiparticle density of states for the non-constant $N(E)$ case.

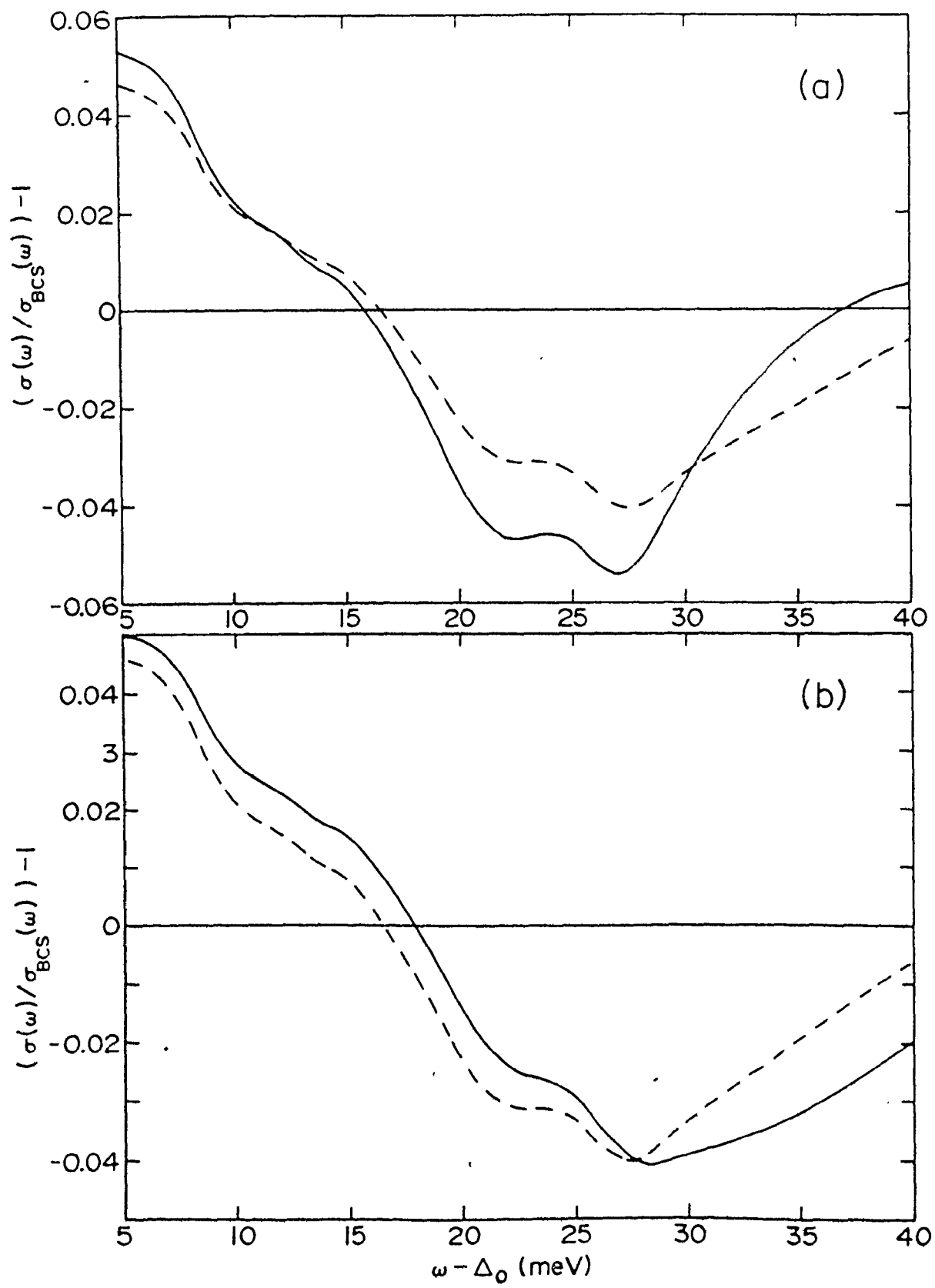
In Fig. (III.2a) we present $(\sigma(\omega)/\sigma_{\text{BCS}}(\omega)) - 1$, where $\sigma_{\text{BCS}}(\omega) = \omega/(\omega^2 - \Delta_0^2)^{1/2}$, calculated from the solution of Eqs. (III.37a)-(III.37c) with $N(E)$ given by (II.40) (solid lines). In the same figure the dashed line is the corresponding quantity for constant EDOS. While no new structure is introduced it is evident that the slopes in $(\sigma(\omega)/\sigma_{\text{BCS}}(\omega)) - 1$ are larger for a nonconstant EDOS near the position of the two lower peaks in the input α^2F -spectrum (dashed line in Fig. (III.3a)), near $\omega - \Delta_0 = 8.4$ meV and $\omega - \Delta_0 = 17$ meV, than the slopes in the corresponding curve for the case of flat EDOS. This effect will cause, as shown below, an overestimate of the weight under α^2F in the lower portion of the spectrum if the solid curve in Fig. III.2a is inverted conventionally³⁰). Another important feature of this $(\sigma(\omega)/\sigma_{\text{BCS}}(\omega)) - 1$ is a sharp swing back towards zero around $\omega - \Delta_0 = 35$ meV. For these large values of ω one can write

$$\sigma(\omega) = 1 + \frac{1}{2\omega^2}(\Delta_1^2(\omega) - \Delta_2^2(\omega)) \quad (\text{III.42})$$

where Δ_1 and Δ_2 are the real and imaginary part of Δ respectively. Therefore, the rapid reduction in $|\sigma(\omega)/\sigma_{\text{BCS}}(\omega) - 1|$ is coming from the rapid decrease in $\Delta_2(\omega)$ in the neighbourhood of $\omega = 35$ meV ($> \omega_{\text{max}} = 28.9$ meV) as can be seen from Fig. (III.1a). We have found such behaviour for $\Delta_2(\omega)$ in all our calculations done with the peak in EDOS around the Fermi

Fig.III.2

Normalized tunneling conductance reduced to the corresponding BCS expression: a) for a peak in EDOS (solid line), b) for a valley in EDOS (solid line). Dashed curves in a) and b) are obtained with a flat EDOS equal to $N(0)$.



level, and the resulting rapid decrease in $|\sigma(\omega)/\sigma_{\text{BCS}}(\omega)-1|$ for ω larger than the maximum phonon frequency in the input α^2F -spectrum. In Fig. (III.3) we show $\sigma(\omega)$ calculated from the analytically continued solution of the modified Eliashberg equations on the imaginary frequency axis (see Sec. III.1) for two symmetric Lorentzian models of $N(\epsilon)$. The analytic continuation was performed by means of N -point Padé approximants⁷⁶⁾ (see Sec. III.1). The solid curve in Fig. (III.3) corresponds to the flat EDOS, while the dashed one and the

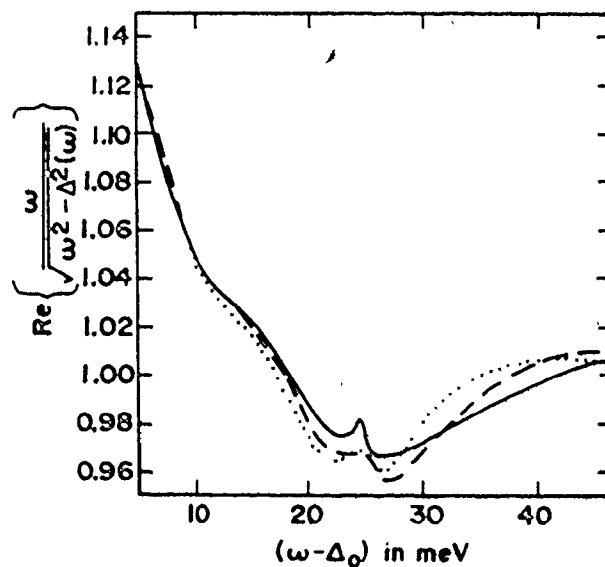


Fig. III.3

dotted one correspond to the Lorentzian model with half-widths of $a = 60$ meV and $a = 15$ meV respectively. Note that in the

case of narrower peak, $\sigma(\omega)$ goes faster to unity for $\omega > \omega_{\max}$.

It is interesting to see what the inversion of the calculated $\sigma(\omega)/\sigma_{\text{BCS}}(\omega)-1$ (solid line in the Fig. III.2a) would give for the electron-phonon spectral function assuming the usual Eliashberg theory, which does not take into account the energy dependence in EDOS, is applicable. To this end we have applied the inversion procedure of Galkin, D'yachenko and Svistunov⁹³). This inversion procedure besides being very simple and unambiguous has a distinct advantage over the more conventional McMillan-Rowell procedure³⁰): during inversion of the gap equations for α^2F , the value of $\mu^*(\omega_c)$ does not enter. Once the α^2F is determined, $\mu^*(\omega_c)$ is fitted to the experimental gap edge.

The central relation of the procedure proposed by Galkin et.al. is the dispersion relation

$$\text{Im} \frac{1}{[\omega^2 - \Delta^2(\omega)]^{1/2}} = \frac{2}{\pi} \int_{\Delta_0}^{+\infty} \left\{ \text{Re} \frac{\omega'}{[\omega'^2 - \Delta^2(\omega')]^{1/2}} \right\} \frac{d\omega'}{\omega^2 - \omega'^2} \quad (\text{III.43})$$

which connects the measured quantity

$$\sigma(\omega) = \text{Re} \frac{\omega}{[\omega^2 - \Delta^2(\omega)]^{1/2}} \quad (\text{III.44})$$

with $\text{Im}[\omega^2 - \Delta^2(\omega)]^{-1}$. Eqs. (III.43) and (III.44) are two equations for two unknowns $\Delta_1(\omega)$ and $\Delta_2(\omega)$. Thus the gap function can be determined directly from the tunneling experi-

ment without reference to the Eliashberg equations. Once $\Delta(\omega)$, and therefore $\tilde{N}_\Delta(\omega) = \text{Re}[\Delta(\omega)/(\omega^2 - \Delta^2(\omega))^{1/2}]$ and $\tilde{N}_Z(\omega) = \sigma(\omega)$, are known, the Eliashberg equations can be used to set up a linear integral equation for $\alpha^2(\Omega)F(\Omega)$. By taking the imaginary part of the gap equation (III.37a), $\mu^*(\omega_c)$ drops out and one has

$$\text{Im}\Delta(\Delta_0 + \omega) Z(\Delta_0 + \omega) = \pi \int_0^\omega d\omega' \text{Re} \frac{\Delta(\Delta_0 + \omega')}{[(\Delta_0 + \omega')^2 - \Delta^2(\Delta_0 + \omega')]^{1/2}} \alpha^2 F(\omega - \omega') \quad (\text{III.45})$$

with

$$Z(\Delta_0 + \omega) = 1 - \frac{1}{\Delta_0 + \omega} \int_0^{+\infty} d\omega' \text{Re} \frac{\Delta_0 + \omega'}{[(\Delta_0 + \omega')^2 - \Delta^2(\Delta_0 + \omega')]^{1/2}} \\ \times \int_0^{+\infty} d\Omega \alpha^2(\Omega) F(\Omega) \left[\frac{1}{\omega' + \omega + \Omega + 2\Delta_0 + i\delta} - \frac{1}{\omega' + \omega + \Omega - i\delta} \right] \quad (\text{III.46})$$

A guess is made for $\alpha^2(\Omega)F(\Omega)$ and Z is calculated from Eq. (III.46). This Z and the known Δ are used in Eq. (III.45) to calculate new spectral function $\alpha^2 F$; then the whole procedure is repeated. This iterative procedure converges rapidly. It is sufficient to assume that $\alpha^2 F$ is a histogram, provided it is defined on a fine enough grid (a bin width of 0.1-0.2 meV is small enough). This fact simplifies the numerical work considerably since for the histogram-like $\alpha^2 F$, Eq. (III.45) has the form

$$\begin{pmatrix} b_1 \\ b_2 \\ \vdots \\ \vdots \\ \vdots \end{pmatrix} = \begin{pmatrix} c_1 & 0 & 0 & 0 & \cdots \\ c_2 & c_1 & 0 & 0 & \cdots \\ c_3 & c_2 & c_1 & 0 & \cdots \\ \vdots & \vdots & \vdots & \vdots & \vdots \\ \vdots & \vdots & \vdots & \vdots & \vdots \end{pmatrix} \begin{pmatrix} a_1 \\ a_2 \\ a_3 \\ \vdots \\ \vdots \end{pmatrix} \quad (\text{III.47})$$

where for the set of equally spaced frequencies

$$0 = \Omega_0 < \Omega_1 < \Omega_2 < \cdots$$

$$\left. \begin{aligned} a_i &= \alpha^2(\Omega) F(\Omega) \quad \text{for } \Omega_{i-1} \leq \Omega \leq \Omega_i \\ b_i &= \frac{1}{\pi} \text{Im} \Delta(\Delta_0 + \Omega_i) Z(\Delta_0 + \Omega_i) \\ c_i &= \int_{\Omega_{i-1}}^{\Omega_i} d\omega' \text{Re} \frac{\Delta(\Delta_0 + \omega')}{[(\Delta_0 + \omega')^2 - \Delta^2(\Delta_0 + \omega')]^{1/2}} \end{aligned} \right\} \quad i = 1, 2, \dots \quad (\text{III.48})$$

Care was to be exercised in calculating the integrals defining the c_i numbers.

Before applying this inversion procedure to the $\sigma(\omega)/\sigma_{\text{BCS}}(\omega) - 1$ (solid line in Fig. III.2a) calculated for the assumed model of $N(\epsilon)$, we tested it for the case of the electron-phonon spectrum of $\text{Nb}^{85)}$ and $\text{Nb}_3\text{Sn}^{91)}$ (which is the input spectrum in all other calculations in this thesis). The procedure works extremely well, giving after a few iterations an

$\alpha^2 F$ spectrum which is indistinguishable from the input $\alpha^2 F$ when examined by eye.

In Fig. III.4a we plot the effective spectrum $[\alpha^2(\Omega)F(\Omega)]_{\text{eff}}$ obtained by the inversion of $\sigma(\omega)/\sigma_{\text{BCS}}(\omega)-1$ from Fig. III.2a. In the inset we give the assumed band structure EDOS $N(E)$. The dashed line in Fig. III.4a is our input $\alpha^2 F$. The main deviations from the input $\alpha^2 F$ are the shift in weight under the spectrum towards the lower frequencies, the attenuated longitudinal peak (at $\Omega = 25$ meV) and the negative tail. The negative in $\alpha^2 F_{\text{eff}}$ does not have a physical meaning if this spectrum is interpreted as the true spectrum, since the electron-phonon coupling function should be a positive quantity. The presence of the negative tail is completely analogous to the problem with the frequency derivative of the inverse life-time at zero temperature in the normal state, Sec. II.2. Only when we allowed during the inversion procedure for the possibility of negative values of $\alpha^2(\Omega)F(\Omega)_{\text{eff}}$ did the recalculated $\sigma(\omega)$ and $\sigma(\omega)/\sigma_{\text{BCS}}(\omega)-1$ agree well with the original functions. In Figs. III.5a-III.5b, dotted lines represent the functions obtained from the solutions of Eqs. (III.37a)-(III.37b) with nonconstant EDOS and $\alpha^2 F$ -spectrum given by the dashed line in Fig. III.4a, while the solid lines were obtained from the solutions of the unmodified Eliashberg equations with $\alpha^2(\Omega)F(\Omega)_{\text{eff}}$ as the input spectrum.

Fig.III.4

Effective electron-phonon spectral densities obtained by inversion of calculated normalized tunneling conductances within the usual Eliashberg theory (solid lines). Dashed lines represent the input electron-phonon spectral density. In insets we give corresponding EDOS.

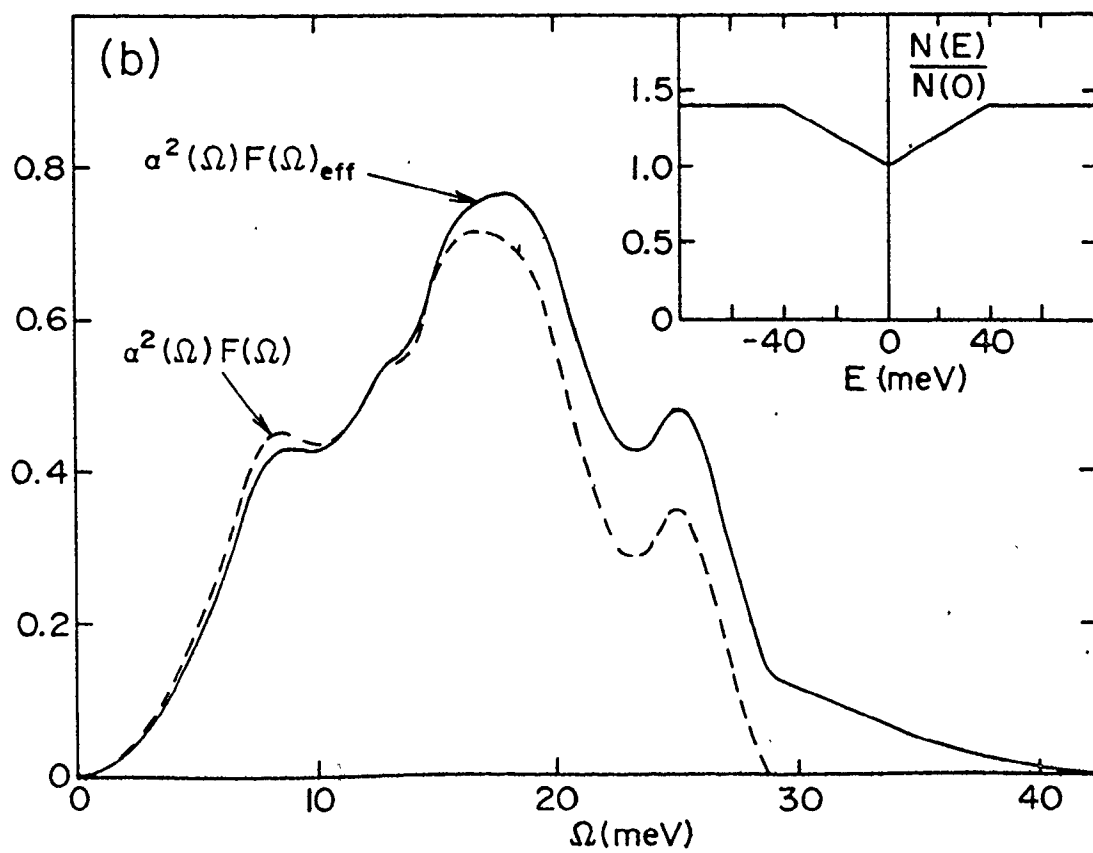
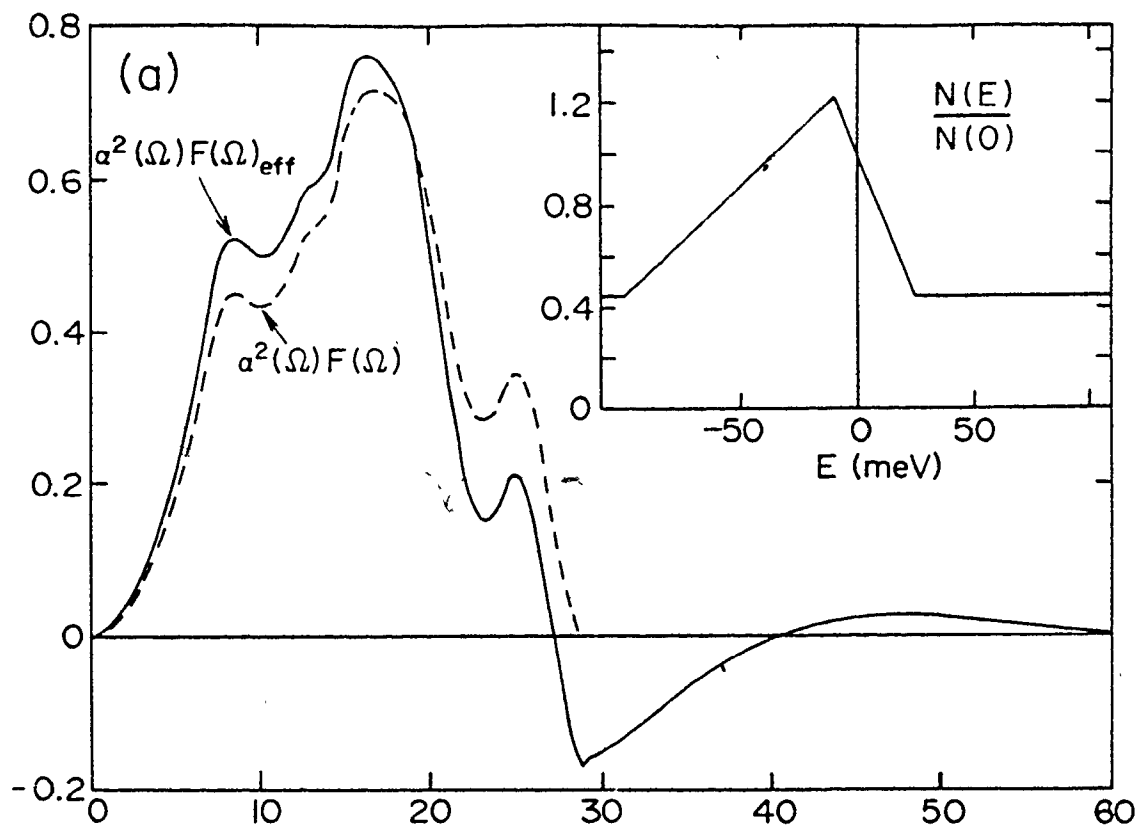
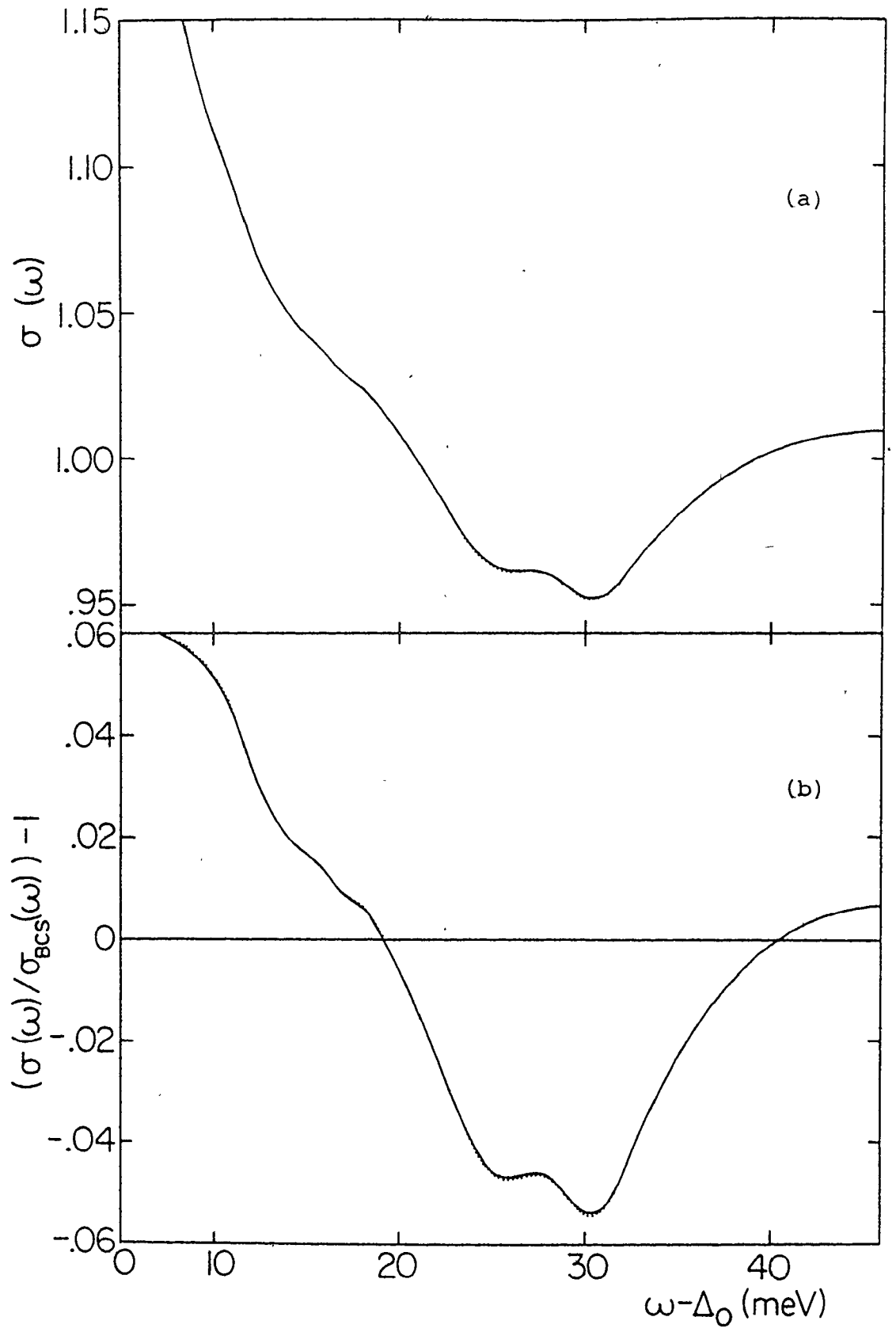


Fig.III.5

- a) Comparison of the normalized tunneling conductance calculated for a peak in EDOS (dotted line) and the one recalculated from the effective electron-phonon spectrum in Fig.III.4a (solid line).
- b) The quantities as in a) normalized to the BCS expression for the normalized tunneling conductance.



Leaving the negative tail out while inverting $\sigma(\omega)$ leads to a poor agreement between this function and the one which is recalculated from an $\alpha^2 F$ with the negative tail omitted, in particular in the range $\omega \gtrsim \omega_{\max}$ (see Figs. III.6a,b and (III.7)). Note that the curvature of the $\sigma(\omega)/\sigma_{\text{BCS}}(\omega)-1$ recalculated from such an $\alpha^2 F_{\text{eff}}$ (Fig. III.7) is in the range $\omega \gtrsim \omega_{\max}$ similar to the one for the case of flat EDOS (dashed line in Fig. III.4a).

In Fig. III.4b, we give another effective $\alpha^2 F$ spectrum obtained for the EDOS presented in the inset of the same figure. The corresponding $(\sigma(\omega)/\sigma_{\text{BCS}}(\omega))-1$ curve is shown in Fig. III.2b (solid line). Here the trend in the change of the $\alpha^2 F$ -spectrum is exactly opposite to the previous case and is connected to the fact that the Fermi level falls in a small valley, not a peak, in the EDOS.

In conclusion, the effects of a nonconstant EDOS on the normalized tunneling conductance $\sigma(\omega)$ are significant and cannot be accounted for in a meaningful way within the standard Eliashberg theory by working with effective values of $\alpha^2(\Omega)F(\Omega)_{\text{eff}}$ and μ_{eff}^* . Needless to say, when we inverted the Eliashberg equations (III.37a)-(III.37c) modified to include the energy dependent EDOS, in a way completely analogous to the previously described inversion technique and starting from the calculated $\Delta(\omega)$, we have obtained back our input electron-




Fig.III.6

- a) Normalized tunneling conductance (solid line) recalculated from the electron-phonon spectral function which was obtained by inversion of the dotted curve. The negative tail in the spectral function was ignored in the process of inversion.
- b) The same quantities as in a) normalized to the BCS formula for the normalized tunneling conductance.

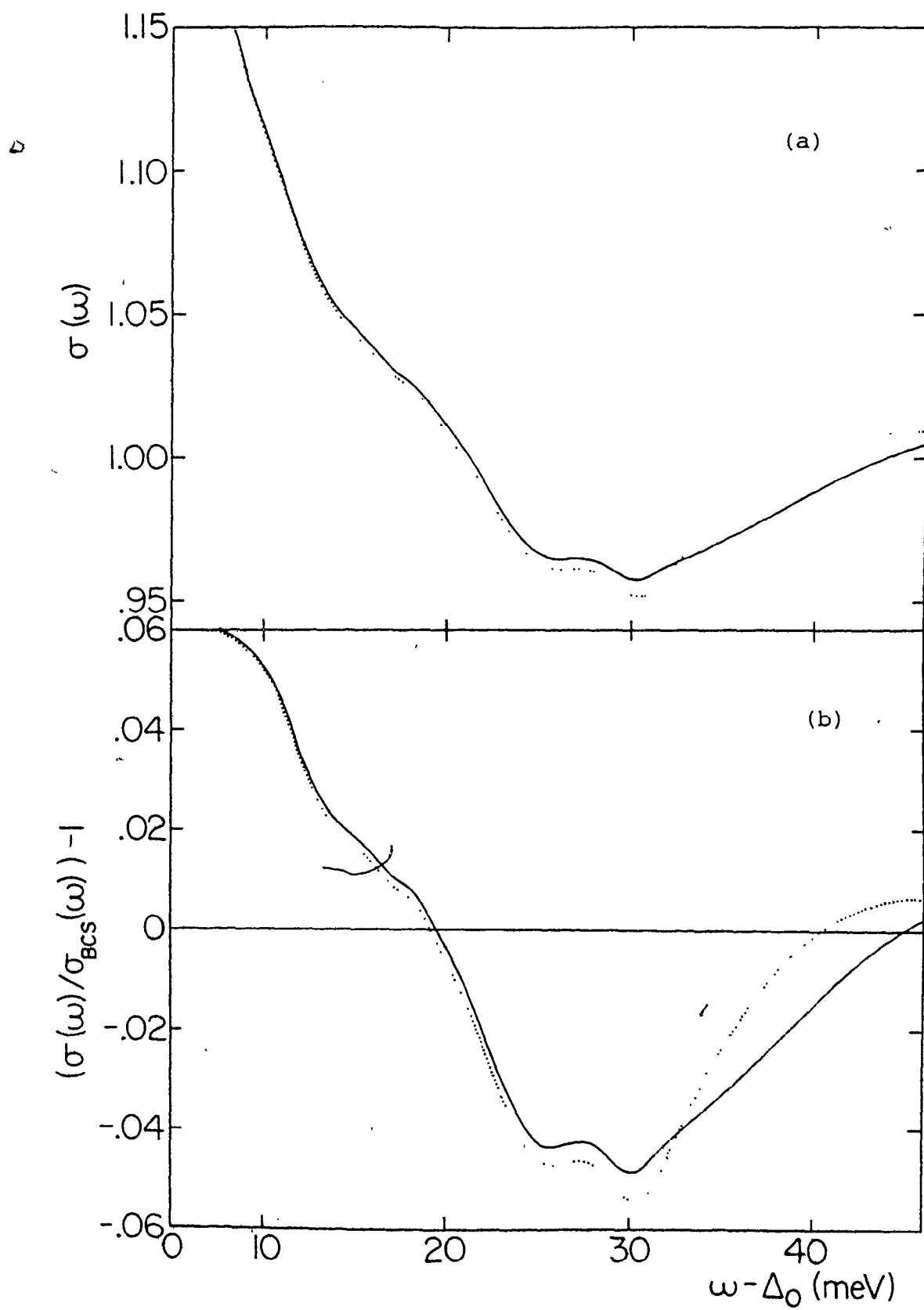
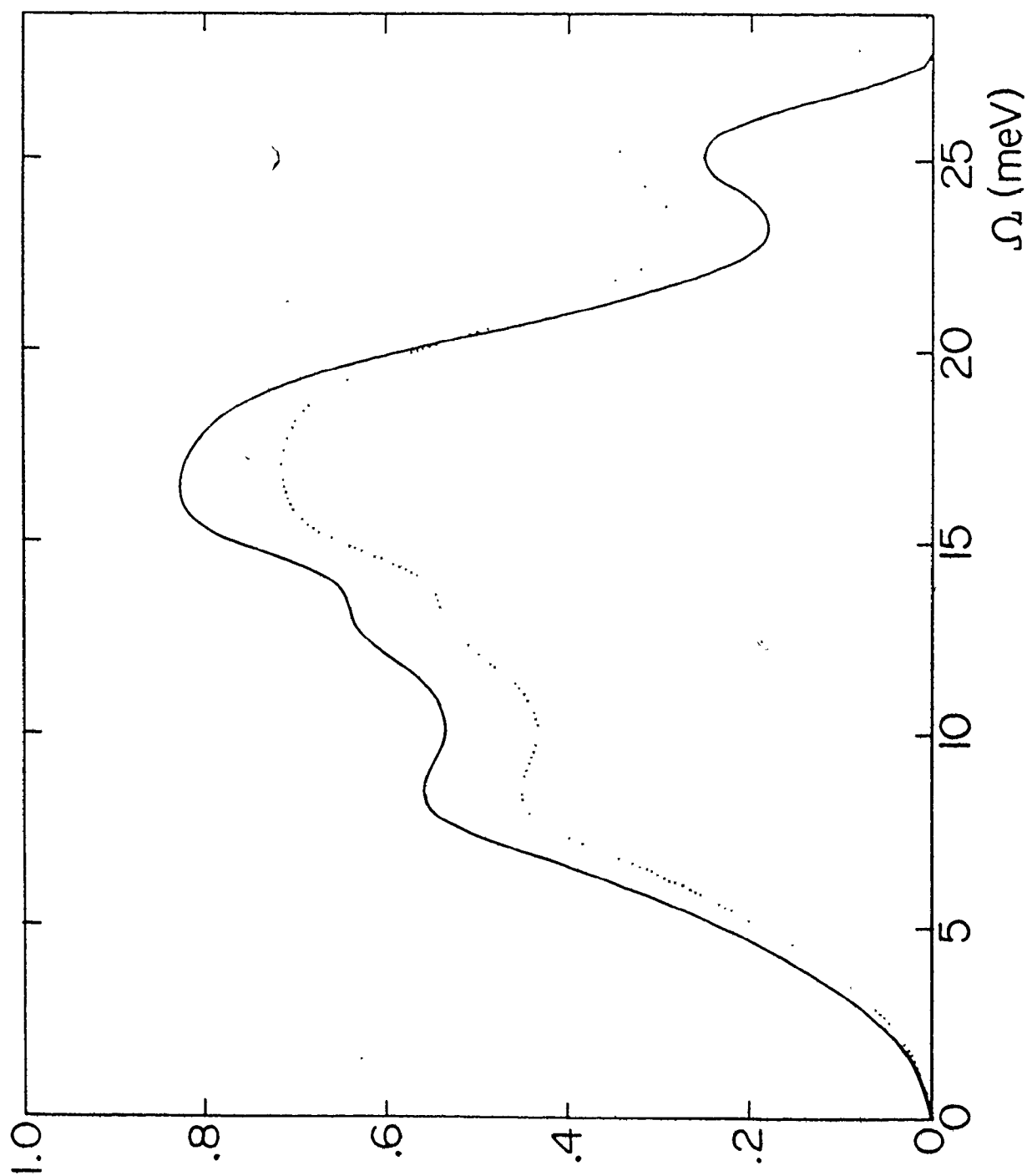


Fig.III.7

The effective electron-phonon spectral density inverted from the calculated normalized tunneling conductance for a peak in EDOS (solid line). The negative tail was ignored during the inversion process. Dotted line is the input electron-phonon spectral function.



phonon spectral density $\alpha^2 F$. This procedure, however, requires a detailed knowledge of the band EDOS.

Note that the dispersion relation (III.43) still remains valid since it results from the energy integration,

$\int_{-\infty}^{+\infty} d\varepsilon_k$, of the equality

$$\text{Re} G_{11}(\varepsilon_k, \omega + i\delta) = P \int_{-\infty}^{+\infty} \frac{d\omega'}{\omega - \omega'} \left\{ \frac{1}{\pi} \text{Im} G_{11}(\varepsilon_k, \omega' + i\delta) \right\} \quad (\text{III.49})$$

which is just the real part of the spectral representation for the 11-component of Nambu's Green's function $\hat{G}(\varepsilon, \omega + i\delta)$. The critical fact is that the various self-energy parts appearing in G_{11} do not depend on the electron energy ε ; this fact follows from our assumption that $\alpha^2 F(\Omega; \varepsilon, \varepsilon')$ does not depend on ε and ε' . Note that the integration of the real part of the spectral representation for G_{11} over the momentum, i.e. $\int_{-\infty}^{+\infty} \frac{d^3 \vec{k}}{(2\pi)^3} = \int_{-\infty}^{+\infty} d\varepsilon_k N(\varepsilon_k)$ would give a more complicated and in fact unnecessary identity.

Now the question is whether there exists some experimental evidence for the effects we have established so far of energy dependence in EDOS on the single-particle tunneling characteristics. The most natural candidates are the A-15 materials, for which successful tunneling experiments have been performed only very recently^{82,89,91}). In all cases the conven-

tional McMillan-Rowell inversion procedure gives anomalous values for the parameters λ and $\mu^*(\omega_c)$; also the resulting α^2F -spectra and $\mu^*(\omega_c)$ give a poor fit^{88,89)} to the experimentally measured $\sigma(\omega)$. These difficulties were ascribed^{88,89)} to the proximity effect, and improved values of the α^2F -spectra and Coulomb repulsion parameters were obtained by applying the modified McMillan-Rowell procedure, which accounts for the presence of the proximity sandwich. With this modification, the inverted parameters give a good fit to the experimentally measured normalized tunneling conductance. In one case only⁸²⁾, the inversion was attempted using the method of Galkin et al. with presumably anomalous results, but the character of the anomalies, unfortunately, was not clearly specified. It is not completely clear whether the two methods necessarily give the same result, once the conventional description of the tunneling experiment is inapplicable for one reason or another.

We find that all published^{82,88,89)} normalized tunneling conductances $\sigma(\omega)$ (or equivalently $\sigma(\omega)/\sigma_{\text{BCS}}(\omega)-1$) for A-15 materials show behaviour in the frequency range $\omega \gtrsim \omega_{\text{max}}$ characteristic of a peak in EDOS around the Fermi level, namely a very rapid approach to unity (or equivalently zero). That something unusual is happening in this frequency range is evident from the very recent work of Kwo and Geballe on Nb_3Al ⁸⁹⁾. They found that if the usual McMillan-Rowell pro-

cedure was employed, a too small cutoff (less than 30 meV) had to be imposed with the result that the structure in $\sigma(\omega)$ between 20 meV and 40 meV ($\approx \omega_{\text{max}}$) was left out of consideration. This omission was necessary in order to prevent the iterative solutions from becoming unstable. However, these difficulties were interpreted as a result of the proximity effect⁸⁴⁾. It should be noted that the α^2F -spectra deduced for Nb_3Sn ^{88,91)} and Nb_3Al ⁸⁹⁾ show a large shift in weight towards lower frequencies compared^{66,82,91)} to the corresponding measured phonon densities of states. Such behaviour is quite different from the one found in other superconducting materials.

By improving the tunneling junctions and by performing systematic studies of tunneling spectra for A-15 materials with varying composition, it will be possible to gain more insight into the microscopic properties of these materials. Some studies of this type have already been performed on Nb_3Sn and Nb_3Al ^{82,89)}. The results are not inconsistent with the hypothesis that changes in stoichiometry result in the smearing of the peak in EDOS (see Fig. III.4).

III.3 THERMODYNAMIC PROPERTIES OF A SUPERCONDUCTOR WITH A SYMMETRIC LORENTZIAN ELECTRONIC DENSITY OF STATES

In this section we will give results of our numerical calculations of the thermodynamic properties of a strong coupling superconductor having an electronic density of states (EDOS) represented by a symmetric Lorentzian

$$N(\epsilon) = N_b \left(1 + \frac{S}{\pi} \frac{a}{a^2 + \epsilon^2} \right) . \quad (\text{III.50})$$

As in Section II.3 of Chapter II we can ignore any shift of the chemical potential μ by assuming that $\mu \gg a$ (see also Appendix 3). This assumption will simplify the treatment considerably since we will then have to solve only two equations for the renormalization function Z and the pairing self-energy ϕ (or equivalently the gap function Δ). This assumption will also simplify the treatment of the free energy difference ΔF between the normal and superconducting state, since ΔF can then be calculated as the difference between the corresponding grand thermodynamic potentials (see Appendices 3 and 4). Thus we restrict ourselves to a study of the effects of decrease in EDOS as one moves away from the chemical potential at $\epsilon = 0$. The problem of calculating the free energy difference between the normal and the superconducting states becomes very complicated with non-constant EDOS because the standard theories cannot be applied directly. In fact it has been shown by

Lie and Carbotte⁹⁴⁾ that when the EDOS cannot be assumed constant, the method due to Wada⁴⁵⁾ does not describe correctly the order of superconductive phase transition. The exact origin of this difficulty remains unclear at present. At the same time a direct application of the method due to Bardeen and Stephen⁴⁶⁾ is not possible, essentially because of the self-consistency of the electron self-energy equation in the normal state (see Ch. II). Like Bardeen and Stephen we start from the general Eliashberg formula for the grand thermodynamic potential Ω of the interacting electron-phonon system³⁶⁾, but then proceed somewhat differently. Since this derivation is fairly complicated and technical we present it in Appendix 4. In Appendix 3 we discuss in some detail the problem of calculating the grand thermodynamic potential of the interacting electron-phonon system in both superconducting and normal state and show how Eliashberg's result can be generalized to include the effects of the screened Coulomb repulsion on the pairing self-energy. We also generalize Eliashberg's result to include scattering by small amounts of ordinary and paramagnetic impurities. It should be noted that our final formula for the free energy difference (Eq. (A4.13) of Appendix 4) with a Lorentzian model of EDOS is applicable when the Coulomb repulsion and scattering by ordinary or paramagnetic impurities are present. Numerical calculations of the superconducting

thermodynamic properties based on our formula, Eq. (A4.13), when the system contains small amounts of ordinary or paramagnetic impurities were performed by Schachinger et al.²⁹⁾ and will be presented elsewhere. In Appendix 4 we explicitly show that the order of superconductive phase transition is described correctly by Eq. (A4.13), i.e. that this transition is not first order.

Before presenting the results of our numerical calculations we will specify the form of the generalized Eliashberg equations, Eqs. (III.27a)-(III.27c), appropriate to the EDOS given by Eq. (III.50). The integrals over ϵ in Eqs. (III.27a)-(III.27c) are evaluated in Appendix 2. The resulting equations are

$$\omega_n Z(i\omega_n) = \omega_n + \pi T \sum_{m=-\infty}^{+\infty} \lambda(n-m) \frac{\omega_m}{[\omega_m^2 + \Delta^2(i\omega_m)]^{1/2}} \hat{N}(i\omega_m) \quad (\text{III.51})'$$

$$\begin{aligned} \Delta(i\omega_m) Z(i\omega_m) = \pi T \sum_{n=-\infty}^{+\infty} [\lambda(n-m) - \mu^*(\omega_c) \theta(\omega_c - |\omega_m|)] \frac{\Delta(i\omega_m)}{[\omega_m^2 + \Delta^2(i\omega_m)]^{1/2}} \\ \times \hat{N}(i\omega_m) \end{aligned} \quad (\text{III.52})$$

$$\chi(i\omega_n) = -\pi T \sum_{m=-\infty}^{+\infty} \lambda(n-m) \frac{N_b}{N(0)} \frac{s}{\pi} \frac{\chi(i\omega_m)}{(a + Z(i\omega_n) \sqrt{\omega_m^2 + \Delta^2(i\omega_n)})^2 + \chi^2(i\omega_n)} \quad (\text{III.53})$$

with

$$\hat{N}(i\omega_n) = \frac{N_b}{N(0)} \left\{ 1 + \frac{s}{\pi} \times \frac{Z(i\omega_n) [\omega_n^2 + \Delta^2(i\omega_n)]^{1/2} + a}{[Z(i\omega_n) [\omega_n^2 + \Delta^2(i\omega_n)]^{1/2} + a]^2 + \chi^2(i\omega_n)} \right\} \quad (\text{III.54})$$

Since the factor multiplying $\chi(i\omega_m)$ under the summation over m in Eq. (III.53) is positive, the solution $\chi(i\omega_m) = 0$ ($m = 0, \pm 1, \dots$) is consistent with Eq. (III.53) as one can anticipate from the fact that $N(\epsilon)$ is symmetric around $\epsilon = 0$. Thus the problem is reduced to solving Eqs. (III.51) and (III.53) with $\hat{N}(i\omega_n)$ given by Eq. (III.54) and χ set equal to zero. These equations can be solved readily for the given input parameters.

At the superconducting critical temperature T_c Eqs. (III.51) and (III.52) become linear:

$$\omega_n Z(i\omega_n) = \omega_n + \pi T \sum_{m=-\infty}^{+\infty} \lambda(n-m) \operatorname{sgn}(\omega_m) \hat{N}_L(i\omega_m) \quad (\text{III.55})$$

$$\Delta(i\omega_m) Z(i\omega_m) = \pi T \sum_{m=-\infty}^{+\infty} [\lambda(n-m) - \mu^*(\omega_c) \theta(\omega_c - |\omega|)] \frac{\Delta(i\omega_m) Z(i\omega_m)}{|\omega_m Z(i\omega_m)|} \hat{N}_L(i\omega_m) \quad (\text{III.56})$$

where the subscript L on $\hat{N}_L(i\omega_n)$ means that Δ^2 has to be set equal to zero in Eq. (III.54). T_c is defined as the highest temperature at which (III.56) has a nontrivial solution.

From the knowledge of the free energy difference ΔF between the normal state and superconducting state (i.e. the condensation energy), one can evaluate the thermodynamic critical field of the superconductor via

$$\Delta F = \frac{H_c^2(T)}{8\pi} \quad (\text{III.57})$$

(we consider a system of unit volume). Also, from the general thermodynamic relation $S = -(\partial F/\partial T)_{V,N}$ one can calculate the entropy difference between the normal and superconducting state as (see Eq. (III.57))

$$\Delta S = - \frac{1}{4\pi} H_C(T) \frac{dH_C(T)}{dT} \quad (\text{III.58})$$

and the electronic specific heat difference

$$C_n(T) - C_s(T) = T \left(\frac{\partial(\Delta S)}{\partial T} \right)_{V,N} = - \frac{T}{4\pi} \left[H_C(T) \frac{d^2 H_C(T)}{dT^2} + \left(\frac{dH_C(T)}{dT} \right)^2 \right] \quad (\text{III.58})$$

Since the measured values of $H_C(T)$ deviate by small amounts from the prediction of the phenomenological two-fluid model (see for instance Ref. 43) which gives

$$H_C(T) = H_C(0) \left[1 - \left(\frac{T}{T_C} \right)^2 \right], \quad (\text{III.60})$$

it is traditional, and in fact very useful, to present the data on $H_C(T)$ in the form of the deviation from the two-fluid model prediction

$$D(t) = \frac{H_C(T)}{H_C(0)} - (1-t^2), \quad t = T/T_C. \quad (\text{III.61})$$

The function $D(t)$ is called the superconducting critical field deviation function (or simply the deviation function). It turns out^{48,57,95)} that the superconductors in which retardation and damping effects are large (the so-called strong coupling

superconductors such as Pb and Hg) show a positive deviation from the prediction of the two-fluid model, with the maximum in $D(t)$ of the order of 0.01 - 0.02, while for the ones in which these effects play a less important role (In, Sn, Al) $D(t)$ is negative with the minimum in $D(t)$ of the order -0.01 to -0.04. Empirically $D(t)$'s order according to the electron phonon mass enhancement parameter $\lambda = 2 \int_0^{+\infty} d\Omega \alpha^2(\Omega) F(\Omega) / \Omega$: for $\lambda \gtrsim 1$ $D(t)$ is positive, for $\lambda \lesssim 1$ $D(t)$ is negative and for $\lambda \approx 1$ $D(t)$ has an S-shape (Nb⁹⁶).

We will present our results for $H_c(T)$ in the form of $D(t)$ since there the absolute value of the parameter determining the magnitude of $N(\varepsilon)$, i.e. N_D , appearing explicitly in the formula for ΔF drops out (see (A4.13)). In all our calculations we have taken the shape of the input $\alpha^2(\Omega)F(\Omega)$ spectrum to be that of Nb₃Sn⁹¹ and the value of $\mu^*(\omega_c) = 0.1747$ with $\omega_c = 8\omega_{\max}$ ($\omega_{\max} = 28.9$ meV is the maximum phonon frequency in $\alpha^2(\Omega)F(\Omega)$). For each choice of Lorentzian parameters, and the scale of $\alpha^2 F \propto N(0)$ the linearized equations (III.55) and (III.56) were solved first to determine the value of T_c . Then the nonlinear equations (III.51), (III.52) were solved at twenty reduced temperatures (T/T_c) and the resulting solutions $\{\Delta(i\omega_n)\}$, $\{Z_s(i\omega_n)\}$, $\{Z_n(i\omega_n)\}$ (where the subscripts n and s are used to indicate the normal and superconducting states) were used to calculate the free energy difference ΔF according

to the formula (A4.b) of Appendix 4. Note that the iteration procedure was more complicated than in the usual case of a flat electronic density of states, because Eq. (III.55) for the normal state renormalization function had to be solved self-consistently. By using the method of N-point Padé-approximants (see Sec. III.1) we analytically continued the lowest temperature solution $\Delta(i\omega_n)$ to the real frequency axis. From the analytically continued $\Delta(\omega+i0^+, T)$ the corresponding gap at the gap edge, $\Delta_0(T)$, was determined by solving the equation

$$\Delta_0(T) = \text{Re}\Delta(\omega = \Delta_0(T), T) .$$

Since the temperature T was such that $T/T_c = 0.1$, we have identified $\Delta_0(T)$ with the zero temperature gap edge $\Delta_0 \equiv \Delta_0(T=0)$, $\Delta(T)$ being almost constant for $T < 0.1 T_c$ ⁵⁷⁾. The main reason for using the above method for calculating the zero temperature energy gap, rather than solving the corresponding Eliashberg equations on the real frequency axis (Sec. III.2) is that the sharp cutoff ω_c on the imaginary frequency axis does not translate into the same cutoff on the real frequency axis ω_c ⁹⁷⁾. The two sets of Eliashberg equations are completely equivalent before the cutoff ω_c and the Coulomb pseudopotential $\mu^*(\omega_c)$ are introduced. After introducing $(\omega_c, \mu^*(\omega_c))$ the two sets of equations are not so directly related. For this reason we have calculated Δ_0 from the imaginary axis solution. Recently we checked this method of obtaining Δ_0 for 30 superconducting ma-

of obtaining Δ_0 for 30 superconducting materials with excellent results⁹⁸⁾.

The ratio $(2\Delta_0)/(k_B T_C)$ is an excellent indicator of the strength of the electron-phonon coupling^{48,57)}. The Bardeen-Cooper-Schrieffer (BCS) theory of superconductivity⁴³⁾, which does not take into account the retardation and damping effects, predicts for this quantity the universal value $(2\Delta_0)/(k_B T_C) = 3.53$. It also gives a universal shape for $D(t)$, which is negative with the minimum of -0.037 ⁹⁵⁾. Since the effective damping of the quasiparticles increases with temperature, T_C is effectively lowered more than Δ_0 ($T=0$) with strong coupling and therefore the ratio $(2\Delta_0)/(k_B T_C)$ increases⁹⁹⁾. It has been suggested by Ho et al.¹⁵⁾ that with a peak in EDOS centred at the Fermi level and a strong electron-phonon interaction, the depletion of the peak with increasing T should also increase the value of $(2\Delta_0)/(k_B T_C)$.

In Fig. (III.8) we present the $D(t)$ calculated for the four sets of Lorentzian parameters in (III.50). The input $\alpha^2 F$ -spectrum was that of Nb_3Sn ⁹¹⁾ in all four cases, and the value of $s/(\pi a)$ which determines the height of the peak over the background was set equal to unity. The only parameter being varied is the half-width a . The solid line in Fig. (III.8) corresponds to $a = 2\omega_{\max}$, the dotted line to $a = 1.5\omega_{\max}$, the dashed curve is for $a = \omega_{\max}$ and the dash-dot for $a = 0.25\omega_{\max}$. Thus the deviations in $H_C(T)/H_C(0)$ from the

prediction of the two-fluid model decrease with decreasing a . This behaviour is to be expected since by reducing a while $s/(\pi a)$ remains fixed one reduces the strength of the effective coupling between the electrons. For large $a \gg \omega_{\max}$ the increase in $D(t)$ with decrease in a is relatively small because the density of states $N(\epsilon)$ does not vary too rapidly in the important energy range from $-\omega_{\max}$ to ω_{\max} . The corresponding values of T_c and the ratio $(2\Delta_0)/(k_B T_c)$ are summarized in Table III.1.

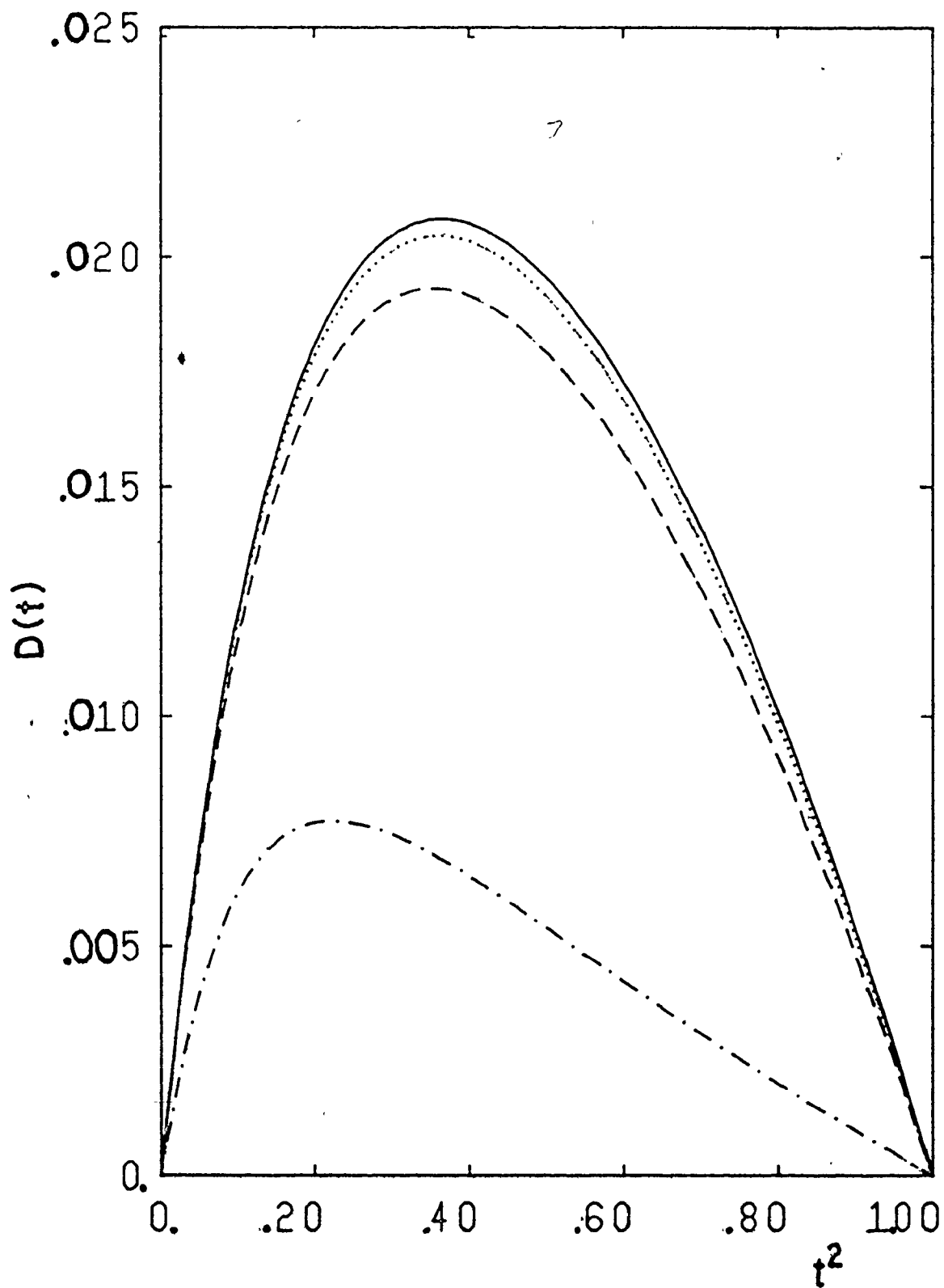
Table III.1

	T_c	$(2\Delta_0)/(k_B T_c)$
$a = 2\omega_{\max}$	17.28°K	4.63
$a = 1.5\omega_{\max}$	17.08°K	4.63
$a = \omega_{\max}$	16.66°K	4.62
$a = 0.25\omega_{\max}$	14.20°K	4.49

Thus the value of the ratio $(2\Delta_0)/(k_B T_c)$ decreases with reducing a , consistently with the behaviour of $D(t)$. However the reduction in $(2\Delta_0)/(k_B T_c)$ between, say, the case of $a = 2\omega_{\max}$ and the case $a = 0.25\omega_{\max}$ is much smaller than the overall reduction in $D(t)$, presumably due to the effect anticipated by Ho et al. which is more pronounced for a narrow peak.

Fig.III.8

Superconducting thermodynamic critical field deviation
function $D(t)$ for four different Lorentzian half-widths.



In Fig. (III.9) we present another set of deviation functions calculated for a fixed peak width $a = 1.5 \omega_{\max}$, fixed value of $N(\varepsilon=0)$ and thereby constant scale of $\alpha^2 F$. Here $s/(\pi a)$, the height of the peak over the background, is varied. The solid line is for $s/(\pi a) = 0.5$, the dotted one is for $s/(\pi a) = 1$, the dashed line is for $s/(\pi a) = 2$ and the dash-dot line is for $s/(\pi a) = 4$. The corresponding values of T_c and the ratio $(2\Delta_0)/(k_B T_c)$ are presented in Table III.2.

Table III.2

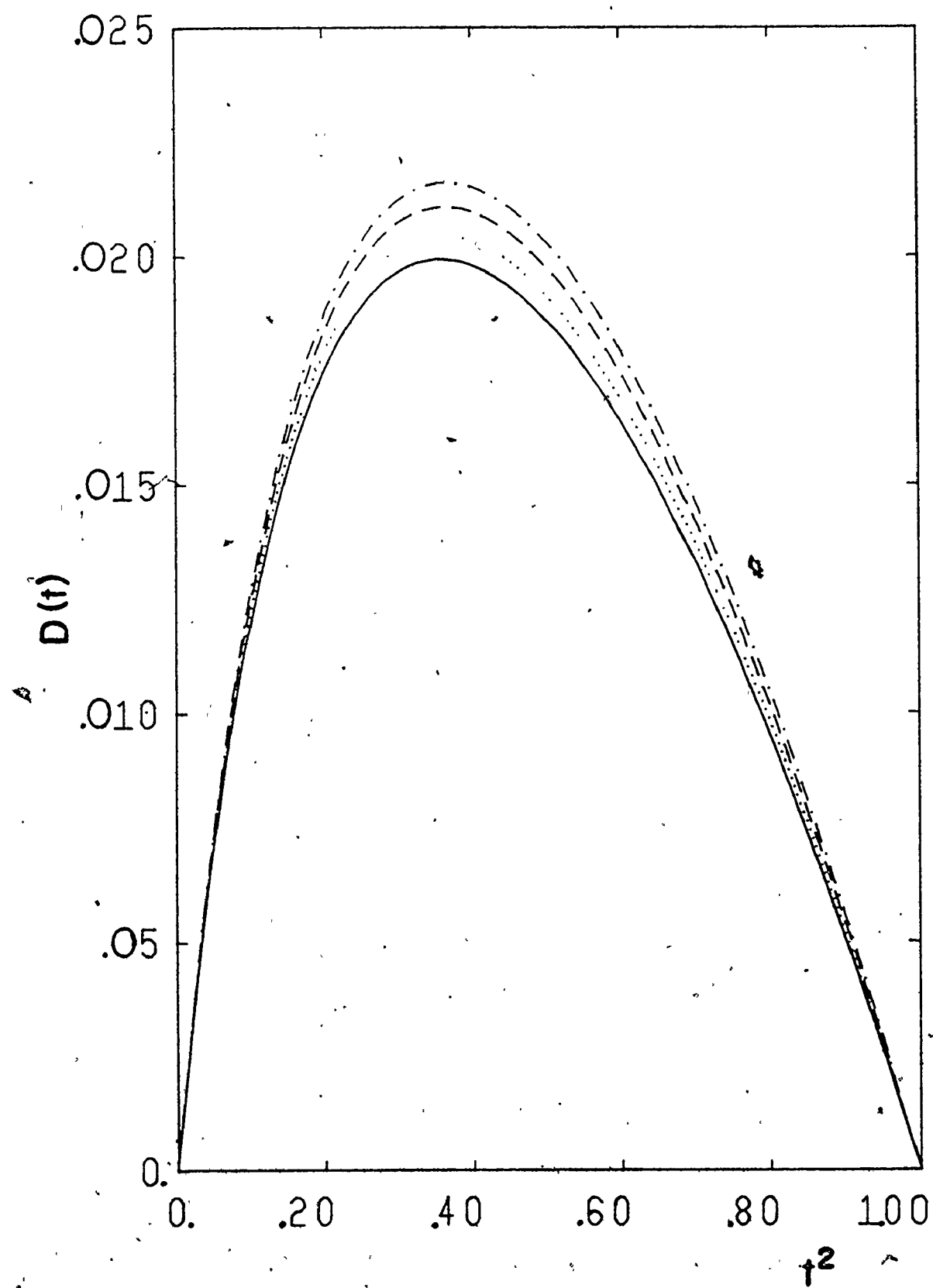
	T_c	$(2\Delta_0)/(k_B T_c)$
$s/(\pi a) = 0.5$	17.21°K	4.60
$s/(\pi a) = 1$	17.08°K	4.63
$s/(\pi a) = 2$	16.97°K	4.66
$s/(\pi a) = 4$	16.90°K	4.69

We find somewhat surprising behaviour. While T_c decreases with increasing $s/(\pi a)$, $D(t)$ and $(2\Delta_0)/(k_B T_c)$ increase with $s/(\pi a)$. However all the changes are very small, presumably due to the fact that the peak is fairly broad ($a = 1.5 \omega_{\max}$).

To see to what extent the above behaviour depends on the width of the peak, in Fig. (III.10) we give two $D(t)$ functions calculated for fixed $a = 0.25 \omega_{\max}$, fixed $N(\varepsilon = 0)$

Fig.III.9

$D(t)$ for fixed $N(0)$, fixed Lorentzian half width $a = 1.5 \omega_{\max}$
and varying ratio of the peak height over the background.



and two difference values of $s/(\pi a)$. The solid line is for $s/(\pi a) = 0.5$ and the dotted one is for $g/(\pi a) = 1$. The corresponding values of T_C and $(2\Delta_0)/(k_B T_C)$ are given in Table III.3.

Table III.3

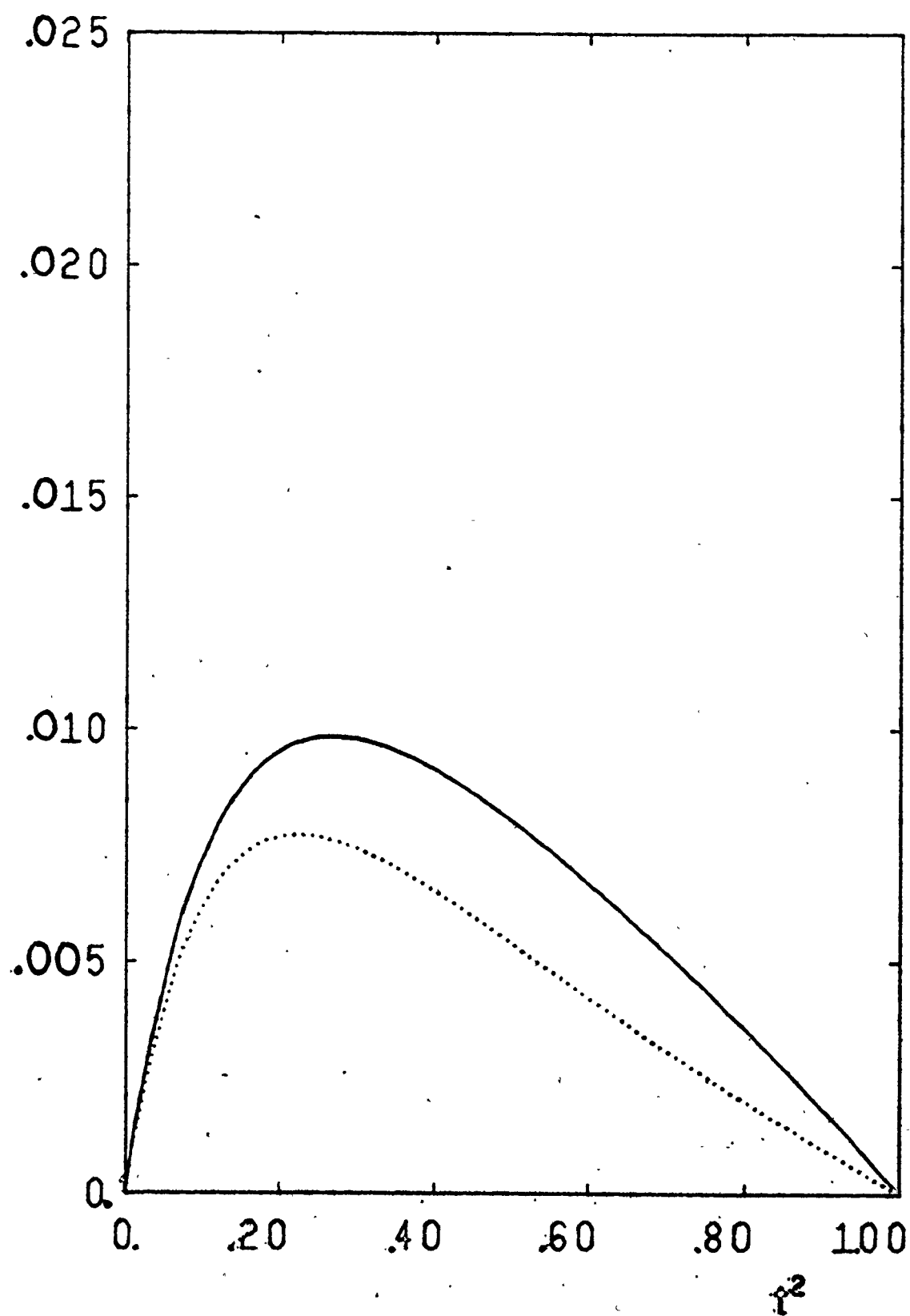
	T_C	$(2\Delta_0)/(k_B T_C)$
$s/(\pi a) = 0.5$	15.14°K	4.48
$s/(\pi a) = 1$	14.20°K	4.49

Thus T_C and $D(t)$ decrease slightly with increasing $s/(\pi a)$, while the ratio $(2\Delta_0)/(k_B T_C)$ remains practically unchanged.

We see that the effects of the interplay between the energy dependence in EDOS and a strong electron-phonon interaction are fairly complex. If the peak is narrow enough ($a \lesssim \omega_D$) T_C and $D(t)$ are reduced by decreasing the weight under the density of states in the important energy range between $-\omega_{\max}$ and ω_{\max} whether this weight is decreased by reducing the a or by increasing the height of the peak above the background. On the other hand for a given height of the peak the ratio $(2\Delta_0)/(k_B T_C)$ is increased by a sharpening of the peak if this sharpening is accomplished by increasing the ratio of peak height over background. For a given ratio $N(\epsilon=0)/N_b$ (see Eq. (III.50)) and given $N(\epsilon=0)$ all three quantities T_C , $D(t)$,

Fig.III.10

$D(t)$ for fixed $N(0)$, fixed Lorentzian half-width $a=0.25 \omega_{\max}$ and varying peak height over the background.



$(2\Delta_0)/(k_B T_C)$ decrease with a sharpening of the peak, the decrease being smallest for $(2\Delta_0)/(k_B T_C)$. Note that only T_C is monotonically decreasing with the reduction of weight under $N(\epsilon)$ at fixed $N(\epsilon=0)$, consistently with the functional derivative $\delta T_C / \delta N(\epsilon)$ of Lie and Carbotte³⁾. However if the peak is broad enough (i.e. $a > \omega_{\max}$) the modifications in all the thermodynamic quantities are small.

In addition Lie et al.⁶⁾ have calculated the behaviour of $(2\Delta_0)/(k_B T_C)$ for the case of a Lorentzian model of $N(\epsilon)$, Eq. (III.50), as a function of a with fixed s and N_0 . The ratio $(2\Delta_0)/(k_B T_C)$ turned out to be a decreasing function of a with the largest decrease at small values of a/ω_D (≤ 1) and was practically constant for a equal to several times ω_{\max} .

In the analysis of the experimental data from radiation damage experiments where the behaviour of T_C with disorder is studied, it is usually assumed that the effects of the peak in EDOS can be accounted for by assuming $\lambda \propto \langle N \rangle$, where $\langle N \rangle$ is the average value of $N(\epsilon)$ in the interval from $-\omega_D$ to ω_D (ω_D is the Debye energy). While this assumption works well for rather broad peaks with no appreciable variation on the scale of ω_D it fails for narrower peaks⁶⁾.

It is interesting to see what the effect is of such an averaging procedure on $D(t)$, i.e. how well $D(t)$ can be described by applying the usual Eliashberg theory and using the averaged value of $N(\epsilon)$ over the range from $-\omega_{\max}$ to ω_{\max} .

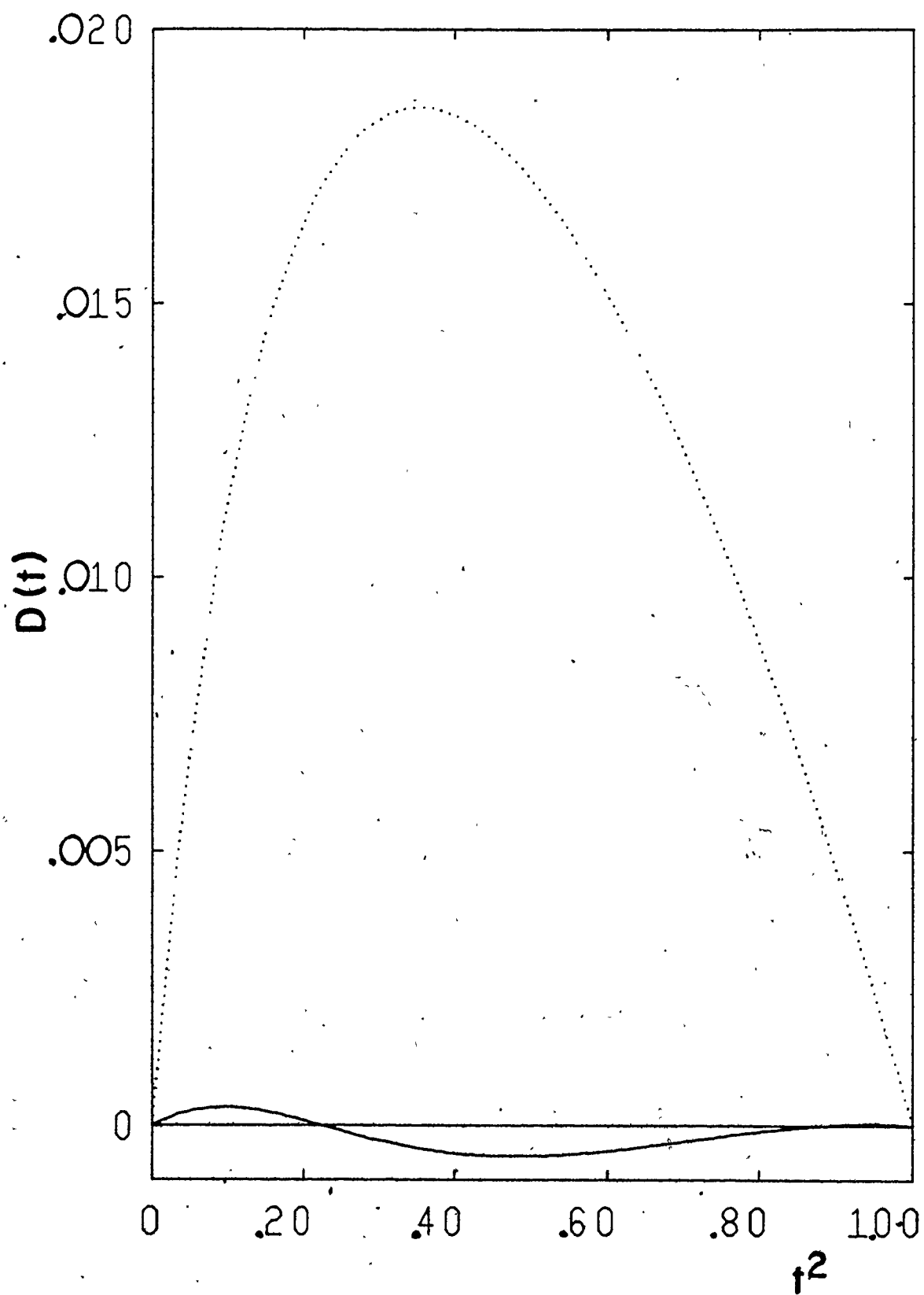
From Figs. (III.8) and (III.9) it is clear that for broad peaks ($a > \omega_{\max}$) the effect of energy dependence in $N(\epsilon)$ on $D(t)$ is rather small. Therefore we consider the case of very narrow peak, $a = 0.25 \omega_{\max}$, $s = 132$ and $N_0/N(0) = 0.335$. The value of T_c and Δ_0 for this choice of Lorentzian parameters is $T_c = 20.9^\circ\text{K}$ and $\Delta_0 = 4.91 \text{ meV}$ ($2\Delta_0/(k_B T_c) = 5.45$). In Fig. (III.11) the solid line represents $D(t)$ calculated for the above values of the Lorentzian parameters while the dotted curve represents $D(t)$ calculated within the usual Eliashberg theory by using the value of averaged EDOS (the average was calculated in the interval from $-\omega_{\max}$ to ω_{\max}). The T_c corresponding to the latter curve is 17.32°K . It is seen that such an averaging procedure fails badly for $D(t)$, while for T_c it gives a fairly close value.

In summary, for the peaks in EDOS near the Fermi level with the half-widths of the order of Debye energy or larger the modifications in all thermodynamic quantities considered here due to the variation in $N(\epsilon)$ are small and the problem of calculating the thermodynamic quantities in the superconducting state can be treated within the usual Eliashberg theory. However, if the scale of variation in $N(\epsilon)$ is less than ω_D one has to apply modified theory in order to account for the thermodynamic properties.

It should be remembered that our treatment is strictly

Fig.III.11

$D(t)$ for a narrow Lorentzian peak in EDOS obtained with modified eliashberg theory (solid line) and $D(t)$ obtained within the usual eliashberg theory by using the average value of the same density of states in the interval from $-\omega_{\max}$ to ω_{\max} (dotted line).



speaking valid only for the case when the EDOS can to a good approximation be represented by a symmetric Lorentzian model. A separate investigation would be required when this assumption ceases to be valid. In particular if the given EDOS does not possess particle-hole symmetry, χ (Eq. III.53) would be non-vanishing; that situation calls for the solution of a more complicated set of equations. Also, the expression for the free energy difference would have to be reconsidered. Since the symmetric Lorentzian models ($a \sim 150^\circ\text{K}$) have been successfully used in fitting the temperature dependence of some A-15 materials^{20,21}) our results should prove useful for those materials at least.

CHAPTER IV

SUMMARY AND CONCLUSIONS

In the A-15 materials, band structure calculations and numerous anomalies in the normal state properties have led to the idea that there may be unusually sharp structures in the electronic density of states (EDOS) of these materials. Any structure in EDOS on the scale of one or two Debye energies around the Fermi level requires careful study of both normal state and superconducting properties. We have analysed this problem within the isotropic approximation.

To understand the combined effects of a nonconstant EDOS and a strong realistic electron-phonon interaction in the superconducting state, we first had to find the effects on the electron quasi-particle properties in the normal state. The effect of smearing of the peak in the electron quasiparticle density of states (QDS) due to lifetime effects was treated from first principles. We showed that the renormalization by a strong electron-phonon interaction affects QDS as much as smearing if EDOS is not constant. The resulting sharpening of the structure in QDS may be related to the fact that in the past pathologically sharp models for EDOS (with square-root singularities or step-like discontinuities) have been needed

to fit some of the experimental data on normal state properties. We have also shown that the frequency dependence of the inverse lifetime due to the electron-phonon interaction is strongly affected by structure in EDOS. The temperature dependence of the electron mass enhancement parameter λ due to coupling with phonons was calculated for two model EDOS and the ratio $\lambda(T)/\lambda(0)$ was found to depend on EDOS as well as on α^2F .

The large superconducting critical fields in those A-15 materials with high superconducting critical temperatures have so far prohibited the experimental study of the effects of the electron-phonon interaction in the normal state at low temperatures. Also the large lattice anharmonicity in these materials makes any detailed analysis of the normal state specific heat data difficult. The analysis of the superconducting properties looks, at present, more promising.

In the superconducting state we have analyzed experimental single particle tunneling into superconductors. We have shown that the structure in EDOS influences the results of these experiments significantly even for a fairly modest amount of structure. Also, the character of the modifications in the normalized tunneling conductance and results obtained if this data is inverted conventionally, without taking non-constant EDOS into account, have been shown to correlate with the type of structure in EDOS. On the basis of several recent tunneling measurements on Nb_3Sn and Nb_3Al ^{82,88,89)} we conclude that the resulting normalized tunneling conductances show behaviour charac-

teristic of a peak in EDOS. However, it seems that similar behaviour could also be caused by the proximity effect. Presumably further improvement of the quality of the tunneling junctions and more experiments on the off-stoichiometric A-15 materials or A-15 ternary alloys will establish whether non-constant EDOS is actually significant.

We have also analysed the thermodynamic properties of a superconductor with rapidly varying EDOS. The expression for the free energy difference between the superconducting and normal state has been derived for a model electronic density of states, namely the symmetric Lorentzian model. We have calculated the resulting critical magnetic field deviation function $D(t)$ for several sets of Lorentzian parameters. The corresponding values of the ratio $(2\Delta_0)/(k_B T_c)$ have also been calculated. We have established that if the characteristic scale of variation in EDOS is greater than the Debye energy ω_D the effects of energy dependence in EDOS on $D(t)$, T_c and $(2\Delta_0)/(k_B T_c)$ are small. However if the peak in EDOS has a half-width less than ω_D , the resulting effects can be described only by a theory which takes the nonconstant $N(E)$ fully into account.

Our results should prove useful in analyzing the effects of non-constant EDOS on the superconducting thermodynamic properties. As with the tunneling experiments, an experimental study of the effects on $D(t)$ of alloying, changing the stoi-

chiometry or the impurity concentration should give information about the importance of the peaks in EDOS in determining the superconducting thermodynamic properties of A-15 materials. At present $D(t)$ has been measured only for V_3Si ¹⁰⁰⁾, among all the A-15 materials. The resulting $D(t)$ has an S-shape characteristic of a medium coupling superconductor (i.e. $\lambda \approx 1$). The measured ratios of $(2\Delta_0)/(k_B T_c)$ range from 3.5 to 3.8^{83,101)}, consistent with this $D(t)$; such values are characteristic of a weak to medium coupling superconductor. However, the recent far infra-red absorption experiments in V_3Si ^{102,103)} suggest a fairly large value, $\lambda \gtrsim 1.3$. Only by considering the overall consistency of various experimental and theoretical results will it be possible to understand the most important features determining the superconducting properties of A-15 materials.

APPENDIX 1

In this appendix we summarize some definitions and properties of the electron Green's functions and list the rules for evaluation of some Feynman diagrams. More details can be found in Ref. (40), (43), (56), (104).

The electron thermodynamic Green's function is defined by

$$G(k, \tau) = - \langle T c_k(\tau) c_k^\dagger(0) \rangle$$

where the index k stands for momentum index and spin. $\langle \rangle$ denotes the average in a grand canonical ensemble, T is Wick's time ordering operator and $c_k(t)$ ($c_k^\dagger(t)$) are electron destruction (creation) operators at time t in the Heisenberg picture. G can be expanded as the Fourier series

$$G(k, \tau) = T \sum_{m=-\infty}^{+\infty} e^{-i\omega_m \tau} G(k, i\omega_m)$$

$$\omega_m = \pi T (2n-1) \quad n = 0, \pm 1, \dots$$

It can be shown that $G(k, i\omega_n)$ has the spectral representation (or form)

$$G(k, i\omega_n) = \int_{-\infty}^{+\infty} d\omega \frac{A(k, \omega)}{i\omega_n - \omega}$$

Using this relation one can define the function $G(k, Z)$ with Z complex. Note that since A is real G has the property

$$G(k, Z^*) = G^*(k, Z) .$$

It turns out that at $i\omega_n$ with $n \geq 1$ G coincides with the retarded Green's function $G_R(k, Z)$ which is analytic and nonvanishing in the upper-half complex plane, while at $i\omega_n$ with $n \leq 0$ G coincides with the advanced Green's function $G_A(k, Z)$ which is analytic and nonvanishing in the lower-half complex plane. One can show that

$$\left. \begin{aligned} G_R(k, Z) &= O\left(\frac{1}{Z}\right) \\ G_A(k, Z) &= O\left(\frac{1}{Z}\right) \end{aligned} \right\} \quad |Z| \rightarrow \infty$$

For real ω

$$G_R(k, \omega) = \int_{-\infty}^{+\infty} d\omega' \frac{A(k, \omega')}{\omega - \omega' + i\delta}$$

$$G_A(k, \omega) = \int_{-\infty}^{+\infty} d\omega' \frac{A(k, \omega')}{\omega - \omega' - i\delta} .$$

Thus

$$A(k, \omega) = -\frac{1}{\pi} \operatorname{Im} G_R(k, \omega) = \frac{1}{\pi} \operatorname{Im} G_A(k, \omega)$$

and

$$G(k, \omega + i0^+) = G_R(k, \omega)$$

$$G(k, \omega - i0^+) = G_A(k, \omega) .$$

It follows that

$$A(k, \omega) = -\frac{1}{\pi} \text{Im} G(k, \omega + i\delta)$$

From the spectral form one can conclude that

$$\text{Im} G(k, z) < 0 \quad \text{if} \quad \text{Im} z > 0,$$

$$\text{Im} G(k, z) > 0 \quad \text{if} \quad \text{Im} z < 0.$$

From the Dyson equation

$$G^{-1}(k, i\omega_n) = i\omega_n - \epsilon_k - \Sigma(k, i\omega_n)$$

many of the properties of G translate into the corresponding properties of Σ .

We will state now the rules for calculating the contribution of various diagrams for the electron-phonon interaction.

1. With each solid internal line of the diagram one associates the noninteracting Green's function $G_0^{\pm}(k, i\omega_n) = [i\omega_n - \epsilon_k]^{-1}$ where ϵ_k is the electronic energy measured with respect to the chemical potential.
2. With each wavy (phonon) line of wave-vector \vec{q} , polarization λ and frequency $i\nu_n$ (see Ch. II) associate the phonon interacting Green's function $D_{\lambda 0}(q, i\omega_n)$.
3. Associate with each electron-phonon vertex in which a phonon of polarization λ and wave-vector \vec{q} is emitted and an electron is scattered from k to k' the factor $g_{k, k', \lambda} (= g_{k', k, \lambda}^*)$.

4. Multiply the result with $T^n (-1)^n (-1)^l$ where n is the number of phonon-lines and l is the number of closed electron loops and sum over all internal k 's and $i\omega_n$'s.

In the superconducting state, within Nambu's formalism, these rules remain unchanged except that the electron's Green's function becomes a 2×2 matrix \hat{G} and with each vertex one associates a $\hat{\tau}_3$ -matrix. One has also to keep matrices in their proper order given by the structure of the diagram and to trace over the free matrix indices for each closed electron loop.

Analogous rules apply for the Coulomb problem. It should be remembered that a given set of diagrammatic rules depend on the actual form of the interactions.

APPENDIX 2

EVALUATION OF SOME INTEGRALS WHICH APPEAR IN THE SELF-ENERGY EQUATIONS

In this appendix we evaluate the integrals

$$-\frac{1}{\pi} \operatorname{Im} \int_{-\infty}^{+\infty} d\varepsilon \frac{N(\varepsilon)}{N(0)} G_N(\varepsilon, \omega + i\delta) , \quad (\text{A2.1})$$

$$\operatorname{Re} \int_{-\infty}^{+\infty} d\varepsilon \frac{N(\varepsilon)}{N(0)} G_N(\varepsilon, \omega + i\delta) , \quad (\text{A2.2})$$

for a Lorentzian model and a triangular model of $N(\varepsilon)$. Here $G_N(\varepsilon, \omega + i\delta)$ is the retarded electron Green's function in the normal state. We also calculate the corresponding integrals for the superconducting state

$$-\frac{1}{\pi} \int_{-\infty}^{+\infty} d\varepsilon \frac{N(\varepsilon)}{N(0)} \hat{\tau}_3 \hat{G}_s(\varepsilon, i\omega_n) \hat{\tau}_3 , \quad (\text{A2.3})$$

$$-\frac{1}{\pi} \int_{-\infty}^{+\infty} d\varepsilon \frac{N(\varepsilon)}{N(0)} \hat{\tau}_3 \hat{G}_s(\varepsilon, \omega + i\delta) \hat{\tau}_3 \quad (\text{A2.4})$$

where $\hat{G}_s(\varepsilon, i\omega_n)$ is Nambu's 2×2 matrix electron thermodynamic Green's function in the superconducting state and $\hat{G}_s(\varepsilon, \omega + i\delta)$ is the retarded Nambu's Green's function just above the real frequency axis.

A2.I NORMAL STATE

In the normal state, assuming that Σ does not depend on ε

$$G_N(\varepsilon, \omega + i\delta) = \frac{1}{\omega + i\delta - \varepsilon - \Sigma_1(\omega + i\delta) - i\Sigma_2(\omega + i\delta)} \quad (A2.6)$$

where $\Sigma_1(\omega + i\delta) \equiv \text{Re } \Sigma_1(\omega + i\delta)$ and $\Sigma_2(\omega + i\delta) \equiv \text{Im } \Sigma(\omega + i\delta)$. Therefore

$$-\frac{1}{\pi} \text{Im } G_N = \begin{cases} -\frac{1}{\pi} \text{sgn}(\alpha) \frac{|\alpha|}{(\varepsilon - \beta)^2 + |\alpha|^2} & , \text{ for } \alpha \neq 0 \\ \delta(\varepsilon - \beta) & , \text{ for } \alpha = 0 \end{cases} \quad (A2.7a)$$

$$\quad \quad \quad (A2.7b)$$

where we have defined

$$\alpha \equiv \Sigma_2(\omega + i\delta) \quad (A2.8a)$$

and

$$\beta = \omega - \Sigma_1(\omega + i\delta) \quad (A2.8b)$$

In formula (A2.7b) $\delta(\varepsilon - \beta)$ is a Dirac delta-function. Also

$$\text{Re } G_N = \begin{cases} -\frac{\varepsilon - \beta}{(\varepsilon - \beta)^2 + |\alpha|^2} & , \text{ for } \beta \neq 0 \\ -\frac{1}{\varepsilon - \beta} & , \text{ for } \beta = 0 \end{cases} \quad (A2.9a)$$

$$(A2.9b)$$

A2.I.1 LORENTZIAN MODEL FOR $N(\epsilon)$

We take

$$N(\epsilon) = N_b \left(1 + s \frac{1}{\pi} \frac{a}{(\epsilon+b)^2 + a^2} \right) \quad (\text{A2.10})$$

where $a > 0$. In order to evaluate integrals (A2.1) and (A2.2) we need the following results

$$\int_{-\infty}^{+\infty} d\epsilon \frac{1}{\pi} \frac{a}{(\epsilon-b)^2 + a^2} = 1 \quad (\text{A2.11})$$

$$\int_{-\infty}^{+\infty} d\epsilon \left[\frac{1}{\pi} \frac{a_1}{(\epsilon+b_1)^2 + a_1^2} \right] \left[\frac{1}{\pi} \frac{a_2}{(\epsilon+b_2)^2 + a_2^2} \right] = \frac{1}{\pi} \frac{a_1 + a_2}{(a_1 + a_2)^2 + (b_1 - b_2)^2} \quad (\text{A2.12})$$

$$\int_{-\infty}^{+\infty} d\epsilon \frac{\epsilon}{\epsilon^2 + a_1^2} \frac{1}{\pi} \frac{a}{(\epsilon+b)^2 + a^2} = - \frac{b}{(a+a_1)^2 + b^2} \quad (\text{A2.13})$$

$$\int_{-\infty}^{+\infty} d\epsilon \frac{1}{\epsilon} \frac{1}{\pi} \frac{a}{(\epsilon+b)^2 + a^2} = - \frac{b}{a^2 + b^2} \quad (\text{A2.14})$$

where we have assumed that $a, a_1, a_2 > 0$. Equations (A2.11)-(A2.13) are most easily obtained by the residue theorem and (A2.14) is to be interpreted as a principal part integral (since the term $1/\epsilon$ in this integral arises from the real part of the Green's function). Then

$$-\frac{1}{\pi} \operatorname{Im} \int_{-\infty}^{+\infty} d\varepsilon \frac{N(\varepsilon)}{N(0)} G_N(\varepsilon, \omega + i\delta) = \begin{cases} -\operatorname{sgn}(\alpha) \frac{N_b}{N(0)} \left(1 + s \frac{1}{\pi} \frac{a + |\alpha|}{(a + |\alpha|)^2 + (b + \beta)^2}\right) & \text{For } \alpha \neq 0 \\ \frac{N_b}{N(0)} \left(1 + s \frac{1}{\pi} \frac{a}{a^2 + (b + \beta)^2}\right) & \text{For } \alpha = 0 \end{cases} \quad (\text{A2.15a})$$

$$(\text{A2.15b})$$

and

$$\operatorname{Re} \int_{-\infty}^{+\infty} d\varepsilon \frac{N(\varepsilon)}{N(0)} G_N(\varepsilon, \omega + i\delta) = \frac{N_b}{N(0)} s \frac{\beta + b}{(a + |\alpha|)^2 + (\beta + b)^2} \quad (\text{A2.16})$$

A2.1.2 TRIANGULAR MODEL FOR $N(\varepsilon)$

Here we consider

$$N(\varepsilon) = \begin{cases} B, & \varepsilon < \varepsilon_1 \\ B + \frac{P-B}{\varepsilon_2 - \varepsilon_1} (\varepsilon - \varepsilon_1), & \varepsilon_1 \leq \varepsilon < \varepsilon_2 \\ B + \frac{B-P}{\varepsilon_3 - \varepsilon_2} (\varepsilon - \varepsilon_2), & \varepsilon_2 \leq \varepsilon < \varepsilon_3 \\ B, & \varepsilon_3 \leq \varepsilon \end{cases} \quad (\text{A2.17})$$

We have

$$\begin{aligned} & -\frac{1}{\pi} \operatorname{Im} \int_{-\infty}^{+\infty} d\varepsilon \frac{N(\varepsilon)}{N(0)} G_N(\varepsilon, \omega + i\delta) = \\ & = -\operatorname{sgn}(\alpha) \frac{1}{N(0)} \left\{ B + \frac{1}{\pi} (P-B) \left[\frac{\beta - \varepsilon_1}{\varepsilon_2 - \varepsilon_1} \left(\operatorname{arctg} \frac{\varepsilon_2 - \beta}{|\alpha|} - \right. \right. \right. \\ & \left. \left. - \operatorname{arctg} \frac{\varepsilon_1 - \beta}{|\alpha|} \right) - \frac{\beta - \varepsilon_3}{\varepsilon_3 - \varepsilon_2} \left(\operatorname{arctg} \frac{\varepsilon_3 - \beta}{|\alpha|} - \operatorname{arctg} \frac{\varepsilon_2 - \beta}{|\alpha|} \right) + \right. \\ & \left. + \frac{1}{2} \frac{|\alpha|}{\varepsilon_2 - \varepsilon_1} \ln \frac{(\varepsilon_2 - \beta)^2 + \alpha^2}{(\varepsilon_1 - \beta)^2 + \alpha^2} - \frac{1}{2} \frac{|\alpha|}{\varepsilon_3 - \varepsilon_2} \ln \frac{(\varepsilon_3 - \beta)^2 + \alpha^2}{(\varepsilon_2 - \beta)^2 + \alpha^2} \right\} \quad (\text{A2.18a}) \end{aligned}$$

For $\alpha \neq 0$

and

$$-\frac{1}{\pi} \operatorname{Im} \int_{-\infty}^{+\infty} d\varepsilon \frac{N(\varepsilon)}{N(0)} G_N(\varepsilon, \omega + i\delta) = \frac{N(\beta)}{N(0)}, \quad \text{for } \alpha = 0 \quad (\text{A2.18b})$$

For the integrals over the real part of the Green's function we get

$$\begin{aligned} \operatorname{Re} \int_{-\infty}^{+\infty} d\varepsilon \frac{N(\varepsilon)}{N(0)} G_N(\varepsilon, \omega + i\delta) = \\ = \frac{P-B}{N(0)} \left\{ \frac{|\alpha|}{\varepsilon_2 - \varepsilon_1} \left[\operatorname{arctg} \frac{\varepsilon_2 - \beta}{|\alpha|} - \operatorname{arctg} \frac{\varepsilon_1 - \beta}{|\alpha|} \right] - \right. \\ - \frac{|\alpha|}{\varepsilon_3 - \varepsilon_2} \left[\operatorname{arctg} \frac{\varepsilon_3 - \beta}{|\alpha|} - \operatorname{arctg} \frac{\varepsilon_2 - \beta}{|\alpha|} \right] - \frac{1}{2} \frac{\beta - \varepsilon_1}{\varepsilon_2 - \varepsilon_1} \ln \frac{(\varepsilon_2 - \beta)^2 + \alpha^2}{(\varepsilon_1 - \beta)^2 + \alpha^2} + \\ \left. + \frac{1}{2} \frac{\beta - \varepsilon_3}{\varepsilon_3 - \varepsilon_2} \ln \frac{(\varepsilon_3 - \beta)^2 + \alpha^2}{(\varepsilon_2 - \beta)^2 + \alpha^2} \right\}, \quad \text{for } \alpha \neq 0; \quad (\text{A2.19a}) \end{aligned}$$

$$\begin{aligned} \operatorname{Re} \int_{-\infty}^{+\infty} d\varepsilon \frac{N(\varepsilon)}{N(0)} G_N(\varepsilon, \omega + i\delta) = \\ = \frac{P-B}{N(0)} \left[\frac{\beta - \varepsilon_3}{\varepsilon_3 - \varepsilon_2} \ln \left| \frac{\varepsilon_3 - \beta}{\varepsilon_2 - \beta} \right| - \frac{\beta - \varepsilon_1}{\varepsilon_2 - \varepsilon_1} \ln \left| \frac{\varepsilon_2 - \beta}{\varepsilon_1 - \beta} \right| \right], \\ \text{for } \alpha \neq 0 \text{ and } \beta \neq \varepsilon_1, \varepsilon_2, \varepsilon_3; \quad (\text{A2.19b}) \end{aligned}$$

$$\begin{aligned} \operatorname{Re} \int_{-\infty}^{+\infty} d\varepsilon \frac{N(\varepsilon)}{N(0)} G_N(\varepsilon, \omega + i\delta) = - \frac{P-B}{N(0)} \frac{\varepsilon_3 - \varepsilon_1}{\varepsilon_3 - \varepsilon_2} \ln \left| \frac{\varepsilon_3 - \varepsilon_1}{\varepsilon_2 - \varepsilon_1} \right|, \\ \text{for } \alpha = 0 \text{ and } \beta = \varepsilon_1; \quad (\text{A2.19c}) \end{aligned}$$

$$\text{Re} \int_{-\infty}^{+\infty} d\varepsilon \frac{N(\varepsilon)}{N(0)} G_N(\varepsilon, \omega + i\delta) = - \frac{P-B}{N(0)} \ln \left| \frac{\varepsilon_3 - \varepsilon_2}{\varepsilon_2 - \varepsilon_1} \right| ,$$

$$\text{for } \alpha = 0 \text{ and } \beta = \varepsilon_2 ; \quad (\text{A2.19d})$$

$$\text{Re} \int_{-\infty}^{+\infty} d\varepsilon \frac{N(\varepsilon)}{N(0)} G_N(\varepsilon, \omega + i\delta) = - \frac{P-B}{N(0)} \frac{\varepsilon_3 - \varepsilon_1}{\varepsilon_2 - \varepsilon_1} \ln \left| \frac{\varepsilon_3 - \varepsilon_2}{\varepsilon_3 - \varepsilon_1} \right| ,$$

$$\text{for } \alpha = 0 \text{ and } \beta = \varepsilon_3 . \quad (\text{A2.19e})$$

We note that in evaluating integrals (A2.19a)-(A2.19e) one has to interpret them as principal part integrals whenever necessary.

Obviously, if an attempt is made to use the $N(\varepsilon)$ obtained from band-structure calculations it would be convenient to assume that it is a piece-wise linear function and hence one would have to solve the same type of integrals as for the triangular model.

A2.II SUPERCONDUCTING STATE

We have

$$\hat{G}_S(\varepsilon, i\omega_n) = \frac{i\omega_n Z(i\omega_n) \hat{\tau}_0 + (\varepsilon + \chi(i\omega_n)) \hat{\tau}_3 + Z(i\omega_n) \Delta(i\omega_n) \hat{\tau}_1}{Z^2(i\omega_n) [(i\omega_n)^2 - \Delta^2(i\omega_n)] - (\varepsilon + \chi(i\omega_n))^2} \quad (\text{A2.20})$$

and

$$\hat{G}_S(\varepsilon, \omega + i\delta) = \frac{(\omega + i\delta) Z(\omega + i\delta) \hat{\tau}_0 + (\varepsilon + \chi(\omega + i\delta)) \hat{\tau}_3 + Z(\omega + i\delta) \Delta(\omega + i\delta) \hat{\tau}_1}{Z^2(\omega + i\delta) [(\omega + i\delta)^2 - \Delta^2(\omega + i\delta)] - (\varepsilon + \chi(\omega + i\delta))^2} \quad (\text{A2.21})$$

where $\hat{\tau}_0 = \begin{pmatrix} 1 & 0 \\ 0 & 1 \end{pmatrix}$, $\hat{\tau}_1 = \begin{pmatrix} 0 & 1 \\ 1 & 0 \end{pmatrix}$ and $\hat{\tau}_3 = \begin{pmatrix} 1 & 0 \\ 0 & -1 \end{pmatrix}$ are Pauli matrices.

We have assumed that Z , χ and Δ do not depend on ε .

A2.II.1 LORENTZIAN MODEL FOR $N(\epsilon)$

Here we assume that $N(\epsilon)$ has the form given by (A2.10).

Note that the $\hat{\tau}_0$ -component and the $\hat{\tau}_1$ -component of

$-\frac{1}{\pi} \hat{\tau}_3 \hat{G}_s(\epsilon, i\omega_n) \hat{\tau}_3$ have the form

$$Y(\epsilon, i\omega_n) = \frac{X(i\omega_n)}{Z(i\omega_n) [\omega_n^2 + \Delta^2(i\omega_n)]^{1/2}} \frac{1}{\pi} \frac{Z(i\omega_n) [\Delta_n^2 + \omega_n^2]^{1/2}}{Z^2(i\omega_n) [\omega_n^2 + \Delta^2(i\omega_n)] + (\epsilon + \chi(i\omega_n))^2} \quad (A2.21)$$

where $X(i\omega_n) = i\omega_n Z(i\omega_n)$ and $\chi(i\omega_n) = -Z(i\omega_n) \Delta(i\omega_n)$ respectively.

Here Z , Δ and χ are real numbers and Z is positive. Using (A2.11) and (A2.12) we obtain

$$\begin{aligned} \int_{-\infty}^{+\infty} d\epsilon \frac{N(\epsilon)}{N(0)} Y(\epsilon, i\omega_n) &= \\ &= \frac{X(i\omega_n)}{Z(i\omega_n) [\omega_n^2 + \Delta^2(i\omega_n)]^{1/2}} \frac{N_b}{N(0)} \left\{ 1 + s \frac{1}{\pi} \times \right. \\ &\times \left. \frac{Z(i\omega_n) [\omega_n^2 + \Delta^2(i\omega_n)]^{1/2+a}}{[Z(i\omega_n) [\omega_n^2 + \Delta^2(i\omega_n)]^{1/2+a}]^2 + (\chi(i\omega_n) - b)^2} \right\} \quad (A2.22) \end{aligned}$$

The $\hat{\tau}_3$ -component gives (see A2.13)

$$\begin{aligned} \int_{-\infty}^{+\infty} d\epsilon \frac{N(\epsilon)}{N(0)} \frac{1}{\pi} \frac{\epsilon + \chi(i\omega_n)}{Z^2(i\omega_n) (\omega_n^2 + \Delta^2(i\omega_n)) + (\epsilon + \chi(i\omega_n))^2} &= \\ &= \frac{N_b}{N(0)} \frac{s}{\pi} \frac{\chi(i\omega_n) - b}{(a + Z(i\omega_n) \sqrt{\omega_n^2 + \Delta^2(i\omega_n)})^2 + (\chi(i\omega_n) - b)^2} \quad (A2.23) \end{aligned}$$

On the real frequency axis calculations for the superconducting state were performed only with a triangular model for $N(\epsilon)$. Therefore we do not give the corresponding integrals for $(-1/\pi)\hat{\tau}_3\hat{G}_S(\epsilon, \omega+i\delta)\hat{\tau}_3$.

A2.II.2 TRIANGULAR MODEL FOR $N(\epsilon)$

In the superconducting state calculations with the triangular model for $N(\epsilon)$, Eq. (A2.17), were performed only on the real frequency axis. Hence we give only the values of $(-1/\pi)\text{Im} \int_{-\infty}^{+\infty} d\epsilon (N(\epsilon)/N(0)) \times \hat{\tau}_3\hat{G}(\epsilon, \omega+i\delta)\hat{\tau}_3$. The quantities which appear in the zero temperature Eliashberg equations generalized to include the energy dependence in the electronic density of states are (see Eqs. (III.37a)-(III.37b)):

$$\tilde{N}_X(\omega+i\delta) = -\frac{1}{\pi} \text{Im} \int_{-\infty}^{+\infty} d\epsilon \frac{N(\epsilon)}{N(0)} \frac{X(\omega+i\delta)}{Q^2(\omega+i\delta) - (\epsilon + \chi(\omega+i\delta))^2}, \quad (\text{A2.24})$$

where

$$X(\omega+i\delta) = \begin{cases} \Delta(\omega+i\delta)Z(\omega+i\delta) & \text{for the } \Delta\text{-equation} \\ \omega Z(\omega+i\delta) & \text{for the } Z\text{-equation} \end{cases} \quad (\text{A2.25})$$

and

$$\tilde{N}_\chi(\omega+i\delta) = \frac{1}{\pi} \text{Im} \int_{-\infty}^{+\infty} d\epsilon \frac{N(\epsilon)}{N(0)} \frac{\epsilon + \chi(\omega+i\delta)}{Q^2(\omega+i\delta) - (\epsilon + \chi(\omega+i\delta))^2} \quad (\text{A2.26})$$

for the χ equation.

The quantities Δ , Z and χ are generally complex and

$$Q \equiv Q(\omega+i\delta) = Z(\omega+i\delta)R(\omega+i\delta) , \quad (\text{A2.27})$$

$$R \equiv R(\omega+i\delta) = [(\omega+i\delta)^2 - \Delta^2(\omega+i\delta)]^{1/2} \quad (\text{A2.28})$$

where for a given $\omega > 0$ the branch of the square-root in Eq. (A2.28) is chosen in such a way that

$$Q_2 \equiv \text{Im } Q > 0 .$$

In general we will denote the real parts of complex quantities by the subscript 1, while the imaginary parts will be labelled by the subscript 2.

Eq. (A2.24) can be written in the form

$$\tilde{N}_x(\omega+i\delta) = J^{(1)} + J^{(2)} \quad (\text{A2.29})$$

where

$$J^{(1)} \equiv -\frac{1}{\pi} \text{Im} \int_{-\infty}^{+\infty} d \frac{B}{N(0)} \frac{X}{Q^2 - (\epsilon + \chi)^2} \quad (\text{A2.30})$$

$$\begin{aligned} J^{(2)} \equiv & -\frac{1}{\pi} \text{Im} \left\{ \int_{\epsilon_1}^{\epsilon_2} d\epsilon \frac{P-B}{N(0)} \frac{\epsilon - \epsilon_1}{\epsilon_2 - \epsilon_1} \frac{X}{Q^2 - (\epsilon + \chi)^2} + \right. \\ & \left. + \int_{\epsilon_2}^{\epsilon_3} d\epsilon \frac{B-P}{N(0)} \frac{\epsilon - \epsilon_3}{\epsilon_3 - \epsilon_2} \frac{X}{Q^2 - (\epsilon + \chi)^2} \right\} . \end{aligned} \quad (\text{A2.31})$$

We calculate J_1 by the residue theorem. The value will depend on the signs of $\chi_2 - Q_2$ and $\chi_2 + Q_2$. It is worth noting that physically, at $T=0$, Q defined by Eq. (A2.27) can vanish only at the gap edge $\omega = \Delta_0$ and that at other values of ω it has a

finite imaginary part (we assume that the phonon frequencies span the range from zero up to some maximum value ω_D). One has the following cases:

1) $Q \neq 0$

1.1) $\chi_2 - Q_2 < 0$ and $\chi_2 + Q_2 > 0$

$$J^{(1)} = \frac{B}{N(0)} \operatorname{Re} \frac{\omega}{[(\omega + i\delta)^2 - \Delta^2 (\omega + i\delta)]^{1/2}} \quad (\text{A2.32})$$

1.2) $\chi_2 - Q_2 < 0$ and $\chi_2 + Q_2 = 0$

$$J^{(1)} = \frac{1}{2} \frac{B}{N(0)} \operatorname{Re} \frac{\omega}{[(\omega + i\delta)^2 - \Delta^2 (\omega + i\delta)]^{1/2}}$$

1.3) $\chi_2 - Q_2 < 0$ and $\chi_2 + Q_2 < 0$, $J^{(1)} = 0$

1.4) $\chi_2 - Q_2 = 0$ and $\chi_2 + Q_2 > 0$, $J^{(1)}$ is the same as in 1.2).

1.5) $\chi_2 - Q_2 > 0$ and $\chi_2 + Q_2 > 0$, $J^{(1)} = 0$.

We do not give the other possibilities since they would contradict our starting convention $Q_2 > 0$.

2) $Q = 0$ and $\chi_2 = 0$ (the situation at the gap edge)

The integral $J^{(1)}$ is equal to zero since in this case X is real.

We now consider the integral $J^{(2)}$.

1') $Q \neq 0$. The integral $J^{(2)}$ can be written in the form

$$J^{(2)} = -\frac{1}{2} \frac{P-B}{N(0)} \left(-\frac{1}{\pi}\right) \text{Im} \left[\frac{\omega}{R} (I(\chi-Q) - I(\chi+q)) \right] \quad (\text{A2.33})$$

where

$$I(Z) = \int_{\epsilon_1}^{\epsilon_2} d\epsilon \frac{\epsilon - \epsilon_1}{\epsilon_2 - \epsilon_1} \frac{1}{\epsilon + Z} - \int_{\epsilon_2}^{\epsilon_3} d\epsilon \frac{\epsilon - \epsilon_3}{\epsilon_3 - \epsilon_2} \frac{1}{\epsilon + Z} \quad (\text{A2.34})$$

1.1') $Z_2 = \text{Im } Z \neq 0$

$$\begin{aligned} \text{Re } I(Z) = & \frac{1}{\epsilon_3 - \epsilon_2} \left[\frac{\epsilon_3 + Z_1}{2} \ln \frac{(\epsilon_3 + Z_1)^2 + Z_2^2}{(\epsilon_2 + Z_1)^2 + Z_2^2} + |Z_2| \times \right. \\ & \times \left. \left(\arctg \left(\frac{\epsilon_3 + Z_1}{|Z_2|} \right) - \arctg \left(\frac{\epsilon_2 + Z_1}{|Z_2|} \right) \right) \right] - \\ & - \frac{1}{\epsilon_2 - \epsilon_1} \left[\frac{\epsilon_1 + Z_1}{2} \ln \frac{(\epsilon_2 + Z_1)^2 + Z_2^2}{(\epsilon_1 + Z_1)^2 + Z_2^2} + |Z_2| \times \right. \\ & \times \left. \left(\arctg \left(\frac{\epsilon_2 + Z_1}{|Z_2|} \right) - \arctg \left(\frac{\epsilon_1 + Z_1}{|Z_2|} \right) \right) \right] \quad (\text{A2.35}) \end{aligned}$$

$$\begin{aligned} \text{Im } I(Z) = & \frac{1}{\epsilon_3 - \epsilon_2} \left[\frac{Z_2}{2} \ln \frac{(\epsilon_3 + Z_1)^2 + Z_2^2}{(\epsilon_2 + Z_1)^2 + Z_2^2} - \text{sgn}(Z_2) (\epsilon_3 + Z_1) \times \right. \\ & \times \left. \left(\arctg \left(\frac{\epsilon_3 + Z_1}{|Z_2|} \right) - \arctg \left(\frac{\epsilon_2 + Z_1}{|Z_2|} \right) \right) \right] - \\ & - \frac{1}{\epsilon_2 - \epsilon_1} \left[\frac{Z_2}{2} \ln \frac{(\epsilon_2 + Z_1)^2 + Z_2^2}{(\epsilon_1 + Z_1)^2 + Z_2^2} - \text{sgn}(Z_2) (\epsilon_1 + Z_1) \times \right. \\ & \times \left. \left(\arctg \left(\frac{\epsilon_2 + Z_1}{|Z_2|} \right) - \arctg \left(\frac{\epsilon_1 + Z_1}{|Z_2|} \right) \right) \right] \quad (\text{A2.36}) \end{aligned}$$

$$1.2') \quad Z_2 = \operatorname{Im} Z = 0$$

$$1.2.1') \quad Z_1 = \operatorname{Re} Z \neq -\epsilon_1, -\epsilon_2, -\epsilon_3.$$

$$\operatorname{Re} I(Z) = \frac{\epsilon_3 + Z_1}{\epsilon_3 - \epsilon_2} \ln \left| \frac{\epsilon_3 + Z_1}{\epsilon_2 + Z_1} \right| \rightarrow \frac{\epsilon_1 + Z_1}{\epsilon_2 - \epsilon_1} \ln \left| \frac{\epsilon_2 + Z_1}{\epsilon_1 + Z_1} \right|, \quad (A2.37)$$

$$\operatorname{Im} I(Z) = 0$$

$$1.2.2') \quad Z_1 = -\epsilon_1$$

$$\operatorname{Re} I(Z) = \frac{\epsilon_3 - \epsilon_1}{\epsilon_3 - \epsilon_2} \ln \left| \frac{\epsilon_3 - \epsilon_1}{\epsilon_2 - \epsilon_1} \right|$$

$$\operatorname{Im} I(Z) \neq 0$$

(A2.38)

$$1.2.3') \quad Z_1 = \epsilon_2$$

$$\operatorname{Re} I(z) = \ln \left| \frac{\epsilon_3 - \epsilon_2}{\epsilon_2 - \epsilon_1} \right|$$

(A2.39)

$$\operatorname{Im} I(Z) = 0$$

$$1.2.4') \quad Z_1 = -\epsilon_3$$

$$\operatorname{Re} I(Z) = \frac{\epsilon_3 - \epsilon_1}{\epsilon_2 - \epsilon_1} \ln \left| \frac{\epsilon_3 - \epsilon_2}{\epsilon_3 - \epsilon_1} \right|$$

(A2.40)

$$\operatorname{Im} I(Z) = 0$$

2') $Q = 0$ and $\chi_2 = 0$ (situation at the gap edge) $J^{(2)} = 0$

For $\tilde{N}_\chi(\omega+i\delta)$, Eq. (A2.26), we have

$$\tilde{N}_\chi(\omega+i\delta) = K^{(1)} + K^{(2)} \quad (\text{A2.41})$$

$$K^{(1)} = \frac{1}{\pi} \text{Im} \int_{-\infty}^{+\infty} d\varepsilon \frac{B}{N(0)} \frac{\varepsilon + \chi}{Q^2 - (\varepsilon + \chi)^2} \quad (\text{A2.42})$$

$$K^{(2)} = \frac{1}{\pi} \text{Im} \left\{ \int_{\varepsilon_1}^{\varepsilon_2} d\varepsilon \frac{P-B}{N(0)} \frac{\varepsilon - \varepsilon_1}{\varepsilon_2 - \varepsilon_1} \frac{\varepsilon + \chi}{Q^2 - (\varepsilon + \chi)^2} + \right. \\ \left. + \int_{\varepsilon_2}^{\varepsilon_3} d\varepsilon \frac{B-P}{N(0)} \frac{\varepsilon - \varepsilon_3}{\varepsilon_3 - \varepsilon_2} \frac{\varepsilon + \chi}{Q^2 - (\varepsilon + \chi)^2} \right\}. \quad (\text{A2.43})$$

We consider first the integral $K^{(1)}$.

1") $Q \neq 0$

$$K^{(1)} = \frac{1}{2} \frac{B}{N(0)} (\text{sgn}(\chi_2 + Q_2) + \text{sgn}(\chi_2 - Q_2)) \quad (\text{A2.44})$$

where in this formula we assume that $\text{sgn}(x) = 0$ for $x = 0$.

Note that in the normal state for $\omega > 0$

$$Q_2 = \omega Z_2(\omega+i\delta) = -\frac{1}{2} [\Sigma_2(\omega+i\delta) + \Sigma_2(-\omega+i\delta)] \quad (\text{A2.45})$$

$$\chi_2 = \frac{1}{2} [\Sigma_2(\omega+i\delta) - \Sigma_2(-\omega+i\delta)] \quad (\text{A2.46})$$

where Σ_2 is the imaginary part of the normal state self-energy $\Sigma(\omega+i\delta) = \omega(1-Z(\omega+i\delta)) + \chi(\omega+i\delta)$ (see Chapter II). Therefore

$$\chi_2 - Q_2 = \Sigma(\omega + i\delta) < 0 \quad (\text{A2.47})$$

and

$$\chi_2^* + Q_2 = -\Sigma_2(-\omega + i\delta) > 0 \quad (\text{A2.48})$$

so that one can expect that the integral $K^{(1)}$ is zero in the superconducting state at least for large enough $\omega > 0$. At any rate, if $Q_2 > |\chi_2|$, which seems to be the case in practice, the integral $K^{(1)}$ is zero.

1.2") $Q = 0$ and $\chi_2 = 0$ (the situation at the gap edge) the integral $K^{(1)}$ is zero.

It can be easily seen that the integral $K^{(2)}$ reduces to

$$K^{(2)} = -\frac{1}{2\pi} \frac{P-B}{N(0)} \text{Im}(I(\chi-Q) + I(\chi+Q)) \quad (\text{A2.49})$$

where the integral $I(Z)$ is defined by Eq. (A2.34).

APPENDIX 3

THE GRAND THERMODYNAMIC POTENTIAL FOR THE INTERACTING ELECTRON-PHONON SYSTEM IN THE NORMAL AND SUPERCONDUCTING STATE. THE FREE ENERGY DIFFERENCE BETWEEN THE SUPERCONDUCTING AND NORMAL STATE

As is well known from statistical mechanics, in order to calculate the thermodynamic properties of a macroscopic system it is sufficient to know the form of the grand thermodynamic potential $\Omega(\beta, \mu, V)$ which is related to the grand partition function $Z_G(\beta, \mu, V)$ by

$$Z_G(\beta, \mu, V) = \exp[-\beta\Omega(\beta, \mu, V)] \quad (A3.1)$$

In the above formula $\beta = 1/T$ (as usual we take a system of units in which Boltzmann's constant $k_B = 1$ and $\hbar = 1$), μ is the chemical potential and V is the volume of the system. A first principal calculation of Ω for a complicated many-body system which consists of strongly interacting particles is a difficult problem. The canonical solution of this problem for an isotropic system of spin 1/2 fermions interacting via instantaneous spin-independent two-body potential was given by J.M. Luttinger and J.C. Ward⁶⁹⁾. They have shown that for such a system of fermions

$$\Omega = -\frac{1}{\beta} \sum_k \sum_{n=-\infty}^{+\infty} \exp(i\omega_n 0^+) \{ \ln[-G^{-1}(k, i\omega_n)] + \Sigma(k, i\omega_n) G(k, i\omega_n) \} + \Omega' \quad (A3.2a)$$

where

$$\Omega' = \left\{ \begin{array}{l} \text{Contribution of all closed linked skeleton} \\ \text{diagrams computed according to the appropriate} \\ \text{diagrammatic rules but with } G_0(k, i\omega_n) \\ \text{replaced by the full } G(k, i\omega_n) \end{array} \right\} \quad (\text{A3.2b})$$

Here $k = (\vec{k}, m)$, where \vec{k} is momentum and m is the spin projection quantum number,

$$\omega_n = \pi(2n-1)/\beta \quad (n = 0, \pm 1, \pm 2, \dots)$$

G is the electron thermodynamic Green's function and Σ is the corresponding self-energy part defined by

$$G^{-1}(k, i\omega_n) = G_0^{-1}(k, i\omega_n) - \Sigma(k, i\omega_n) . \quad (\text{A3.3})$$

Thus, Ω given by Eqs. (A3.2a), (A3.2b) can be considered as a functional of $\{G(k, i\omega_n)\}$. Luttinger and Ward have shown that this Ω is stationary with respect to a first order variation in $\{\Sigma(k, i\omega_n)\}$ if and only if

$$\Sigma(k, i\omega_n) = \left\{ \begin{array}{l} \text{Contribution of all possible skeleton} \\ \text{diagrams with } G_0(k, i\omega_n) \text{ replaced by} \\ G(\vec{k}, i\omega_n) . \end{array} \right\} \quad (\text{A3.4})$$

In other words, the first order change in Ω is zero when one

makes a first order change in $\Sigma(k, i\omega_n)$ around its correct value. This property of Ω which we will call a stationary property, is very useful in various practical calculations.

Eliashberg³⁶⁾ has generalized the procedure of Luttinger and Ward to the interacting electron-phonon system in both the normal and superconducting state. For a homogeneous and isotropic model of a metal Eliashberg's result for the grand thermodynamic potential per unit volume in the normal state can be written in the form

$$\begin{aligned} \Omega = & -\frac{2}{\beta} \sum_P \exp(i\omega_n 0^+) \{ \ln[-G^{-1}(P)] + \Sigma(P)G(P) \} + \\ & + \frac{1}{2\beta} \sum_Q \exp(i\nu_n 0^+) \{ \ln[-D^{-1}(Q)] + \pi(Q)D(Q) \} - \\ & - \frac{1}{\beta^2} \sum_P \sum_{P'} |g_{P-P'}|^2 G(P) D(P-P') G(P') \end{aligned} \quad (A3.5)$$

where

$$\begin{aligned} P = (\vec{k}, i\omega_n) \quad , \quad \omega_n = \pi(2n-1)/\beta \\ Q = (\vec{q}, i\nu_n) \quad , \quad \nu_n = \pi 2n/\beta \end{aligned} \quad \left. \vphantom{\begin{aligned} P = (\vec{k}, i\omega_n) \\ Q = (\vec{q}, i\nu_n) \end{aligned}} \right\} n = 0, 1, \quad (A3.6)$$

$$\sum_P \equiv \sum_{\vec{k}} \sum_{n=-\infty}^{+\infty} \quad , \quad \sum_Q \equiv \sum_{\vec{q}} \sum_{n=-\infty}^{+\infty} \quad (A3.7)$$

$D(Q)$ is the phonon thermodynamic Green's function (we have suppressed phonon polarization index) and $\pi(Q)$ is the polarization part defined by

$$D^{-1}(Q) = D_0^{-1}(Q) - \pi(Q) \quad (A3.8)$$

(see Chapter II). $g_{p-p'}$ is the electron-phonon coupling function. Again, Ω given by Eq. (A3.5) can be considered as a functional of $\{\Sigma(P)\}$ and $\{\pi(Q)\}$ and is stationary with respect to a small variation in these quantities if and only if they are given by Migdal's equations (see Eqs. II.2 and II.15)

$$\Sigma(P) = -\frac{1}{\beta} \sum_{P'} |g_{P-P'}|^2 D(P-P') G(P') \quad (A3.9a)$$

$$\pi(Q) = \frac{2}{\beta} |g_Q|^2 \sum_P G(P+Q) G(P) \quad (A3.9b)$$

We note that one can prove quite generally that for a given model of a metal the grand thermodynamic potential per unit volume in the normal state is given by

$$\begin{aligned} \Omega = & -\frac{2}{\beta} \sum_P \exp(i\omega_n 0^+) \{ \ln[-G^{-1}(P)] + \Sigma(P)G(P) \} + \\ & + \frac{1}{2\beta} \sum_Q \exp(i\nu_n 0^+) \{ \ln[-D^{-1}(Q)] + \pi(Q)D(Q) \} + \\ & + \Omega' \end{aligned}$$

where Ω' is given by

$$\Omega' = \left\{ \begin{array}{l} \text{Contribution of closed linked skeleton} \\ \text{diagrams computed according to the rules} \\ \text{of Appendix 1 with bare Green's functions} \\ \text{replaced by the full Green's functions,} \end{array} \right.$$

Eliashberg's result, Eq. (A3.5), amounts to retaining only the contribution of the lowest order graph in Ω' , which is given in Fig. (A3.1)

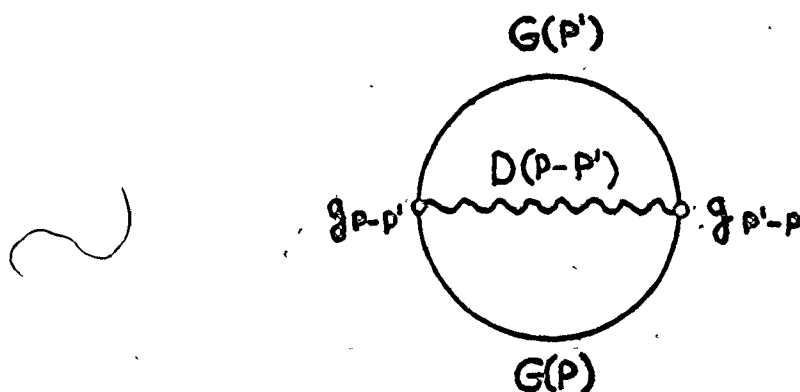


Fig. (A3.1)

The contribution of this graph is equal to (see Appendix 1)

$$-\frac{1}{\beta^2} \sum_P \sum_{P'} |g_{P-P'}|^2 G(P) D(P-P') G(P') e^{i\omega_n O^+} e^{i\omega_{n'} O^+} \quad (\text{A3.10})$$

which is precisely the last term in Eliashberg's result (A3.5). Higher order graphs in Ω' , like the one in Fig. (A3.2)

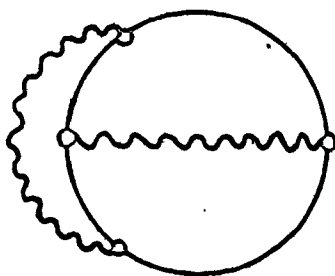


Fig. (A3.2)

can be neglected compared to the lowest order one because of the same type of argument as used by Migdal in his solution of the Dyson equations for the electron-phonon problem. This is precisely the reason why the equations $\delta\Omega/\delta\Sigma = 0$ and $\delta\Omega/\delta\Pi = 0$, with Ω given by Eq. (A3.5) result in Migdal's equations (A3.9a) and (A3.9b).

In passing we note that from the above discussion it should be reasonable to expect that the expression for the electronic part of the specific heat for the interacting electron-phonon system in the normal state obtained from the Eliashberg's result for Ω , Eq. (A3.5), is equal to the one derived by Prange and Kadanoff⁴⁴⁾ in a quite different way. Namely, Prange and Kadanoff analysed the transport equations for the interacting electron-phonon system and obtained the result for several equilibrium properties, like the electronic part of the specific heat, by reinterpreting the partial derivatives with respect to time in their transport equations as the derivatives with respect to temperature. Since Migdal's approximation played a crucial role in their treatment one can expect that the end result for the electronic part of the specific heat, C_V^{el} , should be the same. This was explicitly demonstrated by Grimvall⁵⁵⁾.

For the grand thermodynamic potential per unit volume in the superconducting state Eliashberg has obtained the following result by ignoring the short range Coulomb repulsion between the electrons:

$$\begin{aligned}
\Omega = & - \frac{2}{\beta} \sum_P \exp(i\omega_n 0^+) \left\{ \frac{1}{2} \ln[-\Phi(P)] + \Sigma_1(P)G(P) - \Sigma_2(P)F(P) \right\} \\
& + \frac{1}{2\beta} \sum_Q \exp(i\nu_n 0^+) \{ \ln[-D^{-1}(Q)] + \pi(Q) \} - \\
& - \frac{1}{\beta^2} \sum_{P, P'} |g_{P-P'}|^2 [G(P)D(P-P')G(P') - F(P)D(P-P')F(P')] e^{i\omega_n 0^+ i\omega_n' 0^+}
\end{aligned} \tag{A3.11}$$

The quantities $\Sigma_1(P)$, $\Sigma_2(P)$, $\Phi(P)$, $G(P)$ and $F(P)$ are related to Nambu's 2×2 matrix self-energy $\hat{\Sigma}(P)$ and the electron thermodynamic Green's function $\hat{G}(P)$ (see Ch.III) by

$$\Sigma_1(P) = \hat{\Sigma}_{11}(P) = i\omega_n (1 - Z(i\omega_n)) \chi(i\omega_n) \tag{A3.12a}$$

$$\Sigma_2(P) = \hat{\Sigma}_{12}(P) = \phi(k, i\omega_n) \tag{A3.12b}$$

$$\Phi(P) = \det G^{-1}(P) = (i\omega_n Z(k, i\omega_n))^2 - (\epsilon_k + \chi(k, i\omega_n))^2 - \phi^2(k, i\omega_n) \tag{A3.12c}$$

$$G(P) = (\hat{\tau}_3 \hat{G}^d(P) \hat{\tau}_3)_{11} = \hat{G}_{11}^d(P) = [i\omega_n Z(k, i\omega_n) + (\epsilon_k + \chi(k, i\omega_n))] / \det \hat{G}^{-1}(P) \tag{A3.12d}$$

$$F(P) = (\hat{\tau}_3 \hat{G}^{od}(P) \hat{\tau}_3)_{12} = (-\hat{G}^{od}(P))_{12} = -\hat{\Sigma}_{12}(P) / \det \hat{G}^{-1}(P) \tag{A3.12e}$$

Here $\hat{G}^d(P)$ and $\hat{G}^{od}(P)$ are the diagonal and off-diagonal part of $\hat{G}(P)$, respectively. Also, since we are interested in the equilibrium thermodynamic properties of a superconductor, the phase of the single-particle state $|k\rangle$ used to define the creation operator C_k^\dagger can be chosen in such a way that the $\hat{\tau}_2$ -component of $\hat{\Sigma}(P)$, i.e. $\Phi(P)$ (see Ch.III) is equal to zero.

As before, the expression (A3.11) has the useful property that it is stationary with respect to small changes in $\{\Sigma_1(P)\}$, $\{\Sigma_2(P)\}$ and $\{\pi(Q)\}$ around their correct values given by

$$\Sigma_1(P) = - \frac{1}{\beta} \sum_{P'} |g_{P-P'}|^2 D(P-P') G(P) \quad (\text{A3.13a})$$

$$\Sigma_2(P) = - \frac{1}{\beta} \sum_{P'} |g_{P-P'}|^2 D(P-P') F(P) \quad (\text{A3.13b})$$

$$\pi(Q) = \frac{2}{\beta} |g_Q|^2 \sum_P [G(P+Q)G(P) - F(P+Q)F(P)] \quad (\text{A3.13c})$$

We note that the equations (A3.13a) and (A3.13b) are equivalent to

$$\hat{\Sigma}^d(P) = - \frac{1}{\beta} \sum_{P'} |g_{P-P'}|^2 D(P-P') (\hat{\tau}_3 \hat{G}(P) \hat{\tau}_3)^d \quad (\text{A3.14a})$$

$$\hat{\Sigma}^{\text{od}}(P) = - \frac{1}{\beta} \sum_{P'} |g_{P-P'}|^2 D(P-P') (\hat{\tau}_3 \hat{G} \hat{\tau}_3)^{\text{od}} \quad (\text{A3.14b})$$

which are just the usual Eliashberg equations for a superconductor with the Coulomb repulsion set equal to zero (see Ch.III). Equation (A3.13c) is the equation for the phonon polarization part in the superconducting state. Also, in the limit $\Sigma_2(P) \rightarrow 0$ Eqs. (A3.11), (A3.13a) and (A3.13c) reduce to the corresponding normal state equations (A3.5), (A3.9a) and (A3.9b).

The last term in Eq. (A3.11) is equal to the contribution of the diagram in Fig. (A3.1) where now each vertex is to be interpreted as $g\hat{\tau}_3$ (see Appendix 1 and the first diagram in Fig. A3.3). The contribution of the higher order diagrams can

be neglected as before.

It should be noted that the effects of the Coulomb interaction between the electrons have been included in (A3.5) and (A3.11) only through the electronic energies ϵ_k . A first principle calculation of Ω for the Coulomb interaction, which would include all many-body effects, is a difficult task due to the absence of a small expansion parameter for the Coulomb problem. However, we are ultimately interested in calculating the difference $\Omega_s - \Omega_n$ between the grand thermodynamic potential in the superconducting state, Ω_s , and corresponding quantity in the normal state Ω_n . The major part in $\Omega_s - \Omega_n$ comes from the superconducting correlations and is well described by the BCS theory. The corrections to the BCS result come mostly from the details of the basic interaction which brings about superconductivity - i.e. the electron-phonon interaction. Therefore it seems appropriate to modify the expression for Ω_s by adding to the last term in Eq. (A3.11) the contribution of the second diagrams in Fig. A3.3 which accounts for the effect of the

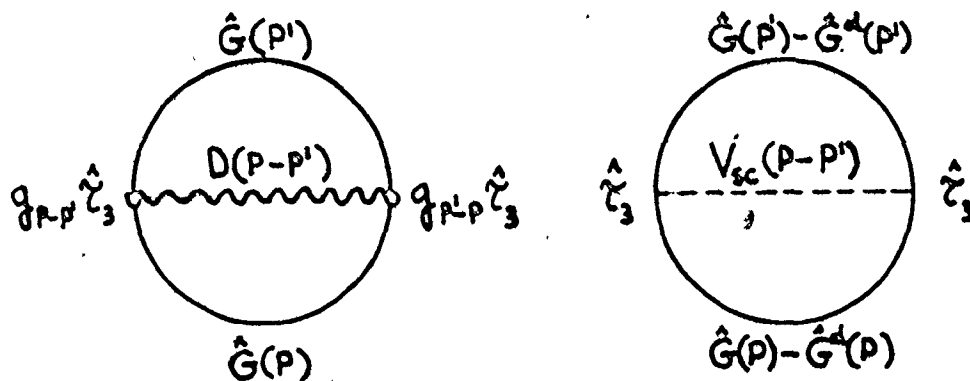


Fig. A3.3

short-range Coulomb repulsion on the pairing self energy. The contribution of the two diagrams in Fig. A3.3 is (from now on we do not write explicitly the small convergence factors $\exp(i\omega_n 0^+)$, $\exp(i\omega_n 0^+)$ etc.)

$$- \frac{1}{\beta^2} \sum_{P, P'} \{ |g_{P-P'}|^2 \overline{G(P) D(P-P') G(P')} - F(P) [|g_{P-P'}|^2 D(P-P') +$$

(A3.15)

$$+ V_{SC}(P-P')] F(P') \}$$

and the last term in Eq. (A3.11) is replaced by the expression (A3.15). $V_{SC}(P-P')$ denotes the screened Coulomb matrix element. Note that the expression (A3.11) modified in the described manner is now stationary with respect to the small changes in $\{\Sigma_1(P)\}$ and $\{\Sigma_2(P)\}$ around their values given by the Eliashberg equations extended to include the effects of the short-range Coulomb repulsion (see Ch.III):

$$\Sigma_1(P) = - \frac{1}{\beta} \sum_P |g_{P-P'}|^2 D(P-P') G(P') \quad (A3.16a)$$

$$\Sigma_2(P) = - \frac{1}{\beta} \sum_{P'} [|g_{P-P'}|^2 D(P-P') + V_{SC}(P-P')] F(P') \quad (A3.16b)$$

(Equation (A3.13c) which is equivalent to $\delta\Omega/\delta\pi = 0$ remains unchanged.) Here again, the effects of the Coulomb interaction in the normal state are included via band-structure energies ϵ_k and fully screened and Coulomb vertex corrected electron-

phonon coupling function $g_{p-p'}$.

In the case when a small amount of ordinary (nonmagnetic) impurities is present the last term in Eq. (A3.15) should be supplemented by the contribution of the diagram in Fig.

(A3.4)

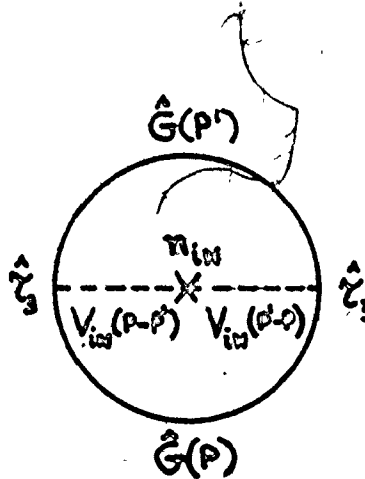


Fig. A3.4

and the last term in Eq. (A3.5) for Ω in the normal state by the contribution of the analogous diagram for the normal state, after appropriate configuration averaging over the impurity configurations. The contribution of this diagram is

$$\frac{1}{\Omega} \sum_P \sum_{P'} [G(P)n_{iN}|V_{iN}(P-P')|^2 G(P') - F(P)n_{iN}|V_{iN}(P-P')|^2 F(P)] \quad (A3.17)$$

where n_{iN} is the impurity concentration (number of impurities per unit volume) and V_{iN} is the change in the crystal potential due to impurity. Again, with this term added to the expression (A3.15) (which is already modified to include the

Coulomb repulsion) Ω is stationary with respect to small changes in $\{\Sigma_1(P)\}$ and $\{\Sigma_2(P)\}$ around the values given by

$$\Sigma_1(P) = -\frac{1}{\beta} \sum_{P'} |g_{P-P'}|^2 D(P-P') G(P) + n_{iN} \sum_{P'} |V_{iN}(P-P')|^2 G(P') \quad (\text{A3.18a})$$

$$\begin{aligned} \Sigma_2(P) = & -\frac{1}{\beta} \sum_{P'} [|g_{P-P'}|^2 D(P-P') + V_{sc}(P-P')] F(P') + \\ & + n_{iN} \sum_{P'} |V_{iN}(P-P')|^2 F(P') \end{aligned} \quad (\text{A3.18b})$$

which are the Eliashberg equations extended to include scattering by small amounts of ordinary impurities.

A similar treatment is applicable in the case of small amounts of paramagnetic impurities. Then Ω is to be corrected by the contribution of the diagram analogous to the one in Fig. A3.4, with the main difference that the $\hat{\tau}_3$ -matrices at the vertices are now unit $\hat{\tau}_0$ -matrices:

$$\begin{aligned} & \frac{1}{\beta} \sum_P \sum_{P'} [G(P) n_{iP} S(S+1) V_{iP}(P-P') G(P') + \\ & + F(P) n_{iP} S(S+1) V_{iP}(P-P') F(P')] \end{aligned} \quad (\text{A3.19})$$

where n_{iP} is the concentration of the paramagnetic impurities, S is the magnitude of the impurity spin and V_{iP} is the change in the crystal potential due to the paramagnetic impurity.

The problem of the free energy difference between the normal and superconducting state has been treated by Wada⁴⁵⁾ and by Bardeen and Stephen⁴⁶⁾. Wada's treatment starts from a first

principle calculation of the thermodynamic average $\langle \hat{H} - \mu \hat{N} \rangle$ where \hat{H} is the total Hamiltonian of the system. In order to eliminate the ion kinetic energy from the problem he uses the so-called Chester's relation which is of thermodynamic nature. The effects of the Coulomb interaction were included in his treatment from the beginning but there appears to be an implicit restriction on the size of the Coulomb repulsion in order to have the simple isotope effect $T_c \propto M^{1/2}$, where M is the mass of the ion. However, in practice, this difficulty has been ignored by computational theorists and the results of the numerical calculations have been in good agreement with the experiments.

Bardeen and Stephen have started from the Eliashberg's expression for the grand thermodynamic potential in the superconducting state, which also gives the appropriate formula for the normal state upon taking the limit $\Sigma_2 \rightarrow 0$. By assuming that there is no change in the chemical potential due to the superconducting transition, which is an excellent approximation (this change is of the order of $\Delta^2/4\mu_n$, where μ_n is the chemical potential in the normal state) the free energy difference is given by $\Omega_s - \Omega_n$. Furthermore, they have exploited the fact that both Ω_s and Ω_n are stationary with respect to small changes in various self-energy parts and in the expression for Ω_n they have replaced Σ_{ln} by Σ_{ls} and π_n by π_s (indices n and s refer to the normal and superconducting state respectively), since the differences $\Sigma_{ln} - \Sigma_{ls}$ and $\pi_n - \pi_s$ are small ($Z_s - Z_n$ is of the order of $\lambda_0 (\Delta_0/\omega_D)^2 \ln(\omega_0/\Delta_0) [1 + \theta(\omega - \omega_D) (\frac{\omega_D}{\omega})^2]$ where

$\lambda_0 = |g_{P-P'}|^2 N(0)$, $N(0)$ being the single spin electronic density of states, and ω is the excitation energy; $\pi_s - \pi_n$ is of the order of $(\lambda_0/8) (\Delta_0^2/\mu_n) \ln(2\omega_D/\Delta_0)$. The resulting quantity is called Ω_{ns} and the free energy difference is calculated as

$$\begin{aligned} \Omega_s - \Omega_{ns} = & - \frac{1}{\beta} \sum_P \left[\ln \left(\frac{\Phi_s(P)}{\Phi_{ns}(P)} \right) - \Sigma_2(P) F(P) \right] - \\ & - \frac{1}{\beta^2} \sum_{P, P'} |g_{P-P'}|^2 [G(P) - G_{ns}(P)] D(P-P') [G(P') - G_{ns}(P')] \end{aligned} \quad (A3.20)$$

where

$$\Phi_{ns}(P) = (i\omega_n Z_n(k, i\omega_n))^2 - (\epsilon_k + \chi_n(k, i\omega_n))^2 \quad (A3.21a)$$

$$G_{ns}(P) = \frac{1}{i\omega_n Z_n(k, i\omega_n) - (\epsilon_k + \chi_n(k, i\omega_n))} \quad (A3.21b)$$

In the next step Bardeen and Stephen neglect the momentum dependence of Σ_1 and Σ_2 and the energy dependence in the electronic density of states. The first approximation is retained in this thesis (essentially because $\alpha^2 F(\Omega; \epsilon, \epsilon')$ is assumed to be independent of ϵ and ϵ') while the second one is relaxed since it is the subject of central interest in the present work. Then χ_n vanishes (see Ch. III), i.e. $\Sigma_1(i\omega_n)$ is an odd function of $i\omega_n$, and

$$- \frac{1}{\beta} \sum_{P'} |g_{P-P'}|^2 D(P-P') G_{ns}(P') = \Sigma_{1n}(P) . \quad (A3.22)$$

We note at this point that the above equality is an important part of Bardeen and Stephen's derivation and that it breaks

down if the self-energy is momentum dependent and/or electronic density of states cannot be assumed to be a constant in the energy range of the order of ω_D around the Fermi level. This will force us to use a somewhat different procedure in evaluating the free energy difference for a Lorentzian model of the electronic density of states (see Appendix 4) from that used by Bardeen and Stephen. The final result of Bardeen and Stephen's calculation of the free energy difference is

$$\Omega_s - \Omega_{ns} = \frac{2\pi N(0)}{\beta} \sum_{n=1}^{\infty} \left\{ \frac{\Delta^2(i\omega_n) Z_s(i\omega_n)}{(\omega_n^2 + \Delta^2(i\omega_n))^{1/2}} - 2Z_s(i\omega_n) [(\omega_n^2 + \Delta^2(i\omega_n))^{1/2} - \omega_n] - \right. \\ \left. - \omega_n (Z_s(i\omega_n) - Z_n(i\omega_n)) \left(1 - \frac{\omega_n}{(\omega_n^2 + \Delta^2(i\omega_n))^{1/2}} \right) \right\} \quad (A3.23)$$

where $\Delta(i\omega_n) = \phi(i\omega_n)/Z(i\omega_n)$.

It should be noted that the above formula, (Eq. A3.23), is valid when the Coulomb interaction between the electrons is included in the way previously described. It expresses the free energy difference in terms of various self-energy components in the superconducting and normal states, which are to be determined from the solutions of the Eliashberg equations at finite temperature with appropriate input parameters $\alpha^2(\Omega)F(\Omega)$ and $(\mu^*(\omega_c), \omega_c)$.

As shown by Bardeen and Stephen their expression for the free energy difference is equivalent to Wada's formula for this quantity, which, from the numerical point of view, converges

more slowly. The key step in this proof is the identity

$$\sum_P G_n(P) \Sigma_{1s}(P) = \sum_P G_s(P) \Sigma_{1n}(P) \quad (\text{A3.23})$$

which is the consequence of the obvious identity

$$\sum_P \sum_{P'} G_n(P) |g_{P-P'}|^2 D(P-P') G_s(P') = \sum_P \sum_{P'} G_s(P) |g_{P-P'}|^2 D(P-P') G_n(P) ,$$

the assumption that $\pi_s(Q) = \pi_n(Q)$ and the Migdal-Eliashberg equations (A3.9a) and (A3.14a) (see Fig. A3.5). We note here that the equation (A3.23) is valid in the case of a momentum

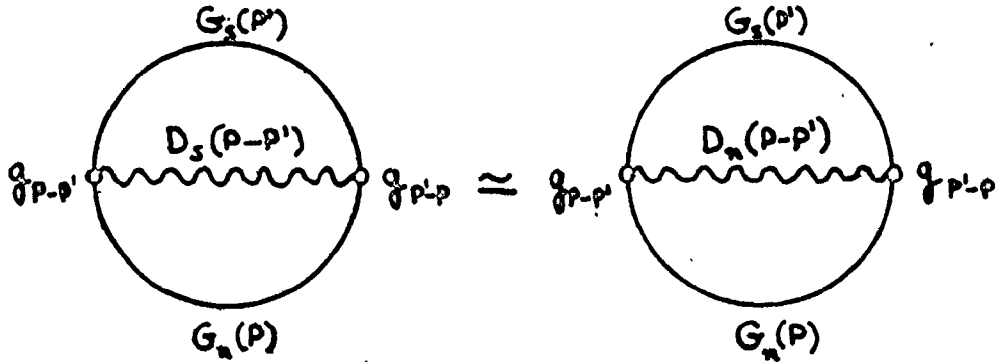


Fig. A3.5

dependent Σ_1 and/or energy dependent electronic density of states $N(\epsilon)$ as long as one can assume that the phonon propagator remains unchanged by the superconducting transition. We will use this equality, Eq. (A3.23), in our generalization of the formula for the free energy difference to the case of a noncon-

stand electronic density of states (Appendix 4).

Finally, we note that the last term in Eq. (A3.11) for Ω_s exactly cancels against one half of

$$- \frac{2}{\beta V} \sum_P \exp(i\omega_n O^+) [\Sigma_1(P)G(P) - \Sigma_2(P)F(P)]$$

in the first term upon using the Eliashberg equations. This is also the case if the last term in Eq. (A3.11) is replaced by (A3.15) in order to include the effects of the Coulomb repulsion, or if it is extended to include impurities, so that one has

$$\begin{aligned} \Omega_s = & - \frac{1}{\beta V} \sum_P \{ \ln[-\phi_s(P)] + \Sigma_{1s}(P)G_s(P) - \Sigma_{2s}(P)F(P) \} + \\ & + \frac{1}{2\beta V} \sum_Q \{ \ln[-D_s^{-1}(Q)] + \pi_s(Q)D_s(Q) \} \end{aligned} \quad (A3.24)$$

and similarly

$$\begin{aligned} \Omega_n = & - \frac{1}{\beta V} \sum_P \{ \ln[-\phi_s(P)] + \Sigma_{1n}(P)G_n(P) \} + \\ & + \frac{1}{2\beta V} \sum_Q \{ \ln[-D_s^{-1}(Q)] + \pi_s(Q)D_s(Q) \} . \end{aligned} \quad (A3.25)$$

By assuming that $\pi_s(Q) = \pi_n(Q)$ (and consequently $D_s(P) = D_s(Q)$) Eqs. (A3.24) and (A3.25) give

$$\begin{aligned} \Omega_s - \Omega_n = & - \frac{1}{\beta V} \sum_P \left\{ \ln \left[\frac{\phi_s(P)}{\phi_n(P)} \right] + \Sigma_{1s}(P)G_s(P) - \Sigma_{1n}(P)G_n(P) - \right. \\ & \left. - \Sigma_{2s}(P)F(P) \right\} . \end{aligned} \quad (A3.26)$$

This will be our starting formula for finding the expression for the free energy difference between the superconducting and the normal state for a Lorentzian model of $N(\epsilon)$.

APPENDIX 4

DERIVATION OF THE FORMULA FOR THE FREE ENERGY DIFFERENCE
BETWEEN THE SUPERCONDUCTING AND NORMAL STATE FOR THE SYM-
METRIC LORENTZIAN MODEL FOR $N(\varepsilon)$

We take

$$N(\varepsilon) = N_b \left(1 + s \frac{1}{\pi} \frac{a}{\varepsilon^2 + a^2} \right) \quad (\text{A4.1})$$

as a model for the electronic density of states (EDOS) and calculate the free energy difference $\Omega_s - \Omega_n$ between the normal and superconducting state per unit volume (see Appendix 3):

$$\begin{aligned} \Omega_s - \Omega_n = & - \frac{1}{\beta} \sum_P \left[\ln \frac{\phi_s(P)}{\phi_n(P)} + \sum_{1s}(P) G_s(P) - \sum_{1n}(P) G_n(P) - \right. \\ & \left. - \sum_2(P) F(P) \right] \end{aligned} \quad (\text{A4.2})$$

where

$$P = (\vec{p}, i\omega_n) , \quad (\text{A4.3a})$$

$$- \frac{1}{\beta} \sum_P = - \frac{1}{\beta} \sum_{n=-\infty}^{+\infty} \int \frac{d^3 \vec{p}}{(2\pi)^3} \left(- \frac{1}{\beta} \sum_{n=-\infty}^{+\infty} \int_{-\infty}^{+\infty} d\varepsilon N(\varepsilon_P) \right) , \quad (\text{A4.3b})$$

$$\phi_s(P) = - [Z_s^2(i\omega_n) (\omega_n^2 + \Delta^2(i\omega_n)) + \varepsilon_P^2] , \quad (\text{A4.3c})$$

$$\phi_n(P) = - [Z_n^2(i\omega_n) \omega_n^2 + \varepsilon_P^2] , \quad (\text{A4.3d})$$

$$\Sigma_{1s}(P) = i\omega_n(1 - Z_s(i\omega_n)) , \quad (A4.3e)$$

$$G_s(P) = - \frac{i\omega_n Z_s(i\omega_n) + \epsilon \frac{1}{P}}{Z_s^2(i\omega_n)(\omega_n^2 + \Delta^2(i\omega_n)) + \epsilon \frac{1}{P}} , \quad (A4.3f)$$

$$\Sigma_{1n}(P) = i\omega_n(1 - Z_n(i\omega_n)) , \quad (A4.3g)$$

$$G_n(P) = - \frac{i\omega_n Z_n(i\omega_n) + \epsilon \frac{1}{P}}{Z_n^2(i\omega_n)\omega_n^2 + \epsilon \frac{1}{P}} , \quad (A4.3h)$$

$$\Sigma_2(P) = \Delta(i\omega_n) Z_s(i\omega_n) , \quad (A4.3i)$$

$$F(P) = \frac{\Delta(i\omega_n) Z_s(i\omega_n)}{Z_s^2(i\omega_n)(\omega_n^2 + \Delta^2(i\omega_n)) + \epsilon \frac{1}{P}} . \quad (A4.3j)$$

Here, $Z_s(i\omega_n)$ and $Z_n(i\omega_n)$ are renormalization functions in the superconducting and normal state, respectively. Since the peak in the electronic density of states given by Eq. (A4.1) is symmetric with respect to $\epsilon = 0$, i.e. $N(-\epsilon) = N(\epsilon)$, and since $N(\epsilon)$ does not change rapidly for $|\epsilon| \ll a$ we have ignored small symmetric components $\chi_s(i\omega_n)$ and $\chi_n(i\omega_n)$ in the off diagonal self-energy parts. Also, for the temperatures which are at most $\sim 0.1 a$ (or $\sim 0.1 \omega_D$) we do not have to take into account any change of the chemical potential (assuming that the model (A4.1) describes the EDOS only in the range of several ω_D around the Fermi level).

Instead of evaluating $\Omega_s - \Omega_n$ in the form given by Eq. (A4.2) it is more convenient to calculate this difference in the form which is obtained by adding and subtracting $\Sigma_{1s}(P)G_n(P)$ from the expression in the square brackets in Eq. (A4.2):

$$\begin{aligned} \Omega_s - \Omega_n = & -\frac{1}{\beta} \sum_P \left\{ \ln \frac{\phi_s(P)}{\phi_n(P)} + \Sigma_{1s}(P)G_s(P) - \Sigma_{1s}(P)G_n(P) + \right. \\ & \left. + \Sigma_{1s}(P)G_n(P) - \Sigma_{1n}(P)G_n(P) - \Sigma_2(P)F(P) \right\}. \end{aligned} \quad (\text{A4.5})$$

We will first integrate various combinations of the terms in Eq. (A4.5) over the electronic energies. Since

$$\int_{-\infty}^{+\infty} d\varepsilon \ln \frac{a^2 + b^2 + \varepsilon^2}{a^2 + \varepsilon^2} = 2\pi[(a^2 + b^2)^{1/2} - |a|] \quad (\text{A4.6})$$

where a and b are real numbers and

$$\int_{-\infty}^{+\infty} d\varepsilon \frac{\ln(a^2 + \varepsilon^2)}{b^2 + \varepsilon^2} = 2 \frac{\ln(|a| + |b|)}{|b|}. \quad (\text{A4.7})$$

For real a , $b \neq 0$, we have

$$\begin{aligned} \int_{-\infty}^{+\infty} d\varepsilon N(\varepsilon) \ln \frac{\phi_s(\varepsilon, i\omega_n)}{\phi_n(\varepsilon, i\omega_n)} = & \int_{-\infty}^{+\infty} d\varepsilon N_b \left(1 + s \frac{1}{\pi} \frac{a}{\varepsilon^2 + a^2} \right) \times \\ & \ln \frac{z_n^2(i\omega_n)\omega_n^2 + [z_s^2(i\omega_n) - z_n^2(i\omega_n)]\omega_n^2 + z_s^2(i\omega_n)\Delta^2(i\omega_n) + \varepsilon^2}{z_n^2(i\omega_n)\omega_n^2 + \varepsilon^2} = \end{aligned}$$

$$\begin{aligned}
&= N_b \, 2\pi \{ [Z_s(i\omega_n) (\omega_n^2 + \Delta^2(i\omega_n))^{1/2} - Z_n(i\omega_n) |\omega_n|] + \\
&+ s \, \frac{1}{\pi} \ln \frac{a + Z_s(i\omega_n) (\omega_n^2 + \Delta^2(i\omega_n))^{1/2}}{a + Z_n(i\omega_n) |\omega_n|} \} . \quad (A4.8)
\end{aligned}$$

We have used the fact that Z_s and Z_n are positive. By using the identity (A3.23) of Appendix 3

$$\sum_P \Sigma_{ls}(P) G_n(P) = \sum_P \Sigma_{ln}(P) G_s(P)$$

we can write

$$\sum_P [\Sigma_{ls}(P) G_s(P) - \Sigma_{ln}(P) G_n(P)] = \sum_P [\Sigma_{ls}(P) G_s(P) - \Sigma_{ln}(P) G_s(P)]$$

and

$$\begin{aligned}
&\int_{-\infty}^{+\infty} d\epsilon N(\epsilon) [\Sigma_{ls}(i\omega_n) G_s(\epsilon, i\omega_n) - \Sigma_{ln}(i\omega_n) G_s(\epsilon, i\omega_n)] = \\
&= i\omega_n (Z_s(i\omega_n) - Z_n(i\omega_n)) \int_{-\infty}^{+\infty} d\epsilon N_b \left(1 + s \, \frac{1}{\pi} \frac{a}{a^2 + \epsilon^2} \right) \times \\
&\quad \times \frac{i\omega_n Z_s(i\omega_n) + \epsilon}{Z_s^2(i\omega_n) (\omega_n^2 + \Delta^2(i\omega_n)) + \epsilon^2} \\
&= \pi \omega_n (Z_s(i\omega_n) - Z_n(i\omega_n)) \frac{\omega_n}{(\omega_n^2 + \Delta^2(i\omega_n))^{1/2}} \times \\
&\quad \times N_b \left[1 + s \, \frac{1}{\pi} \frac{1}{a + Z_s(i\omega_n) (\omega_n^2 + \Delta^2(i\omega_n))^{1/2}} \right] \quad (A4.9)
\end{aligned}$$

(see Eqs. (A2.12)-(A2.14) of Appendix 2). In the same way we get

$$\begin{aligned} & \int_{-\infty}^{+\infty} d\epsilon N(\epsilon) \{ \Sigma_{1s}(i\omega_n) G_n(\epsilon, i\omega_n) - \Sigma_{1n}(i\omega_n) G_n(\epsilon, i\omega_n) \} = \\ & = -\pi\omega_n (Z_s(i\omega_n) - Z_n(i\omega_n)) \operatorname{sgn}(\omega_n) N_b \left[1 + s \frac{1}{\pi} \frac{1}{a + Z_n(i\omega_n) |\omega_n|} \right] . \end{aligned} \quad (A4.10)$$

Finally,

$$\begin{aligned} & \int_{-\infty}^{+\infty} d\epsilon N(\epsilon) \Sigma_2(i\omega_n) F(\epsilon, i\omega_n) = \Delta(i\omega_n) Z_s(i\omega_n) \int_{-\infty}^{+\infty} d\epsilon N_b \left(1 + s \frac{1}{\pi} \frac{a}{a^2 + \epsilon^2} \right) \times \\ & \times \frac{\Delta(i\omega_n) Z_s(i\omega_n)}{Z_s^2(i\omega_n) (\omega_n^2 + \Delta^2(i\omega_n)) + \epsilon^2} = \\ & = \pi \Delta(i\omega_n) Z_s(i\omega_n) \frac{\Delta(i\omega_n)}{(\omega_n^2 + \Delta^2(i\omega_n))^{1/2}} N_b \left[1 + \right. \\ & \left. + s \frac{1}{\pi} \frac{1}{a + Z_s(i\omega_n) (\omega_n^2 + \Delta^2(i\omega_n))^{1/2}} \right] . \end{aligned} \quad (A4.11)$$

Putting all these results together and using the symmetry properties

$$\Delta(-i\omega_n) = \Delta(i\omega_n) , \quad Z_s(-i\omega_n) = Z_s(i\omega_n) , \quad Z_n(-i\omega_n) = Z_n(i\omega_n) ,$$

and

$$\omega_{-n} = \pi T[2(-n)-1] = -\pi T[2(n+1)-1] = -\omega_{n+1} ,$$

when converting the sum over the Matsubara frequencies on the negative imaginary axis into the sum over the Matsubara frequencies on the positive imaginary axis, i.e.

$$\sum_{n=-\infty}^{+\infty} f(i\omega_n) = \sum_{n=1}^{\infty} [f(i\omega_n) + f(i\omega_{-n+1})] = \sum_{n=1}^{\infty} [f(i\omega_n) + f(-i\omega_n)]$$

(where it is assumed that all series converge absolutely so that the terms can be rearranged at will), we obtain

$$\begin{aligned} \Omega_s - \Omega_n &= \frac{2\pi N_b}{\beta} \sum_{n=1}^{\infty} \left[\frac{\Delta^2(i\omega_n) Z_s(i\omega_n)}{(\omega_n^2 + \Delta^2(i\omega_n))^{1/2}} - \right. \\ &\quad \left. - 2(Z_s(i\omega_n)(\omega_n^2 + \Delta^2(i\omega_n))^{1/2} - Z_n'(i\omega_n)\omega_n) + \right. \\ &\quad \left. + s \frac{1}{\pi} \left[\frac{\Delta^2(i\omega_n) Z_s(i\omega_n)}{(\omega_n^2 + \Delta^2(i\omega_n))^{1/2}} \frac{1}{a + Z_s(i\omega_n)(\omega_n^2 + \Delta^2(i\omega_n))^{1/2}} - \right. \right. \\ &\quad \left. \left. - 2 \ln \frac{a + Z_s(i\omega_n)(\omega_n^2 + \Delta^2(i\omega_n))^{1/2}}{a + Z_n(i\omega_n)\omega_n} + \omega_n (Z_s(i\omega_n) - Z_n(i\omega_n)) \times \right. \right. \\ &\quad \left. \left. \times \left(\frac{1}{a + Z_n(i\omega_n)\omega_n} + \frac{\omega_n}{(\omega_n^2 + \Delta^2(i\omega_n))^{1/2}} \frac{1}{a + Z_s(i\omega_n)(\omega_n^2 + \Delta^2(i\omega_n))^{1/2}} \right) \right] \right] \end{aligned} \quad (A4.12)$$

By adding and subtracting $2Z_s(i\omega_n)\omega_n$ from the expression in the first square bracket in the above formula and $2 \ln(a + Z_s(i\omega_n)\omega_n)$, $\omega_n(Z_s(i\omega_n) - Z_n(i\omega_n))/(a + Z_s(i\omega_n)\omega_n)$ from the expression in the second square bracket (this is done to obtain a form of $\Omega_s - \Omega_n$

which is more convenient for the analysis of the order of the phase transition) we can rewrite Eq. (A4.12) in the form

$$\begin{aligned}
 \Omega_s - \Omega_n = & \frac{2\pi N_b}{\beta} \sum_{n=1}^{\infty} \left\{ \left[\frac{\Delta^2(i\omega_n) Z_s(i\omega_n)}{(\omega_n^2 + \Delta^2(i\omega_n))^{1/2}} - 2 Z_s(i\omega_n) (\omega_n^2 + \Delta^2(i\omega_n))^{1/2} - \omega_n \right] \right. \\
 & - \omega_n (Z_s(i\omega_n) - Z_n(i\omega_n)) \left(1 - \frac{\omega_n}{(\omega_n^2 + \Delta^2(i\omega_n))^{1/2}} \right) \Big] + \\
 & + s \frac{1}{\pi} \left[\frac{\Delta^2(i\omega_n) Z_s(i\omega_n)}{(\omega_n^2 + \Delta^2(i\omega_n))^{1/2}} \frac{1}{a + Z_s(i\omega_n) (\omega_n^2 + \Delta^2(i\omega_n))^{1/2}} - \right. \\
 & \left. - 2 \ln \frac{a + Z_s(i\omega_n) (\omega_n^2 + \Delta^2(i\omega_n))^{1/2}}{a + Z_s(i\omega_n) \omega_n} \right. \\
 & \left. - \omega_n (Z_s(i\omega_n) - Z_n(i\omega_n)) \left(\frac{1}{a + Z_s(i\omega_n) \omega_n} - \right. \right. \\
 & \left. \left. - \frac{\omega_n}{(\omega_n^2 + \Delta^2(i\omega_n))^{1/2}} \frac{1}{a + Z_s(i\omega_n) (\omega_n^2 + \Delta^2(i\omega_n))^{1/2}} \right) \right. \\
 & \left. + \omega_n (Z_s(i\omega_n) - Z_n(i\omega_n)) \left(\frac{1}{a + Z_s(i\omega_n) \omega_n} + \frac{1}{a + Z_n(i\omega_n) \omega_n} \right) - \right. \\
 & \left. - 2 \ln \frac{a + Z_s(i\omega_n) \omega_n}{a + Z_n(i\omega_n) \omega_n} \right] \Big\} . \tag{A4.13}
 \end{aligned}$$

Equation (A4.13) is our final expression for the free energy difference between the superconducting and the normal state for an isotropic superconductor with electronic density of states which is described by equation (A4.1). There are several im-

portant points to be noted:

1) In the limit $a \rightarrow +\infty$ (or equivalently $s \rightarrow 0$), equation A(4.13) reduces to

$$\begin{aligned}
 (\Omega_s - \Omega_n)_{\text{B.S.}} = & \frac{2\pi N_b}{\beta} \sum_{n=1}^{\infty} \left\{ \frac{\Delta^2(i\omega_n) Z_s(i\omega_n)}{(\omega_n^2 + \Delta^2(i\omega_n))^{1/2}} - \right. \\
 & - 2Z_s(i\omega_n) ((\omega_n^2 + \Delta^2(i\omega_n))^{1/2} - \omega_n) \\
 & \left. - \omega_n (Z_s(i\omega_n) - Z_n(i\omega_n)) \left(1 - \frac{\omega_n}{(\omega_n^2 + \Delta^2(i\omega_n))^{1/2}}\right) \right\} \quad (\text{A4.14})
 \end{aligned}$$

which is just the Bardeen-Stephen's result for the case of a flat electronic density of states equal to N_b . In order to show that the phase transition is not of the first order it is sufficient to demonstrate that for each n all the terms which are proportional to the second power of $\Delta(i\omega_n)$ (and 'weaker' functions of $\Delta(i\omega_n)$) explicitly cancel in the limit $T \rightarrow T_c - 0^+$, assuming that at T_c $\Delta \propto (T_c - T)^{1/2}$. The last assumption is presumably valid for strong coupling superconductors (it is exact in the BCS theory) since near T_c the damping effects on $\Delta(T)$ and T_c are the same and the strong-coupling effects 'cancel'. Indeed, expanding in powers of Δ and keeping only (explicitly) the terms up to the second order in Δ we get for the (general) n -th term in the series (A4.14) for $(\Omega_s - \Omega_n)_{\text{B.S.}}$

$$\begin{aligned}
& \frac{\Delta^2(i\omega_n) Z_s(i\omega_n)}{\omega_n} - 2Z_s(i\omega_n)\omega_n \left(1 + \frac{1}{2} \frac{\Delta^2(i\omega_n)}{\omega_n^2}\right) - \\
& - \omega_n (Z_s(i\omega_n) - Z_n(i\omega_n)) \left[1 - \left(1 - \frac{1}{2} \frac{\Delta^2(i\omega_n)}{\omega_n^2}\right)\right] = \\
& = - (Z_s(i\omega_n) - Z_n(i\omega_n)) \Delta^2(i\omega_n) / (2\omega_n) , \quad T \rightarrow T_c - 0^+ .
\end{aligned}$$

Since $Z_s(i\omega_n) - Z_n(i\omega_n) = o(\Delta(i\omega_n))$, $\Delta(i\omega_n) \rightarrow 0$ (see Appendix 3) the general term in the series (A4.17) is $o(\Delta^3(i\omega_n))$ near T_c .

2) To prove the same property for the expression (A4.13) it remains to analyze the term in the second square bracket, since the one in the first square bracket has the same form as the general term in Bardeen-Stephen's formula (A4.14). The expression in the second square bracket in (A4.13) can be written in the form

$$A + B + C \quad (A4.15)$$

with

$$\begin{aligned}
A = & \frac{\Delta^2(i\omega_n) Z_s(i\omega_n)}{(\omega_n^2 + \Delta^2(i\omega_n))^{1/2}} \frac{1}{a + Z_s(i\omega_n) (\omega_n^2 + \Delta^2(i\omega_n))^{1/2}} - \\
& - 2 \ln \frac{a + Z_s(i\omega_n) (\omega_n^2 + \Delta^2(i\omega_n))^{1/2}}{a + Z_s(i\omega_n) \omega_n} \quad (A4.16)
\end{aligned}$$

$$B = \omega_n (Z_s(i\omega_n) - Z_n(i\omega_n)) \left(\frac{1}{a + Z_s(i\omega_n)\omega_n} - \frac{\omega_n}{(\omega_n^2 + \Delta^2(i\omega_n))^{1/2}} \frac{1}{a + Z_s(i\omega_n)(\omega_n^2 + \Delta^2(i\omega_n))^{1/2}} \right) \quad (A4.17)$$

$$C = \omega_n (Z_s(\omega_n) - Z_n(\omega_n)) \left(\frac{1}{a + Z_s(i\omega_n)\omega_n} + \frac{1}{a + Z_n(i\omega_n)\omega_n} \right) - 2 \ln \frac{a + Z_s(i\omega_n)\omega_n}{a + Z_n(i\omega_n)\omega_n} \quad (A4.18)$$

Near the T_c A becomes

$$\begin{aligned} A &= \frac{\Delta^2(i\omega_n) Z_s(i\omega_n)}{\omega_n} \frac{1}{a + Z_s(i\omega_n)\omega_n} - \\ &\quad - 2 \ln \frac{a + Z_s(i\omega_n)\omega_n [1 + \frac{1}{2}(\Delta^2(i\omega_n)/\omega_n^2)]}{a + Z_s(i\omega_n)\omega_n} + o(\Delta^2(i\omega_n)) \\ &= \frac{\Delta^2(i\omega_n)}{\omega_n} \frac{Z_s(i\omega_n)}{a + Z_s(i\omega_n)\omega_n} - 2 \ln \left[1 + \frac{1}{2} \frac{Z_s(i\omega_n)}{a + Z_s(i\omega_n)\omega_n} \frac{\Delta^2(i\omega_n)}{\omega} \right] + \\ &\quad + o(\Delta^2(i\omega_n)) \\ &= \frac{\Delta^2(i\omega_n)}{\omega_n} \frac{Z_s(i\omega_n)}{a + Z_s(i\omega_n)} - \frac{\Delta^2(i\omega_n)}{\omega_n} \frac{Z_s(i\omega_n)}{a + Z_s(i\omega_n)} + \\ &\quad + o(\Delta^2(i\omega_n)) = o(\Delta^2(i\omega_n)). \end{aligned}$$

For the B we have

$$\begin{aligned}
 B &= \omega_n (Z_s(i\omega_n) - Z_n(i\omega_n)) \left(\frac{1}{a + Z_s(i\omega_n)\omega_n} - \left(1 - \frac{1}{2} \frac{\Delta^2(i\omega_n)}{\omega_n^2}\right) \frac{1}{a + Z_s(i\omega_n)\omega_n} \right) + \\
 &+ o(\Delta^2(i\omega_n)) = \frac{Z_s(i\omega_n) - Z_n(i\omega_n)}{2\omega_n(a + Z_s(i\omega_n)\omega_n)} \Delta^2(i\omega_n) + o(\Delta^2(i\omega_n)) \\
 &= o(\Delta^2(i\omega_n)) \quad , \quad T \rightarrow T_c - 0^+
 \end{aligned}$$

since $Z_s(i\omega_n) - Z_n(i\omega_n) = o(\Delta(i\omega_n))$, $\Delta(i\omega_n) \rightarrow 0$.

Finally, near T_c C becomes

$$\begin{aligned}
 C &= \omega_n (Z_s(i\omega_n) - Z_n(i\omega_n)) \frac{1}{a + Z_s(i\omega_n)\omega_n} \left(2 + \frac{\omega_n (Z_s(i\omega_n) - Z_n(i\omega_n))}{a + Z_n(i\omega_n)\omega_n} \right) - \\
 &- 2 \ln \left(1 + \frac{\omega_n (Z_s(i\omega_n) - Z_n(i\omega_n))}{a + Z_n(i\omega_n)\omega_n} \right) = \\
 &= 2 \frac{\omega_n (Z_s(i\omega_n) - Z_n(i\omega_n))}{a + Z_s(i\omega_n)\omega_n} - 2 \frac{\omega_n (Z_s(i\omega_n) - Z_n(i\omega_n))}{a + Z_n(i\omega_n)\omega_n} + o(\Delta^2(i\omega_n)) \\
 &= o(\Delta^2(i\omega_n))
 \end{aligned}$$

since, as before $Z_s(i\omega_n) - Z_n(i\omega_n) = o(\Delta(i\omega_n))$, $\Delta(i\omega_n) \rightarrow 0$.

Thus, the formula (A4.13) for the free energy difference per unit volume, ΔF , describes a phase transition which is not of the first order. This is a very important property of the expression for the free energy difference and accounts for the superconductive transition. Also, this point is nontrivial, since an approach to the problem of finding the formula for ΔF when the electronic density of states cannot be taken as constant,

which was based on Wada's method has led to a formula for ΔF which does not correctly describe the order of the superconductive transition⁹⁴). The exact origin of this difficulty with Wada's method remains unclear at present.

3) At least formally we can take the limit $a \rightarrow +0$ in the formulas (A4.1) and (A4.13). The electronic density of states is then given by

$$N(\varepsilon) = N_D (1 + s \delta(\varepsilon)) \quad . \quad (A4.19)$$

It is not hard to see that in this limit Eq. (A4.13) reduces to the form which would be obtained by direct calculation of (A4.5) with the electronic density of states given by (A4.19) and that the resulting expression describes the phase transition which is not of the first order.

4) Bardeen and Stephen, in their treatment of the free energy difference between the superconducting and normal state, have calculated $\Omega_s - \Omega_{ns}$, instead of $\Omega_s - \Omega_n$, where (see Eq. (A3.11) of Appendix 3).

$$\begin{aligned} \Omega_s = & - \frac{1}{\beta} \sum_P \{ \ln[-\Phi_s(P)] + \sum_{1s} (P) G_s(P) - \sum_2 (P) F(P) \} + \\ & + \frac{1}{2\beta} \sum_Q \{ \ln[-D_s^{-1}(Q)] + \Pi_s(Q) D_s(Q) \} \end{aligned} \quad (A4.20)$$

and



$$\begin{aligned}
\Omega_{ns} = & -\frac{2}{\beta} \sum_P \left\{ \frac{1}{2} \ln[-\phi_{ns}(P)] + \Sigma_{1s}(P) G_{ns}(P) \right\} + \\
& + \frac{1}{2\beta} \sum_Q \left\{ \ln[-D_n^{-1}(Q)] + \Pi_n(Q) D_n(Q) \right\} - \\
& - \frac{1}{\beta^2} \sum_P \sum_{P'} G_{ns}(P) D_n(P-P') G_{ns}(P')
\end{aligned} \tag{A4.21}$$

and $\phi_{ns}(P)$ is obtained from $\phi_n(P)$ by replacing $\Sigma_{1n}(P)$ with $\Sigma_{1s}(P)$ and similarly $G_{ns}(P)$ is obtained from $G_n(P)$ by replacing $\Sigma_{1n}(P)$ with $\Sigma_{1s}(P)$. Note carefully that for Ω_s we have cancelled the last term in Equation (A3.11) against one half of $(-2/\beta) \sum_P \Sigma_{1s}(P) G_s(P)$ is the first term of the same equation, while in the corresponding expression for the normal state (which is obtained by setting $\Sigma_2(P) = 0$) we have replaced Σ_{1n} with Σ_{1s} and G_n with G_{ns} without performing the analogous cancellation (which is obtained upon using the Migdal-Eliashberg equations). This is the tricky point of the derivation since it ensures that the final expression (see for instance Eq. (A4.14)) has a form which gives the right order of the phase transition.

This replacement of $\Omega_s - \Omega_n$ with $\Omega_s - \Omega_{ns}$, as it was explained in Appendix 3, is based on the fact that Ω is stationary with respect to the small changes in various self-energy parts around their correct values and that Σ_{1s} and Σ_{1n} differ by a small amount. By using the same property of Ω , $\Pi_n(Q)$ can be replaced with $\Pi_s(Q)$ (and consequently $D_n(Q) = D_s(Q) \equiv D(Q)$) so that one has

$$\begin{aligned} \Omega_s - \Omega_{ns} = & -\frac{1}{\beta} \sum_P \{ \ln[\phi_s(P)/\phi_{ns}(P)] - \Sigma_2(P)F(P) \} - \\ & - \frac{1}{\beta^2} \sum_{P,P'} |g_{P-P'}|^2 (G_s(P) - G_{ns}(P)) D(P-P') (G_s(P') - G_{ns}(P')) . \end{aligned} \quad (A4.22)$$

Now, if the self-energy $\Sigma_{1s}(P)$ does not depend on momentum and the electronic density of states can be assumed as constant one has

$$\sum_{P'} |g_{P-P'}|^2 D(P-P') G_{ns}(P) = \sum_{P'} |g_{P-P'}|^2 D(P-P') G_n(P') \quad (A4.23)$$

so that Eq. (A4.21) reduces to

$$\begin{aligned} \Omega_s - \Omega_{ns} = & -\frac{1}{\beta} \sum_P \{ \ln[\phi_s(P)/\phi_{ns}(P)] - \Sigma_2(P)F(P) \} + \\ & + \frac{1}{\beta} (\Sigma_{1s}(P) - \Sigma_n(P)) \sum_P [G_s(P) - G_{ns}(P)] \end{aligned}$$

and direct evaluation of the integrals over the electronic energies leads to the formula (A3.23).

However, if the electronic density of states cannot be assumed as a constant the equality (A4.23) breaks down and one has to introduce the quantity $Z_{ns}(i\omega_n)$ defined by

$$i\omega_n (1 - Z_{ns}(i\omega_n)) \equiv \Sigma_{1ns}(P) \stackrel{d}{=} -\frac{1}{\beta} \sum_{P'} |g_{P-P'}|^2 D(P-P') G_{ns}(P') \quad (A4.24)$$

(We assume that the various self-energy parts do not depend on momentum.) In that case one has

$$\Omega_s - \Omega_{ns} = -\frac{1}{\beta} \sum_p \{ \ln[\phi_s(P)/\phi_{ns}(P)] - \Sigma_2(P) F(P) \} + \\ + \frac{1}{\beta} (\Sigma_{1s}(P) - \Sigma_{1ns}(P)) \sum_p [G_s(P) - G_{ns}(P)]$$

and evaluation of the integrals over the electronic energies with the $N(\epsilon)$ given by the Eq. (A4.1) gives

$$\Omega_s - \Omega_{ns} = \frac{2\pi N_D}{\beta} \sum_{n=1}^{\infty} \left\{ \left[\frac{\Delta^2(i\omega_n) Z_s(i\omega_n)}{(\omega_n^2 + \Delta^2(i\omega_n))^{1/2}} - \right. \right. \\ \left. \left. - 2 Z_s(i\omega_n) ((\Delta_n^2 + \omega_n^2(i\omega_n))^{1/2} - \omega_n) - \right. \right. \\ \left. \left. - \omega_n (Z_s(i\omega_n) - Z_{ns}(i\omega_n)) \left(1 - \frac{\omega_n}{(\omega_n^2 + \Delta^2(i\omega_n))^{1/2}} \right) \right] + \right. \\ \left. + s \frac{1}{\pi} \left[\frac{\Delta^2(i\omega_n) Z_s(i\omega_n)}{(\omega_n^2 + \Delta^2(i\omega_n))^{1/2}} \frac{1}{a + Z_s(i\omega_n) (\omega_n^2 + \Delta^2(i\omega_n))^{1/2}} - \right. \right. \\ \left. \left. - 2 \ln \frac{a + Z_s(i\omega_n) (\omega_n^2 + \Delta^2(i\omega_n))^{1/2}}{a + Z_s(i\omega_n)} \right. \right. \\ \left. \left. - \omega_n (Z_s(i\omega_n) - Z_{ns}(i\omega_n)) \left(\frac{1}{a + Z_s(i\omega_n) \omega_n} - \frac{\omega_n}{(\omega_n^2 + \Delta^2(i\omega_n))^{1/2}} \right) \right. \right. \\ \left. \left. \left. \frac{1}{a + Z_s(i\omega_n) (\omega_n^2 + \Delta^2(i\omega_n))^{1/2}} \right] \right\}. \quad (A4.25)$$

The above expression, Eq. (A4.25), for $\Omega_s - \Omega_{ns}$ is very similar to the Eq. (A4.13) for $\Omega_s - \Omega_n$ except that the last two terms in the second square bracket in (A4.13) (i.e. C given by (A4.18)) are missing in Eq. (A4.25) and that Z_n in (A4.13) is replaced

by Z_{ns} . The unpleasant feature of the formula (A4.25) is that the artificial quantity Z_{ns} , defined by Eq. (A4.24), appears. One would certainly prefer to have the expression for the free energy difference in which only various self-energy parts in both the superconducting and the normal state appear, since they are the quantities with the physical meaning. In order to illustrate the difference between $Z_s(i\omega_n)$, $Z_n(i\omega_n)$ and $Z_{ns}(i\omega_n)$ we have solved the generalized Eliashberg equations for EDOS given by Eq. (A4.1) (see Eqs. (III.51), (III.52)) and the corresponding linearized equation (II.55) at low temperature, where one would expect the difference between these quantities to be large. In Table A1 we give the values of $Z_s(i\omega_n)$, $Z_n(i\omega_n)$, $Z_{ns}(i\omega_n)$, $Z_{ns}(i\omega_n) - Z_n(i\omega_n)$, $Z_n(i\omega_n) - Z_s(i\omega_n)$ at several low Matsubara frequencies for $T = 1.5^\circ\text{K}$. The solutions $\{Z_s(i\omega_n)\}$ and $\{Z_n(i\omega_n)\}$ were obtained for the $\alpha^2(\Omega)F(\Omega)$ spectrum measured by Shen for Nb_3Sn ($\lambda = 1.7$), $a = 28.9$ meV (which is \sim the maximum phonon frequency in α^2F) and $s = \pi a$. $\{Z_{ns}(i\omega_n)\}$ was calculated from $\{Z_s(i\omega_n)\}$ by using Eq. (A4.24). It can be seen that at small values of ω_n (on the scale of the maximum phonon frequency) $(Z_{ns} - Z_n)$ is several percents of $(Z_n - Z_s)$ while at values of ω_n which are larger than the maximum phonon frequency $(Z_{ns} - Z_n) / (Z_n - Z_s) \sim 0.1$. Since Ω is stationary with respect to the small changes in self-energy parts it seems justified to use $Z_n(i\omega_n)$ instead of $Z_{ns}(i\omega_n)$ in Eq. (A4.25). Then the two equations for $\Omega_s - \Omega_n$, Eq. (A4.13), and $\Omega_s - \Omega_{ns}$, Eq. (A4.25),

Table A1

n	ω_n (mev)	$Z_s(i\omega_n)$	$Z_n(i\omega_n)$	$Z_{ns}(i\omega_n)$	$Z_{ns}-Z_n$	Z_n-Z_s
1	0.4061	2.1762	2.3386	2.3420	0.0034	0.1624
5	3.6546	2.1297	2.2345	2.2375	0.0030	0.1048
10	7.7152	2.0176	2.0725	2.0748	0.0023	0.0550
20	15.8366	1.7919	1.8084	1.8095	0.0011	0.0165
40	32.0797	1.5081	1.5105	1.5108	0.0003	0.0024
60	48.3218	1.3621	1.3627	1.3628	0.0001	0.0006

would differ only by term C given by Eq. (A4.18).

As shown by Bardeen and Stephens in the case when the momentum dependence of the self-energies can be ignored and electronic density of states can be taken as a constant

$\Omega_n - \Omega_{ns} = 0$, that is no error is introduced into the formula for the free energy difference by replacing Σ_{ln} with Σ_{ls} in the calculation of Ω_n . From the previous analysis it is clear that when the density of states cannot be taken as constant

the two equations (A4.13) and (A4.25), wherein the second one Z_{ns} is replaced by Z_n , give slightly different formulas for the free energy difference per unit volume between the superconducting and the normal state, the difference being the term C given by Eq. (A4.18). However, by expanding the expression for C into powers of $Z_s(i\omega_n) - Z_n(i\omega_n)$ one obtains

$$C = O((Z_s(i\omega_n) - Z_n(i\omega_n))^2)$$

which indicates that this correction is small (i.e. of second order in the difference $|\Sigma_{ls}(P) - \Sigma_{ln}(P)|$). Indeed, several numerical tests of these two equations have given almost identical thermodynamic properties of a superconductor. Still from the computational point of view it is not difficult to use the exact result, Eq. (A4.13).

REFERENCES

- (1) P. Horsch and H. Rietschel, Z. Phys. B27, 153 (1977)
- (2) S.J. Nettle and H. Thomas, Solid State Comm. 21, 683 (1977)
- (3) S.G. Lie and J.P. Carbotte, Solid State Comm. 26, 511 (1978)
- (4) W.E. Pickett, Phys. Rev. B21, 3897 (1980)
- (5) S.G. Lie and J.P. Carbotte, Solid State Comm. 35, 127 (1980)
- (6) S.G. Lie, B. Mitrović and J.P. Carbotte, Inst. Phys. Conf. Ser. No. 55, 559 (1980)
- (7) P. Müller, G. Ischenko, H. Adrian, J. Bieger, M. Hehmann and E.L. Haase in Superconductivity in d- and f-Band Metals Ed. by H. Suhl and M.B. Maple (Academic Press, New York ; 1980), p. 369
- (8) B. Mitrović and J.P. Carbotte, accepted for publication in Solid State Comm. (1981)
- (9) L.R. Testardi in Physical Acoustics Ed. by W.P. Mason and R.N. Thurston, (Academic Press, New York ; 1973), Chap. 10, p. 193
- (10) M. Weger and I.B. Goldberg, Solid State Physics Ed. by M. Enrenreich, F. Seitz and D. Thurnbull (Academic Press, New York ; 1973) 28, 1
- (11) Yu, A. Izymov and Z.Z. Kurmaev, Usp. Fiz. Nauk 113, 193 (1974) ; Sov. Phys.-Usp., 17, 356 (1974)
- (12) A.M. Clogston and V. Jaccarino, Phys. Rev. 121, 1357 (1961)

- (13) M. Weger, Rev. Mod. Phys. 36, 175 (1964)
- (14) B.M. Klein, L.L. Boyer and D.A. Papaconstantopoulos,
Phys. Rev. B, 18, 6411 (1978)
- (15) K.M. Ho, M.L. Cohen and W.E. Pickett, Phys. Rev. Lett.,
41, 815 (1978)
- (16) W.E. Pickett, K.M. Ho and M.L. Cohen, Phys. Rev. B, 19,
1734 (1979)
- (17) W.E. Pickett in Superconductivity in d- and f- Band
Metals Ed. by H. Suhl and M.B. Maple (Academic Press,
New York ; 1980), p. 77
- (18) B.M. Klein, D.A. Papaconstantinopoulos and L.L. Boyer in
Superconductivity in d- and f- Band Metals Ed. by
H. Suhl and M.B. Maple (Academic Press, New York ;
1980), p. 455
- (19) J. Ruvalds and C.M. Soukoulis, Phys. Rev. Lett., 43,
1263 (1979)
- (20) A. Handstein, B. Pietrass and G. Behr, Phys. Stat. Sol. (b)
95, 131 (1979)
- (21) B. Pietrass, A. Handstein and G. Behr, Phys. Stat. Sol. (b)
98, 597 (1980)
- (22) J. Labbé and J. Friedel, J. Phys. Radium. 27, 153 (1966)
- (23) J. Labbé, S. Barišić and J. Friedel, Phys. Rev. Lett. 19,
1039 (1967)

- (24) J.W. Garland, Phys. Rev. 153, 460 (1967)
- (25) G. Gladstone, M.A. Jensen and J.R. Schrieffer,
Superconductivity Ed. by R.D. Parks, Vol. 2 (Marcel
Dekker, New York ; 1969)
- (26) A.K. Ghosh and Myron Strongin in Superconductivity in d-
and f- Band Metals, Ed. by H. Suhl and M.B. Maple
(Academic Press, New York ; 1980), p. 305
- (27) D.E. Farrell and B.S. Chandrasekhar, Phys. Rev. Lett. 38,
788 (1977)
- (28) M. Gurvitch, A.K. Ghosh, B.L. Gyorrfy, H. Lutz, O.F. Kammerer,
J.S. Rosner and M. Strongin, Phys. Rev. Lett. 41, 1616
(1978)
- (29) E. Schachinger, B. Mitrović and J.P. Carbotte, to be
published in Phys. Rev. B.
- (30) W.L. McMillan and J.M. Rowell, Superconductivity Ed. by
R.D. Parks, Vol. 1 (Marcel Dekker, New York ; 1969)
- (31) E.L. Wolf, Rep. Prog. Phys. 41, 1439 (1978)
- (32) F.Y. Fradin, Solid State Comm. 16, 1193 (1975)
- (33) A.B. Migdal, J. Exptl. Theoret. Phys. 34, 1438 (1958) ; Soviet
Phys. JETP 7, 996 (1958)
- (34) G.M. Eliashberg, J. Exptl. Theoret. Phys. 38, 966 (1960) ;
Soviet Phys. JETP 11, 696 (1960)
- (35) G.M. Eliashberg, J. Exptl. Theoret. Phys. 39, 1437 (1960);
Soviet Phys. JETP 12, 1000 (1960)

- (36) G.M. Eliashberg, J. Exptl. Theoret. Phys. 43, 1005 (1962) ;
Soviet Phys. JETP 16, 780 (1963)
- (37) P. Morel and P.W. Anderson, Phys. Rev. 128, 1263 (1962)
- (38) S. Engelsberg and J.R. Schrieffer, Phys. Rev. 131, 993 (1963)
- (39) J.R. Schrieffer, D.J. Scalapino, J.W. Wilkins, Phys. Rev.
Lett. 10, 336 (1963)
- (40) A.A. Abrikosov, L.P. Gorkov and I.E. Dzyaloshinski, Methods
of Quantum Field Theory in Statistical Physics (Dover ;
1975)
- (41) E.G. Batyev and V.L. Pokrovskii, J. Exptl. Theore. Phys.
46, 262 (1964) ; Soviet Phys. JETP 19, 181 (1964)
- (42) T. Holstein, Ann. Phys. (N.Y.) 29, 410 (1964)
- (43) J.R. Schrieffer, Theory of Superconductivity (Benjamin,
New York, 1964)
- (44) R.E. Prange and L.P. Kadanoff, Phys. Rev. 134A
- (45) Y. Wada, Phys. Rev. 135, A1481 (1964)
- (46) J. Bardeen and M. Stephen, Phys. Rev. 136, A1485 (1964)
- (47) D.J. Scalapino, Y. Wada and J.C. Swihart, Phys. Rev. Lett.
14, 102 (1965)
- (48) J.C. Swihart, D.J. Scalapino, Y. Wada, Phys. Rev. Lett.
14, 106 (1965)
- (49) W.L. McMillan and J.M. Rowell, Phys. Rev. Lett. 14, 108 (1965)

- (50) V. Heine, P. Noziérs and D. Wilkins, *Phil. Mag.* 13, 741 (1966)
- (51) D.J. Scalapino, J.R. Schrieffer and J.W. Wilkins, *Phys. Rev.* 148, 263 (1966)
- (52) R.E. Prange and A. Sachs, *Phys. Rev.* 158, 672 (1967)
- (53) J. W. Wilkins, Observable Many-Body Effects in Metals, NORDITA Lectures, Copenhagen (1968)
- (54) C.P. Enz in Theory of Condensed Matter, Lectures at ICTP, Trieste 1967, p. 729. IAEA, Vienna, 1968
- (55) G. Grimvall, *Phys. Kondens. Materie* 9, 283 (1969)
- (56) L. Hedin and S. Lundquist, Solid State Physics Ed. by F. Seitz, D. Thurnbull and H. Ehrenreich (Academic Press, New York ; 1969) 23, 1
- (57) D.J. Scalapino in Superconductivity Ed. by R.D. Parks, Vol. 1 (Marcel Dekker, New York ; 1969)
- (58) G. Grimvall, *Physica Scripta* 14, 63 (1976)
- (59) P.B. Allen, *Phys. Rev. B* 18, 5217 (1978)
- (60) P.B. Allen, Theory of the Superconducting T_c , Lecture Notes for the XVI Karpacz Winter School of Theoretical Physics, Karpacz, Poland, 1979 (For possible publication in Lecture Notes in Physics (Springer-Verlag))
- (61) S. Doniach and E.H. Sondheimer, Green's Functions for Solid State Physics (Benjamin, 1974)

- (62) I. Tüttö and J. Ruvalds, Phys. Rev. B 11, 5641 (1979)
- (63) W.B. Cowan and J.P. Carbotte, Phys. Lett. 64 A, 470 (1978)
- (64) P. Horsch, Solid State Comm. 18, 27 (1976)
- (65) G.S. Knapp, S.D. Bader, H.V. Culbert, F.Y. Fradin and
T.E. Klippert, Phys. Rev. B 11, 4331 (1975)
- (66) B.P. Schweiss, B. Renker, E. Schneider and W. Reichardt
in Superconductivity in d- and f- Band Metals Ed. by
D.H. Douglass (Plenum Press, New York ; 1976), p. 189
- (67) S. L. Williamson, C.S. Ting and H.K. Fung, Phys. Rev.
Lett. 32, 9 (1974)
- (68) S.Z. Huang, C.W. Chu and C.S. Ting, Phys. Rev. B 20, 2971
(1979)
- (69) J.M. Luttinger and J.C. Ward, Phys. Rev. 118, 1417 (1960)
- (70) L.P. Kadanoff and G. Baym Quantum Statistical Mechanics
(Benjamin, 1962)
- (71) A.B. Migdal, J. Exptl. Theoret. Phys. 40, 684 (1961) ;
Sov. Phys. JETP 13, 478 (1961)
- (72) L.R. Testardi and L.F. Mattheis, Phys. Rev. Lett. 41,
1612 (1978).
- (73) V.Z. Kresin and G.O. Zaitsev, Zh. Eksp. Teor. Fiz. 74,
1886 (1978) ; Sov. Phys. JETP 47, 983 (1978)
- (74) A.J. Arko, D.H. Lowndes, A.T. Van Kessel, H.W. Myron,
F.H. Mueller, F.A. Muller, L.W. Roeland, J. Wolfrat, and
G.W. Webb, J. de Physique Colloque C6 (Supplement to
Vol. 39, #8) 1385 (1978)

- (75) Y. Nambu, Physical Review 117, 648 (1968)
- (76) H.J. Vidberg and J.W. Serene, J. Low Temp. Phys. 29,
179 (1977)
- (77) L. Tewordt, Phys. Rev. 129, 657 (1963)
- (78) L.Y. Shen in Superconductivity in d- and f- Band Metals
Ed. by D.H. Douglass (AIP, New York ; 1972), p. 31
- (79) J. Bostock, K.H. Lo, W.N. Cheung, V. Diadiuk and
M.L.A. MacVicar in Superconductivity in d- and f- Band Metals
Ed. by D.H. Douglass (Plenum Press, New York; 1976), p. 367
- (80) B. Robinson, T.H. Geballe and J.M. Rowel in Superconductivity
in d- and f- Band Metals Ed. by D.H. Douglass (Plenum
Press, New York ; 1976), p. 381
- (81) P.H. Schmidt, E.G. Spencer, D.C. Joy and J.M. Rowell in
Superconductivity in d- and f- Band Metals Ed. by
D.H. Douglass (Plenum Press, New York ; 1976), p. 431
- (82) D.F. Moore, H.R. Beasley and J.M. Rowell, Journal de Physique,
Colloque C6, Suplement au No. 8, Tome 39 (1978)
- (83) D.F. Moore, R.B. Zubek, J.M. Rowell and M.R. Beasley, Phys.
Rev. B20, 2721 (1979)
- (84) G.B. Arnold, T. Zasadzinski and E.L. Wolf, Phys. Lett.
69A, 136 (1978)
- (85) E.L. Wolf and R.J. Noer, Sol. State Comm. 30, 391 (1979)

- (86) J. Bostock, M.L.A. MacVicar, G.B. Arnold, J. Zasadzinski and E.L. Wolf in Superconductivity in d- and f- Band Metals Ed. by H. Suhl and M.B. Maple (Academic Press, New York ; 1980), p. 153
- (87) J. Zasadzinski, W.K. Schubert, E.L. Wolf and G.B. Arnold in Superconductivity in d- and f- Band Metals Ed. by H. Suhl and M.B. Maple (Academic Press, New York ; 1980), p. 159
- (88) E.L. Wolf, J. Zasadzinski, G.B. Arnold, D.F. Moore, J.M. Rowell and M.R. Beasley, Phys. Rev. B 22, 1214 (1980)
- (89) J. Kwo and T.H. Geballe, Phys. Rev. B 23, 3230 (1981)
- (90) Yu. F. Revenko, A.I. Diachenko, V.M. Svistunov and B. Schöneich, Fizika Nizkih Temperatur 6, 1304 (1980)
- (91) L.Y. Shen, Phys. Rev. Lett. 29, 1082 (1972)
- (92) W.A. Harrison, Phys. Rev. 123, 85 (1961)
- (93) A.A. Galkin, A.I. D'yachenko and V.M. Svistunov, Zh. Eksp. Teor. Fiz. 66, 2262 (1974) ; Sov. Phys. - JETP 39, 1115 (1974)
- (94) S.G. Lie and J.P. Carbotte, (unpublished)
- (95) J.M. Daams, Ph.D. Thesis, McMaster University, Hamilton, Ontario 1978 (unpublished)
- (96) J.M. Daams and J.P. Carbotte, J. Low Temp. Phys. 40, 135 (1980)

- (97) C.R. Leavens and E.W. Fenton, Solid State Comm. 33,
597 (1980)
- (98) B. Mitrović, M.Sc. Thesis, McMaster University, Hamilton,
Ontario 1979 (unpublished)
- (99) Y. Wada, Rev. Mod. Phys. 36, 253 (1964)
- (100) Y. Muto N. Toyota, K. Noto, K. Akutsu, M. Isino and
T. Fukase, J. Low Temp. Phys. 34, 617 (1979).
- (101) D.B. Tanner and A.J. Sievers, Phys. Rev. B 8, 1978 (1973)
and references therein.
- (102) S.W. McKnight, S. Perkowitz, D.B. Tanner and L.R. Testardi,
Phys. Rev. B 19, 5689 (1979)
- (103) S. Perkowitz and G.S. De, Bull. Am. Phys. Soc. 26, 212 (1981)
- (104) J.M. Luttinger, Lectures at Bell Telephone Laboratories
1965-1966 (unpublished)